Technical Report

TR-12-01

KBS-3H Complementary studies, 2008–2010

Svensk Kärnbränslehantering AB

October 2012

Svensk Kärnbränslehantering AB
Swedish Nuclear Fuel
and Waste Management Co

Box 250, SE-101 24 Stockholm
Phone +46 8 459 84 00

ISSN 1404-0344
SKB TR-12-01
ID 1256551

KBS-3H Complementary studies, 2008–2010

Svensk Kärnbränslehantering AB

October 2012

This report is a result of a joint project between SKB and Posiva. This report will also be printed as a Posiva report, Posiva 2013-03.

Abstract

KBS-3H is a joint project between Svensk Kärnbränslehantering AB (SKB) in Sweden and Posiva Oy in Finland. The main goal during the project phase Complementary studies of horizontal emplacement KBS-3H 2008–2010 was to develop KBS-3H to such a state that a decision to go ahead with full-scale testing and demonstration could be made.

The KBS-3H design is a variant of the KBS-3 method and an alternative to the KBS-3V design. In KBS-3H multiple canisters containing spent nuclear fuel are emplaced in parallel, 100–300 m long, horizontal deposition drifts at a depth of about 400–500 m in the bedrock whereas the KBS-3V design calls for vertical emplacement of the canisters in individual deposition holes.

Further development and evaluation of the main KBS-3H design alternatives developed in earlier work, DAWE (Drainage, Artificial Watering and air Evacuation) and STC (Semi Tight Compartments) (Autio el al. 2007) has now enabled a well-founded KBS-3H reference design selection, DAWE has been selected.

Regarding long-term safety; bentonite-metal interactions have been in focus and studies have given a good basis for material selection for the Supercontainer, plugs and other supporting structures and titanium is selected. The selections and evaluations made during this project phase will be used in the safety evaluations planned for Forsmark and Olkiluoto in the upcoming project phase.

KBS-3H specific production lines have been outlined and layout adaptations for both Forsmark and Olkiluoto have been developed. Full-scale tests of system components have also been carried out with good results; the full-scale compartment plug test shows the ability to install a plug that separates drift compartments hydraulically.

Sammanfattning

KBS-3H är ett projekt som drivs gemensamt av Svensk Kärnbränslehantering AB (SKB) i Sverige och Posiva Oy i Finland. Huvudmålet under projektfasen ”Complementary studies of horisontal emplacement KBS-3H 2008–2010” var att utveckla KBS-3H till en sådan nivå att ett beslut om att gå vidare med fullskaliga tester och demonstrationer kunde göras.

KBS-3H är en variant av KBS-3 metoden och ett alternativ till KBS-3V. I KBS-3H alternativet placeras ett flertal kapslar med använt kärnbränsle på ca 400–500 meters djup, i parallella 100–300 meter långa horisontala deponeringshål i berget, medan KBS-3V alternativet bygger på vertikal placering av kapslar i individuella deponeringshål.

Fortsatt utveckling och utvärdering av de huvudsakliga KBS-3H alternativen vilka utvecklats i tidigare projektfaser, DAWE (Drainage, Artificial Watering and air Evacuation) och STC (Semi Tight Compartments) (Autio el al. 2007) har nu möjliggjort ett välgrundat val av en KBS-3H referensdesign, DAWE har valts.

Rörande långsiktig säkerhet har fokus legat på bentonit–metall interaktion och studier har gett en bra grund för materialval i stödkonstruktioner såsom Supercontainer, pluggar och rör, titan har valts. De val och utvärderingar som gjorts under denna projektfas kommer att användas i de säkerhetsanalyser som planeras för Forsmark och Olkiluoto i nästa projektfas.

En struktur för KBS-3H specifika produktionslinjerapporter har utvecklats och layouter för ett KBS-3H förvar har tagits fram för både Forsmark och Olkiluoto. Goda resultat har uppnåtts i tester av ett antal systemkomponenter. Fullskaletester med en compartment plug visar förmågan att installera täta pluggar som hydrauliskt avgränsar deponeringshålssektioner.

Executive summary

KBS-3H is a variant of the KBS-3 method and an alternative to the KBS-3V reference design. KBS-3H is based on horizontal emplacement of several canisters in long drifts whereas KBS-3V calls for vertical emplacement of the canister in individual depositions holes within a deposition tunnel see Figure ES-1. Horizontal emplacement has been studied in parallel with the development of the KBS-3V reference design since the late 90's.

The *Complementary studies of horizontal emplacement KBS-3H 2008–2010* which is described in this report is the fourth phase and follows the Prestudy, Basic Design and Demonstration phases of the KBS-3H project. The aim of the recent phase was to reduce the knowledge gap between KBS-3V and KBS-3H to raise the knowledge of horizontal emplacement to a level where it provides a basis for a decision to go ahead with a new project phase including safety evaluations and full-scale sub-system tests could be made. The recent phase is hence closely coupled with the upcoming KBS-3H System Design phase and the purpose of these two phases is to facilitate a detailed comparison and a possible future change of reference design from KBS-3V to KBS-3H.

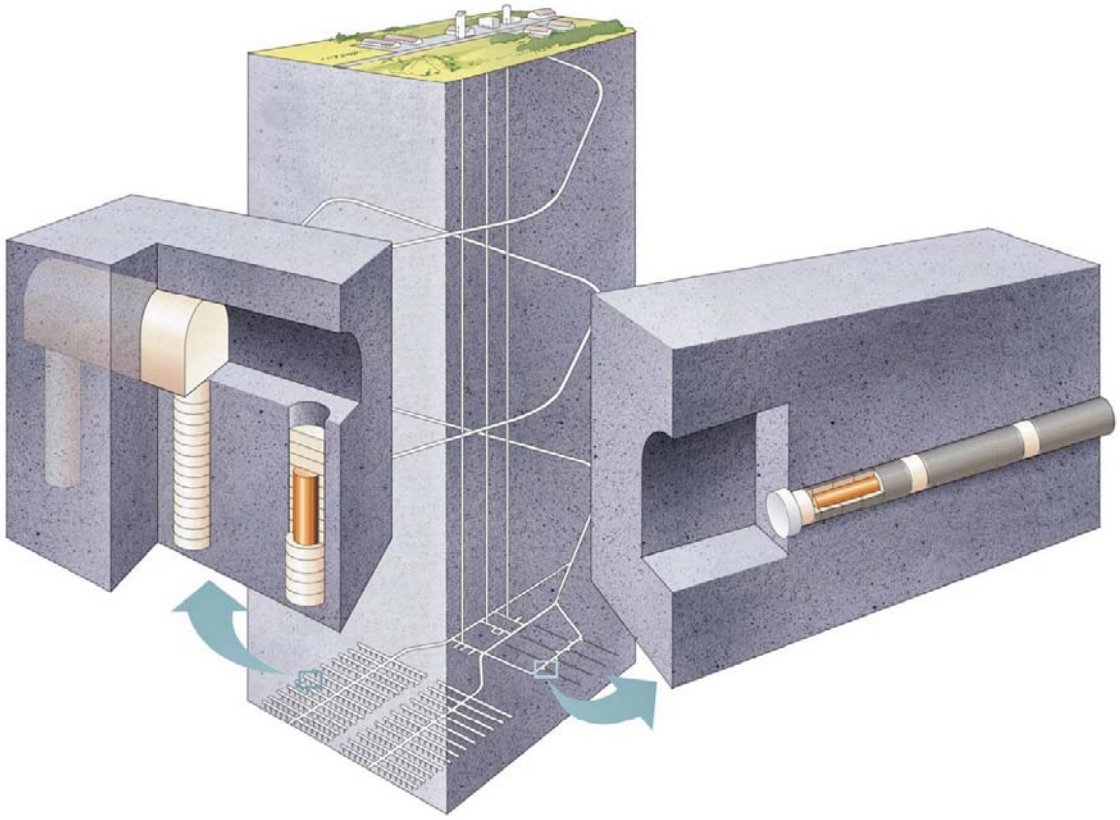

Figure ES-1. *Schematic drawing of the KBS-3V reference design (to the left) and KBS-3H (to the right).*

Progress made during the Complementary studies of horizontal emplacement KBS-3H 2008–2010

Figure ES-2 is an overview of the KBS-3H Project 2008–2010 with the design options that were studied. The text in green indicates the main alternatives for future studies.

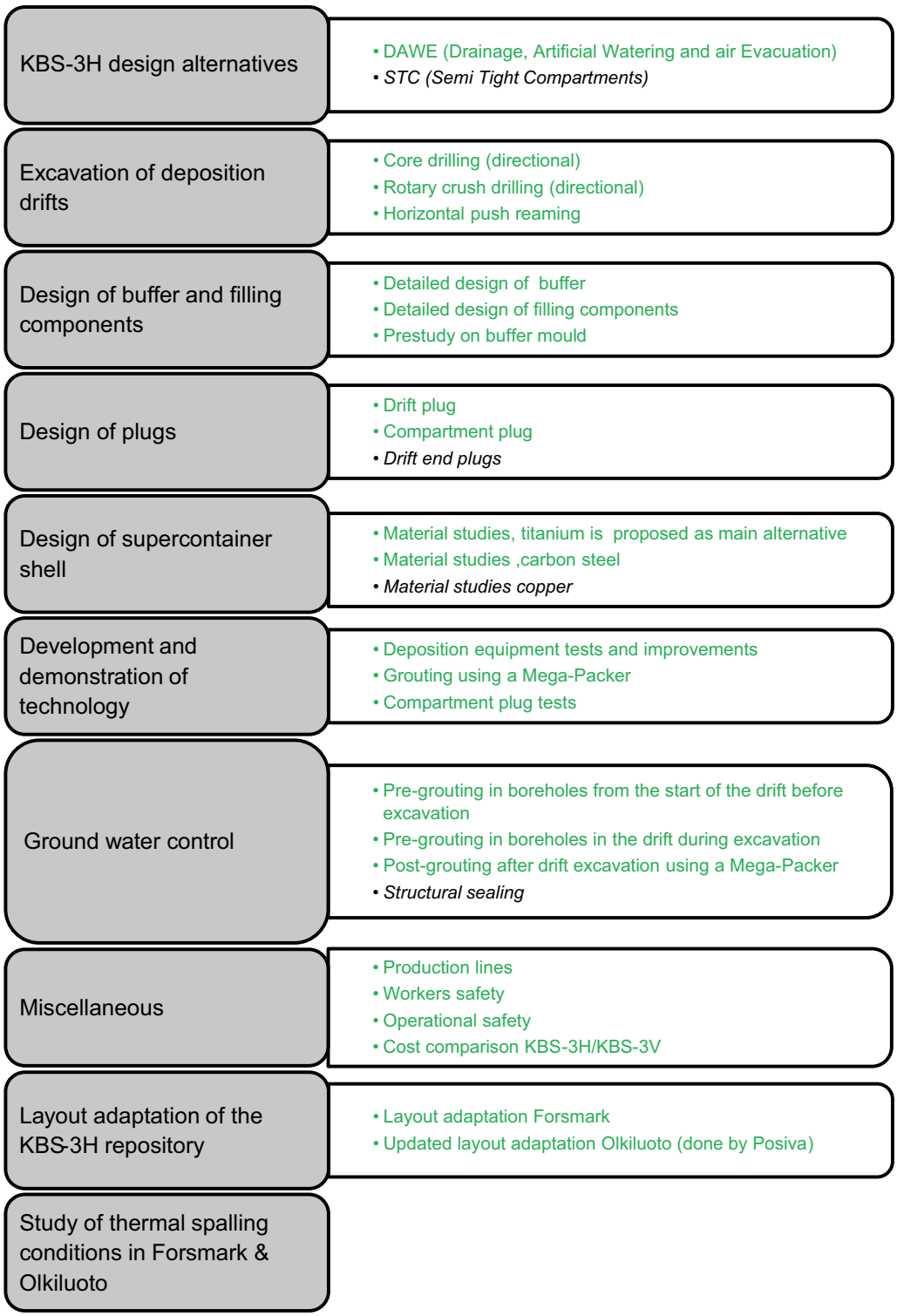

Figure ES-2. *Overview of the KBS-3H project 2008–2010 and design options that were studied. The texts in green font indicate main design alternatives and issues for future studies. The text in black indicates alternatives that were discarded.*

One of the priority targets of this project phase was the establishment of a robust drift design, i.e. a design that yields a well-defined and consistent initial state and subsequently ensures long-term safety. To achieve this several uncertainties related to design and buffer that were identified during earlier project phases had to be handled. These can be divided into four large areas:

- Drift components.
- Thermal spalling of rock.
- Buffer issues.
- Wetting technique.

Drift components

Several KBS-3H key components have been brought to the conceptual design level of maturity during this project phase. Conceptual design of the filling components has also lead to an updated drift design as presented in Figure ES-3.

The new drift design is a considerable simplification of the system with an improved degree of utilization. The filling components have been designed with the same material as the buffer and will hence behave in a similar manner. Studies and scoping calculations have given tentative estimates for the respect distance needed between Superontainer sections and water-conductive fractures with specific inflows ranging from 0.1–0.5 l/min, 0.5–1 l/min and > 1 l/min. Based on these tentative estimates it has been suggested that filling blocks can be placed in sections with higher inflows which would eliminate the need for the previously used double compartment plug sections. It should be noted that where the initial inflow is higher than a certain limit, tentatively > 1 litre per minute in a 10 m drift section, two compartment plugs with a permeable filling material between (currently not designed) may be installed rather than filling blocks to isolate the fractures responsible for this inflow. This is because of concerns regarding the early mechanical erosion, and longer term chemical erosion, of bentonite in such drift sections. The chemical erosion remains an unresolved feature, this issue has high priority and will be re-evaluated in the upcoming project phase, this time using the latest results presented in SR-site (SKB 2011).

The new drift design still requires one compartment plug for operational reasons since the drift needs to be sectioned in two approximately 150 m long sections to enable water filling and de-airing.

The buffer components inside the Supercontainer and the distance blocks which are placed between Supercontainers have also been brought to conceptual design during this project phase.

A new feature is the drift plug which replaces the combined compartment and concrete drift end plug which was the previous solution. The drift plug is basically a stronger compartment plug made of titanium that can withstand both full hydrostatic pressure and buffer swelling pressure during the repository operational period. This design further increase drift utilization and reduces the time for drift installation considerably since no concrete plug casting is required after finalizing the deposition process.

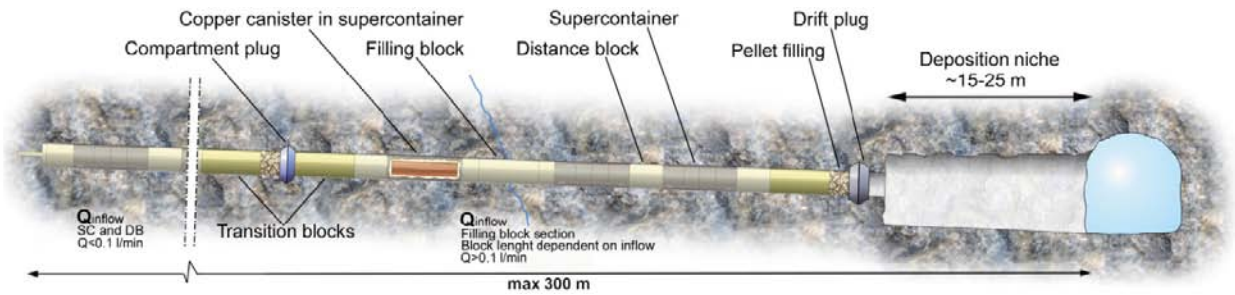

Figure ES-3. *Updated KBS-3H drift design. Updated features are the recently designed filling blocks for different inflow cases, the drift plug and the possible removal of double compartment plugs to separate fractures of higher inflow from the rest of the drift, tentative calculations indicate that these inflows can be handled with filling blocks.*

Thermal spalling of rock

Rock spalling occurs when rock stress around an excavation exceeds the rock strength. There is a spectrum of such spalling, ranging from slight to more severe fracturing. Rock spalling can increase/occur due to the increased stress state induced by thermal stresses. Thermal spalling of rock can lead to new flow paths between Supercontainer sections that are unfavourable from a safety point of view and should therefore be avoided.

Thermal spalling of rock has been evaluated for Forsmark. The repository is planned to be located at a depth of 470 m and in two rock domains of different rock strength. The rock is relatively weaker in the rock domain RFM029 that has a lower uniaxial compressive strength than in the rock domain RFM045 where the rest of the drifts are located. The angle between the deposition drifts and the maximum horizontal *in situ* stress was less than 22°. The thermal field stresses were estimated based on the vertical design results (Lönnqvist et al. 2010). The results indicate that for the most likely *in situ* stress conditions the excavation of the deposition drifts will not induce spalling of rock. However, minor to moderate spalling of rock will be encountered in the deposition drifts located in weaker rock domain when the thermal stresses reach a maximum (about 50 years after deposition). In the stronger rock domain no spalling of rock is predicted. For the unlikely maximum *in situ* stress conditions the excavation of the deposition drifts will induce minor spalling of rock in weaker rock domain. There is also a very minor risk for thermally-induced spalling of rock in stronger domain.

Based on the results of thermal stress evolution presented by Lönnqvist et al. (2010) the modelled rock spalling initiation would take roughly from 1 to 10 years depending on the parameter values used in thermal calculations in case of most likely *in situ* stress conditions. In the event of the unlikely maximum *in situ* stress, rock spalling can initiate right after the drift excavation and any heating will increase the severity of rock spalling.

Noteworthy is that the results above assume that there is no confinement pressure caused by the bentonite material, which could mitigate the rock spalling. The swelling pressure in dry drift sections have been studied extensively in the recent project phase and thermally induced spalling of rock can most likely be mitigated/avoided if there is sufficient buffer swelling pressure working against the rock surface. Buffer swelling pressure is in turn dependent on the availability of water and the issue has hence been studied for the worst case with a totally dry drift. Although the drift is dry the artificial watering used in the DAWE design guarantees that a certain amount of water is accessible for initial buffer swelling. The conclusions from the studies are that despite no access to additional water there will be a significant mechanical pressure (50–500 kPa) acting on the rock surface which would indicate that the issue of thermally induced spalling of rock could be avoided for the DAWE design.

Buffer issues

Extensive work has been put into several buffer issues to increase the understanding of buffer behaviour with the final objective of solving them entirely. It should be stated that not all issues have been solved but the ones that have not been solved have been further constrained during this project phase. There are separate buffer issues that apply to both DAWE and STC and some that apply only to DAWE or only to STC. Since DAWE was eventually selected as the KBS-3H reference design those issues are summarized below, while STC-specific issues are presented in the chapter on buffer issues.

From a long-term safety perspective, the buffer needs to maintain a certain minimum and maximum density in order to function properly. The risk of erosion by artificial wetting in the DAWE-design was identified in previous work. The problem has been studied during the recent project phase and the conclusion is that artificial wetting can be carried out without causing critical erosion. It has also been indicated that it would be preferable to use fresh water in the artificial wetting since there are several advantages with this e.g. the erosion rate would be lower and the internal redistribution of material would be smaller compared to the case when salt water is used.

The extent of homogenization of the bentonite after erosion in KBS-3H is of crucial importance for the long-term safety since the buffer must not lose so much density that advective condition will prevail around the canister. An attempt to model this issue has faced difficulties due to the complexity of the problem; this will be a prioritised research subject for SKB and Posiva in the coming years. However, the effect of erosion before water saturation is not expected to be a problem for DAWE since the bentonite loss is not critical and is very local, as concluded in the study presented above.

Buffer swelling and sealing in heterogeneous inflow conditions (e.g. internal piping) was considered an uncertainty that required additional evaluation (Autio et al. 2008). Internal piping refers to channelled flow inside a closed compartment, but not extending out of the system and therefore the total flow volume is limited. This issue has not been solved, there are, however, indications that the possible axial displacement of buffer is insignificant and internal piping may have a favourable impact on the saturation of the buffer. However, it must be concluded that the process of internal piping especially in context of desiccating buffer is not fully understood and there is a clear need to develop the understanding with respect to buffer desiccation, saturation times, swelling pressures, water transport and physical effects etc. The issue as a whole is, however, not deemed critical for the fulfilment of the requirements for KBS-3H.

A possible scenario within the drift that has been identified in earlier work is that buffer blocks can crack and material can fall down onto the drift floor where it may be moved away by the water flowing down the drift. This erosion will contribute to a loss of material or its redistribution within a deposition drift. Suggested new sentence (page 9): The ring shaped buffer blocks inside the Supercontainer would be at highest risk since they are especially sensitive to high relative humidity due low initial water content, about 11%. Studies show that there will be buffer cracking and subsequent flaking but at such a slow rate that it will not lead to any local density variations outside the allowed range. The distance blocks will be manufactured with an initial water content of 20–22% and are hence more robust.

Wetting technique

Up to 150 m long pipes were previously needed in the DAWE design, with several wetting pipes and one air evacuation pipe. The removal of these before the buffer swells and locks them against the rock wall was early identified as a potential weakness in the DAWE design. Although studies indicate that it would be possible to remove them all by working fast after wetting it would be preferred to exclude as many pipes as possible. A new wetting technique with shorter pipes was therefore developed and found feasible. This would leave just one long pipe, the air evacuation pipe, which would speed the pipe removal process up considerably. The conclusion from the studies that have been carried out is that both the short wetting pipes as well as the long air evacuation pipe can be removed easily within the first day after wetting.

KBS-3H reference design

Work on drift components and buffer issues together with safety-related studies carried out in this and earlier project phases produced the basis for selecting a main design alternative; two designs remained, DAWE and STC. DAWE was selected as the reference design in the recent project phase.

Long-term safety is the critical aspect in selecting a reference design. The selected design must fulfil not only all long-term safety and functional requirements, but also design requirements and operational requirements. When comparing the two designs, their respective ability to fulfil these requirements has been evaluated; for example their respective ability to achieve the initial state, how they manage the inflow conditions expected at Forsmark and Olkiluoto with respect to piping and erosion and how well they can mitigate thermally induced rock spalling.

The DAWE-design allows all inflowing water to flow along the drift floor out of the drift during installation while the STC-design collects all water in each Supercontainer section and does not allow the water to leave the section until the empty slots are filled with water. Natural groundwater inflow hence slowly fills the deposition drift in the STC-design while artificial wetting is used to fill the open slots of the drift in the DAWE-design after installation of the plug. This is the main difference between the two designs and the initial state of DAWE will thus be far better defined.

The period before the buffer swells and provides a swelling pressure at the buffer-rock interface will, for the reason presented above, be considerably longer in the case of STC. This delay will increase the risk of thermally induced spalling of rock which in turn could lead to connected pathways for flow and mass transport along the drifts. This is a critical factor working against the STC-design. DAWE in contrast has proven to develop a significant mechanical counter pressure against the “rock” in several laboratory tests. These tests were run with no additional access to water after the initial water filling, simulating a dry section, the worst case from a buffer swelling point of view. DAWE is hence evaluated to handle the risk of thermally induced spalling of rock considerably better than STC and could probably avoid the problem entirely.

Bentonite piping and erosion is another critical issue to consider when selecting a reference design since large variations in buffer densities are not allowed for long-term safety reasons. In both DAWE and STC water inflows into the drift will cause some mass loss of buffer by erosion, since bentonite particles will be entrained in the flow, transported as suspended solids and eventually settle down. Swelling and sealing in heterogeneous inflow conditions along the long deposition hole and erosion rates at expected inflows has, as presented above, been studied as part of the KBS-3H design development but remains subject to significant uncertainties. This is one of the most significant uncertainties remaining in the STC-design which is avoided to a large extent in the DAWE-design. For DAWE the overall conclusion is that piping and erosion is not a problem when using artificial water filling, given that fresh water can be used. The erosion at groundwater inflow positions is not a problem either since the artificial water filling initially creates a large water-filled volume and in that way controls the erosion points.

Erosion of dropped bentonite particles arising from buffer cracking is another issue that has been considered that could pose a problem. The decisive difference between the two designs is that in STC, especially in dry drifts, the buffer will stay exposed to high humidity (RH) for longer time than in DAWE, where early wetting will lead to early swelling of the buffer against the drift wall. The estimates made for DAWE indicate that the amount of buffer lost in this way will be low.

Pipe removal is a potential problem in DAWE since remaining pipes could lead to flow pathways along the drift. The solution with shorter pipes for wetting and just one long pipe for de-airing minimises this problem and the requirements should still be fulfilled. The air pockets left in STC are a considerable disadvantage for this design that could compromise the long-term safety requirements.

One of the bases for the safety assessment is from which point in time to start the calculations, it is vital that the initial state of the engineered barriers is well defined at that time. This point in time may differ for different parts of the system and there is no obvious definition for the system as a whole. Deposition and building of the drift plug may be the natural starting point for the engineered barrier system, and in DAWE the subsequent artificial water filling ends the man-made actions. With this definition, at least for a comparison point of view, it is clear that DAWE presents a better defined initial state than STC which fully relies on natural inflows for both initial and long-term buffer saturation. For DAWE initial swelling of the buffer is guaranteed by the artificial watering, the buffer and canisters are locked in place and axial displacement and significant buffer erosion can be avoided. Altogether DAWE is a more robust design and the risk of problems resulting in an initial state outside the design requirements should be very low.

Material aspects are basically the same for both designs although STC has the addition of sealing rings but from a long-term safety perspective both designs should be able to fulfil the requirements.

Given all this a well founded decision on selecting DAWE as the KBS-3H reference design can be made, the main advantages of DAWE are summarized in the list below:

- The design has a well defined initial state.
- It can possibly reduce the risk of thermally induced spalling of rock.
- Early swelling of the buffer ensures that axial displacement of the system components can be avoided.
- It reduced groundwater inflow to the drift which minimised the risk of erosion.

The current KBS-3H design is presented in Figure ES-3.

Material selection

Selection of material for the design of the Supercontainer shell, compartment plug and other supporting structures was the other critical technical decision taken in this project phase, the KBS-3H reference design DAWE being the first. Prior to this decision bentonite interaction with iron, copper and titanium was studied by collecting available reported relevant information, as well as by experimental and modelling studies. Titanium is expected to be the most inert, having lowest corrosion rate and lowest rate of production of hydrogen. In addition, this element is already present in various amounts in natural bentonites which have been shown to display favourable properties as buffer

materials. Titanium has been selected. A steel based Supercontainer is not excluded entirely and if additional research verifies that its implications on long-term safety are within the requirements the selection should be re-evaluated.

KBS-3H description

One essential part of the project phase was to update the compiled KBS-3H description.

A structure for KBS-3H specific production lines have been developed. The Production line reports will provide information on the design; how to produce, handle and inspect the engineered barriers and underground openings as well as the initial state within the facilities of the KBS-3H system. The main work with the production lines will be carried out in the upcoming project phase.

Drilling techniques, geometrical requirements and measurement techniques have been re-evaluated and recommendations made for the upcoming project phase. The demanding requirement on waviness means that real time guided drilling probably can't be used and the drilling system should preferably be stiff.

The programme for hydraulic characterization has also been revisited, as have characterization methodology and grouting techniques. A model for predicting the conditions in the fully reamed drift from measurements taken in a core hole has also been proposed. It is under evaluation and its practical application will have to be evaluated in coming work together with KBS-3Vs DETUM (*Vidareutveckling av metoder, verktyg och detaljerat program för undersökningar och modellering inför byggstart*) and OMTF (Olkiluoto Modelling Task Force) when the KBS-3H investigation programme is developed in coming years.

KBS-3H operational and personnel safety analyses have been carried out according to the "what if" methodology. The analysis focused on three main areas; the preparation of a drift, the reloading station and the deposition area with deposition work. In addition to this analysis, a list of initiating events (risks) defined for the assessment of KBS-3V was checked to verify that no additional events had to be considered. Several risks have been identified and corresponding risk-reducing measures proposed.

Layout adaptations have been developed for both Forsmark and Olkiluoto. The KBS-3V layout has been used as a basis and no KBS-3H specific adaptations have been carried out. There are hence still optimizations with respect to utilization, rock strength and fracture orientations to be made.

Full-scale demonstrations

The previous project phase 2004–2007 focused on demonstrating the KBS-3H technology. Some of the tests that were initiated then have continued throughout the current project phase. The deposition machine has been run for 50 km both with a Supercontainer and distance blocks made of concrete as well as without any load. The tests have proven that the technique works and development has continued to ensure long-term functionality of the equipment. The Mega-Packer tests have also been finalized with very good results giving KBS-3H a solution if post-grouting would be required.

A full-scale demonstration of the compartment plug has also been carried out at the Äspö HRL. The test indicates that the concept of compartment plugs is feasible and preliminary results from tests including bentonite pellets indicate that the pellets seal the section behind the plug very efficiently in just a couple of weeks.

Evaluation by the authorities

The Finnish Radiation and Nuclear Safety Authority (STUK), have carried out a review of the KBS-3H Safety Case reporting, in which they have raised several critical issues regarding KBS-3H long-term safety, including piping and erosion, bentonite material interactions, thermally induced spalling of rock etc. The Swedish Radiation Safety Authority (SSM) has also done an evaluation of the joint research, development and demonstration (RD&D) programme carried out by SKB and Posiva in 2002–2007. SSM requested its external expert group BRITE (the Barrier Review, Integration, Tracking and Evaluation) to evaluate the reporting (SSM 2009). They also presented a comprehensive list of key issues for KBS-3H.

SKB's and Posiva's planning for the KBS-3H project is well in line with the comments by the authorities and the issues brought up have been addressed in the recent project phase or are being considered in upcoming work. Some issues are shared with KBS-3V and will hence be addressed together. Several of the issues require full-scale tests to confirm feasibility and confidence in the KBS-3H design. The BRITE group comments: "*bounding analyses are unlikely to be suitable for resolving outstanding construction, operations and emplacement issues*; *only eventual full-scale, reproducible demonstration under in situ conditions can fulfil the necessary requirements for confidence in the KBS-3H design*". This is in line with the current planning where focus is put on increased integration of the components in full-scale sub-system tests.

Conclusions

One of the main objectives of the recent project phase was the selection of a KBS-3H reference design. This milestone was reached when DAWE was selected; and this decision has defined a clear way forward for the KBS-3H project. The DAWE design will be used as a basis for further technical development, planning, safety analysis, radiation protection and work on environmental influence. Selection of a reference design required evidence on the long-term performance of the buffer including interaction with other materials. Bases for material selections have been established and titanium is selected for the Supercontainer, compartment plugs and other supporting structures. The buffer and filling components have all been brought to a conceptual level of design and although not all buffer issues are solved they have been constrained further during the recent project phase.

A structure for the KBS-3H specific production lines have been developed. The full production line reports will be written in the upcoming project phase and will provide information on how to produce, handle and inspect the engineered barriers and underground openings within the facilities of the KBS-3H system.

The overall goal of the KBS-3H project 2008–2010 was to develop the KBS-3H solution to such a state that a decision to go ahead with full-scale testing and demonstration could be made. No "show-stoppers" have been identified and a good base for continuation has been established. A new project phase has also been approved by SKB and Posiva boards with the final goal of enabling a detailed comparison and a possible change of reference design from KBS-3V to KBS-3H. It will include safety evaluations for Forsmark and Olkiluoto, an update of the KBS-3H description and performance of full-scale sub-system tests.

Contents

1 Introduction

Both Sweden and Finland have been using electricity from nuclear power for over 30 years. SKB (www.skb.se) in Sweden and Posiva (www.posiva.fi) in Finland are responsible for developing a solution for waste disposal that does not require monitoring or inspection after sealing, and also is sustainably safe. This requires that the waste is isolated for at least 100,000 years, according to present Posiva VAHA requirements for several hundreds of thousands of years (VAHA is Posiva's requirements management system, for further detailes see Appendix D).

Research and development have been conducted for a period of three decades and a method for safely handling and storing the spent nuclear fuel for long periods of time has been developed. Both SKB and Posiva have selected a deep geological disposal approach with multiple barriers as the reference design, the KBS-3 method, see Figure 1-1. The principle of the KBS-3 method is that the spent nuclear fuel is held in place by a cast-iron insert encapsulated in a copper canister. The canister is placed in a repository constructed in a crystalline host bedrock about 400–500 metres below the surface. The canister is surrounded by highly compacted bentonite clay and the tunnel system is backfilled with bentonite clay.

Safety will always be the number one criterion when disposing of spent nuclear fuel and the repository must comply with all international guidelines and standards, national regulations and the general design requirements for the facility. Long-term safety has hence set the framework when developing the engineering solutions, including underground opening and construction, buffer and backfilling, canister and plug designs.

The engineering solutions have been developed in parallel with site investigations and locations for the final repositories have been chosen in both Sweden and Finland. SKB carried out site investigations at Forsmark in Östhammar and at Laxemar in Oskarshamn. Forsmark was concluded to be the best location and was selected in 2009. SKB submitted an application for a permit to build a final repository for Sweden's spent nuclear fuel at Forsmark, in Östhammar municipality in March 2011. The site chosen for the Nuclear Fuel Repository is close to the Forsmark Nuclear Power Plant. A general description of the overall programme to implement the repository in Sweden is to be found in the latest Research, Development and Demonstration Programme (SKB 2010b).

Posiva applied for the first Decision in Principle (DiP) for a spent fuel disposal at Olkiluoto based on the KBS-3 method in spring 1999. The Government issued the DiP in December 2000 and Parliament endorsed it in May 2001. Since then two more DiP have been issued, one for the disposal of the spent fuel of Olkiluoto 3 (2002) and the newest one for the disposal of the spent fuel of Olkiluoto 4 (2010).

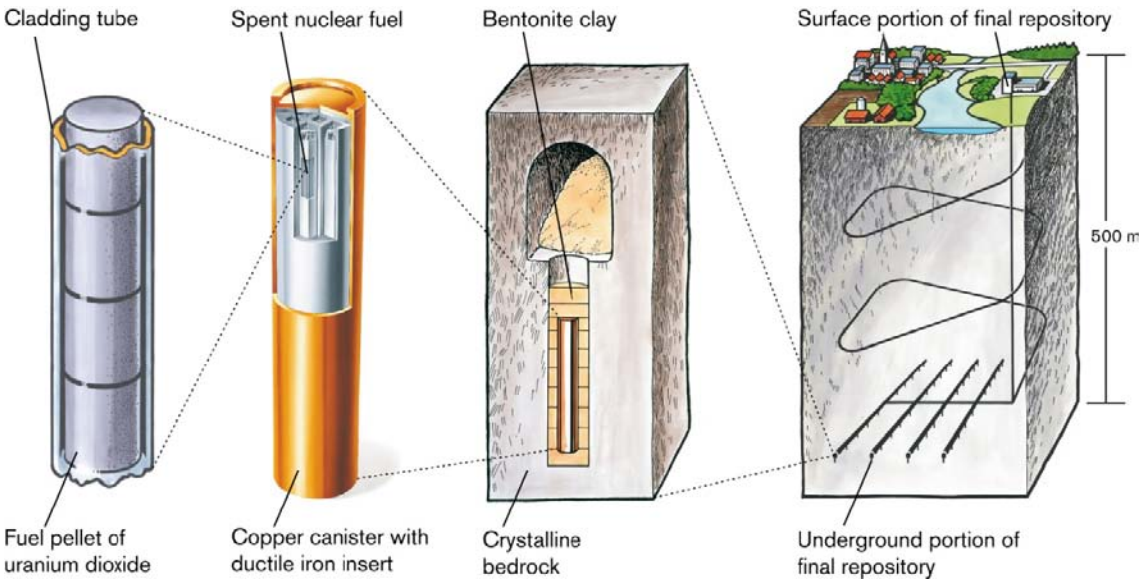

Figure 1-1. *The barriers of the KBS-3 method. The figure illustrates the KBS-3V reference design.*

In June 2004, Posiva started construction of the Olkiluoto Underground Rock Characterisation Facility, ONKALO, for site-specific underground investigations. ONKALO may also be used as part of the future repository. On the basis of site confirming investigations both from the surface and in ONKALO and the monitoring programme as well as other research, technical design and development work, Posiva will plan the repository in detail, prepare construction engineering solutions and assess safety. According to the decision of the Ministry of Trade and Industry on 23 October 2003, Posiva is to submit an application for the construction licence for the encapsulation plant and the KBS-3 disposal facility by the end of 2012. In 2009, Posiva submitted the first outline version of the Construction license application and other licensing documents, among which was the first outline version of the Preliminary Safety Analysis Report (PSAR) in support of the demonstration of the preparedness for the construction license application. The necessary licensing documents including the PSAR will be gradually updated in 2010–2012 to become the actual licensing application. A Final Safety Analysis Report (FSAR) and a final Safety Case will be submitted at the time of the operational license application in 2018. The target is to begin disposal operations in 2020.

Both SKB and Posiva are applying for the KBS-3 method. The vertical emplacement design, KBS-3V, is the reference design and has been so for the last 30 (SKB) and 20 (Posiva) years. The vertical reference design has been developed in parallel by both organisations for the last 20 years and there has been cooperation on several parts of the programme. Evaluations have also been made of alternative designs within the KBS-3 method (Sandstedt et al. 2001). One alternative was long horizontal drifts with serially emplaced canisters instead of the vertical emplacement of single canisters in a deposition hole. The design with horizontal emplacement was later referred to as KBS-3H. Figure 1-2, illustrates a schematic drawing of the KBS-3V and the KBS-3H repositories.

KBS-3H has been studied since the late 90's as a joint SKB/Posiva undertaking and is part of the national programmes for the geological disposal of spent nuclear fuel in Sweden and Finland. The investigation of horizontal emplacement has so far been carried out in three phases. It has been supported throughout by the authorities, SSM in Sweden, and STUK in Finland who sees potential benefits in evaluating alternatives to the KBS-3V reference design. During the recent project phase (covered in this report) SSM required its external expert group BRITE (the Barrier Review, Integration, Tracking and Evaluation) to evaluate the reporting (SSM 2009). The sentence on page 18 "STUK, also carried out a review of the KBS-3H Safety Case reporting (STUK 2009)." I would change by removing just the reference because the information that STUK has also carried out the review is valuable in my understanding. Another option would be to add "The review is available upon request from STUK.

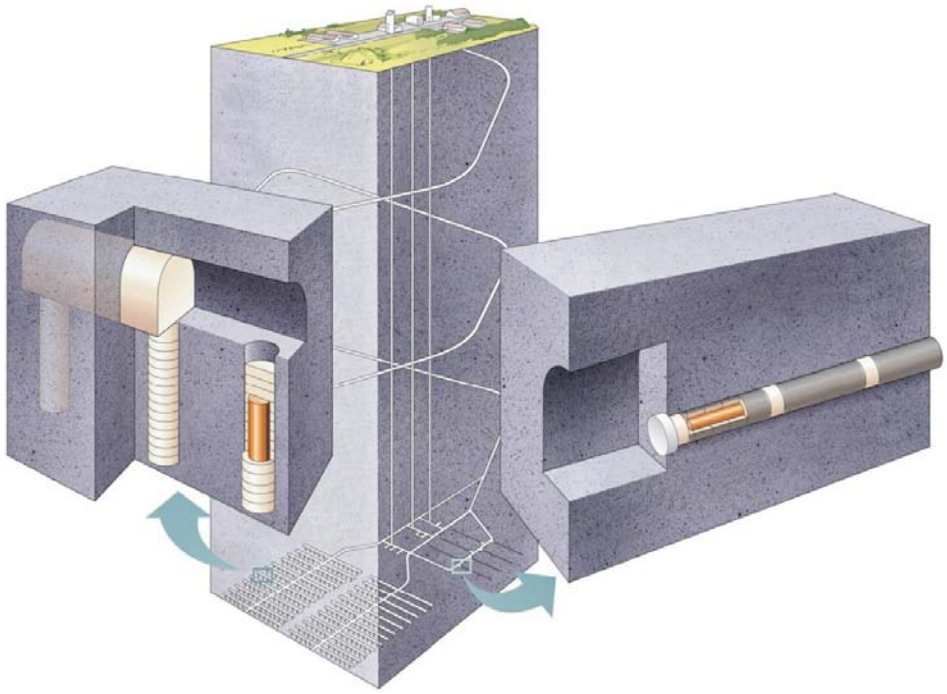

Figure 1-2. *Schematic drawing of the KBS-3V and KBS-3H repositories.*

1.1 Purpose and scope of this report

The purpose of this report is to describe and document the results of the latest project phase; *Complementary studies of horizontal emplacement KBS-3H 2008–2010*. To provide background for readers new to the project a short compilation detailing the history is also included. Additionally the report will serve as a basis for future plans. The recent project phase is closely connected the forthcoming project phase including safety evaluations, a full KBS-3H description update and performance of full-scale sub-system tests. Together these two phases aim at producing a KBS-3H basis for a decision on a possible future change of reference design from KBS-3V to KBS-3H.

The main goal during 2008–2010 was to develop KBS-3H to such a state that a decision to go ahead with full-scale testing and demonstration could be made.

Two designs, the DAWE design, see Section 4.3, and STC, see Section 4.1.2, have been studied; however, focus was early put on DAWE which was also chosen as the KBS-3H reference design at the end of the project phase, see Chapter 6. Critical in choosing a reference design were to understand the processes involved and the early evolution of the buffer. This required extensive work on several buffer and design issues as well as studies on combined issues such as buffer design wetting techniques, buffer material interaction and buffer-rock mechanical (thermal spalling of rock) issues, see Chapter 5.

When it comes to long-term safety the recent project phase has focused on material studies to enable a material selection for the system components, see Chapter 7; the Supercontainer (packages with both canister and buffer inside a metal shell, Section 4.4), plugs (Section 4.7 and 4.8) and other supporting structures. A safety evaluation including these material studies and other recent results was not included in the project phase; this was a prerequisite when the project was set-up. These safety evaluations will be carried out for both Forsmark and Olkiluoto in the upcoming project phase.

The KBS-3H design description has been updated including repository layout adaptations for Forsmark and Olkiluoto, see Chapter 8, work on Operational/Workers safety (Section 9.6 and 9.7) and recommendations for drilling (Section 9.2) and grouting techniques (Section 9.3). The KBS-3H specific production lines have also been outlined (Section 9.1) and will be written in the upcoming project phase. Full-scale tests including the finalisation of the Mega-Packer tests (post-grouting, see Section 4.9) and tests of the compartment plug have been successfully carried out at the –220 level at the Äspö HRL (Section 4.7).

In addition to the achievements presented above, a preliminary outlining for the upcoming project phase is presented in Chapter 10.

This report is to a large extent based on internal documents written for the KBS-3H project and it is hence somewhat detailed in places in order to provide sufficient background information. It should also be stated that all data from all tests, etc, have not been possible to include in this report.

A KBS-3H glossary of technical terms is presented in Appendix D. The terminology differs occasionally between SKB and Posiva, but efforts have been made to harmonise the language in the report.

1.2 Objectives of the Complementary studies phase

The main objective of the project phase during 2008–2010 was to develop the KBS-3H solution to such a state that a decision to go ahead with full-scale testing and demonstration could be made. The issues identified during the demonstration phase during 2004–2007 were used when formulating the objectives for the new project phase. These required additional:

- Evidence on the behaviour of the buffer and other components after emplacement.
- Evidence on the long-term performance of the buffer including interaction with other materials.
- Evidence on construction, manufacturing and installation of the system.

The actual objectives were described, as much as possible, as practical targets and were compiled in seven different groups since the project covers many aspects. These objectives were related to:

1. **Technical solutions**
   a. Critical design issues shall be resolved.
   b. Main design alternative shall be selected and optimised.
2. **Acceptance**
   a. Critical issues regarding construction, manufacturing and installation shall be resolved.
   b. Critical issues affecting short- and long-term system performance shall be resolved.
3. **Licensing**
   a. Assessment of long-term safety for the design alternative shall be possible.
   b. The implementation of the design, construction, manufacturing and installation shall fulfil the requirements of operational safety.
4. **Programme planning**
   a. A plan shall be developed for full-scale tests of the system components under realistic conditions.
   b. A plan shall be developed for demonstration of sub-system tests under realistic conditions.
   c. Resources shall also be secured by performing joint studies with third parties.
5. **Environmental aspects and worker safety**
   a. In the selection of materials and in the construction the impact on the environment shall be minimised and handled.
   b. Methods for implementation and operation of the selected design alternative shall be planned for occupational safety.
6. **Quality aspects**
   a. Methods for construction and manufacturing shall be documented and suitable for licensing, practical use and implementation.
7. **Project operation and human resources**
   a. Project operational objectives.
      - Common issues with the KBS-3V solution shall be recognised and work coordinated to avoid duplicating similar work for KBS-3V.
      - Common issues of interest with other organisations shall be studied and coordinated jointly with the third parties.
   b. Human resource objectives.
      - resources for design, development and planned full-scale tests and demonstration shall be secured by engaging additional experts and training new personnel or engaging third parties

The main objective of the project was to fulfil the technical (1a–b) and acceptance objectives (2a–b) to enable maturity for a decision regarding a full-scale sub-system test phase. The main bulk of the project work comprised the efforts to develop a design, which fulfils the requirements in terms of long-term safety. Solving the issues of the main objectives and selecting a KBS-3H reference design enabled work with the objectives set for licensing and programme planning. The objectives set forth for environment, quality and project management include challenges to coordinate the project work, for example, with the work similar to KBS-3V elsewhere. Results from the work that has been carried out is summarised in this public report.

1.3 Restrictions and assumptions

The project should focus its work on solving issues specific to KBS-3H. Common issues with the reference design KBS-3V should be recognised and coordinated.

The project is based on using information from Olkiluoto and Forsmark as the reference sites. The design data (e.g. canisters, drift spacing etc.) are based on Posiva's and SKB's reference data for KBS-3V unless separately specified for KBS-3H in the project.

It was set as a prerequisite that the project phase should not contain a safety evaluation; this will instead be part of the upcoming project phase.

2 Development of the KBS-3H alternative for geological disposal

This chapter gives a description of the previous KBS-3H related projects and describes the main reasons for developing an alternative KBS-3 method.

2.1 Alternative methods and KBS-3 designs

Development of systems for disposal of long-lived radioactive waste from nuclear power plants was initiated in Sweden in the mid 1970s. The work resulted in the KBS-3 method which was approved by the Swedish government in 1984. Since then the KBS-3 method has constituted the reference method in the Swedish programme, and later also in the Finnish Programme.

In 1987–1989 the WP-Cave method was evaluated and compared to the KBS-3 method (SKB 1989). The conclusion was that it entailed greater uncertainty with regards to the possibility of achieving acceptable safety and would require greater resources for research and development at the same time as the costs of building the repository would be higher, it was hence discontinued.

Several other disposal alternatives have since been developed and evaluated by SKB and Posiva to ensure that KBS-3 is the most suitable method. Concepts that have been studied are: Very Deep Boreholes (2–4 km below the ground surface), Very Long Holes (the deposition of relatively large canisters in 3–5 km long horizontal drifts) and Medium Long Holes (MLH). The results from these studies were summarised by the PASS project over the period 1990 to 1992 (SKB 1993). The conclusion was that KBS-3V and Medium Long Holes based on 200 m long horizontal deposition drifts, later called KBS-3H were judged more favourable than the other two studied alternatives.

In 1996 project JADE was initiated to study different KBS-3 designs. Horizontal KBS-3 with one canister per drift and vertical deposition with two canisters per deposition hole were rejected. In 2001 it was concluded by the JADE project that KBS-3V should be kept as the reference repository design and that the MLH alternative should be studied further with the aim of clarifying the technical feasibility of emplacement and the means of handling water inflow which is of special importance since water leaking in to one section will eventually flow over into the next in a horizontal drift.

The actual starting point of the KBS-3H development work was then SKB's RD&D-Programme in 2001 (SKB 2001b). One important conclusion that had been drawn in earlier work was that the canister and the buffer should be emplaced as an integrated waste package and not as separate components. Various emplacement techniques were studied and the conclusion reached was that a waste package – "Supercontainer" – should be developed.

Figure 2-1 summarises the alternative methods and designs evaluated in the PASS and JADE projects. The remaining alternatives after evaluation are shown in green text. The final part of the figure introduces the KBS-3H projects phases.

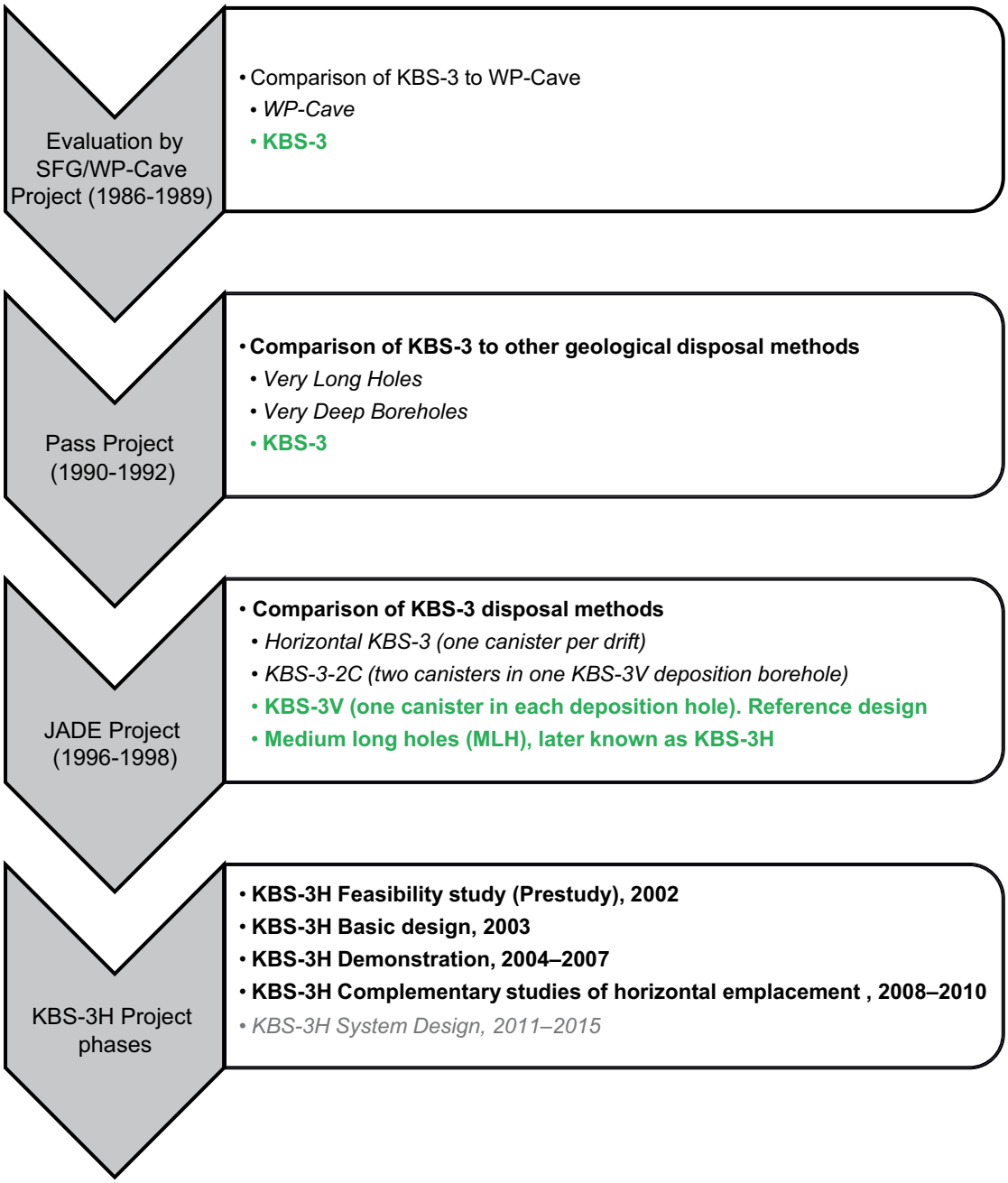

Figure 2-1. *The design selection process for geological disposal from 1990–1998 studied in the PASS and JADE projects. Green text indicates design alternatives that remain after the successive evaluations. The final part of the figure presents the KBS-3H project phases.*

2.2 Differences between KBS-3V and KBS-3H and main reasons for developing horizontal deposition

As described earlier, the KBS-3 reference design for both SKB and Posiva is based on vertical emplacement. It is important to stress that there are more similarities than differences between KBS-3V and KBS-3H; both have basically the same multi-barrier systems relying on the mechanically and chemically stable bedrock conditions, a long-lived manufactured canister, a buffer surrounding the canister to limit the inflow of corroding agents and water flow around the canister, and to retard the migration of nuclides in case the canister is damaged. Thus much of the information gained in the studies of the reference design KBS-3V is directly applicable to KBS-3H. Regulation and overall requirements are identical for KBS-3V and KBS-3H, but construction and deposition would be different for horizontal emplacement as well as some long-term safety issues that may be different or are different in the significance to, or potential impact of, an issue to each of the alternatives.

The main differences between KBS-3H and KBS-3V are listed and described below:

- Absence of deposition tunnels.
- Long horizontal deposition drifts instead of vertical deposition holes.
- Emplacement technique.
- Artificial wetting of the bentonite.
- Supercontainers and compartment plugs.

From an engineering point of view building a KBS-3H or a KBS-3V repository will be rather similar until the deposition drifts are constructed. The horizontal deposition holes of KBS-3H eliminate the need to excavate deposition tunnels and hence the need to backfill these tunnels after deposition. There is also a large difference in emplacement work. In the KBS-3H alternative several Supercontainers, see Section 4.4, consisting of both canister and buffer and weighing approximately 46 tonnes, need to be moved into a deposition drift of up to 300 m in length whereas in the KBS-3V the buffer is lowered into the vertical deposition holes in several steps before the canister, weighing some 25 tonnes is emplaced.

The deposition holes of KBS-3H imply increased sensitivity to groundwater inflow since water flowing into one canister position will eventually pass into the next. A key consideration in the KBS-3H design is hence to minimise the risk of rapidly developing hydraulic pressure differences, since these could result in mechanical displacement of the distance blocks, see Section 4.5, and Supercontainers as well as piping and erosion along the buffer – rock interface. The selected reference design, DAWE, see Section 4.3, eliminates these problems to a large extent since inflowing groundwater is drained during the emplacement work and the drift is then filled artificially allowing the buffer to initiate the accelerated swelling simultaneously in the entire drift.

The major advantage with KBS-3H is due to the smaller volume of excavated rock, approximately 60% of the KBS-3Vvolume, see Chapter 8. This is, as mentioned a consequence of the deposition tunnels being eliminated in the horizontal variant. Examples of potential positive effects of KBS-3H are:

- a more industrialised process during construction and disposal (drilling, Supercontainers, distance blocks and plugs),
- prefabricated disposal container (Supercontainer), which enables an easier quality assurance of the canister and adjacent buffer,
- reduced disturbance on the rock mass during construction and operation (no blasting of deposition tunnels),
- less environmental impact during construction (less excavated rock volumes and hence less filling material),
- reduced cost for construction (including reinforcement),
- reduced cost for backfilling.

KBS-3H includes more prefabricated industrial components and a reduced amount of human involvement in the deposition process which is preferable and should result in small deviations and high quality. The assembly of the Supercontainer is done in an industrial process in a controlled environment, which is likely to be more consistent than "manual" emplacement of canister, backfill and buffer separately. The mechanical excavation (drilling) of deposition drifts will also be more consistent than the "manual" excavation of deposition tunnels, although it should of course be mentioned that the deposition holes of KBS-3V are also made by means of mechanical excavation.

Another reason for developing KBS-3H is that it strengthens the KBS-3 method and can potentially introduce new solutions and technology that can be beneficial to KBS-3V.

In the end, it will come down to long-term safety and feasibility when comparing and deciding between KBS-3V and KBS-3H. A change from KBS-3V to KBS-3H will only be considered if it can be clearly shown that the horizontal emplacement is technically feasible and as safe as KBS-3V. If a change is made there is also the possibility of economical gain in using KBS-3H.

2.3 KBS-3H design development

This Section presents the KBS-3H design development carried out from 2001 up to the current planning for the upcoming project phase.

2.3.1 KBS-3H Research and Development and Demonstration programme 2001

In 2001 SKB presented a Research Development & Demonstration (RD&D) programme for a KBS-3 repository with horizontal emplacement (SKB 2001a). This programme has acted as a basis for the development of the KBS-3H design and is presented in the Section below.

The degree of bedrock utilization, i.e. how many canisters could be deposited within a certain volume of a repository was regarded as important to investigate. The programme hence proposed that an underground layout adaptation should be made. This would also stand as a basis for a preliminary safety assessment. Since KBS-3H and KBS-3V uses the same system of engineered barriers and are designed for similar geological environment, the KBS-3V safety assessment methodology was considered applicable for KBS-3H as well. Several KBS-3H specific issues were identified as needing further attention in the preliminary safety assessment, such as modelling of the following:

- evolution of the Supercontainer including the waste, the canister, the buffer and a Supercontainer shell,
- the degradation of the bentonite due to chemical interaction with the corrosion products of the Supercontainer shell,
- thermo-hydro-mechanical evolution during the saturation, and
- the effects of plugs and distance blocks (bentonite blocks that separate canisters) in the local groundwater flow.

Issues related to buffer behaviour were deemed to be of high priority, such as thickness of the buffer, the swelling and homogenization of the buffer, local saturation of the buffer, the risk of piping/erosion, the mineralogical effects due to contact with the Supercontainer steel shell and the effect of groundwater inflows into the deposition drift before closure. A need to verify methods of groundwater control for horizontal drifts was identified.

Several techniques for excavation of drifts were investigated and it was proposed that a 50 m test drift should be excavated at the Äspö Hard Rock Laboratory (HRL) using either horizontal push-reaming or cluster drilling. This would in turn enable testing of another key issue; the technique to be used for deposition. It was proposed that the Supercontainer design and deposition equipment should be developed further so they could be manufactured and demonstrated in the test drift.

A deposition drift that has been filled with Supercontainers and distance blocks needs to be sealed with a drift end plug. It was proposed that various drift end plug alternatives should be investigated and that one should be selected for design, manufacture and demonstration at the Äspö HRL.

The final key issue identified in the programme was retrievability, i.e. removal of the canister after the buffer has absorbed water and become deformed or after plugging and sealing of the drift. It was proposed that the RD&D Programme should establish the technical assumptions and identify efficient solutions for retrievability that would not compromise canister integrity.

It was preliminarily assumed that the deposition drifts should be 1.75 m in diameter e.g. the same diameter as the deposition holes for KBS-3V. The length of the drifts could be 200–500 m and they should be straight and parallel, and slightly inclined upward from the drift entrance.

2.3.2 KBS-3H development during the period 2002–2003

The development of KBS-3H was initiated with the *Feasibility study phase* which dealt mainly with technical matters such as rock excavation techniques, the handling of deposition equipment and the design of the Supercontainer. The main conclusion from this project phase was that the design is technically feasible and would meet the requirements for long-term safety. The results were summarised in the SKB R&D Programme 2004 (SKB 2004).

A *Basic Design phase* (BD, Section 4.1.1) was devised in 2003, comprising straight drifts of up to 300 m in length and with a diameter of 1.85 m, meeting strict dimensional tolerances so that deposition could proceed smoothly. Deposition of Supercontainers and distance blocks were planned to be carried out using a machine utilising water cushioning technology.

The main purpose of this project phase was to identify critical points with regard to long-term safety in the programme. The work involved three areas: technical development, preparations for a demonstration, and initial studies of the long-term safety of the design.

The results of the Basic Design Phase, which were reported in Thorshager and Lindgren (2004), were as follows:

- There are good possibilities to design and manufacture the equipment necessary for the construction and operation of a repository based on the KBS-3H design. Conclusions on the overall performance of the design and further optimizations can only be reached after completion of the demonstration tests at the Äspö HRL.
- A study regarding the behaviour of the buffer during and just after operation shows that there are many factors which affect the function of the buffer and that it is difficult to design a simple yet robust system.
- Information on the early evolution of the buffer and the processes following the saturation of the bentonite buffer is limited and further information may affect requirements of the design.

The issues identified served as the basis for planning the Demonstration Phase 2004–2007.

2.3.3 KBS-3H development during the period 2004–2007

The *Demonstration phase* in 2004–2007 was planned on the basis of the understanding developed up to 2003 and the issues identified that needed to be resolved to demonstrate the feasibility of the KBS-3H design. Thus, the overall objectives for the project phase were set to use practical trials to demonstrate that the horizontal deposition alternative was technically feasible and that it fulfilled the same long-term safety requirements as the reference design KBS-3V. It was decided to focus on KBS-3H specific issues. Aspects that SKB and Posiva already demonstrated in the framework of KBS-3V or a discussion of techniques that exist in normal industrial applications, such as handling in a reloading station, were not included.

The overall objectives were split into several subsidiary, detailed objectives such as demonstrating a technique for excavating the horizontal drift with a high degree of accuracy, developing equipment for emplacing the heavy Supercontainers in the drift, developing candidate designs and layout adaptation as well as the preparation of a safety case based on Olkiluoto site data and a fundamental understanding of the behaviour of the engineered barrier and the host rock.

Figure 2-2 is an overview of KBS-3H Project 2004–2007 with the design options that were studied. The text in green indicates the main alternatives for future studies.

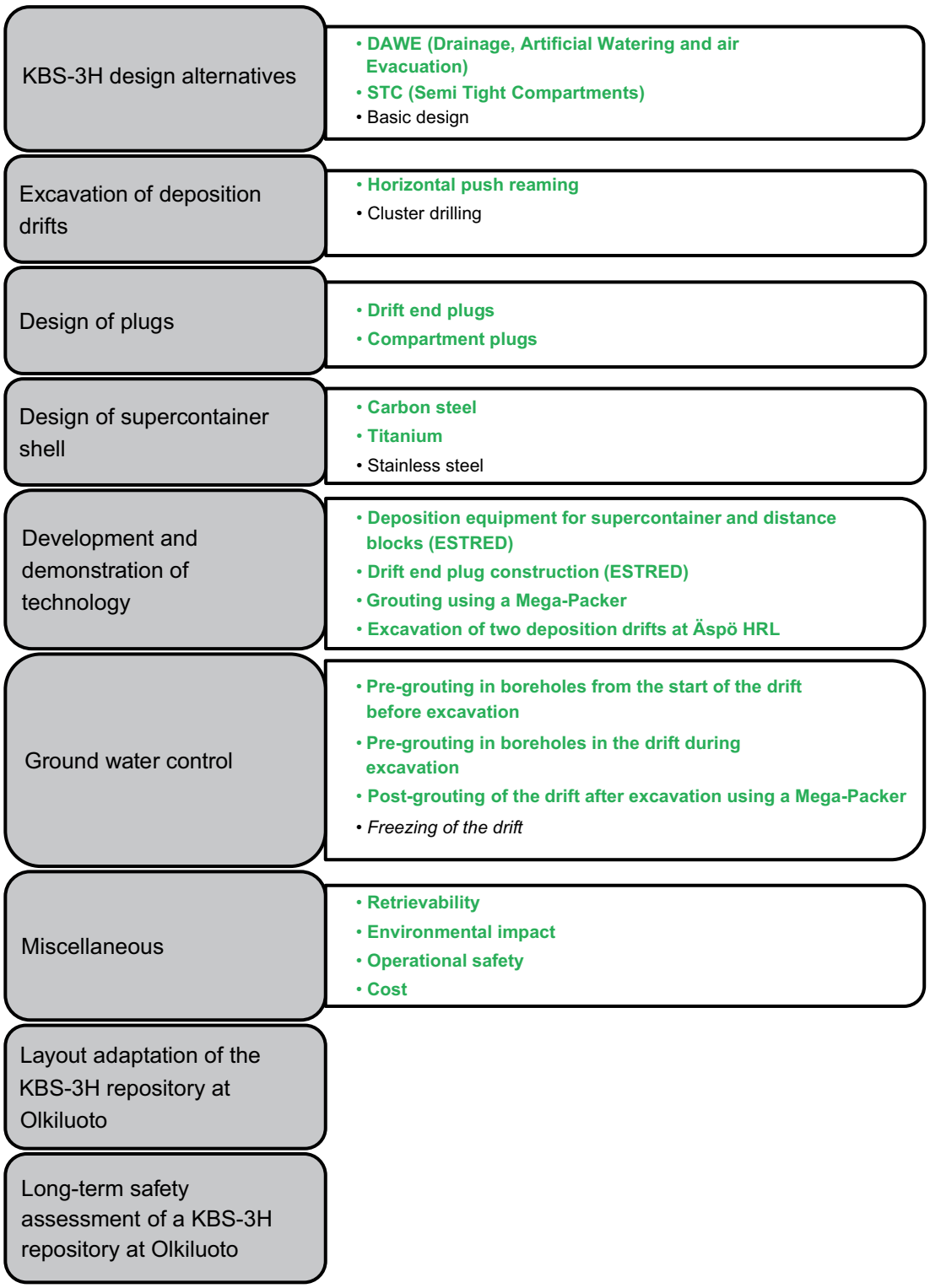

Figure 2-2. *Overview of the KBS-3H project 2004–2007 and design options that were studied. Green text indicates main design alternatives and issues for future studies. The text in black indicates alternatives that were discarded.*

A key issue during 2004–2007 was the development of the barrier design. The work was conducted in close cooperation with the safety assessors to set-up the requirements and potential design alternatives. Important requirements are, for example, the requirements for the deposition drift with respect to geometrical variations and permissible groundwater inflow into the deposition drifts. The work on layout adaptation, barrier design development and systems for groundwater control was reported in annual Design Description Reports, the latest being Autio et al. (2008).

A key KBS-3H element that was studied extensively during this project phase was the Supercontainer. Efficient horizontal emplacement requires the canister and the buffer to be assembled into one unit – the Supercontainer – which is then transported into the deposition drift, see Section 4.4.

The project was a continuation of the work done with the BD where the idea is that each Supercontainer is hydraulically isolated from the next Supercontainer section with thermal dimensioning also included in the isolation aspect. Figure 2-3 illustrates the BD. This is mainly achieved by the use of distance blocks which are designed to prevent water flow between sections during installation as well as during the following saturation process. However, after further studies the robustness of this design was seriously questioned. Therefore a new design was proposed to better control the saturation process, Drainage, Artificial Watering and air Evacuation (DAWE), Section 4.3. In the DAWE design the drift is drained from inflowing groundwater during the deposition phase, a compartment plug is then installed and water is subsequently pumped into the compartment through the plug using pipes. Hereby water will fill the empty space between the drift wall and buffer inside a sealed compartment which will accelerate the swelling of the distance blocks and the buffer inside each Supercontainer. As connected void spaces are filled with water at hydrostatic pressure simultaneously, no significant pressure gradients will exist that may cause mechanical displacement of the Supercontainers or distance blocks. The pipes that are needed for air evacuation and artificial watering will be removed through the compartment plug before drift closure. From an outlining point of view DAWE is similar to the BD; with the fixing rings removed (steel rings positioned to lower the risk of buffer displacement).

One additional design, STC, see Section 4.1.2, was proposed in mid-2007. In the preliminary STC design alternative, each Supercontainer section will be sealed with distance blocks and sealing rings that temporarily prevent water from flowing from one Supercontainer section to another before the section is filled with inflowing water. Once the section is filled with water, the water flows into the next section.

The safety assessment work started in 2005. The BD was then regarded as the KBS-3H reference design and no major differences, relevant for long-term safety, were identified between the BD and DAWE by that time. It was judged that the differences between the design alternatives principally affected the early evolution phase, prior to any possible release of any radionuclides. The final saturated state of the repository is essentially the same whichever option is implemented. The BD was hence chosen for the safety assessment work.

The input to the safety assessment is outlined in Appendix C of Design Description 2007 (Autio et al. 2007). The site data used was originally based on the Olkiluoto Site Description 2005 (Posiva 2005) but was then updated to incorporate data from the Olkiluoto Site Description 2006 (Andersson et al. 2007) whenever possible. The BD alternative was described in the Design Description Report 2007 (Autio el al. 2008). The safety assessment focuses on those aspects which are different or potentially have different significance for KBS-3H as compared to the KBS-3V repository.

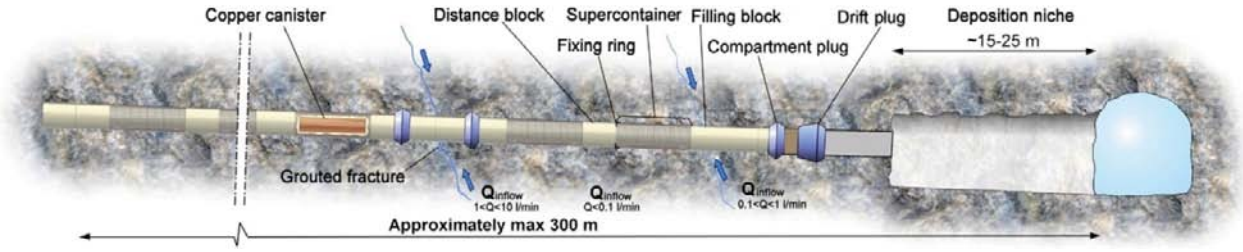

Figure 2-3. *The KBS-3H Basic Design (BD).*

One essential aspect of Project 2004–2007 was the demonstration of technology, and most of these activities were carried out at the Äspö HRL in a realistic environment. Two full-scale horizontal drifts, 95 and 15 m long were bored, and prototype equipment for deposition of a 46 tonnes mock-up Supercontainer was developed and successfully tested. The two drifts were also used for testing techniques for drift end plugging and for reducing groundwater inflows into the deposition drifts.

Overall substantial achievements were made by the KBS-3H project during 2004–2007. Some major uncertainties were, however, detected during this project phase of which several are common with KBS-3V. For example the behaviour of the buffer during the operational period and subsequent period of buffer saturation, where the risk for piping and erosion of bentonite may occur even for very low water inflow, the estimated limit for one Supercontainer section (~10 m) is 0.1 l/min (Autio et al. 2007). KBS-3H specific issues were also identified based on the safety assessment. Many of these are related to the impact of the Supercontainer steel shell and other steel structural materials present in the drift.

In addition to the uncertainties that were detected several components still remained to be demonstrated after this project phase, for example the manufacture and deposition of distance and filling blocks and the construction and installation of compartment plugs.

2.3.4 KBS-3H development during the period 2008–2010

The *Demonstration project* phase was followed by the project phase covered in this report, the *Complementary studies of horizontal emplacement KBS-3H, 2008–2010,* including critical design and material selections and plans for a *KBS-3H System Design* phase.

2.3.5 Increasingly integrated KBS-3H design

Table 2-1 summarises the increased integration in the KBS-3H development, it illustrates how more and more components are tested and evaluated in combination with each other. The table also illustrates the main activities in the upcoming project phase and continuing further on including design optimisations and eventually a possible system test including all components of the KBS-3H reference design.

Table 2-1. KBS-3H design evolution.

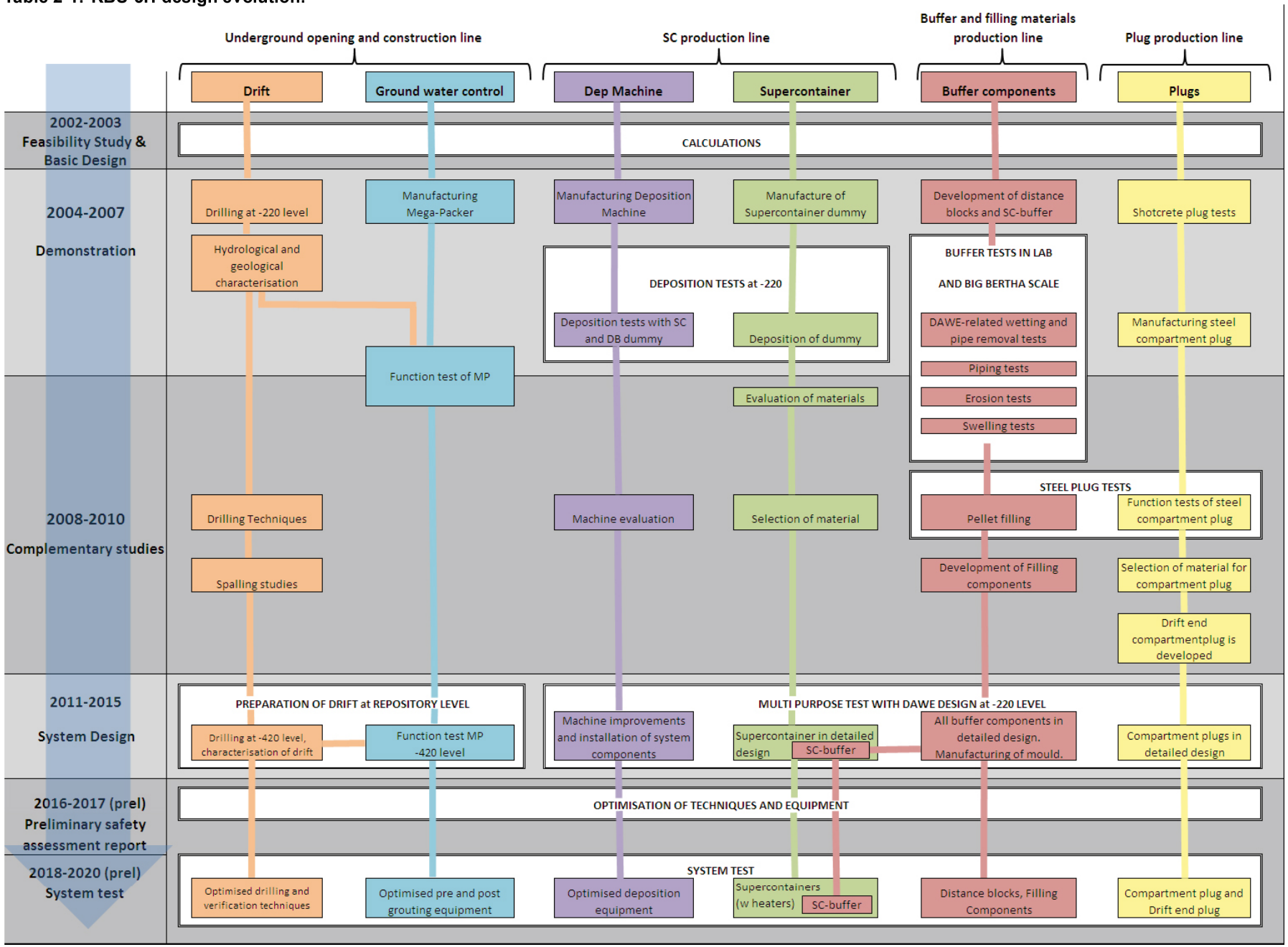

3 General KBS-3 and KBS-3H-specific requirements

This chapter presents the requirements related to design and long-term safety for the KBS-3 method as well as specific requirements identified related to the KBS-3H design. It should be noted that although this report is finalised during 2012, the requirements presented represents the status at the end of the Complementary Studies phase, early 2011. Updates and changes have been made to some requirements during the finalisation of the report but these will be reported in the new project phase.

The KBS-3 method is the method proposed in Finland and Sweden for geologic disposal of spent nuclear fuel. Therefore, especially requirements of the host rock related to long-term performance of engineered barriers will, to a large extent, be similar. Still, there are site specific features and differences in available site data to be considered in development of the practical criteria. There are, however, differences in the definitions and the terminology applied which are partly arising from the differences in the regulations in Sweden and Finland. There is a difference in the basic starting point for defining the requirements in the regulations by the Finnish and Swedish authorities; whereas the focus in the Finnish regulations is in the expected evolution scenarios, the Swedish regulations point out the "*scenarios that can be shown to be especially important from the standpoint of risk"*

3.1 Regulatory requirements and guidance

In Sweden, regulatory requirements, including criteria for judging the safety of a geological repository, are defined in regulations originally issued by SKI and SSI and now by SSM. Two regulations of particular relevance, issued under the Nuclear Activities Act and the Radiation Protection Act, respectively, are:

- *"The Swedish Radiation Safety Authority's regulations concerning the protection of human health and the environment in connection with the final management of spent nuclear fuel or nuclear waste" (SSMFS 2008:37)*. (SSM 2008a)
- *"The Swedish Radiation Safety Authority's regulations concerning safety in final disposal of nuclear waste" (SSMFS 2008:21)*. (SSM 2009b)

According to SSMFS 2008:37, protection of human health shall be demonstrated by compliance with a risk criterion that states that:

"the annual risk of harmful effects after closure does not exceed 10^{-6} for a representative individual in the group exposed to the greatest risk".

"Harmful effects" refer to cancer and hereditary effects. The risk limit corresponds, according to SSM, to an effective dose limit of about $1.4 \cdot 10^{-5}$Sv per year. This, in turn, corresponds to around one percent of the natural background radiation in Sweden.

SSM has also issued General guidance concerning the application of SSMFS 2008:37. In the General guidance, it is indicated that the time scale of a safety assessment should be one million years after closure. A detailed risk analysis is required for the first thousand years after closure. Also, for the period up to approximately one hundred thousand years, the reporting is required to be based on a quantitative risk analysis. For the period beyond one hundred thousand years, however, the general guidance to SSM 2008:37 states that a strict quantitative comparison of calculated risk in relation to the criterion for individual risk in the regulations is not meaningful. Rather, it should be demonstrated that releases from both engineered and geological barriers are limited and delayed as far as reasonably possible using calculated risk as one of several indicators. The demonstration of this is in the regulation seen as part of the demonstration of the use of best available technique, BAT.

The regulatory requirements for the long-term safety of a geological repository in Finland are set out in the Government Decree on the safety of disposal of nuclear waste (DG 736/2008) and, in more detail, in YVL Guide D.5, (Draft 4, 22.9.2010 in Finnish only) by STUK.

Different regulatory requirements on radiological protection are given in DG 736/2008 and in the YVL Guide D.5 for different time windows. *In an assessment period during which the radiation exposure of humans can be assessed with sufficient reliability, and which shall extend at a minimum over several millennia*, Section 4 of DG 736/2008 states:

"The annual dose to the most exposed people shall remain below the value of 0.1 mSv".

and

"The average annual doses to people shall remain insignificantly low".

The way in which *"annual dose to the most exposed people"* and *"average annual doses to* (larger groups of) *people"* is to be interpreted in safety assessment is explained in Guide YVL D.5. It is also stated (YVL Guide D.5 Para. 317) that:

"Disposal shall not affect detrimentally to species of fauna and flora".

In the longer term, the quantitative regulatory criteria relate directly to the release rates of radionuclides from the geosphere to the biosphere ("geo-bio fluxes"). According to YVL Guide D .5, Paragraph 313:

"*The sum of the ratios between the nuclide specific activity releases and the respective constraints shall be less than one".*

The regulatory constraints with which the activity release rates are compared are specified in YVL Guide D.5 Paragraph 312.

3.2 Safety functions and safety-related guidance to KBS-3 design

The primary safety function of the KBS-3 method is to completely contain the spent fuel within copper canisters over the entire assessment period, which is one million years. Should a canister be damaged, the secondary safety function is to retard any releases from the canisters. Other key elements of the safety concept are the existence of multiple barriers so that it is unlikely that any single detrimental phenomena or uncertainty could undermine the safety of the whole system. These are the basis for the safety concept for a KBS-3 repository (see Figure 7-6 in Posiva 2010),

SKB presented in SR-Can (SKB 2006), the concept of safety functions, safety function indicators and safety function indicator criteria. These are also used in the SR-Site (SKB 2011). By introducing these concepts, transparency between long-term safety and any practical criteria can be enhanced. The concepts are defined in the following way:

- A **safety function (**SF**)** is a role through which a repository component contributes to safety.
- A **safety function indicator** (SFI) is a measurable or calculable property of a repository component, which indicates the extent to which a safety function is fulfilled.
- A **safety function indicator criterion** (SFIC) is a quantitative limit, such that if the relevant safety function indicator fulfils the criterion, the corresponding safety function is maintained.

Safety functions are an aid in the evaluation of safety, but the fulfilment of all safety function indicator criteria is neither necessary nor sufficient to argue safety. The different safety function indicator criteria are furthermore determined with varying margins to acceptable performance.

Safety function indicator criteria *are meant to be fulfilled* throughout the one million year assessment period, whereas design premises relate to the initial state of the repository. Design premises need to be defined with sufficient margin to allow deterioration of the system components over the assessment period so that safety is still fulfilled, i.e. so that, ideally, all the safety function indicator criteria are fulfilled also at the end of the assessment period

The concept of safety functions defining the way a specific barrier contribute to the overall safety of the repository system is identical both for SKB and Posiva. Also the actual safety functions defined by Posiva and SKB are practically the same. In SR-Site the safety functions and correspondingly the safety function indicators are divided into two groups; those related to containment and those related to retardation; for Posiva this division has not been made. Safety function indicator criteria for the Forsmark site considered in SR-Site for containment is summarised in Figure 3-1. The corresponding SFIC for retardation is summarised in Figure 8-3 of the SR-Site Main Report (SKB 2011).

According to the Finnish regulations (YVL Guide d.5, Draft version 4, 22.9.2010, in Finnish), targets shall be specified for the performance of each safety function. **Performance targets** for the engineered barriers and **target properties** for host rock are defined considering the safety functions. The performance targets for the EBS and target properties for the host rock defined by Posiva correspond to the safety-function indicators and criteria defined by SKB. The performance targets for the barriers and target properties for the host rock are defined in the Tables 7-1 to 7-4 in Posiva's recent TKS-2009 report (Posiva 2010).

3.2.1 Host rock and repository layout

The safety functions of the host rock are to provide:

- isolation of the spent fuel from the biosphere and normal human habitat and limit the possibility of human intrusion,
- favourable and predictable mechanical, geochemical and hydrogeological conditions for the engineered barriers, and
- a natural barrier that limits transport and retards the migration of harmful substances to the biosphere that could be released from the repository.

In order to fulfil these safety functions of the bedrock, the depth of the repository is chosen such that:

- the host rock adequately isolates the repository from human and the surface environment and protects it from events and processes associated with climate changes.

By locating the repository at a site where the host rock can be assumed to be of no interest to future generations, the risk of human intrusion is reduced. The depth, location and layout of the repository panels, including the directions of the drifts and the positions for canister and buffer emplacement within the drifts, are chosen such that, as far as practicable:

- excessive mechanical, thermal or chemical loads that could compromise the safety functions of the canisters and buffer are avoided (see the discussion of rock suitability criteria in Section 3.3.1).

Layout adaptations for the selected sites at Forsmark in Sweden and in Olkiluoto in Finland are presented in Chapter 8.

Thermal loads must be controlled to avoid adverse mineralogical changes in the buffer; the current requirement is that the temperature of the buffer is kept below 100ºC. Thus, the rock mechanical and thermal properties are taken into account when defining the orientation and mutual distance of the drifts. The requirement on the minimum temperature of the rock at the repository level is set –4°C to avoid freezing of the buffer (SKB 2009b).

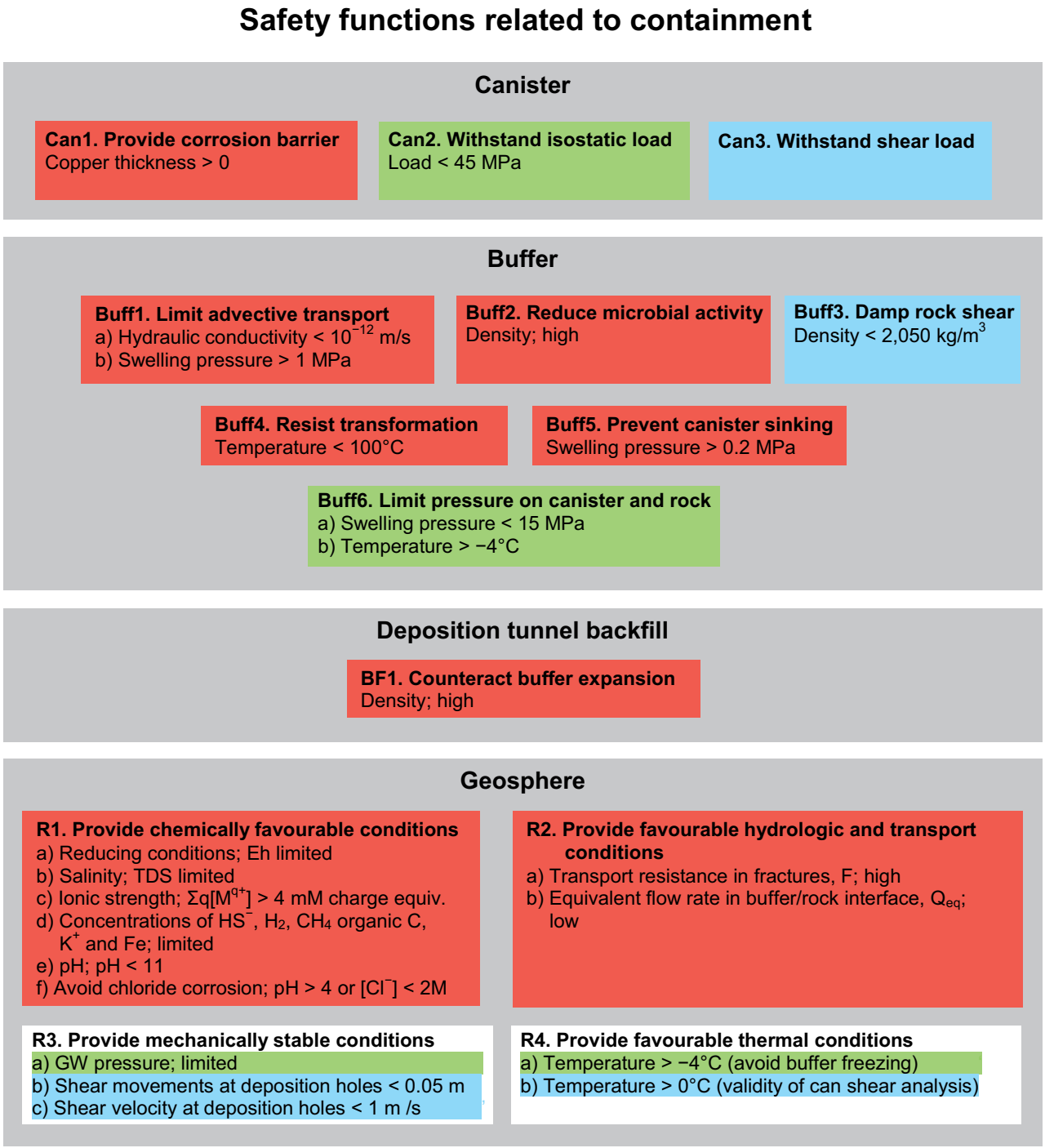

Figure 3-1. *Safety functions (bold), safety function indicators and SFIC related to containment. When quantitative criteria cannot be given, terms like "high", "low" and "limited" are used to indicate favourable values of the safety function indicators. The colour coding shows how the functions contribute to the canister safety functions Can1 (red), Can2 (green) and Can3 (blue) (Figure 8-2 in SKB 2011).*

3.2.2 Canister

Ensuring a prolonged period of complete containment of the spent fuel and its associated radionuclide's is the main safety function of the canister. Thus, the canister must be designed and manufactured in such a way that, with a high probability, it will remain water tight and gas tight for a period of at least several hundred thousands of years (Posiva 2010) (performance requirements) in the conditions expected to prevail in the disposal facility. The spent fuel will then interact with the environment only by means of heat generation and low level radiation penetrating through the canister walls.

This requires that the canister must:

- withstand an isostatic load,
- withstand shear load, and
- provide a corrosion barrier.

Further the canister must not endanger the performance of other release barriers outside the canister, and the fuel inside the canister must not develop a critical configuration in the conditions that are expected to prevail.

This is kept under control by e.g. having a well planned and controlled inventory of each canister as well as by design and configuration measures of the canister and the repository near-field. Credit for burnup has to be taken to demonstrate that the canister remains subcritical for all reasonably conceivable scenarios. The probability of criticality inside or outside the canister is considered to be negligibly small (SR-Site Main report section 13.3 and references therein).

3.2.3 Buffer

According to Posiva's TKS 2009 (Posiva 2010), the safety functions of the buffer are:

- to contribute to mechanical, geochemical and hydrogeological conditions that are predictable and favourable to the canister, and to protect canisters from external processes that could compromise the safety function of complete containment of the spent fuel and associated radionuclide's, and
- to limit and retard radionuclide releases in the event of canister failure.

In the case of KBS-3H, the buffer is defined as the swelling clay initially in the Supercontainer (Section 4.4) and the swelling clay in the distance blocks (Section 4.5). This latter part of the buffer has the additional safety function of separating the Supercontainers hydraulically one from another, thus preventing the possibility of preferential pathways for flow and advective transport along the buffer/rock interface. This is required because the buffer/rock interface near the canisters may locally be perturbed by a number of factors (see Section 3.3.5).

To meet these safety functions the buffer should:

- protect the canister mechanically in the case of shear movements on fractures intersecting the drifts of a few centimetres. The likelihood of larger shear movements is expected to be reduced by the application of appropriate rock suitability criteria; see Section 3.3.1),
- hold the canisters in position, such that a continuous buffer remains present around the canisters,
- limit the rate at which corrosive agents present in the groundwater reach the canister surface,
- allow for gas release of the possible large quantities of gas that may be formed in a damaged canister without compromising its safety functions,
- provide a tight contact with the host rock and the canister soon after emplacement, and
- provide mechanical support for the rock, consequently reducing the possibility of mechanical damage due to excavation- and/or thermally-induced spalling.

To meet these requirements over a prolonged time period, the buffer is also required to be chemically (mineralogically) and mechanically stable in the conditions expected to prevail in the disposal facility. As noted in Section 3.2.1, thermal loads must be controlled to avoid adverse mineralogical changes in the buffer. The thermal properties of the buffer are taken into account when designing the layout of the repository to control thermal loads. It should also contain only limited amounts of constituents that have a negative effect on the performance of the other repository barriers.

3.3 Design requirements to support the long-term safety functions

KBS-3V design requirements to support safety functions are documented in SKB's report of design premises (SKB 2009b) and in Posiva's TKS 2009 (Posiva 2010).

The terms design basis and design premises are used with different meaning by Posiva and SKB. For Posiva design premises means being the starting point for defining the design basis. On the other hand for SKB the design basis cases are the starting point for defining the design premises. The design requirements and in case of host rock, rock suitability criteria (RSC) defined by Posiva are closely related to the design premises.

It is also important to note that the safety function indicator criteria are not the same as design criteria, formally described as design premises in SR-Site (SKB 2011). The former should ideally be upheld throughout the assessment period whereas the design premises should be fulfilled initially. In general, the design premises should assure that the system is robust to the extent that the safety functions indicator criteria are fulfilled over time. For example, the copper canister must be designed such that its initial thickness (the design premise) ensures that it will sustain corrosion for a very long time, i.e. such that the thickness is non-zero (the function indicator criterion) during this time. Design premises typically concern specification on what mechanical loads the barriers must be able to withstand, restrictions on the composition of barrier materials or acceptance criteria for the various underground excavations.

It should be noted that since the compilation of this report started Posiva's requirements management system VAHA has been developed and the performance targets/target properties and design requirements and the justification of these is now reported in the Design Basis report (Posiva 2012). This also means that much of the discussions presented in this chapter would rather now better be included under the safety functions and safety-related guidance to design than to design requirements.

In the following sections, design requirements specific to SKB or to Posiva are indicated in the text by the words "SKB" or "Posiva", enclosed in parentheses.

3.3.1 Requirements on rock volumes for drift construction and canister emplacement

The suitability of a volume of rock for the construction of deposition drifts and for receiving spent fuel canisters must be assessed to ensure that the canisters and their surrounding buffer are protected against excessive mechanical, thermal or chemical loads and, more generally, to ensure that, with a high degree of probability, that the safety functions of the host rock will be achieved (see also Section 3.2.1). For this purpose, Posiva is developing the Rock Suitability Criteria (RSC) (Hellä et al. 2009, Posiva 2010) and SKB has defined the design premises (SKB 2009b, Hellä et al. 2009), which guide and constrain the repository design to meet this goal and which form the basis for demonstrating the repository safety. It is noted that the rock suitability criteria and design premises can be modified later on based on more detailed site data and a more developed understanding of the processes of importance for long-term safety.

When developing the RSC and design premises, the target properties with incidental deviations and safety function indicators (and criteria) are considered by Posiva and SKB respectively. The target properties and the safety function indicator criteria for the host rock describe conditions when the host rock maintains its safety functions i.e. provides conditions under which the perturbing

phenomena is not likely to impair the performance of the EBS and the transport of radionuclide's is limited. The safety functions can be met even if a few of the target properties or the safety function indicator criteria are not fulfilled, but further analyses are required to assess the safety of the whole system. In Posiva case failure to meet the target properties lead to variant or disturbance scenarios as in the base scenario the target properties need to be met. The target properties and safety function indicator criteria in principle apply to the whole assessment period. Target properties/safety function indicator criteria include properties related to the chemical composition of groundwater and retention characteristics that can usually be examined only indirectly by modelling or can be coupled with other properties that can be observed, measured or modelled in the case of retention characteristics or are known to be broadly favourable at repository depth at the selected Swedish and Finnish sites in the case of the chemical composition of groundwater. Posiva has defined RSC to consider observable, measurable present day rock properties that will contribute to fulfilment of the target properties and further the safety functions, especially in the canister near field. The criteria need to be defined in a way that fulfilment of the criteria can be demonstrated. In the Production Line reports for each component SKB describes i) the design premises to be fulfilled, ii) the reference design selected to achieve the requirements, iii) verifying analyses that the reference design does fulfil the design premises, iv) the production and control procedures selected to achieve the reference design, v) verifying analyses that these procedures do achieve the reference design and vi) an account of the achieved initial state. All aspects will be considered when the reports are compiled for KBS-3H, an activity included in subproject "Production and Operation" in upcoming project phase.

Target properties related to thermomechanical stability concern the limited magnitude of mechanical disturbances, and are translated to the RSC shown in Table 3-1. Taking into account the thermal properties of the rock and the heat generation in the canister, the spacing between the deposition tunnels and holes (KBS-3V) is designed to meet the temperature criteria. SKB gives a SFIC that the host rock temperature is above the buffer freezing temperature. The target properties/safety function indicator criteria related to hydrological and transport properties of rock concern initial inflow rates and long-term flow rates at deposition locations and the geosphere transport resistance. The properties of the near-field rock should also be favourable for matrix diffusion and sorption. Again, these properties are translated to the RSC shown in Table 3-1.

The Posiva RSC programme for KBS-3V is described in Section 3.3 of Posiva (2010). The KBS-3V RSC criteria will, according to present plans, be updated after 2012 to also include KBS-3H. However, based on the current planning, the suitability of a certain rock volume for final disposal is likely to be assessed in stages using the classification scales of repository, deposition drift and disposal location within the drift (for KBS-3V, the scales are repository, tunnel and deposition hole), and, as discussed below, at least some of the criteria developed for a KBS-3V repository are expected to be directly transferable to a KBS-3H repository. The repository scale classification applies the site scale model. A detailed scale model based on site scale model and local information becoming available from the rock volume in question is applied for the classification at the tunnel and deposition-hole scale."

The current, preliminary RSC for a KBS-3V repository presented in Table 3-1 is based on an assessment of the properties that the rock should have in order to perform its safety functions. Criteria at the tunnel scale have not yet been developed. The RSC considers the following rock properties: deformation zones and hydrogeological zones at site and detailed scales, their zones of influence, the FPI (Full Perimeter Intersection) fractures intersecting the deposition holes and groundwater inflow to the deposition holes. Deformation zones considered in the RSC are fault zones representing reactivated, earlier non-brittle features. The faults are complex structures consisting of either one or more, possibly branching fault cores surrounded by an influence zone showing signs of less intense deformation than the fault core, but also, for example, hydrothermal clay mineralisation (Pastina and Hellä 2010, p 39, Hellä et al. 2009, Figure 5-3). Hydrogeological zones describe the most extensive and transmissive features of the rock. The hydrogeological zones are linked to fault zones, but based on the observed hydraulic connections are not fully coinciding with them (Posiva 2009, pp 535–536). Specifically, no significant hydraulic connectivity is observed in connection with many of the fault zones.

Table 3-1. Summary of the KBS-3V rock suitability criteria suggested for Olkiluoto in the RSC-I phase (Hellä et al. 2009) and their connection to the target properties of the host rock. Note that the rock shear displacement upper bound of 10 cm is expected to be reduced to 5 cm, in accordance with the design premises given in SKB (2009b). The criterion is based on an assumed maximum shear velocity of 1 m s^{-1}.

Target property	Scale	RSC-Criteria
Inflow to deposition holes < 0.1 L/min. Low flow rate around deposition hole in saturated conditions (in the order of 1 L/year. Transport resistance in the order of few thousands of years per metre in the vicinity of deposition hole.	Repository scale.	Avoid the influence zones of the site-scale hydrogeological zones. In general, 20 metre is considered as an adequate distance.
	Tunnel scale.	No additional criteria.
	Deposition hole scale.	Deposition hole cannot be positioned within the influence zone of a hydrogeological structure (a zone or a fracture). Maximum allowed inflow to a deposition hole is 0.1 L/min.
Limited mechanical disturbances. Rock shear in deposition hole < 10 cm.	Repository scale.	Avoid the influence zones of site-scale brittle deformation zones.
	Tunnel scale.	No additional criteria (however, FPIs need to be taken into account in the degree of utilisation).
	Deposition hole scale.	Deposition hole must not intersect an FPI fracture; a preliminary respect distance of 0.5 metres is suggested. Deposition hole cannot intersect minor brittle deformation zones and the influence zones of these must be avoided.

At the repository scale, RSC for a KBS-3H repository are expected to be identical to those defined for a KBS-3V repository. In particular, there is an identical requirement to provide adequate respect distances to the rock structures that determine the layout of the drifts (so-called LDFs, Layout Determining Features). The LDFs include those deformation zones that have potential for rock movements in either the current or future stress fields, as well as zones that are main groundwater flow routes (extensive zones with transmissivity > 10^{-5} m^2 s^{-1}). The respect distance is based on the zone of influence next to fault core. The zone of influence is affected by deformation caused by earlier geological processes and, most likely, any significant changes will be limited to this zone also in the future. The zone of influence (Hellä et al. 2009, Section 5.2.2) is, where possible, defined on the basis of observations on increased fracturing, alteration, occurrence of hydraulically conductive fractures and changes in the host rock characteristics close to the fault core observed in geophysical measurements. If there are no direct observations, the zone of influence is defined based on the extent of the zone by applying scaling laws (see Table 3.1 in Scholz 2002).

At the scale of a deposition drift and disposal location within the drift, a possible criterion is that there may be no FPI (Full Perimeter Intersection) fractures intersecting the deposition drifts at canister emplacement locations, analogous to the corresponding KBS-3V criterion that FPI fractures must not intersect a deposition hole. The adoption of such a criterion would reduce the probability that secondary rock shear movements on rock fractures larger than a few centimetres that may occur in the event of a large earthquake near the site will damage the canisters (the buffer is designed to meet the requirement to protect the canisters from smaller shear movements). However, the practicality of such a criterion has still to be evaluated in terms of its consequences for unnecessarily discarding deposition holes in case they are intersected by an FPI fracture that in reality has a limited size and thus unlikely to undergo damaging shear movements.

Other potential criteria relate to initial inflows to the drifts, both the total inflow to the drift and local inflow into drift sections. From the point of view of long-term safety, such inflows are of concern since they may potentially lead to mechanical erosion of the bentonite buffer, as well as other bentonite filling components emplaced along the drift (Section 4.6) before artificial watering of the void spaces in the drift takes place and inflow largely ceases. Furthermore, a high initial inflow is an indication of a high transmissivity of the fracture from which the inflow occurs, and hence an increased likelihood of high long-term flow rates around the drift following buffer saturation. High long-term flow rates around the drift have a number of implications for long-term safety, including:

- relatively high fluxes of corrosive agents (notably sulphide) around the drift that could diffuse through the buffer and lead to increased corrosion rates of the canisters,
- the possibility of low ionic strength glacial melt water reaching the buffer/rock interface, leading to chemical erosion of the buffer, reducing the protection afforded to the canisters by the buffer and hence increasing the risk of canister failure, and
- reduced transport times of radionuclide's through the geosphere, and less attenuation of releases to the biosphere by radioactive decay during transport, in the event of canister failure (low geosphere transport resistances).

Drip shield may be installed to reduce the possibility of mechanical erosion of bentonite components by inflowing groundwater prior to artificial watering. Furthermore, initial inflows may be reduced by grouting the fractures intersecting the drifts, or compartment plugs (Section 4.7) can be installed to isolate the highest-inflow fractures from bentonite components. It should be noted that slow degradation means that any grouting material cannot be relied upon to limit water flows in the long-term. Thus, KBS-3H-specific criteria related to initial inflow of groundwater to the drift are expected to distinguish between inflows prior to and after any grouting of the intersecting fractures (requirements related to control of groundwater inflow are described in Section 3.4.2). Site characterisation data and modelling is applied to address this and define the limits to be applied, which may be different for the pilot hole and drift phase.

Very tentatively, an inflow limit of 0.1 litres per minute has been set for fractures intersecting a drift section of about 10 m containing one Supercontainer and one distance block (no grouting is allowed in this section). This limit is based on scoping calculations of the transport of radionuclides from a failed canister. These scoping calculations suggest that, if fractures giving inflows greater than about 0.1 litres per minute are avoided as canister emplacement locations, the likelihood of transport paths with resistances less than 50,000 yr m^{-1} beginning near canister locations will be significantly reduced, although these calculations are subject to significant uncertainties especially regarding the relationship between initial inflow and long-term flow. Scoping calculations also show that a geosphere with a transport resistance of 50,000 yr m^{-1} provides an effective barrier to the migration of many shorter lived and/or more sorbing radionuclide's (Figure 3-2). Although such radionuclide's are expected to be significantly attenuated by the EBS, the geosphere provides "defence in depth"; i.e. provides a significant barrier if the EBS is less effective than expected. Still as noted earlier the inflow limit is very tentative and the limit and the rationale behind it as well as the analysis of how the system performs has to be evaluated after a complete and comprehensive safety assessment has been performed for KBS-3H.

Where bentonite filling components are used, higher pre-grouting inflow limits from fractures intersecting the drift are likely to be acceptable (see Section 3.3.6). The possibility of early mechanical erosion and later chemical erosion may make the use of bentonite filling components unacceptable where initial inflows are particularly high. In this case, the affected drifts section would need to be isolated using compartment plugs. However, no corresponding inflow criteria have as yet been developed. Chemical erosion and its consequences for the long-term safety of a KBS-3H repository is a key issue to be addressed in the next phase. This will also include a re-evaluation of the set requirements for the whole drift and its components and the criteria for the host rock and intersecting fractures.

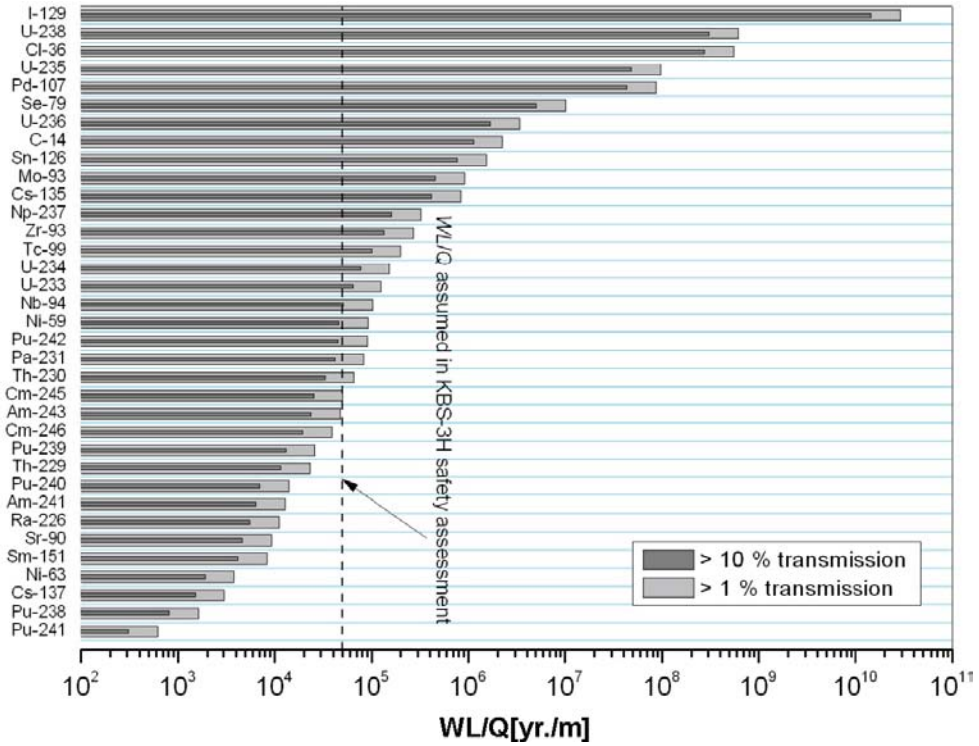

Figure 3-2. *Illustration of the relationship between geosphere transmission and hydrodynamic transport resistance. The extent of the horizontal bars indicate how high the transport resistance (WL/Q) has to be before the steady-state release rate of a radionuclide from the geosphere to the biosphere is significantly attenuated by radioactive decay during transport. The highest transport resistances are required for long-lived or poorly sorbing radionuclides, such as I-129. The dark and light grey bars indicate where host rock transport resistance gives a geosphere transmission greater than 10% and 1%, respectively. Transmission is the ratio of the steady state release rate from the geosphere divided by the release rate to the geosphere. Note that a low transmission does not necessarily mean that there will be little reduction in the amplitude of a short-duration near-field release pulse, since such reduction may also occur due to spreading during geosphere transport.*

3.3.2 Requirements common to all engineered components

All engineered system components, including not only the canister and the buffer, but also the auxiliary components discussed later in this chapter, must be designed mutually compatible. Although all components will inevitably undergo physical and chemical changes over time e.g. due to chemical alteration or corrosion, saturation, swelling, none should evolve in such a way as to significantly undermine either the long-term safety functions or the design functions of the others. Thus:

- no component should contain any chemical constituents that lead to significant negative effects on the performance of the others,
- no component should generate gases at rates that could lead to a build-up of potentially damaging gas pressure taking into account the gas permeability of the other components, and
- no component should give rise to mechanical stresses that could lead to significant damage to the canisters; and no component should undergo volume changes due, e.g. to swelling, compaction, corrosion or alteration that could lead to significant changes in density of the adjacent buffer.

In the case of the canister, the buffer and the host rock, significant negative effects include, in SKB terminology, any that compromise their ability to meet their respective safety function indicator criteria and, in Posiva terminology, any that compromise their ability to meet their respective performance targets in the case of the canister and buffer or achieve target properties in the case of the host rock. If these criteria or targets are not met, then a component may not perform its allocated safety functions.

It should be noted that the criteria or targets for the canister, buffer and host rock are largely identical for the KBS-3V and KBS-3H design options.

Additional, more specific requirements on the repository components are given in the following sections.

3.3.3 Requirements specific to the canister

The functional requirement of resistance to mechanical (isostatic and shear) loads and chemical loads are achieved primarily by the mechanical strength of the cast iron insert and the corrosion resistance of the copper surrounding it, and a manufacture and quality control procedure that ensures a low probability of occurrence of initial defects that could compromise containment.

Consistent with its functional requirements, the canisters must be designed to have:

- sufficient corrosion resistance in the chemical environment of the repository near-field as it evolves over time,
- sufficient strength to withstand the mechanical loads to which it may be subjected over time, including isostatic loads and shearing loads,
- a low probability of initial defects that could allow water ingress and release of radionuclide's, which is in line with Posiva VAHA requirement the canister shall initially be intact except for incidental deviations when leaving the encapsulation plant for disposal, and
- in the expected repository conditions, the canister shall remain intact for hundreds of thousands of years, except for incidental deviations.

Sufficient strength to withstand both isostatic and dynamic mechanical loads is a performance target/ SFIC for the canister. Another is that the canister shall be water and gas tight, with copper completely covering the canister interior. These performance targets/safety function indicator criteria are applicable at all times addressed by safety assessment.

According to SKB (2009b), the requirement for sufficient corrosion resistance gives rise to the design premise of a nominal copper thickness of 5 cm, also considering the welds (where any defects are most likely). The requirement for sufficient mechanical strength gives rise to the design premises that:

- the canister shall withstand an isostatic load of 45 MPa, this being the sum of the maximum swelling pressure and maximum buffer porewater pressure. The corresponding figure for Posiva is 39 MPa, the difference being due largely to the lower maximum isostatic glacial load of 20 MPa assumed by Posiva for the Olkiluoto site, compared with 28 MPa assumed by SKB for Forsmark due to the different locations and expected maximum thickness of ice sheet during the glacial period, and
- the copper shell shall remain intact, and the insert to retain its pressure-bearing properties, after a 5 cm shear movement at 1 m s^{-1} for buffer material properties of a 2,050 kg m^{-3} Ca-bentonite, and for all locations and angles of the shearing fracture, and for temperatures down to 0°C.

Note that the dynamic mechanical loads to which the canister will be subjected will be constrained by the application of RSC (Hellä et al. 2009, Table 3-1) and by the design premises (SKB 2007). Although there are differences in the exact requirements, the principle applied by Posiva is the same: deposition holes are not allowed to be placed close to deformation zones and large fractures that may have potential for shear larger than the canister can withstand are avoided in the deposition holes

The need to ensure sub criticality of the fuel in the canisters also imposes constraints on the design of the canister insert, as well as on quality-control measures in choosing the fuel bundles to be disposed of in the canisters. A design premise is that criticality is to be avoided, even if water should enter a defective canister.

3.3.4 Requirements specific to the buffer

The buffer is designed such that, after artificial watering, it will fill all the void spaces in the deposition drift between canisters and the rock wall. As in the case of the KBS-3V buffer, it is also required to be:

- plastic enough to mitigate the effects of small rock movements on the canisters,
- stiff enough to support the weight of the canisters and keep the canister in position in the deposition drift,
- dense enough to suppress microbial activity that might otherwise lead to unfavourable chemical conditions at the canister surface, and
- impermeable enough that the movement of water is insignificant and diffusion is the dominant transport mechanism for both the corrosive agents present in the groundwater that may degrade the canisters and for the radionuclide's that may be released from damaged canisters.

In the case of KBS-3H, this last requirement implies, in particular, that no items are allowed to be left in or around the distance blocks that may give rise to a hydraulic connection between Supercontainer sections.

The buffer should also have:

- a sufficiently fine pore structure so that microbes and colloids are immobile and microbe- or colloid-facilitated radionuclide transport will not occur,
- a gas permeability that is sufficient to allow for gas release of the possible large quantities of gas that may be formed in a damaged canister,
- a swelling pressure that is sufficient to ensure a contact between the buffer and the rock and between the buffer and the canister, but is no higher than the canister can withstand,
- a self-sealing capability, which means that any cavities or potential advective pathways for flow and transport that may arise, for example, as a result of piping and erosion, sudden rock movements or the release of gas formed in a damaged canister are rapidly closed, and
- heat conduction properties shall be such that heat from the canisters will not lead to unacceptable physical and chemical changes in the buffer.

Swelling pressure and low permeability will develop over time as the buffer saturates. A further tentative requirement is that sufficient swelling pressure to prevent the rock surrounding the deposition drift from spalling because of increased temperature must be established sufficiently promptly. This requirement will be re-evaluated after a complete safety assessment has been done. The requirements are translated into safety function indicator criteria related to containment in e.g. Figure 3-1. Corresponding performance targets for the buffer have been presented in the Table 7-2 in TKS-2009 (Posiva 2010).

The target properties/safety function indicator criteria are, in general, applicable at all times addressed by safety assessment, although an initial period when the buffer is not fully saturated and thus does not provide full swelling pressure or a tight contact with the rock is expected. This must be shown not to have a significant detrimental impact on the safety functions of the buffer in the longer term. Furthermore, the criterion on maximum temperature is most relevant during early times, when there is significant heat output from the canisters.

Competing requirements related to buffer density must be balanced in the design process. For example, excessive density would offer less protection of the canisters from rock movements. On the other hand, insufficient density would lead to the possibility of colloid-facilitated radionuclide transport. The choice of MX-80 bentonite as a buffer material with a design target for saturated density of 1,950–2,050 kg m^{-3} is made with a view to balancing these various requirements (SKB 2007).

The above requirements on swelling pressure and impermeability must be fulfilled taking into account the groundwater salinity variations that will occur during early evolution of the repository system. Furthermore, the buffer properties themselves must not, as a consequence of the heat released from the canister, change to an extent that would be detrimental. The layout of the reposi-

tory will also be adapted to ensure this is the case, see Section 3.2.1. According to SKB (2009b), these requirement give rise to the design premise that, after swelling, the buffer should meet is requirements related to swelling pressure and hydraulic conductivity independently of the dominating cation and for chloride concentrations up to 1 M. Furthermore, after swelling, the shear strength of the buffer should not exceed the strength used in verifying the analysis of the resistance of the canisters to shear loads. These conditions apply for temperatures as low as ~ 0°C and as high as ~ 100°C.

The following requirements have been defined for buffer material in "Design, production and initial state of the buffer" (SKB 2010d) and SKB (2009b), these are common both for KBS-3V and KBS-3H. Reference is also made to SKB TR-09-22, "Design premises for a KBS-3V repository based on results from the safety assessment SR-Can and some subsequent analyses" and to Smith et al. (2007c, Appendix B.4) for calculations on erosion limits:

- The montmorillonite content of the dry buffer material shall be 75–90%.
- The content of organic carbon of the buffer material should be less than 1 wt-%.
- The sulphide content of the buffer material should not exceed 0.5 wt-% of the total mass.
- The total sulphur content of the buffer material, including the sulphide, should not exceed 1 wt-%.
- The density of the buffer shall be between $1{,}950 < \rho m < 2{,}050$ kg/m^3 after saturation.
- The nominal thickness of the buffer around the canister in any direction should not be less than 350 mm after saturation.
- The buffer shall be possible to manufacture and install with high reliability.

The suitable buffer material is bentonite with the material composition specified in Table 3-2. Examples of commercial bentonite with this material composition are MX-80 (used as the reference material) and Ibeco RWC (Deponit CA-N), which were analysed in Buffer production report – Design, production and initial state of the buffer for the safety assessment (SR-Site).

3.3.5 Requirements on the buffer/rock interface

Some perturbation to the buffer/rock interface is probably inevitable in the vicinity of the Supercontainers. For example, the buffer material that fills the gaps initially present between the Supercontainer shells and the drift walls will be of lower density than the bulk of the buffer. Such density differences in the buffer will only partially homogenize over time due to internal friction within the bentonite. The Supercontainer shell may also rupture and be pressed against the drift wall by the developing swelling pressure of the buffer within the Supercontainer. Depending on the material selected for the shell, its corrosion may lead to the presence of potentially porous or fractured corrosion products in contact with the drift wall, and there may be chemical interactions of the buffer with these corrosion products. Finally, there may be some thermally-induced rock spalling if the buffer swelling pressure does not develop sufficiently rapidly, according to the requirement given in Section 3.3.4. Studies related to these potential perturbations are also discussed in Section 9.2.3.

Such potential perturbations mean that there is requirement for disturbance to the buffer/rock interface adjacent to the distance blocks, which have the safety function of separating the Supercontainers hydraulically, in addition to the other safety functions of the KBS-3H buffer. There is also a requirement that disturbances to the buffer in the vicinity of the Supercontainers should extend to only a limited radial distance inwards towards the canisters from the buffer/rock interface, such that the

Table 3-2. Reference buffer material.

Design parameter	Nominal design [wt-%]	Accepted variation [wt-%]
Montmorillonite content	80–85	75–90
Sulphide content	Limited	< 0.5
Total sulphur content (including the sulphide)	Limited	< 1
Organic carbon	Limited	< 1

remainder of the buffer between the canister and the rock continues to perform its safety functions. In the current design, the distance from the canister surface to the drift wall is about 0.4 m. These requirements will be re-evaluated after a performance assessment for the whole drift has been done.

3.3.6 Requirements on auxiliary components

In addition to the canister and buffer, implementation of the KBS-3 method entails the introduction of a number of auxiliary components such as grouting materials (cement-based materials or colloidal silica, Silica Sol), spray and drip shields, and rock support structures (bolts, nets, etc.). Further auxiliary components specific to KBS-3H include the Supercontainer shells (Section 4.4), filling blocks (Section 4.6), compartment plugs (Section 4.7) and Drift Plug (Section 4.8). Some of these components will degrade significantly over time and so do not serve a long-term safety role. All, however, protect the components that do have safety functions during the operational period and through the early evolution of the repository, and in some cases beyond. Tentative requirements have been set for these components. These requirements will be re-evaluated after a performance assessment for the whole drift has been done.

A general requirement on all these components is that the presence of these components should not significantly impair the safety functions of the host rock, buffer or canister. This implies, in particular, that any chemical or mineralogical changes that they give rise to in the buffer, or volumetric changes that they undergo, should be sufficiently limited as not to compromise the performance of the buffer or that of the canisters.

More specific requirements on the Supercontainer shells, filling blocks, compartment plugs and drift end plugs are presented below.

The Supercontainer shell

Following artificial watering, the buffer inside the Supercontainer must swell and form a tight seal with the drift wall. The perforations in the Supercontainer shell must be such as to allow this to happen. This is needed as to avoid the possibility that pressure differences develop along the drift. Also the likelihood of thermal spalling of rock which is especially a risk in dry drift sections will be minimised by the buffer in contact with rock, as well as the Supercontainer shell getting into contact with rock during the early evolution of the system. Whith regards to a dry drift section it is defined as a section where the inflow is equal or less than what the buffer can absorb over the length of a Supercontainer section. The inflow criteria is currently not known quantitatively but estimated roughly to be of orders 1.4 l/h.

In the longer term, the Supercontainer shell will degrade at a rate that depends strongly on the material chosen for its construction, and its degradation products may interact with the buffer. This leads to the following requirements on the Supercontainer shell:

- the properties of the buffer affected by interaction with the Supercontainer shell must be shown to meet the performance targets for the buffer, or, if this is not possible
- the region affected by this interaction should extend only to a limited radial distance into the buffer, see Section 3.3.5.

In addition, the Supercontainer shell may undergo volume change as it degrades, affecting the buffer density. These requirements impose constraints on material selection for, and the thickness of, the shell.

Filling blocks

Filling blocks are used in drift sections where relatively high initial groundwater inflows render them unsuitable for Supercontainer and distance block emplacement. Their function from a long-term safety perspective is (i), to fill void spaces in the drift, contributing to its mechanical stability, and to confine the buffer as it takes up water, such that its saturated density remains within the range specified by performance target values, (ii), to protect the canisters and buffer from the effects of transient water flows, e.g. piping and erosion, that may occur during the operational period for a drift and the following period leading to saturation, and (iii), to isolate the canisters and buffer from larger and more transmissive geological features that may detrimentally affect the canisters and buffer in the longer term, and provide preferential pathways for radionuclide transport in the event of canister failure.

The following requirements are imposed to support this function:

- The filling blocks shall have a sufficiently low compressibility.

By their low compressibility, the filling blocks should limit the expansion of the adjoining buffer (distance blocks) during its saturation and, also in the longer term, keep the buffer in place so that the density requirements on the buffer are met.

- The filling blocks shall have a sufficient but not excessive swelling capacity.

By their swelling capacity, the filling blocks should ensure that macroscopic void spaces in the drift are filled, and should contribute to the mechanical stability of the deposition drifts and near-field rock. The maximum swelling pressure should not, however, be so high that it would lead to excessive compression of the buffer and buffer densities around the canisters that would compromise the capacity of the buffer to protect the canisters in the event of rock shear.

- The filling blocks shall have a sufficiently low permeability and lateral extent.

By their low permeability, the filling blocks should ensure that water that flows through them does not lead to significant erosion of the adjoining distance blocks. Significant erosion here means sufficient erosion to compromise the capacity of the distance blocks to fulfil performance targets related to density. By their low permeability and lateral extent, they should also prevent the formation of preferential radionuclide transport paths by isolating more transmissive host rock fractures.

The quantitative criteria for the filling blocks with respect to the hydraulic conductivity and swelling pressure has not been evaluated, but likely the criteria for the hydraulic conductivity should be the same as for the buffer. The swelling pressure should also ideally be the same as for the buffer. The maximum deviation needs to be estimated in the future assessment.

The length of the filling block must be such that it provides adequate respect distance between the high inflow fractures and the canisters. The higher the initial inflow, the larger respect distances that are expected to be needed, on the basis that high initial inflows are indicative of high long-term flow rates and low geosphere transport resistances.

Scoping calculations described in Appendix A have been used to suggest tentative criteria for minimum respect distances as a function of given initial inflow. The criteria are provisional, being based solely on considerations of radionuclide release and transport. However, it should also be noted that the scenario analysed may not reflect the most severe impact of having high flows close to a deposited canister. This means that the appropriate distance between a canister and a flowing fracture needs to be reassessed once a complete safety assessment of KBS-3H is carried out.

The scoping calculations consider the maximum rate of release of C-14 emanating from a failed canister to the fracture following its diffusion through the buffer and filling component. Conservatively, only transport along the drift towards the fracture is considered (Figure A-1 in Appendix A). Diffusion away from the fracture in the other direction along the drift is disregarded. Furthermore, also conservatively, all C-14 reaching the position in the drift where the fracture intersects is assumed to be transferred to the fracture, and not to diffuse further along the drift. The governing equation for diffusion along the drift is presented and solved in Appendix C. It is assumed – in accordance with the current design – that the filling blocks are composed of compacted bentonite and have the same properties as the buffer, which are those assumed in the KBS-3H safety assessment.

The model considers the IRF release of C-14 and the release of C-14 from Zircaloy and other metal parts. The approach is quite conservative in that spreading and decay of the C-14 release during geosphere transport is not taken into account, even though this could be significant. Also, it is assumed that C-14 is released instantaneously from Zircaloy and other metal parts, whereas, in reality, C-14 will be released as this material gradually corrodes, and some will decay before it is ever released. On the other hand, the model considers only one failed canister; the consequences of several failed canisters have not as yet been assessed.

In applying the model, a wide range of possible initial inflows is considered (Figure 3-3). In each case, the length of the filling block, and hence the respect distance between high inflow fractures and the canisters, is adjusted until the calculated release rate from the filling block to the fracture is reduced to 0.01 GBq per year. This is 3% of the 3 GBq per year Finnish regulatory geo-bio flux constraint for C-14, and is deemed to represent an adequate safety margin, given the above-mentioned uncertainties.

The choice of compacted bentonite for the filling blocks also satisfies the following additional requirements:

- The composition of the filling blocks should ensure the chemical environment, e.g. nature and concentrations of solutes, does not have an unfavourable effect on the performance of the main barriers.
- The filling blocks should prevent the build up of excessive gas pressure in adjoining drift sections to avoid damage to the main barriers. The drift sections adjoining those occupied by filling blocks may be tight, causing gas pressure to build up most likely at the buffer/rock interface. This gas should be able to escape along the buffer/rock interface and hence either though the filling blocks, or along the filling block/rock interface, to transmissive fractures intersecting the drift sections occupied by the filling blocks.
- The filling blocks should not promote microbial activity that might otherwise lead to unfavourable chemical conditions in the adjacent buffer and at the canister surface.
- By their erosion resistance and suitable chemical composition, the filling blocks should prevent the formation of colloids at the filling block/rock interface that could otherwise detrimentally affect the barrier function of the bedrock with respect to radionuclide transport.

Initial inflow range [litres min^{-1}]	Respect distance [m]
0.1–0.5	3 m
0.5–1	5 m
> 1	6 m

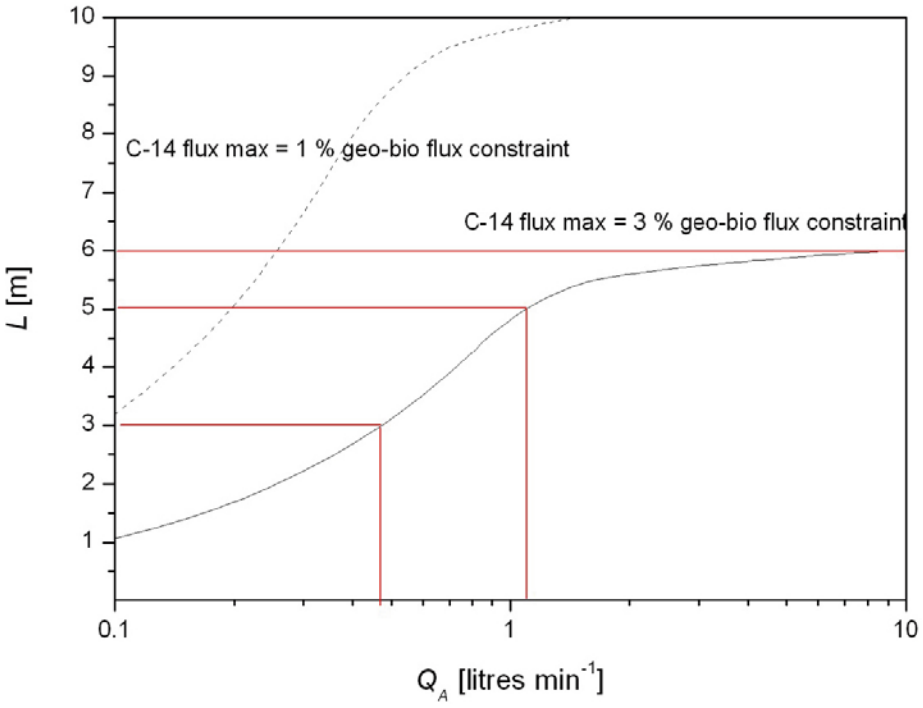

Figure 3-3. *Proposed minimum respect distance (L) between the high inflow fractures and the canisters as a function of initial inflow from fracture intersecting the deposition drift.*

Compartment plugs, as possible alternative to filling blocks

Compartment plugs are mainly used to section the KBS-3H drift, see next page. An additional use is when the initial inflow into a section is higher than a certain limit; tentatively > 1 litre per minute in a 10 m drift section, two compartment plugs may be installed rather than filling blocks to isolate the fractures responsible for this inflow. This is because of concerns regarding the early mechanical erosion, and longer term chemical erosion, of bentonite is such drift sections. The plugs are installed at both ends of the drift section to be sealed off, and filling material emplaced between them, this filling material is currently not designed. The function of this entire assembly from a long-term safety perspective is identical to that of the filling blocks, namely (i), to fill void spaces in the drift, contributing to its mechanical stability, and to confine the buffer as it takes up water, such that its saturated density remains within the range specified by performance target values, (ii), to protect the canisters and buffer from the effects of transient water flows that may occur during the operational period for a drift and the following period leading to saturation (e.g. piping and erosion), and (iii), to isolate the canisters and buffer from larger and more transmissive geological features that may detrimentally affect the canisters and buffer in the longer term, and provide preferential pathways for radionuclide transport in the event of canister failure.

The filling material for use between two compartments plugs has not been completely defined. The key design requirements for this material are that:

- The filling material between compartment plugs shall have a sufficiently low compressibility.

The compartment plugs are designed to withstand the hydraulic pressure at repository depth, but they are not designed to withstand the swelling pressure of the adjoining buffer after sealing of the drift and saturation of buffer. However, by its low compressibility, the filling material between the plugs should limit the expansion and withstand the adjoining buffer expansion during its saturation and also in the longer term and keep the buffer in place so that the density requirements on the buffer are met.

- The filling material between compartment plugs shall not have excessive swelling pressure.

The filling material shall not have a swelling pressure that is so high as to give rise to significant axial movement outwards of the compartment plugs during its saturation that might otherwise cause increase in the density of the adjoining buffer above the maximum density requirement.

Additional requirements related to prevention of filling material loss and to the need for mutual compatibility of the components with each other and with the bedrock are as follow.

- The filling material between compartment plugs has to be designed to allow the water flow through without significant mass loss (Autio et al. 2007, Section 5.7.3 the system of filter zones and transition zones in the design).
- The compartment plugs and the filling material between compartment plugs should not give rise to chemical or mineralogical changes in the adjoining buffer, which compromise the performance of the buffer or that of the canisters.
- The compartment plugs should not undergo volumetric changes which might compromise the performance of the adjoining buffer.
- The compartment plugs should not allow the build-up of excessive gas pressure in adjoining drift sections, i.e. to avoid damage to the main barriers.

Compartment plugs for sectioning the drift, including the adjacent filling material

Compartment plugs are mainly used to section the drift into two compartments, approximately 150 m long. For installation reasons, these plugs cannot be built right up against the distance blocks, and for this reason transition zones; see Section 4.6, consisting of a transition block and bentonite pellets are required.

The filling material in the transition zone should not have an impact on the distance blocks and ensure the functions of the distance blocks. Another function of transition zone is to seal potential pathways around the plug. In case of water leakage in the transition block section the same respect distances between the fracture and the Supercontainer as presented for filling blocks can be applied. The plug will be positioned in good rock avoiding any water leakages close to it in order to prevent any hydraulic pathways around the plug.

The compartment plugs themselves also have certain specific functional requirements during the operational phase and the period immediately thereafter. In particular, they should:

- provide an adequate drift seal that prevents flow through the plug and rock plug interface, to avoid erosion of buffer by transient water flows during the operational phase,
- be capable of supporting a full hydrostatic pressure after installation for as long as there are void spaces in an adjoining drift, and
- form a confining surface to maintain the Supercontainers and other components in position during operation of each drift.

Design requirements corresponding to these functional requirements are that the plugs should be:

- positioned in good-quality rock sections in the drift, with the forces exerted on rock surfaces being compressive, and
- dimensioned to withstand a one-way pressure of 5 MPa prior to installation of the drift end plug.

The drift plugs

The function of the drift plugs, similar to the KBS-3V deposition tunnel plugs, is to avoid significant water flows out of the drift, which could give rise to piping and erosion of the buffer, either through the plug itself, or through the adjacent rock. They also keep the buffer in place prior to the backfilling and saturation of the adjacent central tunnel (in Finland named main tunnel). In the longer term, and over the entire regulatory compliance period, the drift plugs form part of the system of natural and engineered barriers that limit any radionuclide's transport in the event of canister failure.

The requirements on the drift plugs are similar to those on the KBS-3V deposition tunnel plugs. In particular, the plugs are required to:

- withstand full hydrostatic pressure of 5 MPa plus the swelling pressure of the buffer in the disposal drifts of up to 10 MPa for as long as the adjacent central tunnels are not backfilled, to avoid displacement into the central tunnels, with consequences for buffer density and swelling pressure,
- withstand pressure heterogeneity of 2 MPa (estimated) acting on the plug surface,
- be sufficiently tight, particularly during the operational phase before the central tunnels are backfilled but also afterwards together with the backfill and seals of other openings, so as to avoid loss of eroded buffer materials from the deposition drifts, and
- not give rise to volume changes or to chemical or mineralogical changes in the adjoining buffer that compromises its performance or that of the canisters.

The drift plug is required to stay in place under the applied loads until the adjoining central tunnels are backfilled and saturated. Also in the long-term as noted above they should form part of the natural engineered barriers that limit the transport in the event of canister failure.

The backfill of underground openings, including the central tunnels, access tunnels, shafts, and other excavations e.g. boreholes.

- The backfill of underground openings, including the central tunnels, access tunnels, shafts, and other excavations, and the installation of hydraulic plugs and the seals near the surface, will likely be carried out for KBS-3H in the same manner as for KBS-3V. These components have safety functions that are the same for both design variants and the same requirements also apply. Eventual needs for some special design solution for the backfilling of central tunnels for KBS-3H is a question to be considered in the coming project phases. The requirements on the backfill of the central/main tunnels in KBS-3H might differ from the requirements in KBS-3V.

Their safety functions are:

- to prevent these openings from compromising the long-term isolation of the repository from the biosphere and normal human habitat,
- to contributing to favourable and predictable geochemical and hydrogeological conditions for the other engineered barriers by preventing the formation of significant water conductive flow paths through the openings, and
- to limit and retard inflow to and release of harmful substances from the repository.

Requirements are that:

- the backfill, together with plugs and seals, should ensure that the excavated parts of the repository do not form preferential pathways for groundwater flow and radionuclide transport and do not significantly change the bedrock hydrology (over the long-term), and
- the backfilling of the central tunnels should ensure that the buffer in the deposition drifts remains in place. Eventual needs for some special design solution for the backfilling of central tunnels for KBS-3H is a question to be considered in the coming project phases. The requirements on the backfill of the central/main tunnels in KBS-3H might differ from the requirements in KBS-3V.

Furthermore, the backfilling and sealing solutions for the upper parts of the repository are required to be designed in such a way as to discourage inadvertent human intrusion, hence limiting its likelihood.

3.4 Additional requirements from the operational point of view

3.4.1 Construction of the deposition drifts

Additional requirements related to operations have been established for the construction of the deposition drifts.

Construction begins with the drilling of a pilot hole. Requirements on the pilot hole and the drilling technology used to create it are that:

- Technology should permit the drilling of the pilot-holes up to 300 m.
- The vertical inclination upward shall be 2° ± 1°. In no occasion shall inclination be negative.
- The vertical waviness of the pilot-hole should be less than ± 10 mm over a length of 6 m.

Preliminary geometrical requirements, including tolerances, for the drift itself are given in Table 3-3 along with a summary of the reasoning that justifies them. Construction of the drift must also respect requirements concerning the buffer/rock interface given in Section 3.3.5 – in particular, the requirement for very limited disturbance to the buffer/rock interface adjacent to the distance blocks.

3.4.2 Control of groundwater inflow

The groundwater flow out of the deposition drift during its operational period must not be so high that it affects the installation of engineered components. Either pre-grouting in the pilot hole or Mega-Packer post-grouting will be used to limit substantial water inflow into the drift. The grouting will have to be durable for the operational time only. After this time hydrostatic pressure in the drift being equal to the pressure in the adjacent rock mass limits the inflow regardless of the grouting material. For the installation phase it is important to provide conditions where the water flow on the drift floor in the slot (42.5 mm) between floor and the components does not reach the bentonite blocks, which would result in erosion. The flow rate that would cause this erosion would have to be several tens of l/min.

Use of groundwater controlling techniques is proposed to reduce inflows during the whole repository construction phase in order to avoid drawdown of the water table which could lead to upconing of salt water. It is also important to ensure that there are no significant connective flow paths between the drifts and those parts of the repository that remain open for a long period, since these could lead to high flow rates and mechanical erosion of bentonite components. The tests performed with compartment plug have given very promising results regarding the self-sealing capacity of bentonite pellets preventing water (artificial and leakage water) flow from a sealed drift into open parts of the repository, see Section 4.7.

Table 3-3. Justification for preliminary geometrical tolerances for the KBS-3H deposition drifts based on the SKB design. The table is extracted from SKB (2008) with recent comments added.

Issue	Requirement	Justification
Length	< 300m	The repository layout shall be similar to KBS-3V. The length is considered to be feasible from a construction and operational point of view. However, optimisation of this length will be necessary after the KBS-3H technology has been demonstrated.
Diameter	1,850+5 mm	The drift diameter and the given tolerances are based upon operational as well as thermal heat flow, buffer density and swelling pressure considerations. In particular, the tolerances constrain the void space outside the Supercontainer such that acceptable buffer density and swelling pressure are after saturation.
Inclination	2°±1°	A positive inclination is a prerequisite for water drainage.
Deviation of pilot hole	< 2m from the nominal position at a distance of 300 m	A minimum distance between the drifts of 36 m has been adopted in thermal dimensioning of the repository layout for the 40 m layout alternative, see Section 8.1.
Steps	≤ 5 mm	Full-scale laboratory tests have verified that the emplacement equipment can move properly in the drift for steps of up to 5mm.
Roughness	≤ 5 mm	Full-scale laboratory tests have verified that the emplacement equipment functions properly for a roughness up to 5mm.
Straightness (waviness or deviation from the centre line)	± 10 mm over a length of 6,000 mm	The centre line deviation must be kept within small tolerances to prevent the Supercontainer from contacting the rock surface during transport in the drift.

3.4.3 Prevention of mechanical displacement and limitation of piping and erosion

The operation of the drift needs to be such that there will be no significant water pressure built up in the deposition drifts during Supercontainer and distance block emplacement that could cause movement of these components, or cause rupture or piping and transport of bentonite through buffer, prior to artificial watering.

Following artificial watering, high hydraulic pressure gradients and gradients in buffer swelling pressure may develop along the drifts, which could potentially lead to phenomena displacement of the distance blocks and Supercontainers. The distance blocks and filling blocks, together with the compartment and drift plugs, have the important design function of keeping the engineered components in the drift in place, and not allowing any significant loss or redistribution of buffer mass by piping and erosion. The distance blocks and filling blocks have a low hydraulic conductivity at saturation and will develop swelling pressure against the drift wall, such that friction will resist buffer displacement. Furthermore, the compartment plug is designed to stay in place under the applied loads (i.e. no significant displacement are allowed) until the next compartment is filled and a further compartment plug or drift plug installed.

3.4.4 Artificial watering

A favourable initial state of saturation is obtained by using Draining, Artificial Watering and air Evacuation (DAWE), see Section 4.3. After artificial water filling the buffer should swell uniformly and fill all the open space. The bentonite should have sealed the drift so that there is no flow inside the drift that can cause piping and transport of bentonite.

The artificial watering system is required to fill all void spaces in the drift compartment at approximately the same time, thus ensuring that the bentonite will swell and seal the drift uniformly. This minimises the risk of bentonite piping and erosion, as well as water pressure displacement of distance blocks and/or Supercontainers during the saturation phase after sealing of the drift.

3.4.5 Operation schedule

The installation of the engineered components in each deposition drift will be carried out in two steps. Installation in the inner section of the drift will take place first. This section will then be sealed with a compartment plug and subsequently water-filled according to the DAWE methodology. Installation in the second section – i.e. the section from the compartment plug to the drift entrance – will take place, followed by the construction of a drift plug and water filling according to the DAWE methodology. The time from deposition of the first Supercontainer until the drift is sealed and water is filled shall be as short as possible for the reasons stated below:

- The compartment must be filled as fast as possible because of the erosion, cracking of the bentonite in highly humid environment, which are dependent on time.
- The compartment plug shall be mounted without delay as well as the artificial water filling thereafter to accelerate the swelling of the bentonite (prevent erosion and rock spalling).

Inadequate sealing around the compartment plug could cause leaking of the artificially filled water from behind the plug into the open drift section and potentially cause erosion of bentonite components in the filled section.

Filling of the next compartment quickly would mitigate these incidents. Another reason for filling the second compartment and building a drift plug quickly is that the compartment plug is only dimensioned for full hydrostatic pressure assuming that no significant (more than 100 kPa) swelling pressure will occur before the drift is sealed. If the drift is kept open after emplacing the first compartment plug (longer than months), there is risk for increased swelling pressure from filling components and buffer which potentially could compromise the compartment plug.

The operational schedule will be detailed in the upcoming project phase.

4 KBS-3H design

One of the main objectives of the Complementary studies phase was to establish a KBS-3H reference design, see Chapter 6, two main design alternatives remained for comparison coming in to this project phase, the STC design and the DAWE design. DAWE was early identified as the main alternative and was eventually selected as the reference design. It should be noted again that a safety evaluation for DAWE was not carried out in the recent project phase, but it will be done for both Forsmark and Olkiluoto in the upcoming project phase.

This chapter gives a brief presentation of the earlier BD and the STC design and then focuses on presenting the reference design (DAWE), its components and results from full-scale demonstration of these in the recent project phase.

4.1 Evolution of the KBS-3H design

4.1.1 BD

The BD aims to isolate Supercontainer sections hydraulically, one from another, immediately after installation, thus preventing water flow from one Supercontainer section to another. This is mainly achieved by the rapidly sealing distance blocks. Important design features specific to the BD are: 1) the small, approximately 5 mm, gap between the distance blocks and the rock surface; 2) the requirement for a small gap between the Supercontainer and the distance block; and 3) the need for steel fixing rings to prevent the distance blocks from moving when exposed to hydraulic pressure.

The BD is presented in detail in Design Description 2007 (Autio et al. 2008), it was assessed as not being robust enough and it contains severe uncertainties, which are also described in more detail in that report. Based on the identified uncertainties this design alternative was not further examined in the studies during the project phase 2008–2010.

4.1.2 STC

In the preliminary STC design alternative, each Supercontainer section would be sealed with distance blocks and sealing rings that temporarily prevent water from flowing from one Supercontainer section to the next until the section is completely filled with inflowing groundwater. The sealing rings are not designed to withstand full hydrostatic pressure. Thus, once a section becomes filled, water flows into the next section. STC is presented in detail in Design Description 2007 (Autio et al. 2008).

The most significant uncertainties associated with the STC design are related to the potential loss and redistribution of buffer mass by erosion. Processes such as piping and erosion have been studied as a part of the KBS-3H design development (Sandén et al. 2008a). However, buffer swelling and sealing in heterogeneous inflow conditions along the long deposition drift and erosion rates at expected inflows remain subject to significant uncertainties. The behaviour of the new sealing ring design and the possibility of encountering detrimentally high hydraulic pressures because of rapidly sealing distance blocks have not been evaluated.

Thermally-induced rock spalling may take place in drift sections where buffer swelling pressure develops only slowly at the drift wall. There is a concern that thermally-induced spalling of rock could lead to connected pathways for flow and mass transport along the drifts. Thermally-induced spalling of the rock during the thermal period may take place in dry deposition drift sections in all design variants, but especially in the case of the STC design alternative in drift compartments that are relatively dry.

STC was one of the two designs evaluated during the recent project phase; it was, however, put on hold due to uncertainties regarding buffer behaviour, piping and erosion and possible displacement of buffer components.

4.1.3 DAWE

In the DAWE design alternative water is self-drained at the bottom of the drift during the installation phase. The empty space between the deposition drift wall and the Supercontainer, distance blocks and filling components inside a sealed compartment is then artificially filled with water. The water filling is done to accelerate the swelling of the buffer in distance blocks and in the Supercontainers. It is done rapidly and simultaneously in the entire compartment which basically removes the risk of inhomogeneous swelling and subsequent buffer displacement (Autio et al. 2008). The current design for water filling is to use short pipes that extend approximately 2 m into the drift behind the drift compartment plug or drift plug. The water supplied via these pipes will fill the air-filled volume remaining in the drift. The pipes are installed through the compartment plug as well as through the drift plug, see Figure 4-2. During the water filling air will be accumulated at the end of the drift due to its slightly upward inclination and this trapped air needs to be evacuated through a pipe that extends to the rear (~150 m) of the compartment section that is being flooded. After the water filling and air evacuation the pipes are removed from the compartment as required for long-term safety reasons. The deposition drift is sectioned into 2 compartments, each of approximately 150 m by a compartment plug and at the drift entrance by a drift plug. This is done for operational reasons; artificial watering and pipe removal is so far not considered feasible for a 300 m long section.

4.2 Premises for updating the drift design

Significant new information of bedrock properties, engineering design and buffer processes have been introduced since the last design was presented in Autio et al. (2008). This has enabled an update of some of the DAWE design components; the basis for this update is presented below:

- DAWE is based on water filling through a compartment plug or a drift plug. Erosion caused by water filling was identified as one important issue and has been studied in the recent project phase (Section 5.3). The study concluded that the erosion was not a critical issue when using fresh water to fill the void with short pipes.
- It has been suggested that filling blocks can be placed in sections with higher inflows which would eliminate the need for the previously used sections with two compartment plugs to section off inflow. This suggestion is based on studies described in Section 4.6.3.
- The drift plug system has been changed. A drift plug has been designed, effectively removing the need for the combined compartment plug + concrete drift end plug which was used in the previous design. The new plug is designed to take full hydrostatic pressure of 5 MPa and a buffer swelling pressure of 10 MPa, see Section 4.8.
- There is more information available on the groundwater inflows at the selected sites for repositories in Sweden and Finland (Olkiluoto and Forsmark) (Hartley et al. 2009) than in the previous project phase, 2004–2007, when the previous design was implemented (Autio et al. 2008). The newer data indicate that the inflows are smaller and more sparsely distributed than in estimates presented in Autio et al. (2008).
- The Mega-Packer post-grouting technique, see Section 4.9, using colloidal silica has proven to be efficient and can be used to reduce the inflows during the operational and the transient phase during which the buffer swells and fills the open gaps in the deposition drift.
- Understanding of the impact of water inflows on buffer behaviour has improved. The present understanding from a functional point of view clearly indicates that the inflows have less detrimental effects on buffer and filling components than earlier projected. Therefore the water inflow limits for the filling components can be elevated from an engineering point of view without affecting the behaviour of buffer negatively during time period from emplacement to water filling. This is supported by test results presented in Sections 5.3 and 5.8.

The most important conclusion drawn from the new information is that the water inflows in the deposition drift are smaller than the earlier estimates, that there are proven techniques to control the inflows and the buffer design of DAWE is not as sensitive to inflows as in the earlier BD alternative (Autio et al. 2008). The conclusion is that the present DAWE design is far more robust with respect to inflows than in earlier assessments. Therefore the drift design can be updated to correspond to the new information which will improve the technical and economic feasibility of the KBS-3H design in several ways.

It should be stated that one thing has not been taken into account when changing the design; this is the possible detrimental chemical erosion of buffer caused by diluted glacial melt waters which is an issue common with KBS-3V. This issue is of high priority for SKB and Posiva and the KBS-3H design could possibly be more sensitive to this since there is less bentonite in the deposition area and since multiple canisters are placed in one drift and there are no backfilled deposition tunnels. The latest information of SR-site (SKB 2011) will be used to address this issue by scoping calculations early in the upcoming project phase after which the design will be re-evaluated.

4.3 Description of the KBS-3H reference design (DAWE)

4.3.1 General

In the DAWE design alternative, multiple canisters containing spent fuel are emplaced at the depth of about 400–500 m in bedrock in parallel, 100–300 m long, approximately horizontal deposition drifts, see Figure 4-1.

In this report the following denominations are used for the components in the deposition drift:

- Drift entrance, the intersection between the main tunnel and the deposition drift.
- Drift end, earlier called Drift bottom end.
- Drift plug, earlier called Drift end plug.
- Compartment plug, also earlier called Compartment plug.

The deposition drifts with a diameter of 1,850 mm are bored slightly inclined from a niche in the main tunnel. A deposition drift is composed of two compartments (~150 m long each) which are separated by a compartment plug (Section 4.7). The outermost compartment is sealed by a drift plug, which is similar to the compartment plug.

In a compartment the Supercontainers are separated by cylindrical distance blocks (Section 4.5.3) to manage the heat and to seal off each canister position from the next, and to prevent the transport of water and bentonite along the drift. According to this design, about 30–40 Supercontainers depending on the type of spent fuel will be deposited in each drift. Filling components (Section 4.6) are placed in positions which cannot be used for Supercontainers or distance blocks based on positioning criteria e.g. long-term safety reasons dictate that the inflow rate into a Supercontainer position including distance blocks must be less than 0.1 l/min before grouting. Filling blocks are used in the inflow sections and transition blocks together with bentonite pellets, forming a transition zone, adjacent to the plugs. All components, except the pellet filling sections, are centred in the drift so that the slot width between the components and the drift wall is 42.5 mm. The drift components will be deposited using the deposition equipment, which is described in Section 9.4 and in more detail provided by Autio et al. (2008).

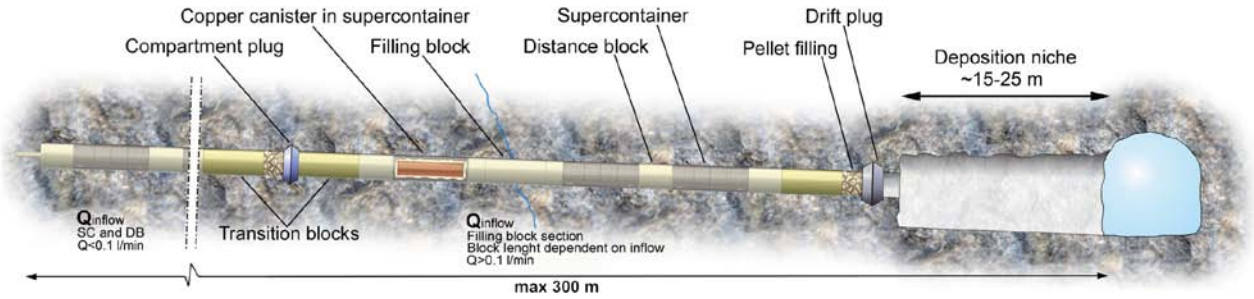

Figure 4-1. *Drift plug and the new filling components possibly removing the need for the dual compartment plugs at high inflow sections.*

Use of Mega-packer (Section 4.9) for groundwater control reduces inflow leakages into the drifts and reduces potential rate of bentonite erosion during the operational phase. The drainage of the compartment during deposition is achieved by the inclination of the drift, water will self-drain along the drift floor out of the drift until the compartment plug or the drift plug is installed. Spray or drip shields, thin titanium sheets, will be mounted in positions of water spraying or dripping in order to protect the buffer against mechanical erosion allowing the leakage water to flow freely down the drift walls to the floor.

In the previous KBS-3H project phase, 2004–2007, two drifts were constructed at the –220 level at Äspö HRL – one 15 metre long drift and one 95 metre long drift. The drifts were used to test grouting with the Mega-Packer and the deposition equipment. The drifts have also been used during the project phase 2008–2010; the longer drift has been used for continued testing of the deposition technique and deposition equipment while the shorter drift has been used for testing of the compartment plug. The Mega-Packer tests have also been finalised during this project phase.

The work on drilling and measurement techniques for production of drifts is discussed in more detail in Chapter 9. The design and requirements of the drifts has not undergone any major changes during the recent project phase, and the current requirements on the drifts are presented in Table 3-3.

4.3.2 Preparations in a drift prior to installation of the components

The plugs, compartment plug and drift plug, will be installed in sound rock with no fractures in drift sections that are determined prior to installation of the components. For the installation of the plug's notches have to be excavated in the drift and fastening rings casted in the notches as a preparatory measure before the installation phase. The fastening rings must allow unrestricted emplacement activity in the drift during the installation phase. Excavation of notches and casting of a fastening ring is described in more detail in Section 4.7.

The artificial water filling and air evacuation procedure requires that the 150-m-long air evacuation pipe is installed in the drift before the emplacement of drift components can be initiated. Installation of the air evacuation pipe is described in more detail in Section 4.10.

4.3.3 Plugging

When the drift components including the pellets have been deposited the compartment is sealed with a plug. Installation of the plug includes welding of the collar to the previously casted fastening ring (Section 4.7). Air and wetting pipes with valves are inserted through the collar lead-in tubes. The cap of the compartment plug, with the pellet filling pipe, is subsequently welded to the collar. The section between the compartment plug and the transition block is filled with bentonite pellets through the pellet filling pipe in the cap. The filling pipe is plugged by a blind flange bolted in place after filling. Installation of the plug is described in Section 4.7. Design of the plugs, compartment plug and drift plug, are described in Sections 4.7 and 4.8 respectively.

4.3.4 Wetting and air evacuation

In the DAWE design alternative the empty space in the slot between the deposition drift wall and the Supercontainer, distance block and filling components inside a sealed compartment will be artificially filled with water. This will ensure initial swelling of the buffer, the development of counter-pressure against drift surface and that the canisters are locked in place and axial displacement and significant buffer erosion can be avoided. The volume of the slot for a 150 m long drift compartment is approximately 40 m^3. The water filling is made rapidly and in order to accelerate the swelling of buffer and filling components simultaneously in the compartment. The ground water inflow into the drift will eventually slow down as the pressure inside the drift increases after installation of the compartment plug or drift plug. Pressure gradient will be even in the drift and in the adjacent rock mass.

Water filling will be done by pumping fresh water through the plug with short (appr. 2 m) wetting pipes. During the water filling air will be compressed and accumulated at the end of the drift compartment due to its slightly upward inclination, this trapped air needs to be evacuated through a pipe (maximum length 150 m) to allow complete filling with water. For water filling and air evacuation

purposes the collar is equipped with four identical lead-troughs with valves, three for the water pipes and one for the air evacuation pipe. The three short water filling pipes extend behind the pellet filling section underneath the transition block, see Figure 4-2. In the compartment end the air evacuation pipe is extended with a short bottom pipe to the highest point of the drift, this ensures complete water filling, see Figure 4-3.

Water is pumped in through the three pipes with a flow rate of about 25 l/min per pipe for approximately 8 hours and after the water starts to come out of the air evacuation pipe all the valves are closed.

4.3.5 Pipe removal and sealing a compartment

Water filling and the subsequent pipe removal were identified as a potential weakness in the DAWE design in the previous project phase and focus was put on developing and studying water filling methods that would minimise the risk involved in removing long pipes. Water filling using shorter pipes was proven feasible in erosion tests carried out during the recent project phase, see Section 5.3, providing advantages both in terms of technical performance due to less preparative work, shorter water filling time etc. and from a long-term safety point of view, because the risk of foreign material left in the drift due to failure in removal is much smaller.

After the water filling and air evacuation have taken place the pipes will be removed from the compartment as required for long-term safety. Removal of the long air evacuation pipe and the short water filling pipes will take place directly after the water filling and air evacuation phase. When removing the long air evacuation pipe a coupling will allow the short bottom pipe to release, the short bottom pipe will be left in the drift.

The winch system for removing the air evacuation pipe is set-up at the deposition niche and the procedure will depend on the location of the plug. In the case of the compartment plug, located approximately at the middle point of the drift, the pipe can be pulled out in one piece to the first half of the drift and then divided into 6 m long pieces. In the case of the drift plug the pipe is pulled out in long sections as allowed by the space (niche and central tunnel) available, probably as 24–30 m long parts. After the pipe is totally removed the ball valve of the lead-through tube is closed.

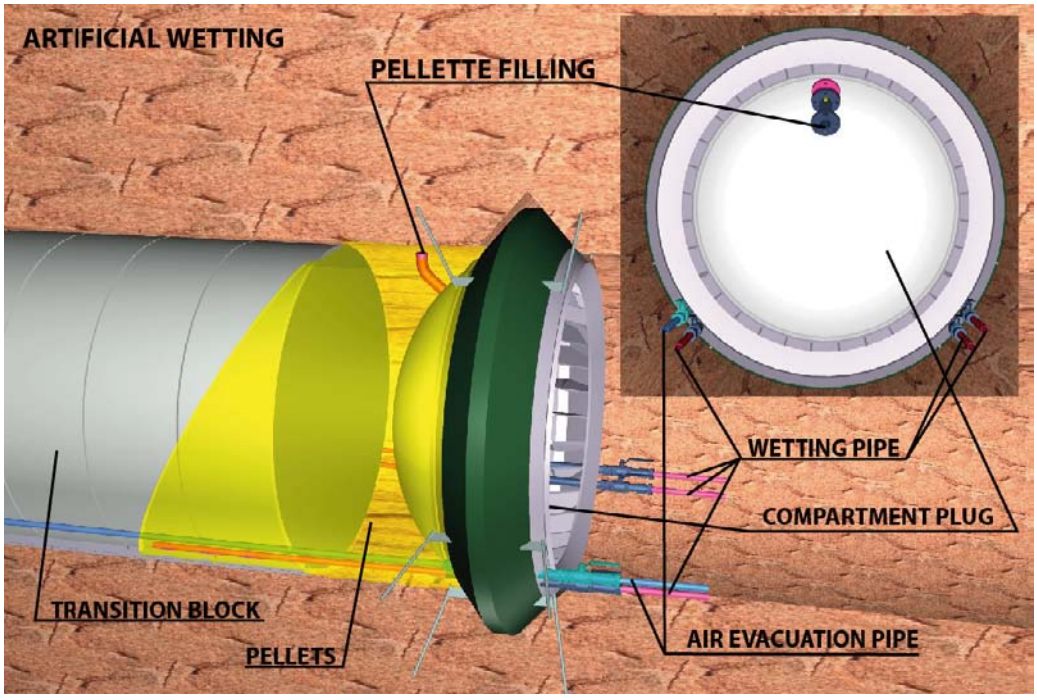

Figure 4-2. *Main components of the water filling system with short pipes through the compartment plug (similar design for the drift plug). The three short water filling pipes lead the water past the pellet filling section underneath the transition block. Perspective view orthogonal to drift axis and view parallel to drift axis, facing the plug.*

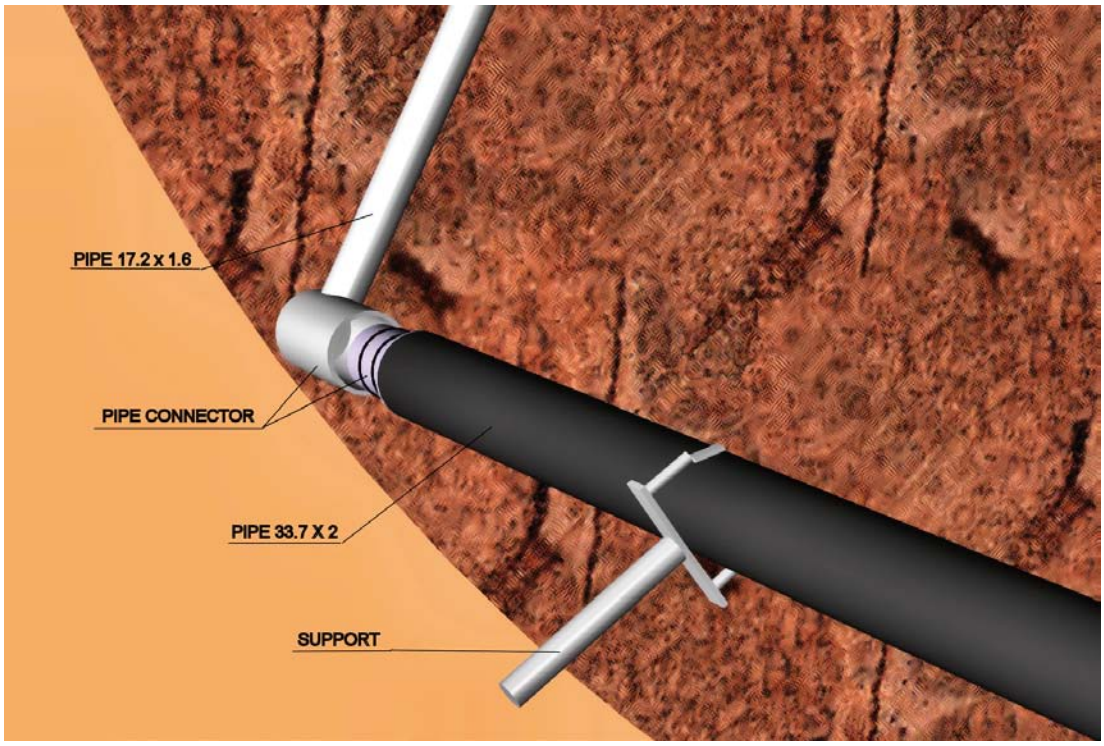

Figure 4-3. *Location of the air evacuation pipe at the rear end of the drift. The short pipe in the rear part of the drift (compartment) that is turned upwards to the roof is needed because the air is accumulated in the upper part of the inclined drift.*

4.4 Supercontainer

4.4.1 General Design

The KBS-3H design is based around the canister and the buffer being emplaced as one unit rather than as in the KBS-3V case, the buffer being installed first followed by the canister in a separate step. The KBS-3H canister-buffer unit including an outer shell is denoted a Supercontainer. The design and assembly of the Supercontainer is described in detail in the design description 2007 (Autio et al. 2008).

One of the main objectives with the Complementary studies of horizontal emplacement KBS-3H 2008–2010 phase was the selection of a material for the Supercontainer shell with the aim of selecting a material that fulfils long-term safety and operational requirements. Titanium and copper together with structural steel have been evaluated. The studies of metal-bentonite interactions including the material selection are elaborated in Chapter 7. Some fabrication considerations and cost implications are presented below.

The Supercontainer is depicted in Figure 4-4 showing the spent fuel canister surrounded by a bentonite buffer and the perforated metal shell. The shell has an outer diameter of 1,765 mm, a length of 5,525 mm and a thickness of 8 mm using structural steel. The Supercontainer shell is provided with five pairs of feet with a height of 42.5 to 45 mm and 73.5° spacing. The shell has a perforation of 60% with 100 mm diameter holes, the end plates are solid and the total weight of the empty shell is 1,108 kg including the feet using structural steel. Fully loaded with canister and buffer the weight of the Supercontainer is approximately 46 tonne.

The Supercontainer is designed to withstand unfavourable load conditions induced by variations in the excavation of the deposition drift. For example, where a step-like unevenness exists on the surface of the deposition drift floor, causing uneven load on the Supercontainer.

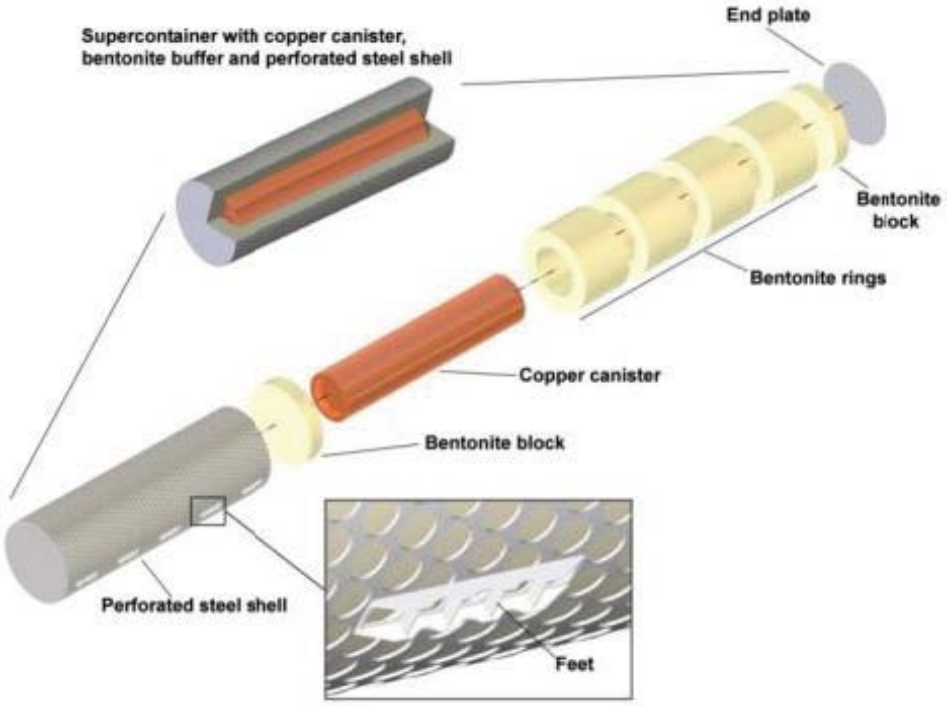

Figure 4-4. *The KBS-3H Supercontainer made up of a canister surrounded by buffer rings and blocks with an outer perforated metal shell to keep the unit together.*

4.4.2 Alternative materials, fabrication considerations and cost aspects

Long-term safety is always the number one requirement when selecting materials for the repository. However, when materials perform similarly with respect to safety and operation, cost is going to be an important aspect in selection of material for use in the Supercontainer.

Several copper, titanium and steel alloys have been considered for use in manufacturing the shell portion of the Supercontainer. There are large differences between different grades of the materials. The overall conclusions for each material in comparison with the originally used structural steel (S235JRG2) are presented below.

There should be no big surprises associated with making the Supercontainer. Bending of plates and making holes in materials of higher tensile strength demand more of the production equipment but this will be taken care of by qualified manufacturers working with qualified procedures. Welding can also be carried out with fairly conventional methods.

Special care must be taken to ensure that manufacturing procedures are correctly adjusted to the grade of material used and manufacturing is performed in accordance with qualified procedures in order to maintain the desired mechanical properties of the welded units.

Titanium is a strong material with good mechanical properties and allows for a thinner Supercontainer which in turn brings additional benefits by enabling some optimisation of the buffer; altered water content or an increased initial amount of buffer. Concerning the titanium grades, grade 2 is the standard and most commonly used. If grade 3 and grade 4 could be used instead, the material volume needed for manufacturing of the Supercontainer could be markedly reduced. A titanium Supercontainer has not been designed in detail during the recent project phase; this will be done in the upcoming project phase. Initial FEM- calculations using titanium grade 3 indicate that the shell thickness can be reduced to 6 mm with acceptable stresses, strains and deformations. The reduction in shell thickness could impact the practicality of production and these aspects will also be addressed in the upcoming project phase.

A copper Supercontainer has previously been designed; it, however, required a redesign with increased material thickness due to coppers poorer mechanical properties compared to steel and titanium.

A study of the cost for manufacturing of the Supercontainers based on different shell materials has been carried out. The cost calculations were based on the established shells of 10 mm for copper, 8 mm for steel and the estimated 6 mm for titanium.

The fact that no design has been done for a titanium shell is a complicating circumstance. Initial estimations on manufacturing procedures indicate that manufacturing costs (material excluded) for a titanium shell will not be significantly different from the steel shell version.

Spot prices to calculate a rough minimum price and plate sales prices from manufacturers to produce more realistic costs together with scrap prices for the selling of excess material were used when doing the calculations for copper. Conclusions from the price study are presented below. Spot price of copper from 18 March 2009 was used; 4,380 US$ per tonnes (~34,300 SEK/~3,270 EUR), at the US$ exchange rate of 7.85 SEK. Titanium price was based on supplier estimate, as of 27th May 2009 at approximately 16,300 US$ per tonnes (~128,000 SEK/~12,200 EUR) at a similar US$ exchange rate.

The production cost (material and manufacturing) for one Supercontainer made of:

- copper is (10 mm thickness) 340,000 SEK
- titanium is (6 mm thickness) 310,000 SEK
- structural steel S235JRG2 is (8 mm thickness) 150,000 SEK

The price for structural steel is only included as a reference to show the consequence of choosing more expensive materials, and based on the actual cost to manufacture the Supercontainer used for the deposition equipment tests at Äspö.

The comparison clearly shows that the price of a Supercontainer will increase considerably if a material other than structural steel is selected. Cost is however of secondary importance to guaranteeing long-term safety. The conclusion arising from safety considerations is that titanium would be better with regard to cost and that steel has potentially undesirable effects on system performance (corrosion and interaction with buffer). Both titanium and copper have high corrosion resistance. The material selection process together with discussion of the impact on material selection is presented in Chapter 7. Titanium has been selected as the material for the Supercontainer shell.

One thing that will require further consideration when calculating costs is that the future cost of materials are difficult to predict because supply, demand and prices fluctuate considerably.

4.5 Conceptual design of buffer components

4.5.1 General

The project phase 2008–2010 included the conceptual design of the buffer components inside the Supercontainer (ring shaped blocks and solid blocks at both ends, see Figure 4-4) and the distance blocks placed between Supercontainers. These buffer components are composed of the same reference buffer material with differences only in dry densities and water contents. In addition to the conceptual design of the components, work during the project phase 2008–2010 has been focused on solving important buffer issues such as swelling/spalling of rock, piping and erosion, and buffer issues related to artificial watering. The results of work on buffer issues have been documented in several reports and the main results and conclusions together with the references to the publications containing this supporting information are presented in Chapter 5. The conceptual design of buffer components is presented below. The design at this stage has not addressed the design of the feet under distance blocks and optimization of slices composing the distance block.

The dimensions of distance blocks and buffer segments in Supercontainers are different for Swedish and Finnish repository designs and depend on the canister length, canister spacing, drift spacing and thermal conductivity of bedrock. It is assumed that the buffer components can be manufactured either by uniaxial or isostatic compaction technique. The differences between uniaxially and isostatically compacted material has not yet been studied thoroughly. This, as well as the size optimization of buffer components, is proposed to be addressed in the future work, see Section 5.9. The KBS-3H

project has so far opted for the more developed uniaxial compression and drawings for such a buffer mould has been developed in the recent project phase, see Section 4.5.4. This mould will be ordered and the technique will be tested in full-scale in the upcoming project phase, see Section 10.

The design presented in this chapter is based on requirements for buffer given in Section 3.3.4.

4.5.2 Buffer blocks in the Supercontainer

The buffer is composed of different types of bentonite sections with different dimensions, dry densities and water contents. Section I corresponds to ring-shaped blocks, Section II to solid cylindrical blocks at both ends inside a Supercontainer and section III to solid cylindrical distance blocks between Supercontainers.

The buffer inside the Supercontainer consists of a sufficient number of ring-shaped blocks and solid blocks depending on the repository design alternative. The reference designs of the blocks are presented in Table 4-1 and Figure 4-5. The densities are given as dry densities.

Table 4-1. Reference buffer blocks inside the Supercontainer.

Design parameter	Nominal design	Accepted variation
Solid blocks inside the Supercontainer		
Dry density	1,753 kg/m^3	± 20 kg/m^3
Water content	17 %	± 1 %
Dimensions	Height: 350 mm	± 1 mm
	Outer diameter: 1,740 mm	+ 1/–2 mm
Ring shaped blocks inside the Supercontainer		
Dry density	1,885 kg/m^3	± 20 kg/m^3
Water content	11 %	± 1 %
Dimensions	Height: 1,211 mm	± 1 mm
	Outer diameter: 1,740 mm	+ 1/–2 mm
	Inner diameter: 1,058 mm	± 1 mm

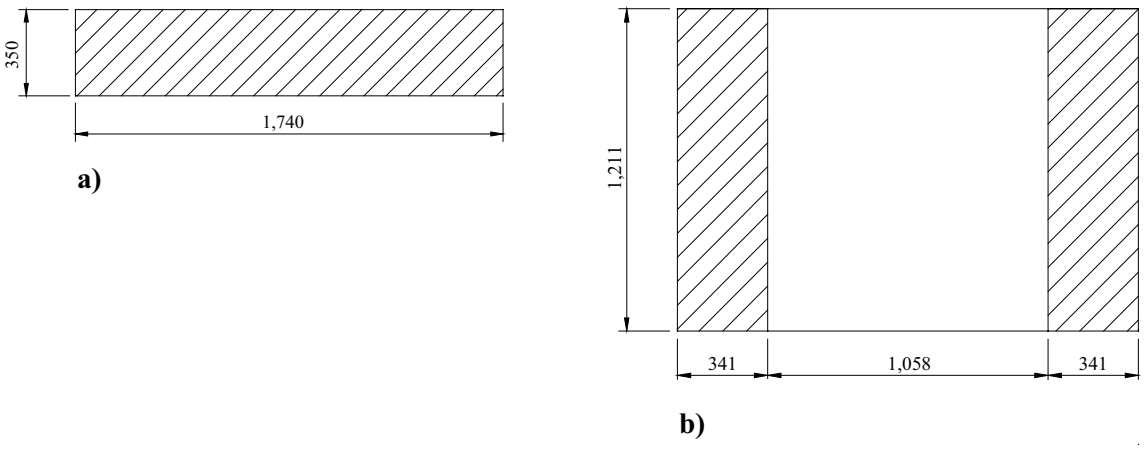

Figure 4-5. *Cross-sections of the cylindrical blocks inside the Supercontainer a) solid blocks, b) ring shaped blocks around the canister. The final thickness of the ring-shaped blocks depends on the selected compaction technique.*

4.5.3 Distance blocks

The distance blocks are placed between the installed Supercontainers in a drift. The reference design of the blocks is presented in Table 4-2 and Figure 4-6. The densities are given as dry densities. The water content of the distance blocks is higher than in the Supercontainer blocks in order to prevent humidity induced cracking during operation.

The length of each distance block section varies dependent on the thermal properties; type of canister, bedrock properties and the layout. The Finnish reference distance block lengths are illustrated in Figure 4-7 and Table 4.3 presents a summary of four different canister spacing's and corresponding distance block lengths for Swedish spent fuel canisters.

Table 4-2. Reference buffer block outside the Supercontainer (distance blocks).

Design parameter	Nominal design	Accepted variation
Solid blocks outside the Supercontainer (distance blocks)		
Dry density (kg/m^3)	1,712 (kg/m^3)	±20 (kg/m^3)
Water content (%)	21 (%)	±1 (%)
Dimensions (mm)	Height: 500 mm Outer diameter: 1,765 mm	±1 (mm)

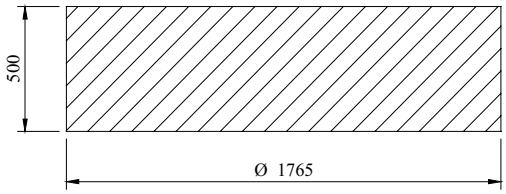

Figure 4-6. *Cross-section of the solid cylindrical distance blocks.*

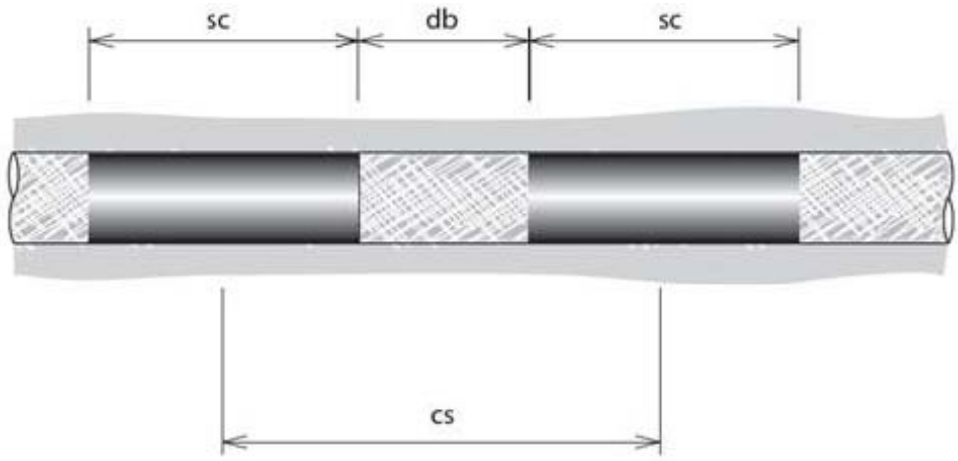

	Canister spacing *cs* (m)	Distance block *db* (m)
LO 1 & 2	7,2	2,875
OL 1 & 2	9,0	3,475
OL 3	10,6	4,625

Figure 4-7. *Different distance block alternatives for Finnish spent fuel canisters (Kirkkomäki and Rönnqvist 2011).*

Table 4-3. A summary of four different canister spacing's and corresponding distance block lengths for Swedish spent fuel canisters with respect to deposition drift spacing and thermal conductivity of bedrock.

Drift spacing	Thermal conductivity 2.9 W/mK		Thermal conductivity 3.57 W/mK	
	Canister spacing (m)	Length of the distance block (m)	Canister spacing (m)	Length of the distance block (m)
40 m	7.9	2.34	6.5	0.94
30 m	8.6	3.04	7.2	1.64

4.5.4 Buffer mould

The buffer blocks of the Supercontainer, the distance blocks and the filling components (Section 4.6) can either be manufactured using isostatic or uniaxal compaction. Since isostatic compaction is under development and there is more experience for the uniaxal technique the KBS-3H project has opted for uniaxally compressed blocks, this can of course be changed later on. The drawings for a buffer mould for uniaxal compaction of KBS-3H buffer was ordered during the recent project phase, the work is ongoing when this report is being compiled. The mould will be designed so it can be used for compaction of Supercontainer rings and blocks as well as distance blocks. The work is based on the mould developed for the KBS-3V buffer. At uniaxial compaction the bentonite is filled and compacted in axial direction. The block is compacted in one step, due to the limitations in the press the length of compacted components are limited to 0.5 metres. To get a homogeneous block lubricant is used on the mould (bentonite contaminated with lubricant will be machined off). Further machining ensures blocks within the requirements, of correct evenness and dimensions.

4.5.5 Verifying analysis of the final buffer density

The nominal values of the parameters yield a final target buffer density of about 2,000 kg/m^3 after saturation, which is the target density with the allowed density range being 1,950-2,050 kg/m^3. The following parameters have been varied in order to evaluate the sensitivity of the final average buffer density:

1. The section of the buffer. The ring shaped blocks (Section I of the buffer) are placed around the canister in the Supercontainer while the solid blocks (Section II of the buffer) are placed at the end sections of the Supercontainer. Distance blocks (Section III of the buffer) are positioned outside each Supercontainer separating the installed Supercontainers.
2. The diameter of the deposition drift can vary between 1,850–1,855 mm.
3. The dry density of the blocks (about ±20 kg/m^3 from the nominal values).
4. The type of Supercontainer shell (steel/copper/titanium), titanium being the reference material.
5. The volume of the corroded Supercontainer shell (constant/twice to triple for the shell made of steel, copper and titanium) – for titanium, due to the very low corrosion rate (1 nm/yr), it will take a very long time to get the volume increase.

The Supercontainer including the perforated titanium shell, selected as the reference design, has an outer diameter of 1,761 mm and an inner diameter of 1,749 mm (i.e. thickness of 6 mm). In the case of using steel the outer diameter of the Supercontainer is 1,769 mm and the inner diameter of 1,749 mm. The third material alternative included in the calculations was copper with the maximum outer diameter of 1,769 mm and the inner diameter 1,749 mm.

Table 4-4. Data extracted from the analyses of the buffer density. The calculations are made for a Supercontainer shell made of titanium with the assumption of having constant volume of the corroded shell.

The green marked numbers in the table are nominal data for the installed system.

Diameter drift (m)	Dry density block (kg/m^3)	Section	Buffer density at saturation (kg/m^3)
1.850	1,885	Section I	2,000
1.850	1,905*)	Section I	2,024
1.855	1,865**)	Section I	1,981
1.850	1,753	Section II	1,998
1.850	1,773*)	Section II	2,019
1.855	1,733**)	Section II	1,981

*) The dry density of the buffer blocks is assumed to be 20 kg/m^3 higher than the nominal value.

**) The dry density of the buffer blocks is assumed to be 20 kg/m^3 smaller than the nominal value.

4.5.6 The effect of gaps on the final buffer density

The calculations made assume that no swelling in axial direction occurs. The dimensions of the canister (diameter 1,050 mm, total length 4,835 mm), Supercontainer shell (length 5,560 mm ± 6 mm) and blocks (see Section 4.5) imply that there is a gap between the canister lid and the solid blocks which will result in axial swelling of the buffer during the saturation. According to the geometry of the reference design of KBS-3H the total gap between the canister and the solid blocks is 9 mm. Assuming that this gap will vanish during the saturation phase, it is possible to calculate an average density of the buffer in the section between the canister lid and the Supercontainer lid, using a dry density of the solid blocks of 1,753 kg/m^3 and corresponding dry density for the ring shaped blocks of 1,885 kg/m^3. The buffer density at saturation calculated at these conditions will be about 1,985 kg/m^3. This density is above the lowest acceptable density at saturation of 1,950 kg/m^3.

4.5.7 Conclusions

The calculations used to estimate system density are based on the data for the drift, the Supercontainer and the buffer blocks presented in this report. The following conclusions can be made from the calculations:

- The calculations of the buffer density at the three investigated sections assuming nominal values of the density and dimensions of the blocks, nominal dimensions of the drift, a Supercontainer shell with constant volume and no axial swelling will give a final buffer density of about 2,000 kg/m^3 at saturation.
- A lower initial block density than the defined nominal value will result in a buffer density at saturation of less than 2,000 kg/m^3. The lowest saturated density, about 1,981 kg/m^3, was calculated for the case of blocks with an initial density of 20 kg/m^3 lower than the nominal both for the distance block (Section III) and for the solid blocks inside the Supercontainer (Section II) in the case of a Supercontainer shell made of titanium. Furthermore it is assumed that the drift has the maximum allowed diameter of 1,855 mm.
- When combining the highest acceptable densities of the blocks, tripled volume of the corroded Supercontainer shell with the minimum acceptable diameter of the drift (1,850 m) the calculated final maximum density at saturation will be about 2,039 kg/m^3 for the case of a Supercontainer shell made of copper.
- The calculations made for a Supercontainer shell made of titanium produce a buffer density at saturation between 1,981–2,024 kg/m^3.
- An axial swelling of the buffer with nominal values of the buffer and the drift will lead to a buffer saturated density of less than 2,000 kg/m^3. A simplified calculation of the buffer density when taking into account an axial swelling yields a final buffer saturated density of 1,985 kg/m^3 at one of the two end sections. This design presumes that the axial gap inside the Supercontainer is assembled at one side.
- The design at this stage has not addressed the design of the feet under distance blocks.

In summary, for all the cases examined for Supercontainer installation in deposition drifts according to the DAWE reference design, the equilibrated, water-saturated density of the buffer was within the allowed range of 1,950–2,050 kg/m^3. This should ensure that this type of installation also meets the thermal, hydraulic and mechanical requirements set for it.

4.6 Conceptual design of Filling Components

4.6.1 General

Significant buffer research, testing and technical development has taken place since the previous drift design was presented. This increased understanding, especially with respect to design requirements and evolution of the system after water filling has been taken into account when designing new filling components. This design work has also lead to a revision of the KBS-3H drift design which incorporates current understanding and results from the extensive testing and research on several issues, such as those presented in Chapter 5. The revised design basis and design is presented in this section. There are still some uncertainties left in the design. These are, however, not being assessed as critical for the feasibility of the design and presented in Section 4.6.4.

The new design has 6 different filling components; the components are shown in Figure 4-8 and listed below:

1. Filling adjacent to drift plug (compartment side).
2. Filling in inflow position.
3. Filling on entrance side of compartment plug.
4. Filling on drift end side of compartment plug.
5. Filling at the drift end.
6. Filling of the pilot hole.

The filling of the deposition drift outside the drift plug has not been developed and will be part of later backfilling design of the deposition niche and other tunnels.

All engineered system components, including not only the canister and the buffer, but also the auxiliary components must be designed to be mutually compatible. Although all components will inevitably undergo physical and chemical changes over time, e.g. due to chemical alteration or corrosion, saturation, swelling, none should evolve in such a way as to significantly undermine either the long-term safety functions or the design functions of the others.

The general KBS-3 and KBS-3H-specific long-term safety requirements and design requirements to support the long-term safety functions are presented in Section 3.3.6.

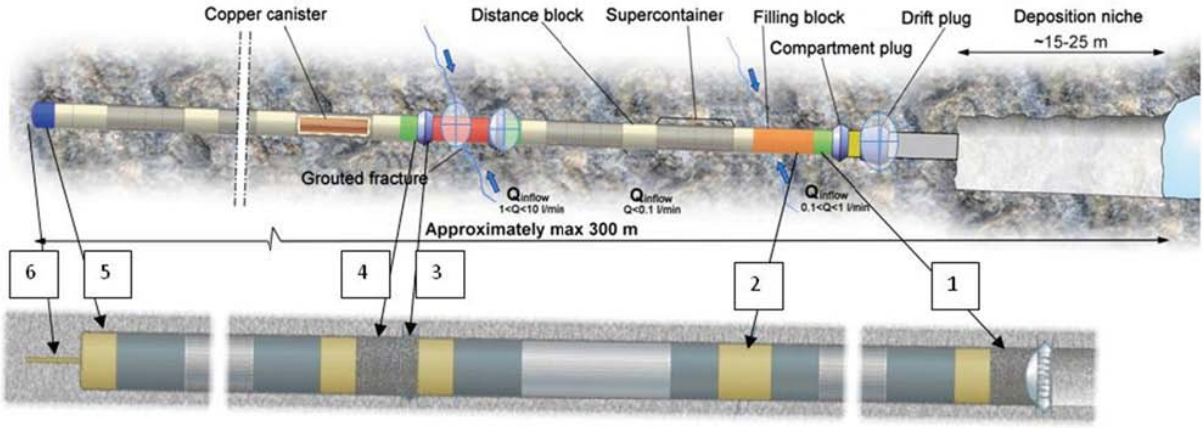

Figure 4-8. *Filling components in KBS-3H drift. The previous design based on Autio et al. (2008) is presented on top and the new design principle in Figure 4.1. The components that are not included in the new design principle are shown inside circles on top figure. Corresponding components in old and new design are shown with numbered arrows that refer to the list below.*

4.6.2 Additional basis for filling component design

Material selection and design

Na-bentonite of similar type to that used for buffer has been selected for use in the filling components; see Section 3.3.4 Table 3-2. This will allow distance blocks and the filling/transition blocks to be merged together.

Material selection was based on engineering judgement and the following arguments:

- It is assumed that the material used for buffer fulfils the requirements specified for buffer and therefore has a potential to fulfil the requirements for filling components as well.
- The recent research on erosion issues (Chapter 5) has shown that Wyoming type Na-bentonite material (commonly referred also as MX-80 type bentonite) used as bentonite buffer in KBS-3H design, can sufficiently resist the erosive action of fresh water being pumped into the drift when the water flows are orders of tens of litres per minute (Section 5.3), which can tolerate the erosion during water filling of the drift (see Section 5.3) when the water flows are orders of tens of litres per minute, which together with inflows from rock has been a main concern previously (Autio et al. 2008). Inflow from rock is not a main concern in the DAWE design alternative because the artificial water filling limits the erosion effect caused by inflows. Mechanical erosion due to inflow from rock is also prevented with spray and drip shields. After water filling the inflow becomes smaller since it is limited by the water absorption capacity of the buffer and filling components. Furthermore, the drift is sealed such that flow along its length is minimized.
- The bentonite clay proposed for use in the filling components is well known when compared to other materials or mixtures of materials with adequate swelling capacity and has been proven to be stable for long periods of time. The material also benefits from the research on buffer both within the KBS-3V and KBS-3H.
- The use of same material for filling components as buffer reduces or eliminates the risk for detrimental or uncertain physical and chemical reactions between filling components and other materials in the drift.
- Use of same material in the filling components as for the buffer gives the system addional buffering capacity which conforms with bentonite buffer.
- There are some uncertainties related to the behaviour of bentonite material such as post glacial erosion or effect of internal piping over long periods of time. These issues will be addressed in future research. It is likely that use of other materials may introduce new uncertainties in chemical and physical short- and long-term processes which have not been addressed and might therefore require initialisation of new research and hence impact on several present RD&D activities.

The design of the filling components is based on use of pellets and cylindrical blocks similar to distance blocks if possible. The blocks can be combined of fixed size thickness cylindrical block or the thickness can be adjusted to specific requirements based on operational considerations. The selection of design for the filling components was based on the following arguments:

- The filling components can be installed using same type of equipment (in principle) as for emplacing Supercontainers and/or distance blocks which has been proven technically feasible and efficient.
- Use of pellets is standard proven technique.
- The properties of filling blocks (e.g. density, length) can be dimensioned so that the diameter is same as for distance blocks.

Control of groundwater inflow

Presently there are no total inflow restrictions from engineering and short-term operational points of view. Since the drift is artificially filled with water in a time period which is less than one day, the effect of inflows from the surrounding rock mass is very small.

The only restriction for the groundwater flow out of the deposition drift during the operational period of the drift is that it must not be so high that it affects the installation of engineered components.

The current requirement is that the total water inflow for the drift can be no more than 10 litres per minute, however, the operation can tolerate larger inflows and it seems justified to increase the inflow limit or remove it from operational point of view.

If needed, inflows into the drifts during the operational period are proposed to be reduced by groundwater control techniques to avoid draw-down of the water table and mixing of the waters during the whole repository construction phase. It is also important to ensure that there are no significant connective flow paths between the drifts and those parts of the repository that remain open for a long period, since these could lead to high flow rates and mechanical erosion of bentonite components.

Prevention of mechanical displacement and limitation of piping and erosion

The operation of the drift needs to be such that there will be no significant water pressure built up in the deposition drifts during emplacement that could cause movement of components and other adverse effects, see Section 3.4.3.

Following artificial watering, high hydraulic pressure gradients and gradients in buffer swelling pressure may develop along the drifts, which could potentially lead to displacement of the distance blocks and Supercontainers. The distance blocks and filling blocks, together with the compartment and drift plugs, have the important design function of keeping the engineered components in the drift in place, and not allowing any significant loss or redistribution of buffer mass by piping and erosion. The distance blocks and filling blocks have a low hydraulic conductivity at saturation and will develop swelling pressure against the drift wall, such that friction will resist buffer displacement. Furthermore, the compartment plug is designed to stay in place under the applied loads (i.e. no significant displacement are allowed) until the next compartment is filled and a drift plug is installed.

Artificial water filling

It is assumed in design that a favourable initial state of saturation is obtained by using draining, artificial water filling and air evacuation as for buffer components, see Section 3.4.4. After artificial water filling the inflow into the drift is reduced significantly because the water pressure in the drift becomes practically same as in the surrounding bedrock. As a result there is only minor pressure gradient between the drift and surrounding rock mass. The water filling will accelerate the swelling of bentonite and the nearly simultaneous water filling and buffer swelling in the whole drift is beneficial regarding piping and erosion. As a result all void spaces in the drift compartment are filled at approximately the same time, thus ensuring that the bentonite will swell and seal the compartment uniformly.

Engineering basis

Compartment and Drift plug

The design and installation procedure of the plugs influences and to some extent determines the design of the adjacent filling components, see Chapters 4.7 and 4.8 for the plug designs. It is assumed that 1.3 m distance is needed between the crown of the cap and adjacent transition block in order to install the cap properly. Presently the length 1.3 m is defined as the distance from the collar of the plug which makes the results conservative from material density point of view.

Pilot hole

The length and diameter of the pilot hole stump at the drift end is approximately 2,000 mm and 152 mm respectively. The pilot hole is needed to steer the cutter head of drift boring machine.

Drift bottom end

Part of the air evacuation pipe will remain permanently at the drift bottom end as well as at the end of the compartment closer to the drift entrance and will be considered in the design. It has been assumed that the shape (curvature) of the drift face would be similar to that from Äspö demonstration which is presented in the Figure 4-9.

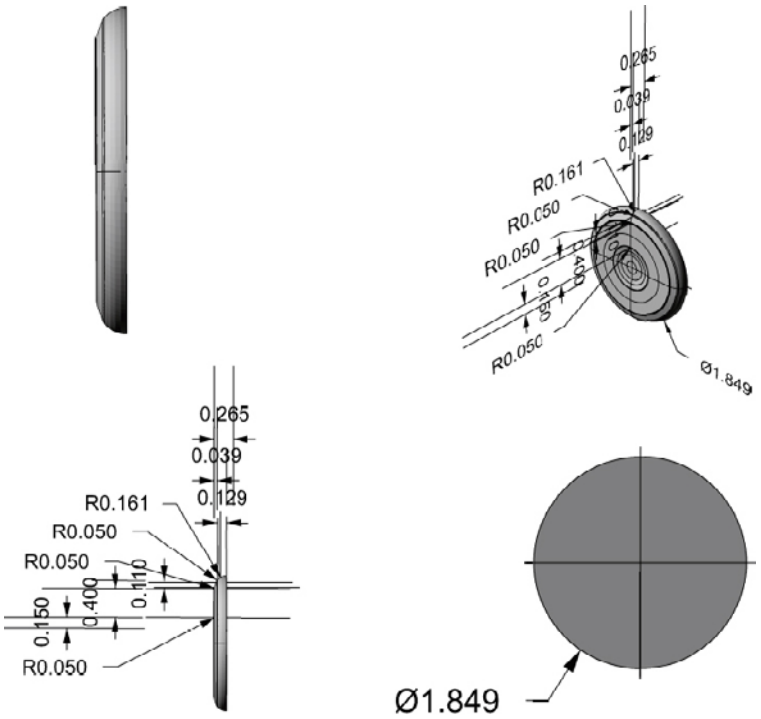

Figure 4-9. *The detailed geometry and shape of a 0.265 m thick section of the drift end with diameter of 1.849 m. Note that the dimensions are in metres. The vertical cross section is shown on top left and the face with dimensions in other pictures.*

Distance block

The distance block design has been presented in Autio et al. (2008) and is described above in Section 4.5.3. There are, however, several alternative lengths for distance blocks based on the type of canister (canister spacing depends on the different types of spent fuel, see Section 4.5.3), layout design and bedrock properties. The distance block length doesn't affect the design of filling components; however, it has impact on the utilization degree of drift and visualization of the whole drift system for readers. The length of 2.875 m was selected based on Table 4.3 and Figure 4-7 as the reference distance block length when designing the filling components because it is closest to the average of Finnish and Swedish distance block lengths.

Operation schedule

The time from the deposition of the first Supercontainer until the drift seal is in operation will be in the order of three months for one 300 m long drift, however, that is based on using concrete plug. The time will be clearly shorter (order of two weeks) if the titanium alloy drift plug (see Section 4.8) is used.

Groundwater inflow estimate updates

A summary is presented in Design description 2007 (Autio et al. 2008). The studies on groundwater flow and expected inflows have continued. Three representative different groundwater cases for Olkiluoto site, normal most likely case and two extreme cases (wet and dry) are presented here based on the results of DFN modelling for Olkiluoto (Hartley et al. 2009). These are all possible in the repository and the objective is merely to qualitatively illustrate the use of filling components in these different cases. The evaluation was based on the following principles:

- The DFN modelling results covered KBS-3V deposition tunnels in 9-metre sections; here we assume that similar inflow distributions apply for a KBS-3H deposition drift with 33 such theoretical sections.
- Three cases (median, dry, wet) were selected from the graph in Figure 4-10, arrived at summing up the contributions of the 9 m sections of individual tunnels, differing by 2 orders of magnitude, however the appropriateness of wet case in this study is not evident and should be addressed separate if needed.

- Expected inflows into unit length of 9 m (composed of a distance block and Supercontainer) were calculated according to the graph in Figure 4-11. The unit lengths were studied because an inflow which exceeds the limit will result in rejection of the unit length to be used for Supercontainer emplacement. This will impact on the number of Supercontainers that can be emplaced in a drift and also the costs associated with disposal.
- Inflow to each section is assumed to be due to one dominating fracture.

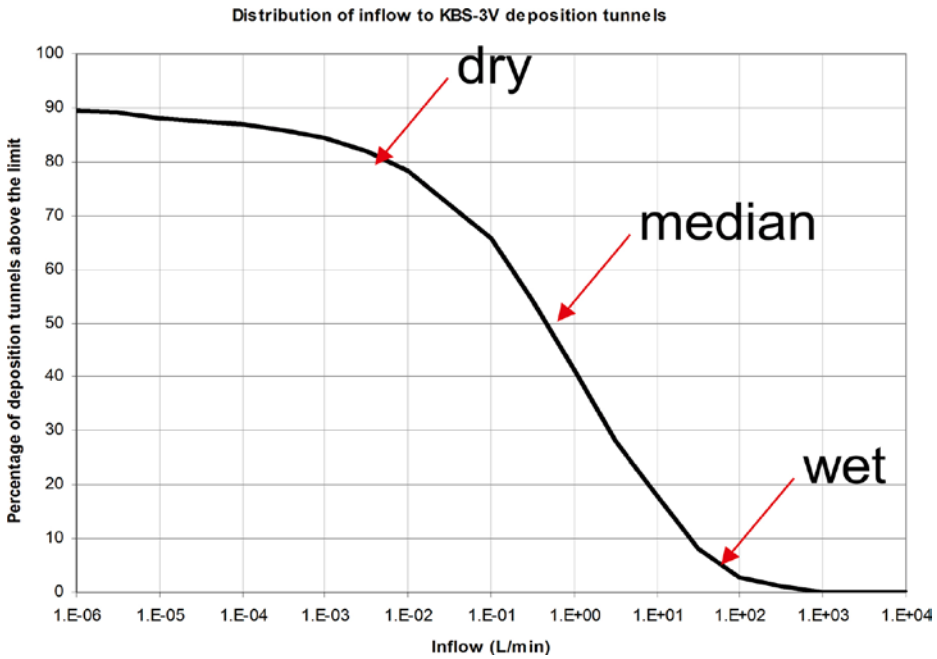

Figure 4-10. *Cumulative distribution of inflows in KBS-3H deposition drift. The three selected cases of total inflows are shown: the dry, median and wet case.*

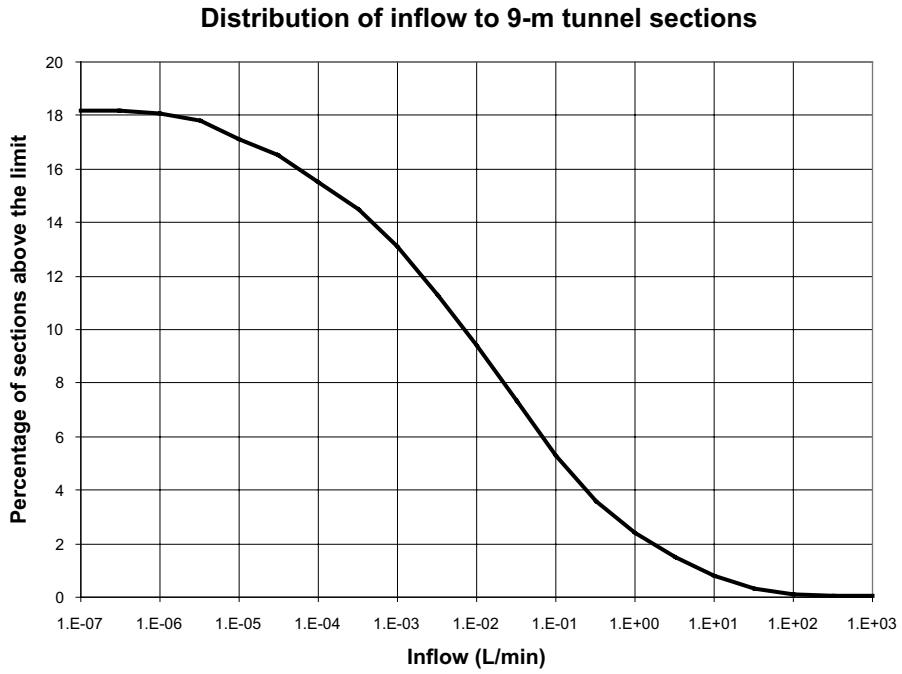

Figure 4-11. *Cumulative distribution of inflows into 9 m unit length drift section (composed of a Supercontainer and distance block) in KBS-3H deposition drift.*

Case 1: Median inflow KBS-3H drift

The results for case 1 simulations indicate the following inflows and inflow positions (see Figure 4-12):

- Total inflow into a 300-metre drift is 0.5 litres/min.
- 6 sections out of 33 have inflow:
  - One between 0.3–1 l/min.
  - One between 0.01–0.1 l/min.
  - Two between 0.001–0.01 l/min.
  - Two below 0.001 l/min.
- Above 0.1 l/min: 1 fracture.
- Above 0.5 l/min: no fractures.

Figure 4-12. *Case KBS-3H Median inflows drift of length 300 m. Inflows and inflow positions are shown.*

Case 2: Wet inflow KBS-3H drift

The results for case 2 simulations indicate the following inflows and inflow positions (see Figure 4-13):

- Total inflow into a 300-metre drift: 50 litres/min.
  - About 5% of drifts are above this limit.
- 10 sections out of 33 have inflow:
  - One between 30–100 l/min.
  - One between 10–30 l/min.
  - One between 1–10 l/min.
  - One between 0.1–1 l/min, two between 0.01–0.1 l/min.
  - Two between 0.001–0.01 l/min, two below 0.001 l/min.
- Above 0.1 l/min: 4 fractures.
- Above 0.5 l/min: 3 or 4 fractures.
- Above 1 l/min: 3 fractures.

Figure 4-13. *Case KBS-3H Wet inflow drift of length 300 m. Inflows and inflow positions are shown (see also Figure 3-16 in Hartley et al. 2010).*

Case 3: Dry inflow KBS-3H drift

The results for case 3 simulations indicate the following inflows and inflow positions (see Figure 4-14):

- Total inflow into a 300-metre drift: 0.005 litres/min.
  - About 20% of drifts are below this limit.
- 2 sections out of 33 have inflow:
  - One between 0.003–0.01 l/min.
  - One between 0.001–0.003 l/min.
- Above 0.1 l/min: no fractures.

The previously calculated inflows to KBS-3H deposition drift by Lanyon and Marshall (2006) and cumulative distribution of inflows were compared to the present results by (Hartley et al. 2010), see Figure 4-15. The comparison shows that the present estimate suggest less inflow (see the red curve in Figure 4-15) The differences are caused by the availability of more data especially on relevant depth and less transmissive fractures for the newer estimates (Hartley et al. 2009) than for the earlier estimates (Lanyon and Marschall 2006). In general, the estimates based on data by Hartley et al. (2009) are considered to be more reliable because of the more comprehensive data set they are based on:

- **Median** inflow 6 l/min (cf. Serco 0.5 l/min).
- **Wet** case (upper 5%) inflow 80 l/min (cf. Serco 50 l/min).
- **Dry** case (lower 5%) inflow 0.6 l/min (cf. Serco lower 20% of tunnels < 0.005 l/min and lower 10% of tunnels < 10–6 l/min).

Figure 4-14. *Case KBS-3H Dry inflow drift of length 300 m. Inflows and inflow positions are shown (see also Figure 3-16 in Hartley et al. 2010).*

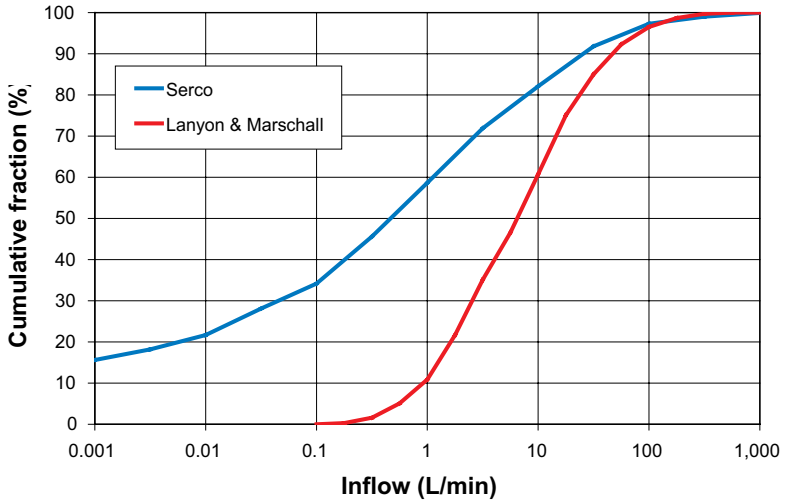

Figure 4-15. *Comparison of cumulative distribution of inflow into a deposition tunnel/drift at Olkiluoto by Lanyon and Marshall (2006) made earlier and the present result based on Hartley et al. (2009). Red curve refers to earlier results and blue curve to present results.*

The fracture directions have effect on the intersection lengths between drift and filling components and therefore affect the length of filling components. Estimates used in the DFN modelling are shown in Table 4-5 to give insight to possible ranges of inclinations. The different properties shown in Table 4.5 refer to following models:

- Model 1; emphasizing a good match to borehole data.
- Model 2; emphasizing a good match to outcrop data.
- Model 3; emphasizing a good match to ONKALO data.

The design of KBS-3H repository is based on avoiding horizontal fractured zones (as well as all fractured zones parallel to the drift) if possible and therefore based on Table 4-5 it is likely that fractures with plunge of 65 deg. will be intersected. The data is presented for illustrative purposes and no more comprehensive or qualitative analysis has been made.

Legend:

P32 is a measure of the volumetric fracture intensity, expressed as fracture surface area per unit of rock volume (m^2/m^3).

SH Set Sub horizontal fracture set.

EW Set Sub vertical fracture set with a pole orientation either to east or west.

NS Set Sub vertical fracture set with a pole orientation either to north or south.

r0 defines the minimum fracture size (in terms of equivalent radius) considered in the power-law distribution describing fracture size distribution.

kr fracture radius scaling exponent, which defines the shape of the power-law distribution describing fracture size distribution.

K (kappa) concentration parameter of the univariate Fisher distribution used to describe the fracture sets, K represents the degree of clustering of fracture poles around the mean pole. Larger values of K indicate higher clustering of fracture poles around the mean poles.

Table 4-5. Fracture orientation sets used in DFN simulation at Olkiluoto (Buoro et al. 2009). Data is used to illustrate effect of fracture direction on the length of filling components.

Parameter	Set / Units	Model 1			Model 2			Model 3		
Fracture Intensity	P_{32} SH Set (m^2/m^3)	1.43			1.15			1.15		
	P_{32} EW Set (m^2/m^3)	0.41			0.41			0.41		
	P_{32} NS Set (m^2/m^3)	0.46			0.46			0.46		
Fracture Size	SH Set r_0	0.35			0.35			0.45		
	SH Set k_r	2.50			2.70			2.80		
	EW Set r_0	0.25			0.25			0.45		
	EW Set k_r	2.30			2.30			2.70		
	NS Set r_0	0.35			0.35			0.45		
	NS Set k_r	2.20			2.20			3.60		
Fracture Orientation	SH Set (Trend, Plunge, κ)	320	65	8.2	320	65	8.2	320	65	8.2
	NS Set (Trend, Plunge, κ)	358	4	8.1	358	4	8.1	358	4	8.1
	EW Set (Trend, Plunge, κ)	268	8	8.1	268	8	8.1	268	8	8.1

4.6.3 Design of filling components

General

As presented earlier the updated KBS-3H drift design includes 5 types of filling components, which are illustrated in Figure 4-16. The design inside the compartment and drift plug are basically the same and 5 different components have been designed.

a) Filling inside the drift plug (and compartment plug).

b) Filling blocks in position of inflows.

c) Filling outside the compartment plug.

d) Filling at drift bottom end.

e) Filling of Pilot hole.

The design of filling components is based on the internal friction of the filling material and therefore permanent density gradients will remain in filling components. This assumption is commonly used in evaluation of buffer performance and is presently being studied in homogenization research (see Section in 5.5) in order to provide more evidence as to its validity.

Material used in filling components

The same material that is used in the buffer has been adopted in the filling components; the reference buffer material is bentonite clay with the material composition specified in Table 3-2. Examples of commercial bentonites with this material composition are MX-80 and Ibeco RWC (Deponit CA-N), which were analysed in SR-Can. The same material is used in the form of compacted blocks and pellets.

Filling blocks in positions of inflows

In the current KBS-3H design, filling blocks will be placed in drift positions intersected by fractures giving initial inflows to the drift above 0.1 l/min (Figure 4-17). Such drift sections are currently excluded as locations for Supercontainer or distance block emplacement.

The following modifications have been made to previous schematic design:

- There is half of a distance block on both sides filling block. This is due to a situation where there is an inflow less than the limit 0.1l/min used to reject it for emplacement of a Supercontainer and where a normal distance block is positioned between Supercontainers in this section.
- The length of filling block depends on: a) distance between transmissive leaking fracture (closest point of the fracture affected by inclination of fracture) and b) length of distance blocks. This is based on the principle that the length of the filling block sets the transport length (and resistance) from a canister embedded in the Supercontainer to the transmissive feature. Note that the design is consequently based on inflows before any possible sealing operations.
- It is assumed that the filling blocks are composed of 50 cm thick slices based on the present production technique and to simplify the operation. This, however, can be adjusted and optimised if needed.

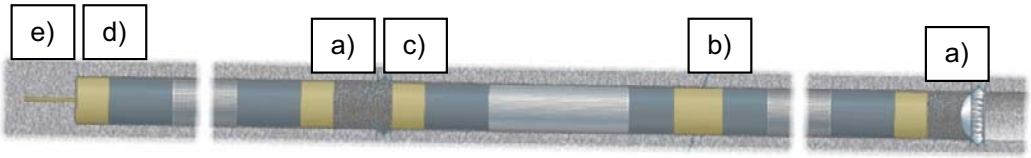

Figure 4-16. *KBS-3H drift design with different filling components.*

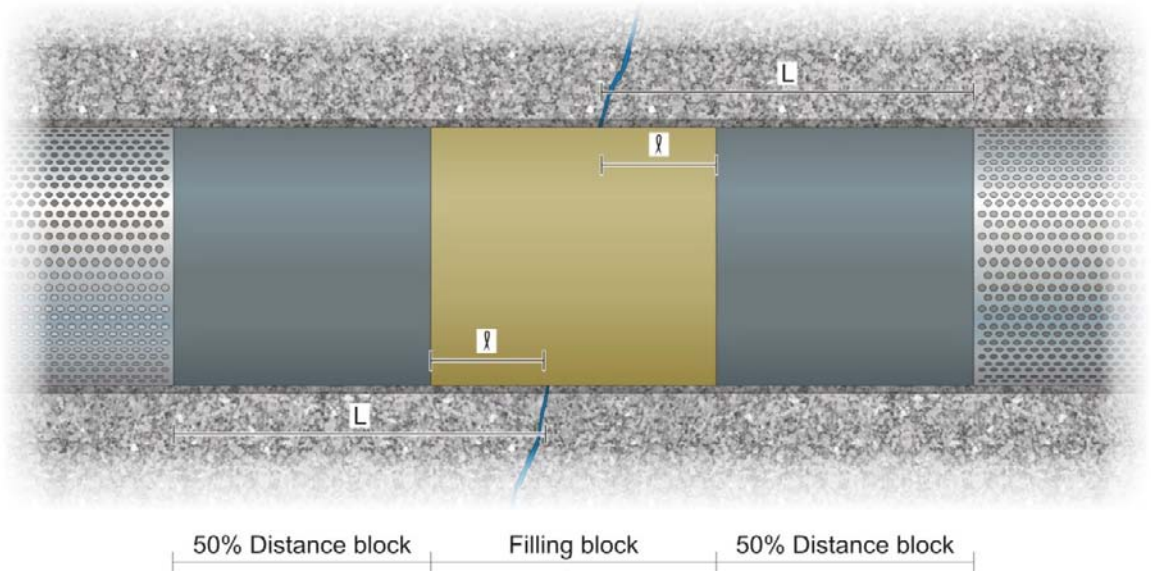

Figure 4-17. *KBS-3H drift, showing the position of a filling block between split distance blocks and 2 Supercontainers. Note that the inclination of fracture has effect on the length of filling block.*

Dimensioning

The length of the filling block has been established as a function of the initial inflow from the fracture using the principles presented above; see section 3.3.6 and Appendix A for details including scoping calculations. The calculations give tentative estimates for the respect distance needed to water-conductive fractures with specific inflows ranging from 0.1–0.5 l/min, 0.5–1 l/min and > 1 l/min. Based on these tentative estimates it has been suggested that filling blocks can be placed in sections with higher inflows which would eliminate the need for the previously used double compartment plug sections. The double compartment plug sections have not been eliminated from consideration and are still an option should conditions require their use. The calculations associated with these inflow conditions are presented in Table 4-6 below.

Design

It should be noted that the respect distances in Table 4-6 includes half a distance block section on each side (see Figure 4-17). The filling block designs corresponding to the selected distance block length and above mentioned respect distances are presented below in Figures 4-18 to 4-20.

The design of filling block is similar to distance blocks and a detailed description of the design can be found in Section 4.5.3. The reference design of the blocks is presented in Table 4-2. The densities are given as dry densities.

Table 4-6. Respect distances (L in Figure 4-16) with respect to inflow rates and allowed components.

Initial inflow range [litres min^{-1}]	Respect distance [m] and allowed component
< 0.1	Supercontainer section.
0.1–0.5	3 m (filling block + half a distance block on each side).
0.5–1	5 m (filling block + half a distance block on each side).
> 1	Alt 1. 6 m (filling block + half a distance block on each side). Alt 2. double compartment plug sections.

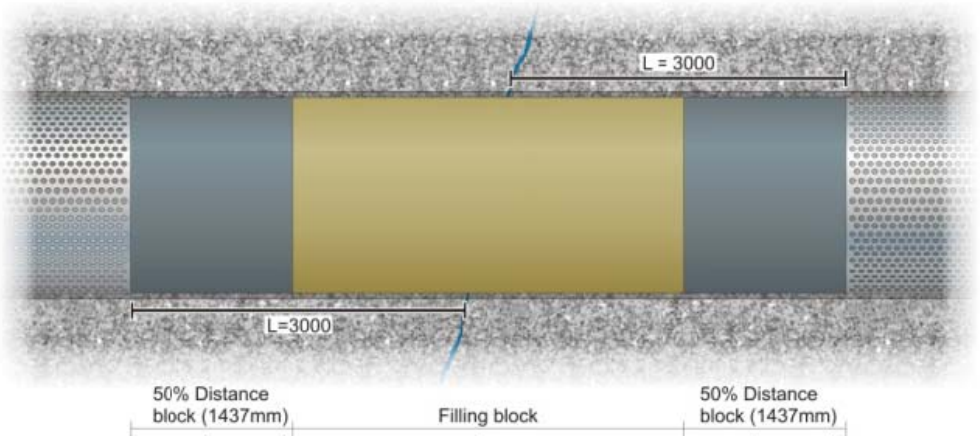

Figure 4-18. *Filling block for positions where inflow is 0.1–0.5 l/min.*

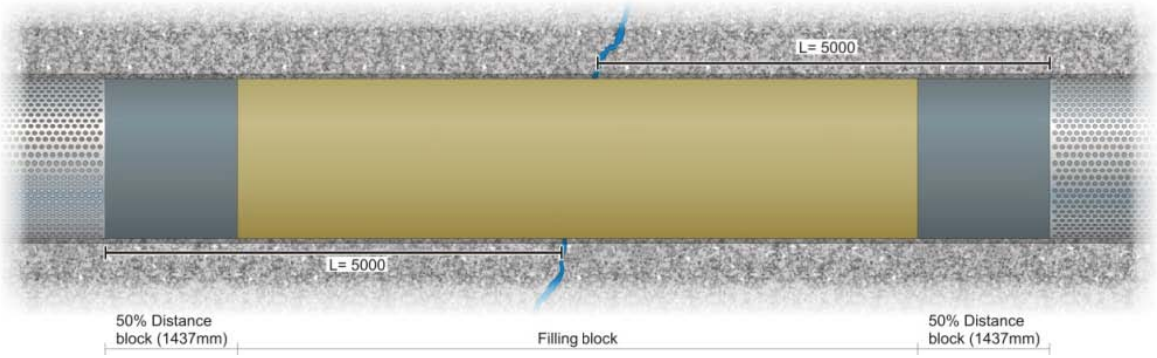

Figure 4-19. *Filling block for positions where inflow is 0.5–1.0 l/min.*

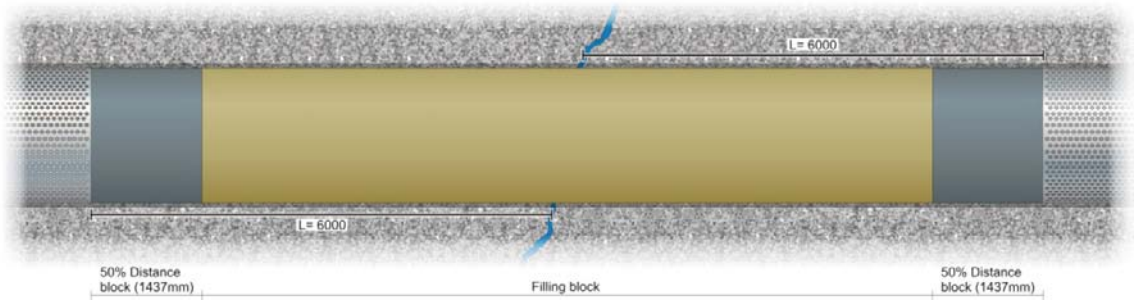

Figure 4-20. *Filling block for positions where inflow is larger than 1.0 l/min.*

Filling adjacent to drift plug and on drift bottom end sealed side of compartment plug

The design for filling components adjacent to the drift plug and for drift end bottom side of compartment plug are identical and therefore presented in this section. The schematic principle of filling adjacent to drift plug is shown in Figure 4-21 and that for filling components for drift end bottom side of compartment plug in Figure 4-22. The key requirements and factors specific to the drift plug and compartment plug affecting the design of filling components are similar with the exception that the compartment plug is exposed to hydrostatic pressure only and not exposed to significant swelling pressure of buffer and adjoining filling components as the drift plug. This difference was not assessed as having impact on the design of these filling components. The preliminary requirements and prerequisites can be summarized as:

- The drift plug must withstand 5.0 MPa hydrostatic pressures plus the swelling pressure of the bentonite inside the drift (10 MPa). The loading from filling should be as even as possible to reduce force heterogeneity on the plug.
- The compartment plug must withstand only hydrostatic pressure and insignificant swelling pressure of order of few tens of kPa's.
- The plug shall be tight assuming the largest allowed water leakage past the plug specified tentatively as 0.1 l/min. The compartment plug was tested in full-scale at ÄSPÖ HRL, see Section 4.7. The leakage during the test was initially at approximately 0.05 l/min and after a couple of days it was reduced to 0.002 l/min. Therefore it is likely that the leakage rate past the plug will be significantly lower than the requirements currently defined.
- The plug shall not under its working time or afterwards affect fulfilment of the requirements of the neighbouring distance block section. In particular, the density of adjacent distance block must not be affected.
- The function of drift plug needs to be maintained for a long time, see Section 4.8.
- It has been found feasible to use pellets to fill empty volumes immediately adjacent to plugs in order to enhance sealing of possible leakages through micro fractures.
- In order to be able to build the plug an empty space of 1.3 m is needed inside the plug in order to emplace the cap of the plug. The length used in this chapter was measured from the crown of the cap. However, present understanding is that it can be measured from the collar so that it is conservative here from filling material density point of view and the design could be optimised by shortening of transition blocks and pellet filling section accordingly. The plug includes lead troughs that allow for artificial water filling of the unfilled space inside the plug and there is a small lid in the plug for filling of bentonite pellets inside the plug.

The design is based on the following principle:

- The empty volume on the sealed side of the drift plug is filled with pellets resulting in lower density fill at the location relative to the remainder of the deposition drift (Figure 4-20).
- A section of compacted blocks of bentonite called transition blocks are placed between the pellet filled volume and adjacent distance blocks. As filling components absorb water and swell, there will be a transition zone from the drift plug to distance block with a density gradient.

Dimensioning

The design implies that the distance block adjacent to filling section is unaffected by the swelling in the transition zone containing transition blocks and pellets shown in Figure 4-21 and corresponding compression of the pellets filling. Since the pellets filling has a much lower density than the transition there will be blocks and pellets in the transition section there will evidently be a transition zone between the distance block and the plug where the density gradually changes. The required length of the transition zone is determined by the density gradient in the transition zone caused by the swelling of the transition blocks into the pellet filling. If some density deviation could be allowed in distance blocks, the length of transition zone could be made shorter. Due to mainly friction between the bentonite and the rock surface, the swelling of the transition zone will be restricted to a distance that can be estimated using equations that are derived from force equilibrium in axial direction.

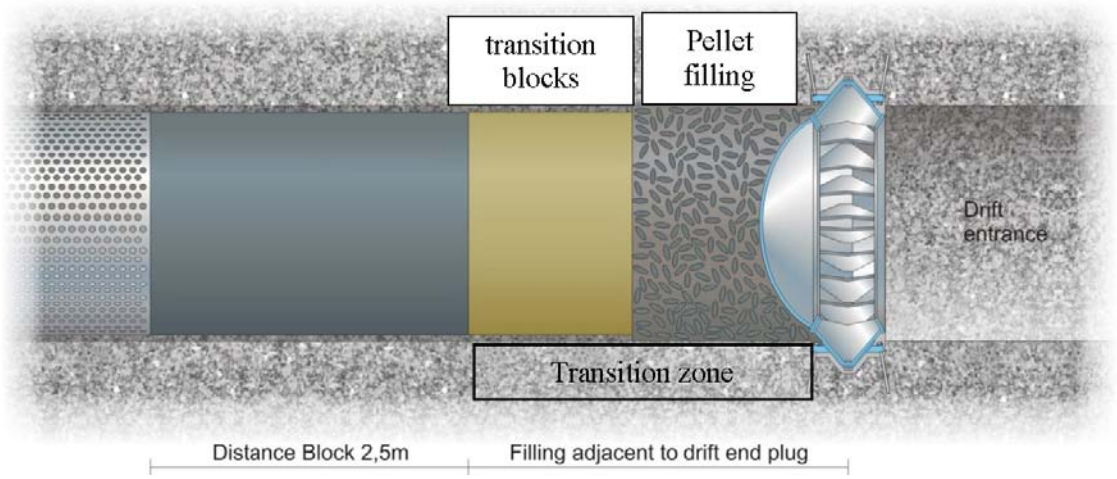

Figure 4-21. *Schematic drawing of Drift Plug position.*

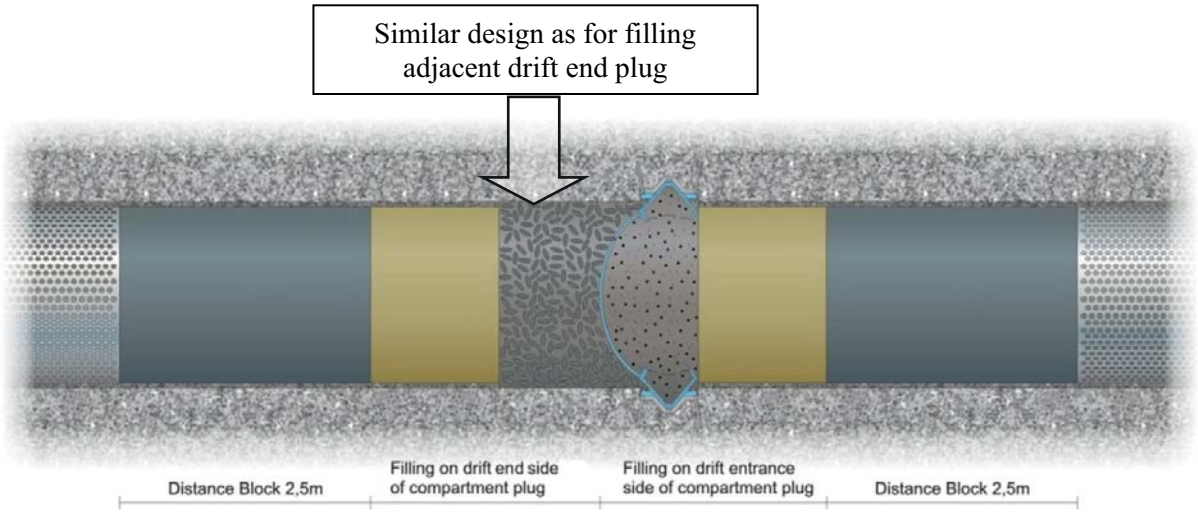

Figure 4-22. *Schematic drawing of the filling components adjacent to a compartment plug. The same design is used for filling components for the sealed side of compartment plug as for filling adjacent to a drift plug.*

The compartment plug and the lead-through are not included in the analysis since they only have minor effect on the system behaviour. Only the filling between the plug and the distance block will be studied. The length of the pellet filling is 1.3 m as measured from the crown of the cap. The length of the transition zone will be dimensioned so that the density of the swelled and homogenized transition zone in contact with the distance block section will be the same as the density of the distance block section assuming that no axial swelling of the distance block section takes place. The dimensions of the transition zone and the expected swelling pressure on the plug are to be determined in the calculation.

The problem can be treated either numerically with FEM calculations or analytically in a simplified way. The analytical solution has been used at this stage, Table 4-7 shows the results and the calculations are presented in Appendix B.

Table 4-7. Results of the calculations.

Friction angle ϕ	Length of the transition zone L_T	Length of the transition blocks L	Swelling pressure on the plug
5°	8.1 m	6.8 m	2.33 MPa
10°	5.8 m	4.5 m	1.40 MPa
20°	4.0 m	2.7	0.46 MPa
30°	3.2 m	1.9 m	0.20 MPa

The required length of the transition zone and the resulting swelling pressure on the plug are thus very dependent on the friction angle. The friction angle for swelling pressures between 1 and 10 MPa is about $\phi = 10°$, which thus can be used as dimensioning value. However, the friction angle between bentonite and a smooth plane surface of rock can be lower (about 50% according to Börgesson et al. 1995), which would motivate to use $\phi = 5°$.

Design

Since the rock surface is not expected to be smooth a friction angle value of $\phi = 10°$ yielding a transition block zone length of 4.5 m is used in the design. The design based on that is shown in Figure 4-23. The material properties used in the design are as follows:

- Dry density of the pellets filling zone rdp = 1,000 kg/m^3.
- Dry density of the transition blocks rdb = 1,712 kg/m^3.
- Average dry density of the transition block zone rdt = 1,635 kg/m^3.

The design of compacted bentonite blocks used in transition block zone is similar to the filling blocks presented in Figure 4-17.

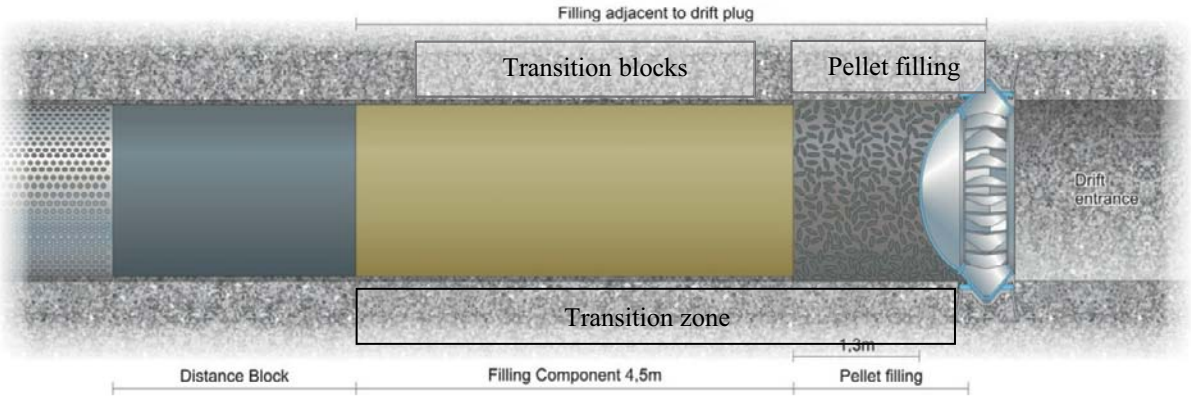

Figure 4-23. *Design of Drift Plug position.*

Filling on drift entrance side of the compartment plug

The same design dimensioning is used for the sealed side of compartment plug as for filling adjacent to drift plug and therefore only the design for filling on drift entrance side of the compartment plug is presented here.

The schematic principle of filling adjacent to drift entrance side of the compartment plug is shown in Figure 4-24. The key requirements and factors specific to the compartment plug and affecting the design of filling components can be summarized as:

- The water leakage flowing from the sealed side to the open side is specified not to exceed 0.1 l/min (a tentative requirement). The compartment plug was tested in full-scale at ÄSPÖ HRL, see Section 4.7. The leakage during the test was initially at approximately 0.05 l/min and after a couple of days it was reduced to 0.002 l/min. Therefore it is likely that the leakage rate will be significantly lower than requirement.
- It is considered beneficial that the swelling pressures of filling components exerted to compartment plug after full saturation from both sides of compartment plug would be roughly equal. This would therefore not lead to any major displacements of plug after long periods of time when the structural strength of the plug has disappeared by e.g. corrosion.

The geometries and initial conditions are identical on both sides of the compartment plug with the exception that the thickness of the pellet filled section is 1.0 m on the entrance side.

The design is based on the following principle:

- A compacted high density transition zone with blocks similar to filling blocks is placed next to compartment plug.
- The empty volume between the compartment plug and transition block zone is filled with pellets resulting in lower density.
- The pellets are installed via a hole in the transition block zone. The hole is filled afterwards with a compacted bentonite cylinder to plug and seal it.
- As filling components absorb water and swell, there will be a transition zone from the compartment plug to the distance block with a density gradient.

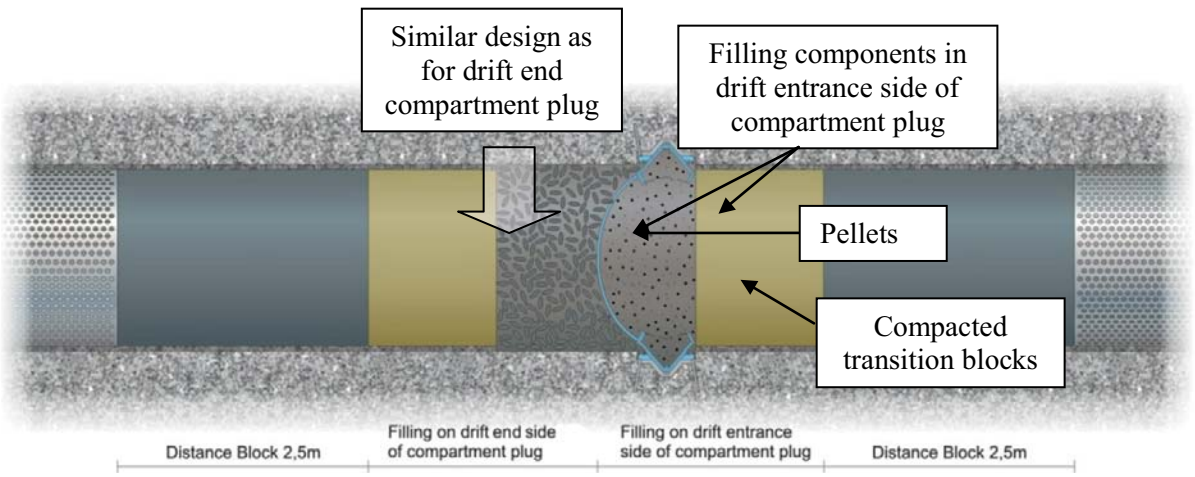

Figure 4-24. *Schematic drawing of filling components in drift entrance side of a compartment plug.*

Dimensioning

The criteria for dimensioning the transition zone are basically the same as for the drift plug. The length of the pellet filling on the entrance side is 1.0 m counted from the crown of the cap. The length of the transition zone will be hence dimensioned so that the density of the swelled and homogenized transition zone in contact with the distance block section will be the same as the density of the distance block section assuming that no axial swelling of the distance block section takes place. The dimensions of the transition zone and the expected swelling pressure on the plug are requested.

The problem has again been treated analytically in a simplified way and the calculations are similar to those presented in Appendix B. There are two ways of treating the influence of the compartment plug:

1. The compartment plug is assumed to be unaffected and can withstand also the swelling pressure from the pellets-filling on both sides. These parts can thus be treated as separate units.
2. The compartment plug is assumed to be completely disintegrated by corrosion and not to affect the compression of the pellets filling on both sides of the plug. These parts can thus be treated as a unity.

For case 1 the dimensioning of the length of the transition zone inside the plug will be identical to the dimensioning the transition zone of the drift plug, which gives results as shown in Table 4-7 and a recommended length of 4.5 m. The outer pellet filling is slightly smaller than the inner one and as reference in this report and the length 1.0 m has been used.

For case 2 the sum of the two pellet filling parts is 2.3 m and if there is no compartment plug the geometry can be treated as having a symmetry plane in the middle of the pellet filling parts, i.e. with a pellets filling length of 1.15 m.

There are thus, with the mentioned subdivision of the two cases, three different lengths of the pellets filling; 1.0 m, 1.15 m and 1.3 m. The effect of the compression of the pellets filling on the length of the transition zone is that the longer pellets filling the longer transition zone is needed. The dimensioning of the transition zone on the sealed side of the compartment plug should thus be done with the pellet filling length of 1.3 m and the transition zone on the drift entrance side of the compartment plug with a pellet filling length of 1.15 m.

Design

The required length of the transition blocks on the entrance side of the plug, where the dimensioning length of the pellets filling is 1.15 m (inside the plug), will be $L = 4.25$ m for $\phi = 10°$. The corresponding swelling pressure on the on the plug will be 1.38 MPa.

Since the rock surface is not expected to be smooth a $\phi = 10°$ yielding a transition block zone length of 4.25 m is proposed to be used in the design assuming 1.15 m length of pellet filling section. The design based on that is shown in Figure 4-25. The material properties used in the design are as follows:

- Dry density of the pellets filling zone rdp = 1,000 kg/m^3.
- Dry density of the transition blocks rdb = 1,712 kg/m^3.
- Average dry density of the transition block zone rdt = 1,635 kg/m^3.

The design of compacted bentonite blocks used in transition block zone is similar to the filling blocks presented above and in Figure 4-17.

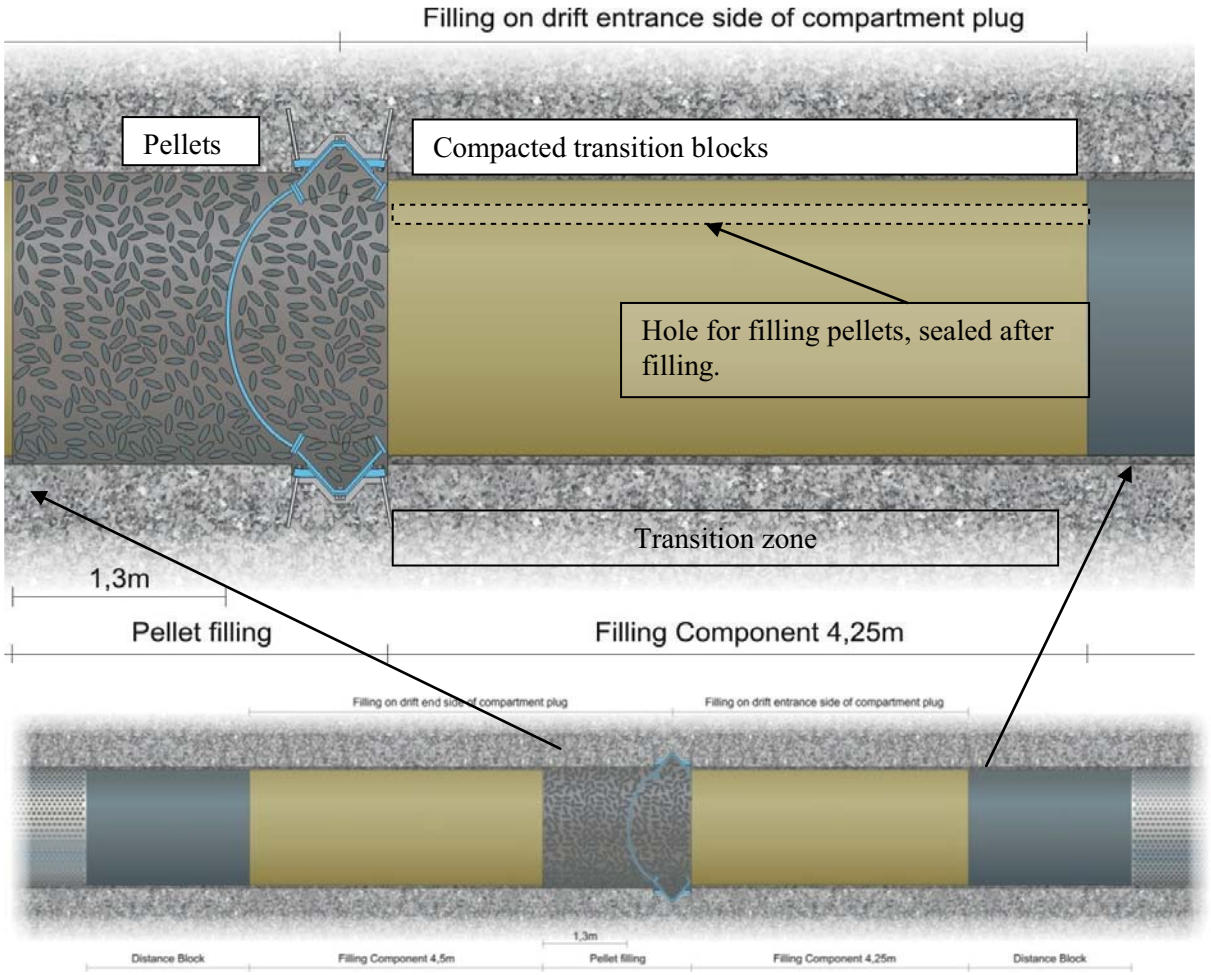

Figure 4-25. *Design of filling on entrance side of compartment plug. Note that the hole for filling can be made shorter if needed depending on the emplacement technique.*

Filling at drift end and pilot hole

It is proposed to emplace a filling component in the KBS-3H deposition drift between the drift face (bottom) and the adjacent distance block, see Figure 4-26. The motivation for placing a distance block section at this location is based on concentrated rock stresses around the corners of the drift end. Therefore the rock adjacent to the drift end might be more vulnerable to smaller scale disturbances and prone to opening of fractures at this location. If there are small deviations in the drift lengths these can also be compensated by adjustments made by using distance blocks and filling components. By emplacing a distance block at the drift end the transport path parallel to the drift axis from canister to the drift end is of the same length as from other Supercontainers axially to the next Supercontainer or a filling component (the shortest transport path from canister to the drift surface is always the same).

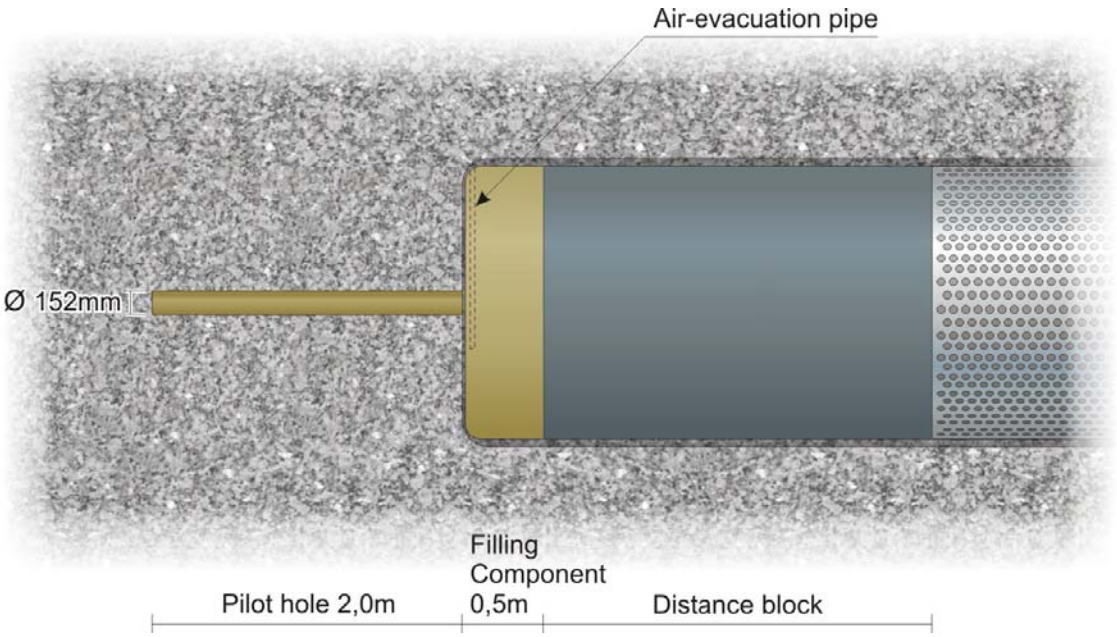

Figure 4-26. *Pilot hole and filling component at drift bottom.*

Dimensioning

The same type of compacted bentonite blocks are used for the filling at the drift end as were used as distance blocks elsewhere.

The dimensioning is based on compensating the open volume in the gaps and the slot made for the air evacuation pipe by adding compacted bentonite so that the required final average density will be the same as for distance blocks.

Design

The design proposed for use in filling the drift end and pilot hole is presented in Figure 4-26 and the dimensions in Table 4-8. The shape of the bottom of the bentonite block is modified to conform to the rock surface. Only one bentonite block of length 0.5 m is placed at the end of the deposition drift.

Table 4-8. Dimensions and properties of bentonite block at the drift end bottom.

Drift end filling component properties	
Ø Ext diameter.	1.85 m
Ø Diameter of filling component alt bentonite blocks.	1.77 m
Gap between drift wall and filling component.	0.04 m
Nominal block length for the filling component.	0.50 m
Gap between filling component and distance block.	0.01 m
Gap between filling component and drift end.	0.05 m
Air evacuation pipe diameter.	0.02 m
Air evacuation pipe length.	2.00 m
Total volume	1.49 m^3
Volume of bentonite blocks.	1.22 m^3
Initial dry density of bentonite blocks.	1,650 kg/m^3
Final dry density of bentonite blocks.	1,350 kg/m^3

Filling of pilot hole

The pilot hole is filled to avoid open cavities that might reduce the density of buffer and other filling components. Another objective is to seal the pilot hole to prevent possible water flow between drift system and host rock.

The pilot hole is filled with cylindrical, highly compacted bentonite blocks with length of 0.1–0.5 m. The dimension will be based on the results of trials to optimize compaction technique and efficiency. The compacted bentonite is of the same type as used for manufacture of the filling blocks. The pilot hole will not be perfectly straight, a small curvature is expected and to compensate for that, several shorter blocks are used for filling instead only one long one. The diameter of the pilot hole is 152 mm and the diameters of the blocks used to fill it are 132 mm. The objective is to reach final saturated density of buffer which is approximately the same as the filling blocks.

4.6.4 Conclusions

Three inflow cases

Three cases were defined in representing hydraulic environment at Olkiluoto: a) wet drift, b) normal (median) drift and c) dry drift, see Figures 4-12 through 4-14 for definition of cases. The design for these different cases is shown in Figures 4-27 through 4-29 to illustrate the use of filling components, assuming nearly perpendicular intersection with leaking fractures and the importance of these to drift utilization efficiency. Note that in the normal case there is only one filling block section in position of 0.4 l/min inflowing fracture in the 300 m long drift and the total length of filling components is about 3 m in a 300 m long drift. In the wet drift there are four filling blocks in position of inflows of 0.8, 2, 12 and 35 l/min and the total length of filling components is about 34 m. In dry drifts there are no filling blocks. The cumulative inflow distribution curve (Figure 4-10) indicates that the dry drift case is more probable than wet drift case.

It should be noted and emphasized that the cases were based on estimates and not made for quantitative purposes but merely for qualitative purposes to illustrate the applicability of design and possible effect of mass and quantities of filling materials on overall feasibility. The results affect the efficiency of disposal and therefore the relevance of these different cases should be re-assessed in case a more detailed design is developed. These designs should of course be based on the most recently updated hydrogeological descriptions available at that time.

Table 4-9. Dimensions and properties of pilot hole filling component.

Pilot hole filling specifications	
Pilot hole length	2.00 m
Ø Ext diameter	0.15 m
Ø Diameter of bentonite blocks	0.14 m
Gap between drift wall and filling component	0.01 m
Length of single bentonite blocks (0.1–0.5 m)	0.50 m
Gap between filling component and pilot hole end	0.01 m
Total volume	0.04 m^3
Volume of bentonite blocks	0.03 m^3
Initial dry density of bentonite blocks	1,650 kg/m^3
Final dry density of bentonite blocks	1,430 kg/m^3

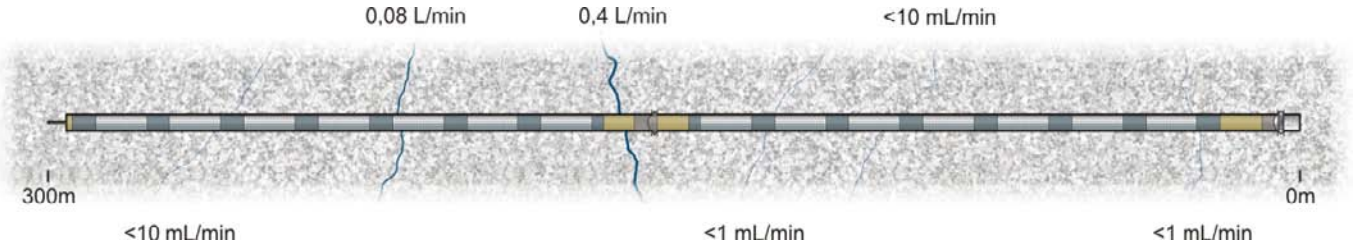

Figure 4-27. *Schematic drawing of the KBS-3H drift design in normal case.*

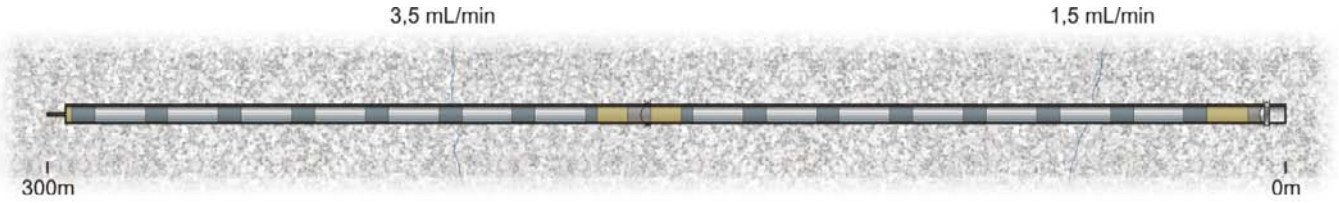

Figure 4-28. *Schematic drawing of the KBS-3H drift design in dry case.*

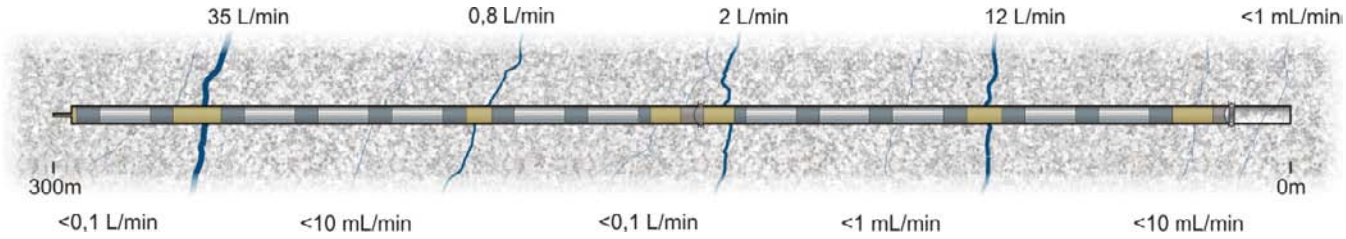

Figure 4-29. *Schematic drawing of the KBS-3H drift design in wet case.*

Uncertainties and important issues

There are several issues including uncertainties in the design of filling components that will have to be addressed in upcoming project phases.

In layout adaptation of the KBS-3H repository, where water leaking into the drift at rates of 0.1 L/min or more via long fracture zones or fractures with a strike in the direction of the axis of the drift should be avoided if possible. This is because such features will have a significant impact on the positioning of Supercontainer sections and lower drift utilization efficiency. Fracture striking perpendicular to the drift should also be avoided to mitigate the impact of earthquakes and also needs to be evaluated with respect to the effects on the buffer components.

The dimensioning of filling components adjacent to drift plug and compartment plugs are based on mathematical calculations and include uncertainties such as the friction angle to be used for the calculations and assumptions that hysteresis has no significant influence on the swelling. The assumption of hysteresis and better definition of the expected effect of such behaviour should be verified in the next project phase, while also taking into account various wetting and saturation alternatives. The scoping calculations done thus far were based on the assumption that high density bentonite filling can maintain density and swelling pressure for long periods of time, which is related to assumed density homogenization of the bentonite.

The dimensioning of filling blocks in positions of leaking fractures was based on a new respect distance approach. This requires that the Supercontainers must be located at least:

- 3.0 m down-tunnel from fractures providing 0.1–0.5 L/m
- 5.0 m down-tunnel from fractures providing 0.5–1.0 L/m or
- 6.0 m down-tunnel from fractures providing > 1.0 L/m

Note that the “respect distances” 3.0 m/5.0 m/6.0 m contain 50% of the filling block length plus 50% of the distance block length, see Figures 4-1 to 4-20. This implicates that the length of the filling block is dependent on the length of distance block (various distance block lengths are used depending on the fuel type in the canisters). The length of the filling block is also dependent on the angle between the fracture and the drift axis.

Furthermore:

- The “one compartment plug” concept differs from previous design with the double compartment plug section and the viability should be evaluated from long term safety point of view.
- The possible consequences of erosion were not considered in design work since there is not adequate design basis for incorporating that into design. Available results hints to some impact on the filling blocks but the degree of effect and design factors to manage it are not yet understood sufficiently for engineering purposes.

Conclusions and need for future development

The design of filling components based on the changes in the drift design presented here simplifies the design. The system is more straightforward since all the filling components behave in a similar manner as buffer. It also improves the utilization degree by allowing adaptation of different solutions of filling blocks and based on different inflows, reduces the number of required distance blocks and eliminates the need for an additional compartment plug. In addition, the change from previous drift end plug design to a single combined drift plug simplifies the design further and improves the drift utilization degree.

There are still uncertainties in design and design premises which are proposed to be resolved in future development work. In general the future work can be divided as follows:

Resolution of important issues. Most of these issues are uncertainties in fulfilment of design requirements to be resolved:

- Effect of chemical erosion due to dilute groundwater Homogenization.
- Ability of compacted bentonite to maintain large density and swelling pressure differences.
- Viability of “one compartment plug” concept from safety point of view.
- Evaluation of drift utilization degree based on fracture data (more accurate fracture estimates and criteria for taking into account e.g. possible canister shearing risk).
- Evaluation of the behaviour of the whole drift system (including all components) from emplacement and fulfilment of the performance requirements is to be resolved in the coming project phase.

4.7 Compartment plug

4.7.1 General

The compartment plugs of KBS-3H are used to hydraulically separate and seal sections (~150 m) of the drift and they also enable the water filling procedures of DAWE, the detailed requirements are presented in Section 3.3.6. The plug consists of three components; the fastening ring which is cast into a rock notch using low-pH concrete, the collar, which is attached to the fastening ring and finally the cap. The collar is fastened to the fastening ring by welding as is the cap to the collar. The plug is designed so that the welds do not carry any load, thus only function as a seal. Possible leakage is expected at the boundary between the steel components and the concrete casting securing the steel to the rock as well as the boundary rock and concrete. The design of the plug is illustrated in Figure 4-30 and elaborated in Autio et al. (2008).

During 2009 and 2010 the compartment plug was tested in the 15 metre long drift, DA1622A01, at the –220 metre level at Äspö HRL. The objective was to verify the ability to divide a KBS-3H drift into hydrological separated compartments. A steel compartment plug was used for testing. Material selection for the compartment plugs and drift plugs was also part of the Complementary studies phase, and they will be made of titanium, see Section 7.5.7.

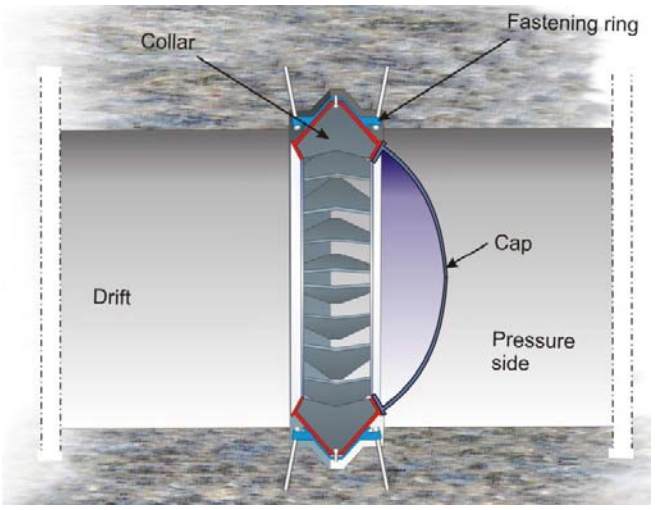

Figure 4-30. *The plug design. In this test a one sided plug is installed and tested. The only difference between a one and two sided plug is the opposite cap on the two sided plug.*

The acceptance criterion had since earlier project phases been tentatively specified as a maximum water leakage of 0.1 l/min through the plug at 5 MPa, this corresponds to an older limit set up for the Compartment plug that relates to the BD where a flow of 0.1 l/min was the limit set for flow from one Supercontainer section to the next and hence also set as a limit for a Compartment plug into the next Supercontainer section. The final target will, however, be to prevent advective flow through the plug and a much lower criterion is foreseen.

4.7.2 Compartment plug installation

Installation of the plug was done during the winter 2008/2009. Demonstrating a method for sawing the notch was part of the test and a notch suitable for plug installation was successfully excavated. Excavation was done by making parallel cuts with a rail-mounted saw. When all cuts were completed the slabs were broken away, creating the notch. The notch position was selected in a section of rock with a low fracture frequency at a distance from the drift face allowing installation, i.e. more than 2 metres from the drift face. In Figure 4-31 the saw and the resulting notch profile are illustrated.

Installation of the compartment plug in the notch was done in four steps:

- Installation of the fastening ring in the notch.
- Casting of the fastening ring.
- Installation of the Collar.
- Installation of the Cap.

Installation of the components was carried out by the manufacturer of the plug. The fastening ring was casted in place by SKB personnel supported by concrete experts who developed the concrete recipe. Low-pH concrete was not used in this test but is likely to be used in a future repository as specified in the KBS-3H design. Despite heavy components and high demands on accuracy the installation was carried out successfully. Initially the casting of the fastening ring was troublesome but after minor adjustments of the concrete mixture the casting could be carried out with good results. In Figures 4-32 and 4-33 the installation of the plug is illustrated.

Figure 4-31. *The rock notch was excavated with parallel-cut sawing. Several cuts were made and the slabs broken away creating a notch. The method proved to be functional. The left image shows the saw mounted in the drift, the resulting notch profile is shown to the right.*

Figure 4-32. *Fastening ring positioned in the rock notch to the left. The right image shows the top of the completed fastening ring casting.*

Figure 4-33. *Installation of the compartment plug collar and cap. The cap was raised using a hand winch.*

A water pressurising system was installed to enable pressure tests. This system was automatic and consisted of pumps, valves and pressure tanks together with a number of pipes leading water in behind the plug and evacuating the air. Multiple sensors were installed to monitor the test, on both in- and outside of the plug. Pressure sensors, sensors for plug deformation and displacement and water leakage measuring equipment were used. The water leakages were measured by building a measurement weir (made of wood) on the drift floor some 50 cm from the compartment plug and the water was led to a holding tank for measurement. In this way the actual leakage through the plug casting could be measured. Water leaking through longer flow paths (fractures in the rock going around the plug and the weir at 50 cm) were not included in the plug leakages measurement, these were instead measured separately at the drift entrance. This set-up allowed for measurement of both changes in the leakage through the plug casting as well as leakage in the rest of the drift.

4.7.3 Compartment plug tests

In total four tests were carried out:

1. Pressurized water behind the plug.
2. Pressurized water behind the plug, casting grouted with Silica Sol.
3. Bentonite pellets behind the plug, casting grouted with Silica Sol.
4. 6 month long-term test with the same set-up as test 3.

The leakage acceptance criterion for all tests was tentatively specified as a maximum leakage of 0.1 l/min through the casting at 5 MPa during 30 days.

The first test was initiated in February 2009. It was immediately noticed that the leakage was much higher than the acceptance level. 1 l/minute was measured through the casting. The high leakage also made it very difficult to raise and maintain pressure. The highest pressure reached during the first test was approximately 2.5 MPa. The test was discontinued after approximately one week due to the high leakage and the fact that the target pressure of 5 MPa could not be reached.

The casting of the fixing ring had been prepared with grouting tubes to enable grouting in case the casting wasn't tight. Silica sol grouting was carried out in this tubing in preparation for the second test. The grouting was carried out prior to summer 2009 and was successful.

The second test was initiated in August 2009. The effect of the silica sol post-grouting was immediately seen. The leakage was considerably lower than in the first test and the target pressure of 5 MPa could easily be reached and maintained. During the first days of the test the leakage was just above the acceptance criteria, 0.1 l/min, but it was continuously reduced during the test period. The reduction could possibly be due to particles naturally sealing the small leakage paths. At the end of the 30 day test period the leakage was as low as 0.002 l/min, it should be noted that at these low flow-rates air humidity and the ventilation probably has an effect on the amount of leakage. The leakage is illustrated in Figure 4-34.

It is also interesting to consider the amount of water needed to maintain the pressure at steady state. Measurements showed that the amount did not vary that much during the second test, between 0.6 and 0.8 l/min. The natural inflow in the 15 metre drift is measured at 0.2 l/min when no pressure is applied to the plug. During the second test the flow measured from the 15 metre drift varied between 0.8 and 1.0, an increase of 0.6 to 0.8 l/min – the same amount that was needed to maintain the pressure behind the plug. The conclusion is that most of the water leaking into the rock is transported in rock fractures around the casting and into the open drift. A very good correlation between the amount of water needed to maintain pressure and the leakage into the 15 metre drift is seen in Figure 4-35. No increased leakage levels into the adjacent 95 metre drift has been observed during these tests.

The low leakage levels through the casting in the second test indicated that the plug fulfils the specified acceptance criteria. In this case without using any bentonite pellets behind the plug. Monitoring the sealing effect of pellets is still highly interesting, especially with respect to the by-pass leakages in fractures around the plug which is of interest not only for KBS-3H but also for the KBS-3V development. Possible decreasing sealing ability of the silica sol is also of interest although most likely difficult to establish when bentonite has been added. For these reasons the plug test series was continued with the bentonite pellets step in accordance with the plan.

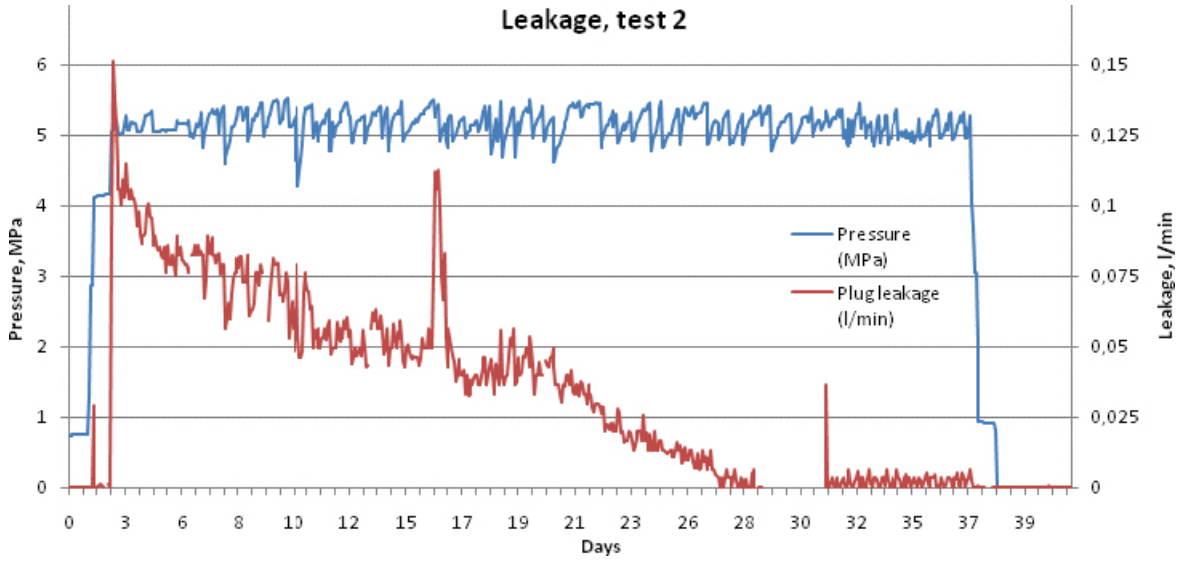

Figure 4-34. *Measured leakage through the plug casting in test 2. The leakage was initially higher than the 0.1 l/min acceptance criteria, but decreased during the test and was remarkably low at the end, 0.002 l/min.*

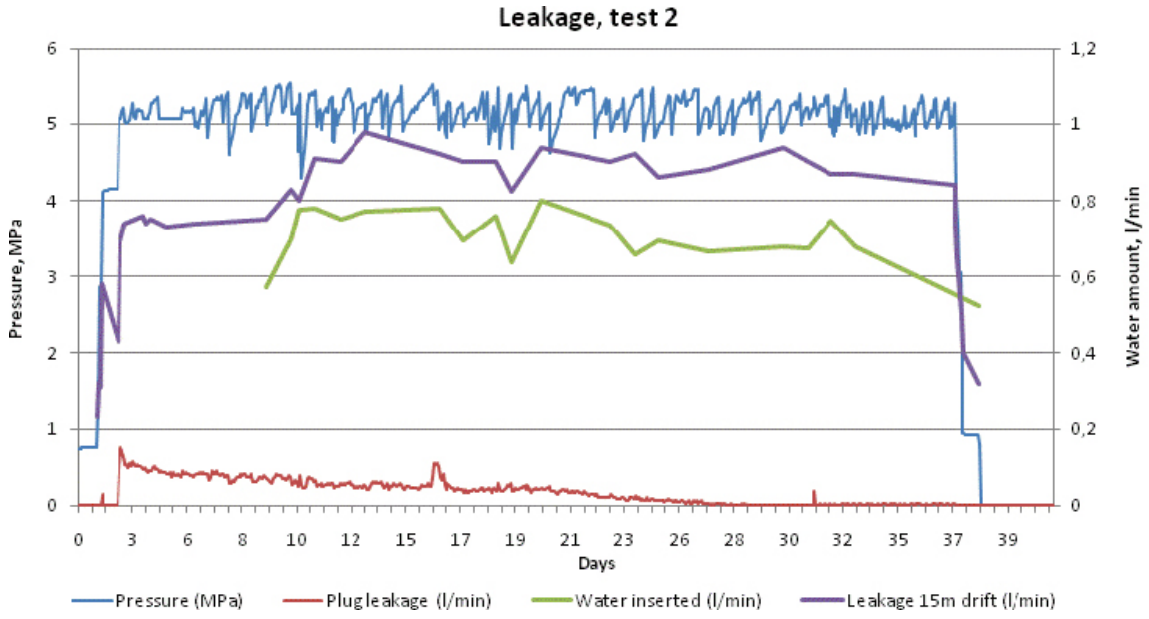

Figure 4-35. *Measured amount of water needed to maintain pressure behind the compartment plug.*

Pellet filling of the void behind the compartment plug was done with a pellet blower. The filling method was tested and verified to function in a full-scale mock-up prior to filling. A good filling was reached using Cebogel pellets with a bulk density of about 1,100 kg/m^3. The gravimetric water content of the pellets was measured at 22–25%. The filling degree was verified using a video camera.

The third test was in operation for a total of 84 days, see Figure 4-36. The extended test period was due to an increase in leakages past the plug at the end of the original test period, the reason for this is unclear. The initial leakage through the plug casting was very low, (approximately 0.002 l/min). However, approximately 20 days into the test a new natural leakage path was opened which resulted in increased leakage levels (approximately 0.4 l/min). After roughly 10 days the leakage was reduced and stabilized at low levels again (approximately 0.002 l/min). This is likely due to the sealing effect of the pellets and illustrates the potential importance of the sealing materials in controlling seepage.

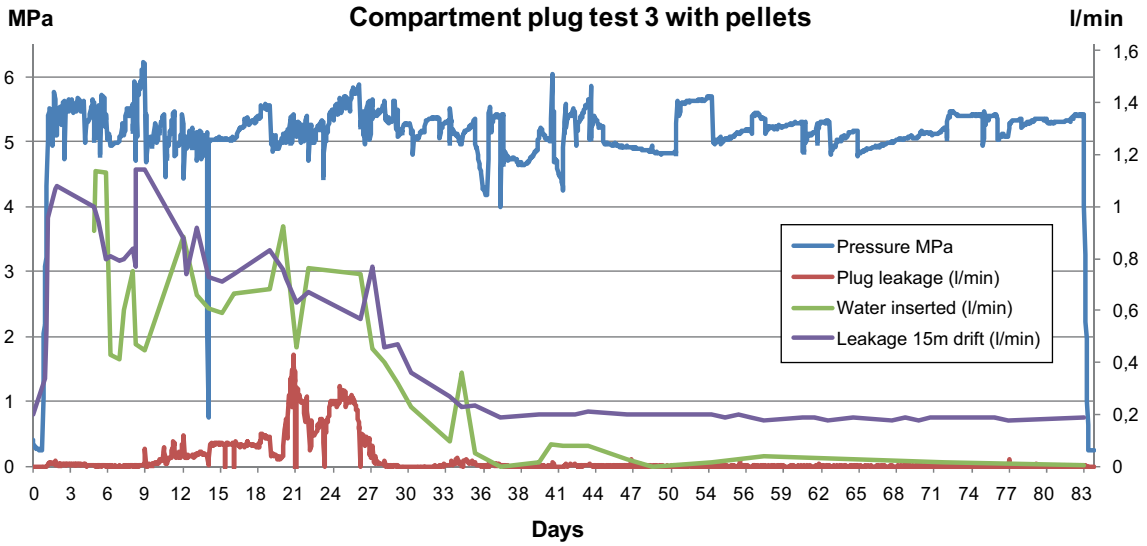

Figure 4-36. *Leakage through the plug during test 3. The amount of water needed to maintain pressure during test 3 is also shown and is as seen remarkably low at the end of the test. The effect of the pellet filling is obvious.*

The very good pellet sealing effect is also quite visible when considering the amount of water needed to maintain the 5 MPa pressure. In the second test and in the beginning of the third test 0.6 to 0.8 l/min was needed. During the first 40 days the water consumption decreased and reached steady state after 40 days where approximately only 0.02 l/min was needed. The reduction in the amount of water needed to maintain pressure also had a significant effect on the impact on the leakage out from the 15 metre drift. The leakage was initially somewhat lower than in the second test, and when the pellets sealed the fractures the leakage from the 15 metre drift was reduced, and at steady state the leakage is measured to be 0.2 l/min, which is the same as the natural leakage into the drift. The conclusion is that the pellets have almost entirely sealed the void behind the compartment plug and the leakage fractures bypassing the compartment plug casting. To summarise, almost no water was needed to maintain pressure and the leakage into the 15 metre test drift was at natural levels and the leakage through the casting was close to zero.

The third test was eventually upgraded to a long-term test to monitor the ability to maintain low leakages through the casting as well as leakage out from the rock volume. It was successfully continued for almost 300 days without any increases in leakages.

4.7.4 Conclusions

The compartment plug tests have shown that the design can fulfil the tentatively set test criteria of 0.1 l/min with a margin. The tightness achieved is in the order of what will be the final requirement on the plugs and it is one of the first demonstrations of a basically tight plug sealing a drift at 5 MPa. The demonstration of the bentonite pellet-sealing effect is of great importance not only for KBS-3H but for KBS-3 as a whole.

However, the results are valid for a depth of 220 m and further testing needs to be done at the actual repository depth.

4.8 Drift Plug

4.8.1 General

In earlier designs the drift end was plugged with a compartment plug followed by a concrete plug. A new design has been developed during the recent project phase and the compartment plug/concrete plug combination has been replaced by an enhanced version of the compartment plug – the drift plug, the old and the new design is illustrated in Figure 4-37.

The function of the drift plug is similar to that of KBS-3Vs deposition tunnel plugs; it is to avoid significant water flows out of the drift, which could give rise to piping and erosion of the buffer, either through the plug itself, or through the adjacent rock. They also keep the buffer in place prior to the backfilling and saturation of the adjacent central tunnel.

4.8.2 Design considerations

During 2010 the positive results from the compartment plug tests led to a re-evaluation of the method used to seal the KBS-3H drifts. It was proposed that a redesigned compartment plug, using a suitable material, could fulfil the function of the previous drift plug structure. Among the advantages of such a change would be reduced use of concrete in the drift, reduction of the installation steps, and an increase in the utilization degree enabling a possible extra canister position in each drift.

The requirements on the drift plug are equal to the requirements on the previously used drift end plug; see Section 3.3.6 for long-term requirements. These are considerably higher than those specified for the compartment plug on which the new design is based, both regarding the pressure tolerances and durability. This is because the compartment plugs have a function only during the installation phase, whereas the drift plugs must withstand the full hydrostatic pressure and the swelling pressure, and be sufficiently tight to form a part of the system of barriers. Therefore the drift plug requires water tightness and the ability to withstand 5 MPa hydrostatic pressure +10 MPa uniform swelling pressure resulting from buffer and filling components. In addition, it is required to withstand a localized variability of 2 MPa in swelling pressure (estimated) which is assumed to be caused by e.g. uneven wetting and swelling.

The compartment plug design has been modified in order to fulfil the preliminary drift end plug criteria. The drift plug design utilises a different rock notch profile, a sturdier collar and a cap with increased strength. The design is illustrated in Figure 4-38.

To make sure that the design fulfils the criteria, the new drift plug will be manufactured in titanium. The drift plug is required to stay in place under the applied loads (no significant displacement allowed) until the adjoining main tunnels are backfilled, which is assumed to be in the order of 30 years.

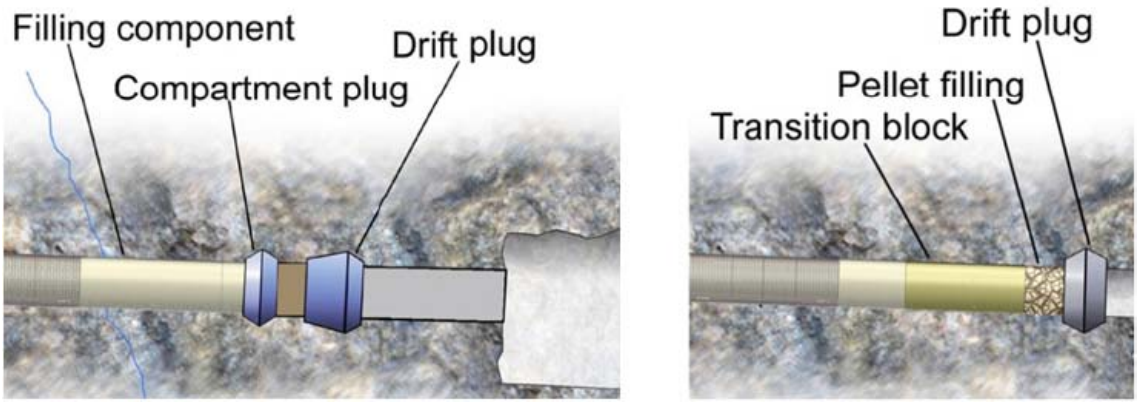

Figure 4-37. *The previous design alternative with one compartment plug and one drift end plug to the left. The right image illustrates how the new drift plug is used.*

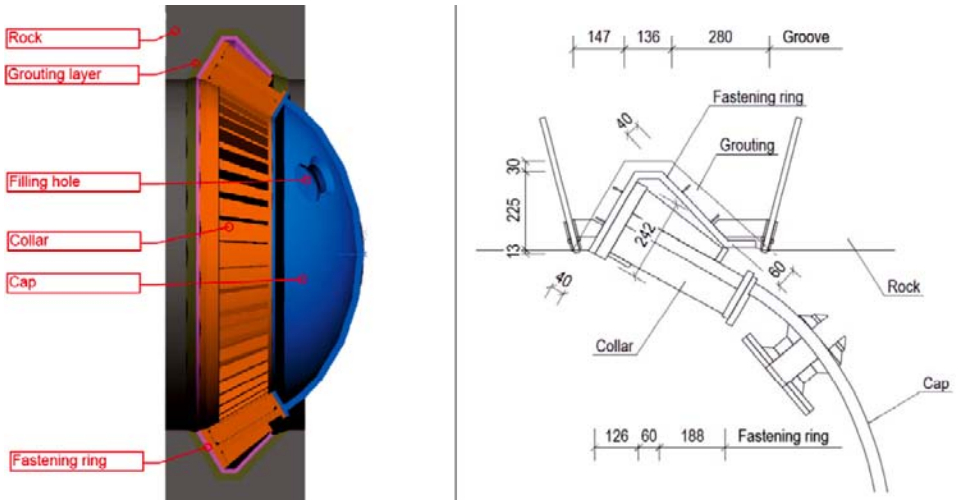

Figure 4-38. *Design of the Drift Plug.*

4.8.3 FEM- calculations

A FEM-analysis has been carried out on the drift plug-design, and its input parameters are summarised in Table 4-10.

The analysis showed that the stresses on the cap are below the acceptance level. According to analysis the drift plug will withstand a load of 22 MPa before failure of the components is expected, which indicates that it will take the design loading of 15 MPa with a high degree of confidence.

The maximum stress in the grouting layer is calculated to be 84 MPa, which is acting on a very limited area. The average stress is 48 MPa. Concrete strength depends on the mixture used, but the tests done so far on low-pH concrete indicate a strength of approximately 88 MPa.

The highest compression stress in the rock is 44 MPa. In addition to the stresses from the plug, stresses from other sources exist after deposition, i.e. in situ rock stresses, and excavation (drift, V-notch) induced stresses as well as thermally induced stresses. Calculations of these were not within the scope of the initial work but will be carried out in the upcoming project phase in order to fully describe the plug and rock interactions and strengths. This will possibly require optimisation of to geometry of the notch and will enable calculations of the minimum required distance between the plug and the entrance of the drift.

Table 4-10. FEM-analysis parameter values for the drift plug-design based on titanium alloy grade 12.

Design data		**Geometry of the model**	
Water pressure **Swelling pressure** **Heterogeneous pressure**	5 MPa (uniform) 10 MPa (uniform) –2 MPa (eventually acting on casual areas)	**Diameter of the cap**	1,650 mm
Material **Safety factor on load (EC)**	Titanium grade 12 (ASTM) 1.0 (water pressure) 1.35 (swelling pressure)	**Hight of the cap** **Thickness of the membrane**	400 mm 36 mm
Material Safety factor	1.0 (titanium grade 12)	**Thickness of grout layer** **Thicknes of rock layer**	40 mm 50 mm

4.8.4 Conclusions

It can be concluded from the compartment plug test results that the ability to seal a drift with a design similar to the drift plug is very good. This, together with the calculations on the more robust drift plug, shows that the new design has potential to be a viable solution that can fulfil high requirements when the deposition process is completed.

4.9 Mega-Packer post-grouting

4.9.1 General

Groundwater control by pre-grouting may not always be sufficiently effective, especially since boreholes are not allowed outside the drift contour. Hence an efficient post grouting methodology would be useful. A post grouting device that can handle the conditions at full repository depth called the Mega-Packer has been developed

Full-scale tests of the Mega-Packer were initiated in the Demonstration phase in 2007 and have been reported in Eriksson and Lindström (2008). The tests were finalised during the Complementary studies phase and the main results are presented here.

Theoretical studies

Theoretical calculations for post-grouting using the Mega-Packer were carried out and reported in Design Description 2007 (Autio et al. 2008). These theoretical studies of different scenarios, variations in fractures and transmissivity, indicated that the inflow requirement of 0.1 l/min after grouting should be possible to achieve.

Mega-Packer description

The Mega-Packer shown in Figure 4-39 is a large steel tube with a wall thickness of 48 mm thick steel and a total length of 1,970 mm. The outer diameter of the Mega-Packer is 1,820 mm and the grouting length is 1,590 mm. It has packers sealing off both ends. The packers are inflated with water at a pressure required to resist grout penetrating out between the packers and the rock wall during grouting. The steel tube has connections for valves, so that the hoses for grouting and measurement equipment can be connected. Silica-sol is the preferred grout but low-pH grouts can also be used, the residual layer of grout on the drift wall is removed after the grouting. To grout longer fracture zones, two Mega-Packers can be connected and used simultaneously. The current design allows for this connection but the functionality has not been included in the tests that have been carried out.

Figure 4-39. *The Mega-Packer positioned outside the 95 m drift at Äspö HRL.*

4.9.2 Full-scale Mega-Packer testing

As mentioned earlier, Mega-Packer tests were initiated during the Demonstration project phase in 2007, the 95 metre deposition drift, DA1619A02, at –220 metre level at Äspö HRL was used for testing. The pilot hole used to steer the reamer head was grouted using cement prior to reaming, this likely meant that all larger inflows were sealed when the Mega-Packer tests were carried out. The excavated drift had an inflow of approximately 12 l/min in 2005; this had been naturally lowered to approximately 4.4 l/min in 2007 when the tests were initiated.

The goal with the test was primarily to verify the Mega-Packer as a possible grouting method and to evaluate the theoretical studies. Establishing a post-grouting method that doesn't require boreholes outside the drift contour would be very beneficial for the KBS-3H design.

A total of five positions were identified as suitable for grouting, that is sections with inflows above 0.1 l/min, Figure 4-40. The inflows in these positions were between 0.145 and 2.40 l/min and the groundwater pressure between 140 to 830 kPa.

Test strategy

The strategy of testing in the 95 m drift was to hydraulically characterise each of the five selected positions in the drift before and after grouting, to evaluate the grouting efficiency.

The test program included:

1. Performance test of the packers.
2. Hydraulic pre-characterisation of the five positions (inflow measurements, pressure build-up tests and water loss measurements).
3. Grouting design.
4. Grouting.
5. Evaluation of the performed grouting – post characterisation (inflow measurements, pressure build-up tests and water loss measurements).

Design of the grouting was made with the target of reaching an inflow of maximum 0.1 l/min per grouting position (Eriksson and Lindström 2008).

The tests were carried out in two series; silica-sol grout was used both times. In the first test series, carried out in November 2007, hydraulic characterisation was carried out for all of the five positions and Position 1 and 3 were grouted. Position 3 was grouted twice due to problems with filling the void with silica-sol and hence a failed grouting in the first attempt. The tests were continued in March 2008, when Positions 2, 4 and 5 were hydraulic characterised and grouted. Position 5 was grouted twice due to equipment problems leading to a too short grouting time in the first attempt. The time between the two test series was used to solve practical problems and improve the equipment and method applied in the characterisation and the grouting. Detailed information regarding the Mega-Packer test can be found in Eriksson and Lindström (2008).

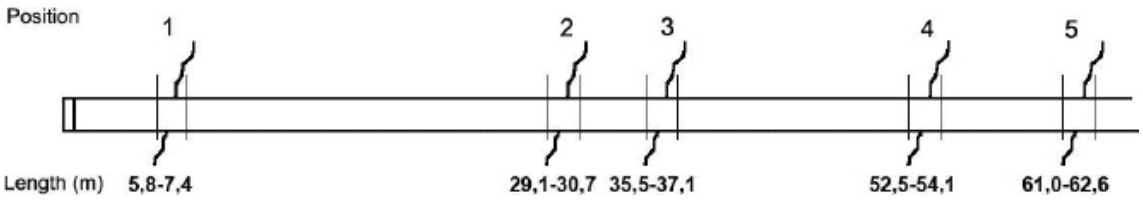

Figure 4-40. *The five positions selected for grouting in DA1619A02.*

Results
Table 4-11 presents the evaluation of the grouting efficiency based on measured inflows before and after grouting. Detailed post characterisation results are found in Eriksson and Lindström (2008). As indicated by the results the performance of the Mega-Packer proved to be good during the tests and grouting efficiency above 85% were reached for all sections, even > 95% was reached for 4 out of the 5 sections. This verifies the theoretical calculations presented in Design Description 2007 (Autio et al. 2008).

As in the case with most post-grouting, there was a tendency to redistribute water to other fractures. New inflow points were noticed in the test drift (a slight increase of flow was also noticed in the neighbouring 15 metre drift); however, the new inflow points in the 95 metre drift were considerably smaller than the original leakages. To give some reference, the total inflow in the 95 meter drift was reduced from approximately 4.4 l/min to 0.4 l/min during the Mega-Packer post-grouting tests.

The flows from the test drift have been followed since the grouting and by January 2011 there is no indication of silica sol deterioration and the inflow has rather continued to naturally decrease.

4.9.3 Conclusions

The tests that have been carried out have demonstrated that the Mega-Packer has the potential to seal horizontal drifts such that the criterion of 0.1 L/min seepage is not exceeded. This is in line with earlier theoretical studies. The test site was however located in a drift that had been pre-grouted with cement and where low groundwater pressures existed. This is likely to have had a considerable influence in the results obtained with the Mega-Packer. Tests at repository level will be required before full confidence in the Mega-Packer can be attained. This is planned for the upcoming project phase.

The above-listed constraints on the results of the Mega-Packer trials aside, the sealing capability observed was at least as good as a well performed traditional pre-grouting using silica sol and showed a better sealing capacity than has been achieved with traditional post-grouting.

Some practical problems were noticed during testing, but these were managed and altogether the method should have good production capability.

Table 4-11. Table showing the evaluated grouting efficiency. Inflow measurements are performed before the grouting started (pre characterisation) and after the grouting was finished at each position (post characterisation).

Position	Inflow before grouting [l/min]	Inflow after grouting [l/min]	Grouting efficiency [%]
1	2.400	0.004	99.8
2	0.145	0.007	95.2
3	0.490	0.015	96.9
4	1.760	0.003	99.8
5	0.190	0.025	86.8

4.10 Wetting techniques related to DAWE

4.10.1 General

As described in Section 4.2, as part of the DAWE design, artificial water filling is carried out as the last stage in a deposition. Artificial water filling has included an issue of pipe removal which was considered critical in the previous project phase (Autio et al. 2008). This issue has been addressed in the recent project phase.

Three alternative water filling methods have been considered in the design work. One of them was basically the method introduced in the earlier project phase "water filling with long pipes". Minor modifications and improvement of the previous design was made in parallel with the design work of the two new water filling techniques in case they would not prove to be feasible.

The new water filling techniques aimed at entirely removing the long water filling pipes included in the earlier design, thus lowering the risk associated with pipe removal. In one of the new techniques considered the idea was to carry out the water filling through the pellet filling hole in the plug, see Figure 4-2. However, this method was discarded due to its disadvantage i.e. the duration of water filling would be too long due to the low flow rate that should be applied to prevent serious erosion.

In the other new method the water filling is carried out with short pipes through the plug. This water filling alternative is described in more detail in Section 4.10.3.

All the considered water filling techniques include one long air evacuation pipe as one essential component, which means that the pipe removal cannot be avoided totally in any of the alternatives. Pipe removal was tested in full-scale at room temperature in the beginning of the project phase in the Äspö Bentonite laboratory.

4.10.2 Pipe removal tests

The objective of the tests was to obtain information about the development of the swelling pressure and the corresponding required pulling force to loosen the pipe resting on small supports inside the profile.

Three tests were carried out. The tests were built around a steel tube, Figure 4-41, which was partly filled with bentonite. The bentonite blocks (MX-80) had an initial water content of 12% and a dry density of 1,732 kg/m^3. Use of blocks with higher dry density and lower initial water ratio compared to distance blocks (see Section 4.5.3) made the test set-up conservative. The buffer was cut to the right dimension and the blocks pushed inside the tube. Effort was made to ensure that the blocks were placed tightly and to the side of the tube. This gave a free gap of 45 mm between the buffer and the tube side simulating the slot 42.5 mm between the rock and buffer in the DAWE design. Once all blocks were in position the flange was secured to the tube and the bolts were tightened. The pipe was inserted via the valve and pushed in all the way to the rear end of the tube. Water was inserted into the free space in the tube via the valves, which started the bentonite swelling, pushing the pipe to the side of the tube and forming a grip around it. To ensure that as little air as possible was left in the tube, one side was raised approximately 30 cm and the water injected in the lower end. When water started to come out of the upper valve the tube was laid horizontally and completely filled with water. The method was used during all three water fillings.

At specific time intervals a pulling force needed to move the pipe loose from the buffer approximately 10 cm was applied to the pipe. The development of swelling pressure and the pulling force needed were measured and logged in a monitoring system. Two swelling pressure sensors were used, one in each end of the tube. The pulling force was measured with a load cell. With data analysis the force needed to loosen and to pull the full pipe assembly length up to 150 m could then be calculated. The general test set-up is shown in Figure 4-41 and the three tests are presented below.

- Test 1. The empty volume was filled with water (using natural Äspö groundwater with salt content of 1% taken from the 420 m level). There was no access to additional water. The force required to pull out the pipe was measured at pre-defined intervals. Test duration was 90 days.

- Test 2. The empty volume was filled with water (same as in Test 1) There was no access to additional water. The pipe was led through the lids in both ends of the test tube. Each measuring time included three pulling forward and three pulling backwards (10 minutes rest between each pulling). Test duration was 30 days.
- Test 3. The empty volume was filled with water (same as in Test 1). The bentonite then had access to additional water from the "rock" side (6 inflow points with a water pressure of 100 kPa). Test duration was 30 days.

The tests were conducted between October 2007 and September 2008.

The major test results are listed below:

1. The bentonite blocks swell and fill up the water-filled slot rather quickly. A swelling pressure acts on the pipe within 24 hours after test start.
2. The force required to pull out the pipe increases rapidly with time. After one day the required force can be higher than the tensile strength of the pipe (150 m pipe).
3. Access to additional water from the rock increases the swelling rate of the bentonite. The result of Test 3 indicated that after 24 hours the required force could be 0.8 kN for a 3 m long test pipe meaning that a pipe with a length of 150 m would require a pulling force of 40 kN.
4. The measurements of the required force are supported by the measured swelling pressure and the measured water content in the clay after termination. The distribution of water content was studied with samples taken from the clay at four cross sections. There was a very clear water content gradient in all tests. The water content around the pipe was about 60–80% in Test 1, 75–100% in Test 2 and 55–85% in Test 3.
5. The tests showed that the removal of one pipe, an air evacuation pipe, after completed water filling should not be an issue in relation to the development of swelling pressure in the compartment.

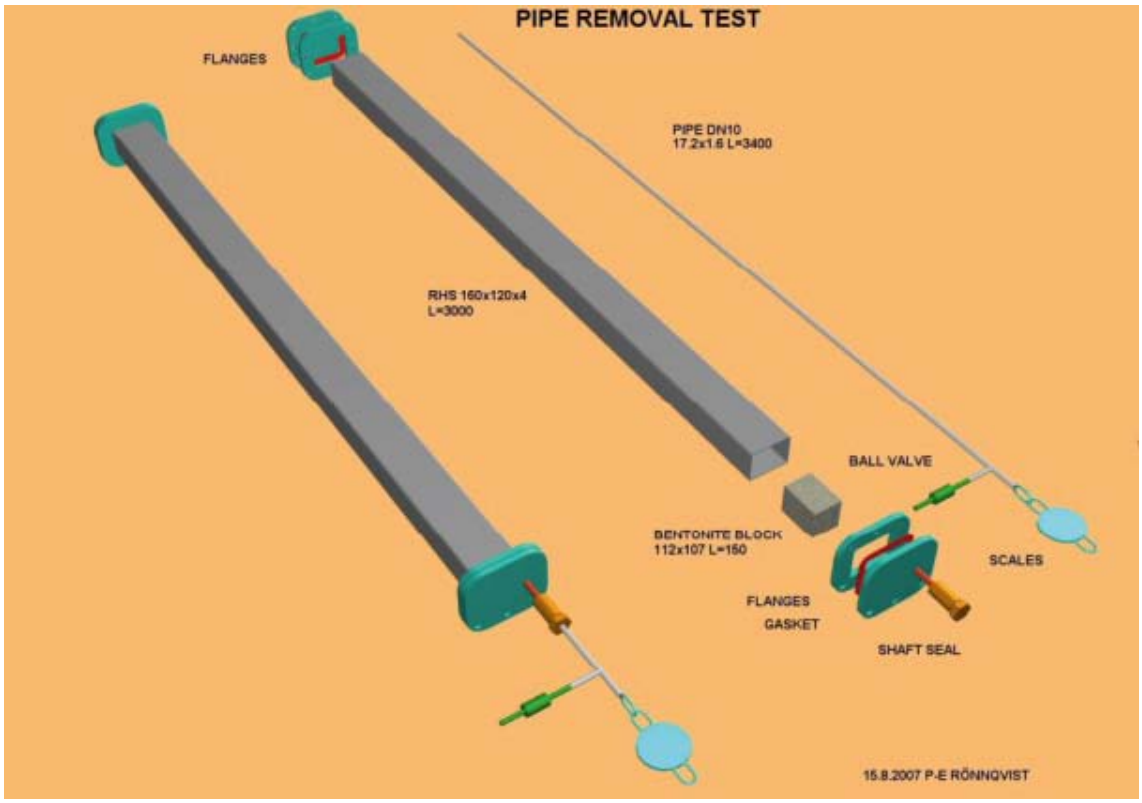

Figure 4-41. *Test equipment for the pipe removal test. Bentonite blocks are inserted in a steel tube leaving a small gap between the blocks and the tube wall. The pipe to be removed is inserted in this gap and the flanges attached.*

4.10.3 Water filling with short pipes and air evacuation

Given the results of the pipe removal tests presented in Section 4.10.2, using several long water pipes to saturate the drift would be problematic as their successful removal in the time avialable before substantial swelling pressure develops cannot be assured. This is not acceptable for long-term safety reasons. A technique using just one long air evacuation pipe and three short water pipes was therefore studied.

Figure 4.2 illustrates this revised concept. In this technique the water filling of the compartment is carried out with three pipes that extend through the plug into the transition zone underneath the transition block that is located between the pellet filling section and the first distance block.

The only remaining long pipe is the air evacuation pipe that stretches the length of the compartment. For air evacuation it is preferable to use the maximum pipe size that can be safely placed in the drift taking into account the space required for the deposition machine, including shifting from side to side which has been observed in the test runs at Äspö. The diameter must be large enough in relation to the inflow rate of water, max 3 l/sec. It has been calculated that an optimal diameter for the air evacuation pipe would be 33.7 mm × 2.0 mm (DN 32**).** The air evacuation pipe will be installed at the lower part of the drift, but in order to function in a proper way the end part at the rear section of the compartment needs to be turned upwards to the top of the drift, where the air will accumulate. This will be achieved by a separate pipe (diameter 17.2 mm) which will be fixed on the end face of the compartment as shown in Figure 4-3. When removing the long air evacuation pipe the coupling will allow it to be released from this bottom pipe, which will be left inside the drift.

The air evacuation pipe will be fixed on the drift surface by drilling small holes in the rock and grouting a support made of titanium. It is also possible to anchor the supports with tight holes without using grout, which would reduce somewhat the amount of grout in the drift (approximately 10 kg/150 m pipe). The mechanism of the support is designed so that the pipe can easily be pushed in and will not hinder removal of the pipe. Spacing of the supports will be 3 metres. The air evacuation pipe will consist of 6 m long pipes which are connected using a screw type coupling. The air evacuation pipe will be made of titanium, the tensile strength of titanium is high enough and the consequences for long-term safety are expected to be less serious if the pipe gets stuck when removing and the pipe has to be left in the drift.

The diameters of the shorter water filling pipes are also set at 33.7 mm × 2 mm (DN32); these will be made of stainless steel.

4.10.4 Conclusions

In this technique the risk of unsuccessful pipe removal has been minimised by having only one long pipe, the air evacuation pipe, which needs to be removed. The removal of short pipes is not deemed to be an issue. Another advantage was confirmed with erosion tests described in Section 5.3. It was concluded that this technique would not cause an increased erosion rate. The total mass loss caused by erosion was concluded to be far from critical.

The water filling using shorter pipes was selected as the preferred design alternative based on its ability to fulfil the requirements and advantages compared to other alternatives.

4.11 Additional studies – structural sealing

Positions of higher inflows are problematic for the KBS-3H design, there is, however, a proposed solution for this, the filling blocks, see Section 4.6. Earlier solutions has been the use of double compartment plug sections (Autio et al. 2008). These are still potential options for very high inflows but are currently not part of the KBS-3H reference design. The structural sealing is another solution that has been developed for these higher inflow positions, it is reported here but is currently ruled out since the filling blocks are the preferred solution together with post-grouting using the Mega-Packer.

4.11.1 General

The structural sealing is an alternative to the earlier used double compartment plug section used in drift sections with higher inflow.

Basically, the structural sealing is a tube made of construction steel S355J2 that would be placed in the drift at the inflow position. As opposed to the double compartment plug section the complete installation of the structural sealing could be carried out before deposition in the drift begins, thus no pause in the deposit work would be needed at the high inflow position.

The inner diameter of the tube matches the drift diameter and the length of the tube can be adjusted in steps of three metres to suit different fractured zones. Seals at both ends provide ability to rapidly seal the fractured zone after the installation, Figure 4-42.

4.11.2 Installation

To be able to have a seamless drift wall the drift would have to be concentrically reamed from Ø1,850 millimetre to Ø2,075 millimetre at the position where the tube is to be installed, Figure 4-43. The inner diameter of the seal will then match the drift diameter.

The structural sealing is made of modules that would be welded together after they have been positioned in the drift. In Figure 4-43, two sections have been welded together to a total length of six metres.

The transportation and the mounting of the sections would principally be carried out as shown in Figure 4-44. Hydraulic controllers mounted on a rig equipped with wheels would handle the positioning of the sections.

When the sections are in position the tube is welded together by an automatic welder placed on the rig. The tube would be centred mechanically in the drift with the help of support pins. After welding the void between the structural sealing and the rock should be grouted, likely with low-pH concrete finalizing the installation. The anticipated installation time would be 18 working days for three workers.

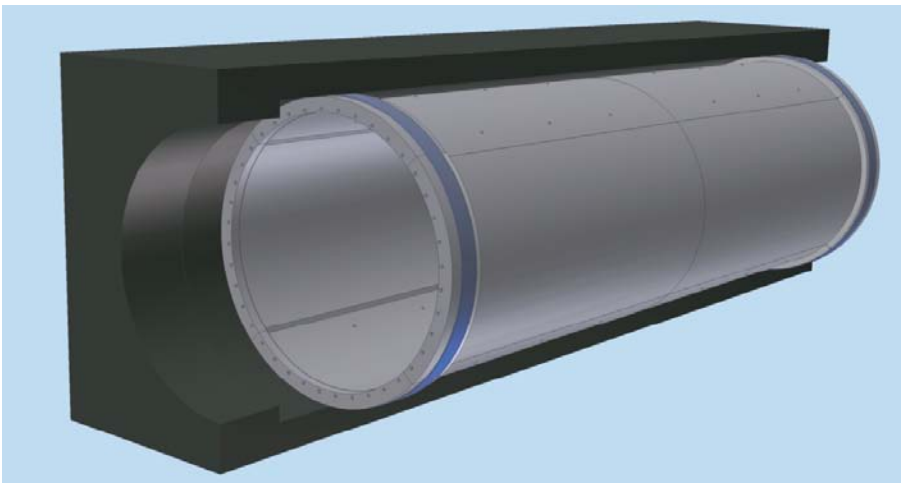

Figure 4-42. *Structural sealing design. The seal is installed in sections with high water inflow.*

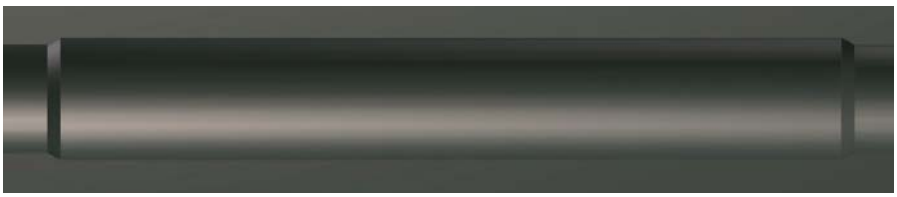

Figure 4-43. *The drift would need to be reamed at the structural sealing position. The diameter would be increased from Ø1,850 millimetre to Ø2,075 millimetre.*

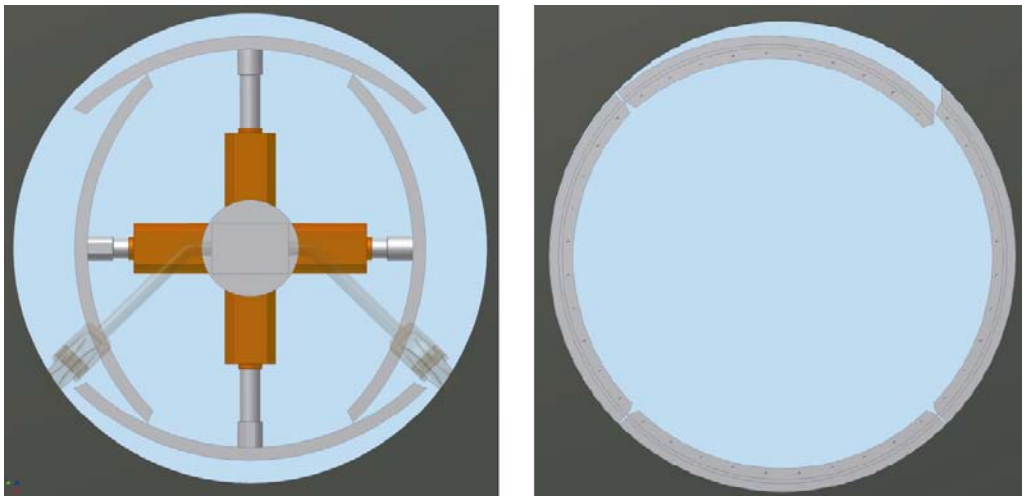

Figure 4-44. *Left: Transportation of tube sections would have been done with a hydraulic rig also being able to position the parts correctly in the reamed section of the drift. Right: The parts are positioned in the reamed section.*

4.11.3 Conclusion

The study concluded that the structural sealing could be an alternative to the double compartment plug section if the fractured zone to be sealed is limited in extent. For longer fractured zones it would be more efficient and economical to use compartment plugs since the installation of the structural seal would be rather complex.

After the structural sealing study was completed a new filling component design has been presented, see Section 4.6. In the new prioritized design double compartment plug sections are no longer used to seal drift sections of higher inflow. The economical incentive to use structural seal instead of compartment plugs is therefore not valid and no further development will take place.

5 Buffer Issues

5.1 Introduction

The smectite content of the bentonite clay used to make the buffer material is responsible for its ability to swell and close gaps or channels and ultimately to form a more homogeneous buffer, which is needed to fulfil the density requirements presented in Chapter 3.

"Water flowing into an unflooded deposition drift containing a newly-installed Supercontainer and distance blocks have a very high potential to induce localised buffer erosion. This redistribution or loss of buffer material could result in reduction of the buffer density to less than an acceptable value. The largest allowed loss of buffer from an inflow point close to the canister has been set at 100 kg due to the potential for the buffer to not come to density equilibrium (Chapter 6). Other mechanisms related to water flow through or adjacent to the deposition drift also have the potential to cause loss of buffer mass and are presented below."

Erosion related to flow of water, that may take place in the KBS-3H deposition drifts can be divided into the following three cases:

- After installation of the compartment plug the drift will be artificially water filled through tubes led through the plug in DAWE design alternative. The water filling will cause considerable water movement in the initially unfilled regions of the drift and it will lead to some mechanical erosion of the buffer adjacent to the water discharge points of the filling tubes.
- Some erosion may occur through natural groundwater inflow from fractures both before and after the water filling. However, this erosion is judged to be very small for the period before water filling as the bentonite blocks will be physically protected by temporary drip shields or else be physically separated from inflowing water by the feet underlying the Supercontainers as well as the other drift components. These feet will keep the Supercontainer above any water flowing along the floor of the drift. After artificial water filling, there is no further substantial empty space in the drift and the inflowing water will be limited to small amounts and will be absorbed by the buffer rather than inducing any erosive behaviour.
- Chemical erosion has been identified as a process that may occur when glacial meltwater penetrates to repository level. Conditions that allow dilute groundwater to enter the drift e.g. after possible earthquakes a fracture of fractured zone will be formed that creates hydraulic connections through which e.g. glacial melting waters can penetrate into the repository, reducing the TDS content in hydraulically-active joints/fractures to essentially zero. This process is very slow as it requires colloidal migration from the buffer into open hydraulic features. However, under certain conditions it could cause large loss of smectite mass and so it needs to be assessed with respect to its potential to affect buffer performance.

Additionally there may be a period shortly after bentonite block installation where clay particles are mechanically eroded by detachment "dropped bentonite particles" from the blocks due to the humidity in the drift air.

The swelling properties of buffer are important with respect to homogenization of the buffer after water filling of the drift compartment. The swelling and homogenization of bentonite is a complex process involving swelling caused by absorption of water and resistance to swelling caused by friction. The friction is both internal in the bentonite and external between the bentonite and the surrounding fixed walls such as the rock surface and in some cases the canister. Both strain-affecting processes are affected by groundwater chemistry, the presence and dimension of the gaps in the installed system and so there are numerous interactions that need to be considered. Additionally there is a need to consider how a system that has experienced erosional loss will recover/respond to this loss and if it is still able to fulfil its barrier functions.

Significant effort has been made in the KBS-3H project to develop buffer design further. Several functional uncertainties and development topics related to buffer behaviour, denoted as buffer issues, were identified in the previous project phase. These issues are important, because they affect the processes that occur during the transient phase when emplaced buffer blocks absorb groundwater and evolve to reach fulfilment of the performance requirements and the issues may have an effect on the redistribution and the homogeneity of the buffer mass. Buffer related issues have been studied for both design alternatives, DAWE and STC.

The KBS-3H specific buffer issues studied in this project phase were:

- Erosion in STC caused by inflows.
- Erosion in DAWE due to artificial wetting.
- Erosion in DAWE due to detachment of bentonite particles from Supercontainer.
- Homogenization of cavities caused by erosion.
- Buffer swelling and sealing in heterogeneous inflow conditions (water transport by internal piping).
- Impact of rock shear on canister.
- Development of swelling pressure in DAWE.

In addition to the KBS-3H specific buffer issues there are buffer issues, which are common for KBS-3V and KBS-3H. These studies are reported elsewhere.

General description of the DAWE design has been presented in Section 4.3.

5.2 Erosion in STC caused by inflows

5.2.1 General

Water inflow into the deposition drift in the STC design alternative will take place mainly through fractures and will wet the buffer. However, before full water saturation has occurred the inflowing water may cause detrimental effects due to erosion on the buffer material in a Supercontainer section, see Figure 5-1.

Groundwater flows into the drift and fills the Supercontainer section where inflow occurs with water before it flows to the neighbouring Supercontainer section according to the STC design; see Section 4.1.2 and Figure 5-1. The inflow will continue until all empty space inside the drift is filled with water. The filling time in STC is dependent on the inflow rate and will possibly take a long time. Eventually the inflow will slow down as the pressure inside the drift rises and the pressure gradient will eventually be even in the drift and in the adjacent rock mass. As a result of inflow a considerable amount of water volume will pass the inflow point and cause some degree of erosion in the bentonite close to the inflow point. It is probable that the loss of eroded material is distributed along the entire water flow channel and not in one point. However, due to lack of knowledge the conservative assumption is made that all eroded material is taken from the inflow point at the rock surface.

The objective of the study was to form a basis for evaluation of the erosion rate due to the process of water filling by natural groundwater leakages in STC design alternative.

Since STC was not selected the issues and associated tests will be presented somewhat shorter than the DAWE issues and focus will be on the conclusions.

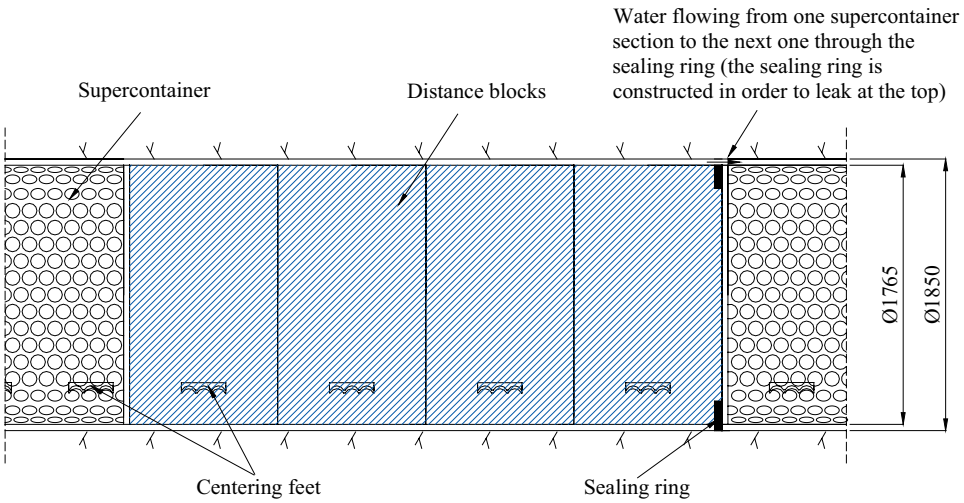

Figure 5-1. *Layouts of the STC design (Autio et al. 2008).*

5.2.2 Description of the results

Gelling tests

Basic tests were carried out in order to understand how the properties of the slurry (water and bentonite) or gel, originating from the inflowing water into a Supercontainer section, changes with time during and after the filling period.

The gelling tests were carried out by exposing small bentonite blocks to water of different salt content, a 1/10 Plexiglas cylinder was used but the slot was kept at a real dimension, 42.5 mm, see Figure 5-2. The tests were left between 1–30 days and then sampled in a number of positions.

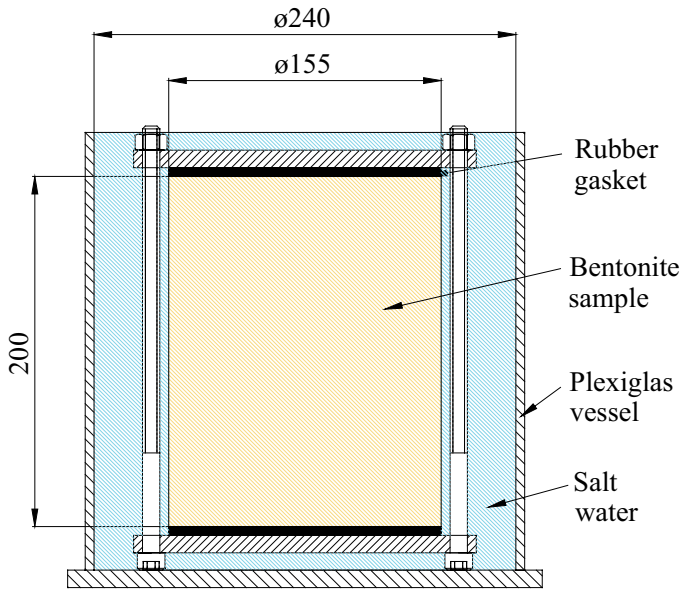

Figure 5-2. *Schematic drawing of the test equipment. The vessel was filled with salt water (1 or 3.5% salt content) and a bentonite cylinder was placed in the middle. After exposing the bentonite sample to water for a certain time, the test was terminated. The water content of the clay in the slot was determined in a number of positions.*

The initial water content (water content is defined as the ratio (%) between mass of water and mass of dry material) of the bentonite blocks seems to be of minor importance regarding the behaviour of the bentonite during the water filling of a STC compartment. The salt content in the inflowing water and the exposure time are the two parameters that seem to mainly influence the consistency of the bentonite gel. A high salt content in the water increases the homogenization rate. The tests with water having a salinity of 3.5% show that after 10 days the gel at the outermost cm (closest to the rock) has a water content between 99 to 167% (corresponds to a saturated density between 1,315–1,473 kg/m^3). The consistency after 30 days' test is in the same range. When water with a salinity of 1% is used, the determined water content after 10 days test is between 173 and 383% (corresponding to a saturated density between 1,152–1,315 kg/m^3). In order to understand the behaviour in detail, especially the time dependence, additional tests would be required.

Tests on erosion from a Supercontainer section

In the STC design the buffer material in a Supercontainer section will be exposed to water during the filling time. With the maximum allowed water inflow, 0.1 l/min (the requirements presented in Chapter 3), into a Supercontainer-section the filling time of the void in one Supercontainer section will be about 20 days. After this time the water will start to leak over to the next Supercontainer section.

Tests were carried out with the aim of investigating the erosion properties (e.g. rate of erosion) and behaviour of the swollen clay (gel) in the slot during the leakage into the next section.

A Plexiglas cylinder was used to simulate a Supercontainer section, the radial scale of the bentonite block and the drift diameter was about 1:10 but the slot width was set to 42.5 mm in order to simulate the real case for a centred distance block, see Figure 5-3. Bentonite blocks with water content of 17% and a bulk density of 2,090 kg/m^3 were used. The lid at the end (outflow side) was sealed with an O-ring with an opening at the top. The opening made it possible to fill up the voids in the test section and after filling let water leak out in order to simulate the expected leakage into the next Supercontainer section.

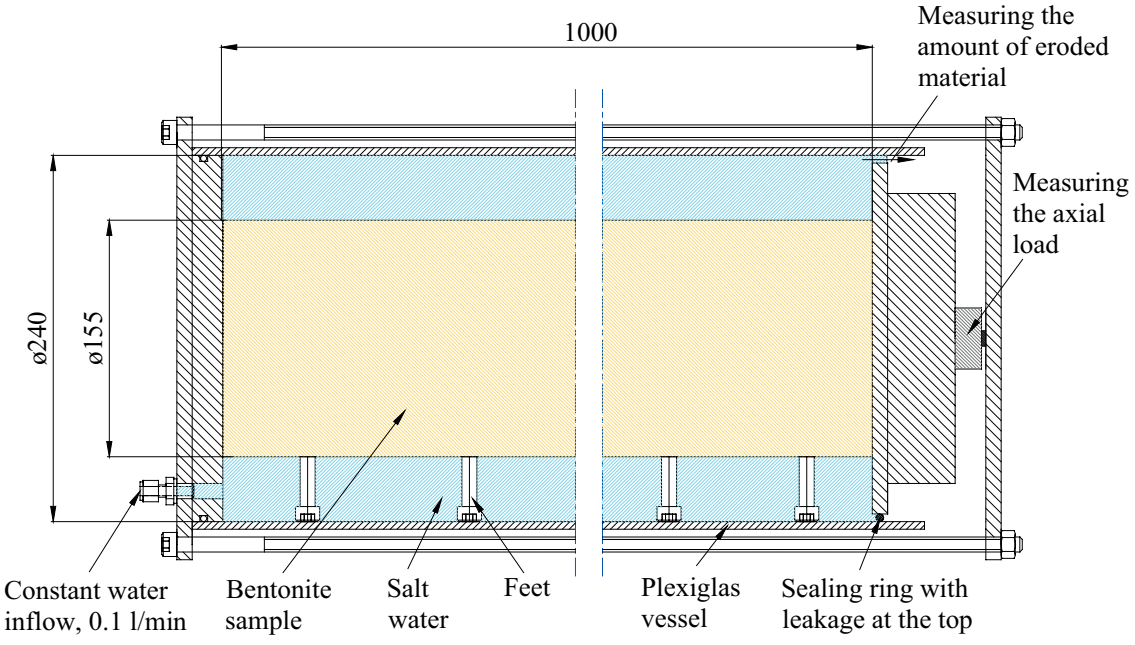

Figure 5-3. *Picture showing the test equipment. Bentonite blocks were placed in the centre of the tube made of Plexiglas, standing on feet. The empty space was filled during a specified time and then a constant flow was applied. The amount of eroded material in the discharging water was determined.*

The following processes were measured and controlled during the tests:

- Water flow into the system (was set to a pre-determined value on a microprocessor controlled pump).
- The pressure of the inflowing water. If the bentonite has swollen and sealed, a water pressure might build up due to the applied constant flow.
- The water-flow out from the system. Samples of the outflowing water were taken at decided intervals and then weighed. With this procedure the amount of water flowing out per time unit could be calculated.
- The amount of eroded material in the water. Samples were taken from the outcoming water at decided intervals and the amount of clay was determined by evaporating the water in an oven at 105°C.
- The axial load. The swelling pressure from the bentonite acting on the axial lid was measured.
- Observation. A digital camera was used in order to register the different phases.

Totally three tests were carried out:

- Test 1. A constant flow rate of 0.1 l/min was applied from the start. 3.5% salt content in the water.
- Test 2. The inflow rate was set in order to fill the section in 10 days (0.002 l/min). After completed filling the water flow rate was increased to 0.1 l/min. 3.5% salt content in the water.
- Test 3. A constant flow rate of 0.1 l/min was applied from the start. 1% salt content in the water.

The results are summarised below:

- Erosion and water flow into the next Supercontainer section. In the two tests where it was possible to measure the erosion rate (Test 1 and Test 3) there were no indications that bentonite gel should flow from one compartment to the other. Instead all water was flowing in a channel at the top of the compartment. The erosion was low in the beginning of the tests depending on the fact that during the filling, the bentonite particles that came loose from the blocks were settling down on the drift floor and the uppermost water was almost clear. The results from the erosion measurements are well inside the limits of the erosion model (Figure 5-4).
- Block behaviour during water filling. The buffer behaviour in Test 2 was very different from Tests 1 and 3. The test was performed using water with a salinity of 3.5%. The water flow rate was set to 0.002 l/min in order to fill the "compartment" in 10 days. After testing for three days the buffer blocks had started to crack severely. After seven days it was observed that the blocks have been pushed upwards by the swelling bentonite at the floor and large cracks have been formed. After about 12 days test the bentonite started to separate in one position and a pocket containing free water was formed. The bentonite had sealed and the water pressure could act on the whole cross section area pushing the bentonite forward. The pocket with free water continued to grow and bentonite gel was pressed out from the compartment. The behaviour seen in this one test is considered indicative since it was not repeated and is assumed to be caused by the slow filling rate, which gives an uneven wetting of the blocks, resulting in cracking and that part of the blocks will fall down to the drift floor. The relative humidity in the compartment during filling is very high and in combination with the rather long exposure time for the bentonite blocks increases the cracking of the blocks.

Evaluation of the results by using the Erosion model

This erosion model presented by Sandén at al. (2008a) was used to estimate the erosion of bentonite caused by a point inflow. The erosion model is based on several different erosion measurements. (Sandén et al. 2008b) found that the following Equation (5-1) gave the best fit for the results, see also Figure 5-4.

$$m_s = \beta \cdot (m_w)^{\alpha} \qquad (5\text{-}1)$$

where

m_s = accumulated mass of eroded bentonite (g)

m_w = accumulated mass of eroding water (g)

β = 0.02–2.0 = parameter defined by the level of erosion at a certain accumulated water flow

α = 0.65 = parameter defined by the inclination of the straight line relation

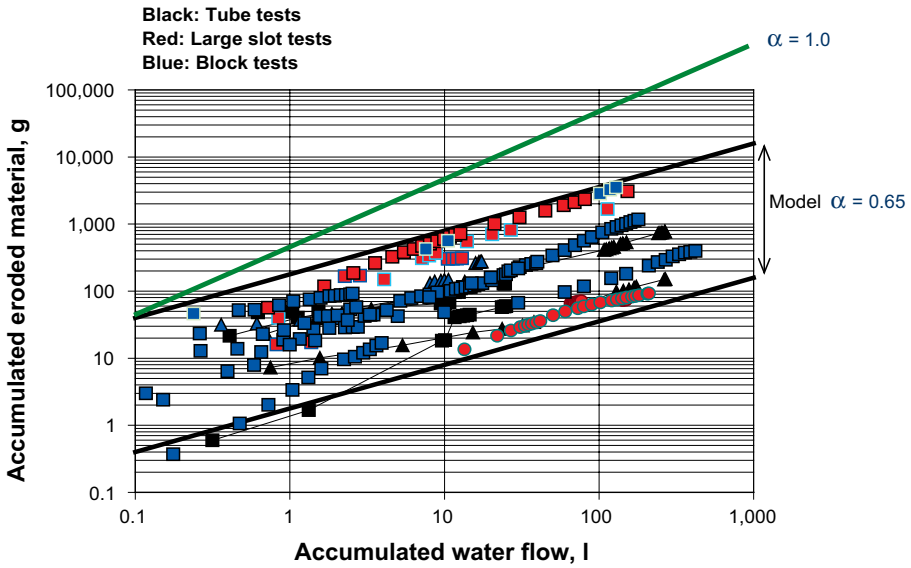

Figure 5-4. *Results of different erosion measurements plotted in one diagram. The lower boundary line corresponds to β = 0.02 and the upper β = 2.0. The inclination corresponding to α = 0.65 is motivated by the figure. α = 1.0 (corresponding to constant erosion rate) is also illustrated, see Sandén et al. (2008b).*

Equation 5-1 describes the total mass of eroded bentonite as a function of the total mass of eroding water; it is derived on empirical results and used to estimate the erosion of the bentonite in deposition drift for different water filling cases.

The parameter ”α” seems not very much affected by the test material or conditions and is according to the measurements constant with the value of 0.65. The parameter “β” must be measured and seems to be dependent mainly on the material type, the salt content, the water ratio, the pellet grain size distribution and the geometry. According to the model, erosion seems to be dependent only on the accumulated flow volume i.e. the flow rate has no influence.

The total volume exposed to flowing water is the empty space in the deposition drift, which is about 80 $m^3 = 8.0 \cdot 10^7$ g. If all water comes from one Supercontainer section the eroding mass of bentonite will according to Equation 5-1 be (using β = 0.02–2.0) $m_s = \beta \cdot (8.0 \cdot 10^7)^{0.65}$ = 2.74–274 kg bentonite, which is more than 100 kg and thus not acceptable (see Section 5.1). The allowed accumulated mass of eroded bentonite, “m_s” = 100 kg, and β = 2.0 yields that 17 m^3 or 21% of the total water volume needed to fill the drift is allowed to flow from one Supercontainer section. Keeping in mind that all tests done have shown that one inflow point usually yields only one channel where the water flows and assuming that the erosion takes place along the flow channel, which is very probable, the maximum allowable inflow rate into a Supercontainer section is 10% of the total inflow rate into the entire drift. In case the flow rate is higher than this it could lead to unacceptable amount of eroded bentonite in a Supercontainer section and to the rejection of the drift. This is a major disadvantage in the STC design alternative.

In addition there is about 60 m^3 left to fill the remaining pore space in the bentonite blocks. The calculation and reasoning above presumes that this pore space will be filled so slowly and evenly distributed that no erosion takes place.

5.2.3 Conclusions

The issue of mechanical erosion of bentonite has been studied in several ways during the project phase 2008–2010. Analyses were performed to see how much bentonite material may erode from the inflow points in different situations and put limits to allowable inflow if required. The critical limits were studied for both candidate designs, although the cause of erosion is different in both designs.

For STC the study concluded:

- The results from the erosion measurements with constant flow rate of 0.1 l/min and a salt content in the water of 1% or 3.5%) were well inside the limits of the erosion model.
- In the work with the issue related to erosion in STC-design an obvious problem was detected in the block behaviour during water filling of a compartment. It was found, that with a slow inflow rate (0.002 l/min, salt content 3.5%) a gel was formed that stopped piping and instead caused separation of water and gel, creating a water-filled pocket and squeezing of bentonite gel from one section to another. The problem was severe and is of course negative for the STC design. Only one test was, however, performed and the uncertainties are still considerable regarding this issue. This scenario could have an effect on the allowed water-filling rate and thus needs to be further investigated.
- The criterion for acceptable loss of bentonite in one Supercontainer section in a deposition drift in the study was set to 100 kg (Section 5.1.). Greater erosion would lead to unacceptable in homogeneities in the buffer density later in the saturation process.
- Allowable inflow rate that limits the amount of material eroded from a Supercontainer section until the drift is filled with water has been found to be 10% of the total inflow rate into the entire drift. This means that the drift should be rejected if the inflow rate into a Supercontainer is higher than this or else some remediation is needed in order to reduce the inflow rate to an acceptable level.

5.3 Erosion in DAWE due to artificial water filling

5.3.1 General

General description of DAWE has been presented earlier in Section 4.3.

The use of artificial water filling in the DAWE design alternative led to work study of mechanical erosion due to the water filling, which is the most important of the three erosion mechanisms described in Section 5.1. The issue of water filling through the compartment plug in the DAWE design is one of the important issues identified in the KBS-3H project. The new design of the water filling system, not using long pipes but instead three short tubes through the plug, means that all water has to flow from a position just inside the plug. Pumping water to fill the voids in the compartment (c. 40 m^3) within about 8 hours will cause considerable water movement in the initially unfilled regions of the drift compartment and will lead to some mechanical erosion and redistribution of the buffer/filling material adjacent to the water discharge points, see Section 5.1.

The main objectives with the tests performed during the current project phase were to study the impact of the water filling technique on the pellet filling section and the buffer blocks especially regarding mechanical erosion and redistribution of material.

Other erosion mechanisms were not studied. Mechanical erosion caused by groundwater inflow is assumed to be negligible due to grouted fractures, spray and drip shields compared to that caused by artificial filling of the compartment. Groundwater inflow to the drift will eventually slow down as the pressure inside the drift rises and the pressure gradient will eventually be even in the drift and in the adjacent rock mass soon after water filling.

5.3.2 Description of work and results

In total four erosion tests were carried out. For each test set-up 22 cylindrical bentonite blocks were needed. The blocks were manufactured using the same mould and technique as the blocks used in the LOT and ABM experiments (Karnland et al. 2000). The blocks were made of MX-80 bentonite. The bentonite was originally delivered with a water content of about 12% but more water was added during mixing (mixing was made at the bentonite laboratory at Äspö) and the measured water content before starting the block manufacturing was 17.0%. The blocks were compacted with a pressure of 100 MPa.

A schematic picture of the test equipment set-up is shown in Figure 5-5. The outer tube is a standard steel pipe DN 350 giving a somewhat smaller gap between the bentonite block and the drift surface (35.8 mm, compared to 42.5 mm for the real case). This small difference is, however, judged to be negligible. The equipment consists of the following main components:

- Test tube, length 2,400 mm, diameter 355 mm, equipped with 6 transparent windows.
- End flanges with lead-ins for water pipes.
- Water pipes with valves: two for leading water in and four for leading water out of the tube.
- Water pump.
- Compacted bentonite blocks (MX-80) with feet (22 pieces including the dummy block, see below), length 100 mm, diameter 280 mm. The blocks available are ring-shaped and therefore the central part is closed by an inner tube with plates at the ends.
- Dummy block (concrete) with feet, length 100 mm, diameter 280 mm. (This was changed to a buffer block in the tests performed.)
- Bentonite pellets placed at the entrance.

The four tests were performed with two water flow rates (1.67 l/min and 21 l/min) and with two water types (fresh water and 1% salt content). A summary of the tests is provided in Table 5-1. In addition, a detailed description of each test is provided in the following sections.

All four tests were performed with the same type of bentonite blocks (MX-80 block compacted with 100 MPa at water content of 17%) and pellets (MX-80 pellets with water content 13.5%).

The tests were running for eight hours except for Test 4. This test was performed with 1% salt in the water and with a flow rate of 21 l/min. The access to large vessels, about 1,000 litres salt water could be prepared in advance corresponding to about 50 minutes test duration, put a limit to the test time.

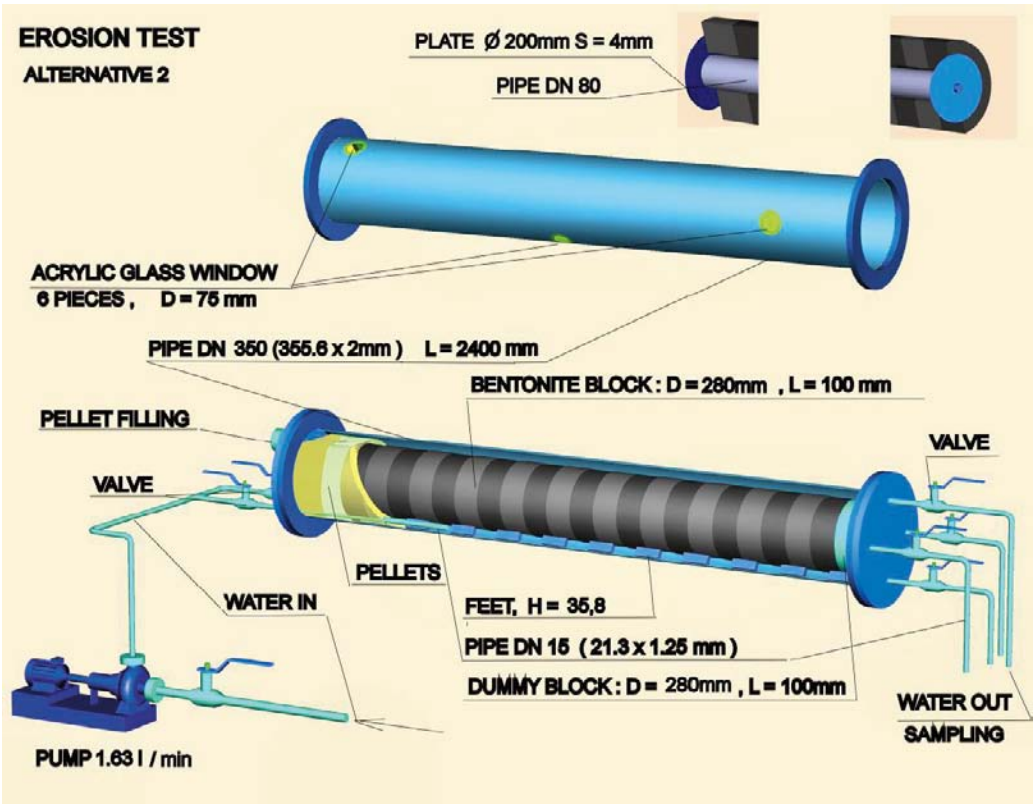

Figure 5-5. *Equipment for bentonite erosion test for the wetting alternative using pipes, which are led through the steel plug.*

Table 5-1. Summary of the performed four tests including the bentonite material used with the initial water content, type of water, water flow rate , duration of the test, volume of the slot between bentonite blocks and the tube as well as the time for water to pass through the system (water in – water out).

Test	Block Material	w, ini. %	Pellets Material	w, ini. %	Water	Water flow rate l/min	Test time hours	Empty space to fill up litres	Time to first leakage minutes	Remark
1	MX-80	17%	MX-80	13.50%	1% salt	1.67	8	72.7	57	Bentonite particles in the water. Bentonite gel on the bottom of the "drift".
2	MX-80	17%	MX-80	13.50%	Tap water	21	8	72.7	4.5	The water looks very clear. No bentonite on the "drift" floor.
3	MX-80	17%	MX-80	13.50%	Tap water	1.67	8	72.7	56	The water looks very clear. No bentonite on the "drift" floor.
4	MX-80	17%	MX-80	13.50%	1% salt	21	1	72.7	4.5	The water is cloudy. Bentonite gel on the bottom of the "drift".

The mechanical erosion rate was measured in all four tests. The accumulated dry weight of eroded material is plotted versus time in Figure 5-6. A large number of erosion tests have been performed earlier within other projects, e.g. Baclo project (Sandén et al. 2008b). With these earlier tests as a basis, a model describing the dry weight of accumulated amount of eroded material plotted versus the accumulated water flow in logarithmic scales has been suggested, see Section 5.2.2. An important finding was that the mechanical erosion rate decreases by time. In Figure 5-7 the data from the new wetting tests have been plotted in such a diagram together with the limits of the suggested model (black lines).

The following observations and conclusions can be drawn from this diagram:

- There is a substantial influence of the salt content in the water. The mechanical erosion is almost a factor 10 larger when the water contains 1% salt compared to when fresh water is used.
- There are irregularities in the salt water curves at the accumulated flow 50–100 l, see Figure 5-7. This is probably caused by the difference in the behaviour before and after the slot in the tube is filled with water. The slot contains about 70 l of water. The inclination of the relation (at the accumulated water flow larger than 100 l, i.e. after the slot has been filled with water) differs between the measurements and the model. While the model has an inclination (Dm/DV) of 0.65, which is less than 1.0 and thus means a decrease in erosion rate with time (or increased accumulated flow), the new results indicate an inclination close to 1.0, which means a constant erosion rate with time. This has been observed earlier in similar tests and is probably caused by the difference in flow conditions. In the tests, on which the model is based, the flow has taken place in channels, while the flow in these DAWE specific tests takes place in a large slot along a bentonite surface area. The consequences of this difference are mainly the following two:
  - The water velocity over the bentonite surface is lower in the DAWE specific tests since the slot is wider than radius of the channels in the earlier tests, which should lead to a lower erosion rate.
  - The surface area is constant in the DAWE specific tests, while when the flow takes place in a channel the diameter may be reduced leading to a reduced surface area and a reduced erosion rate.

Another explanation is that parallel to the erosion process, material is settling within the test volume which may not be the case when erosion takes place in a channel. This means that there probably is some internal erosion, contributing to a certain re-distribution of material within the “drift”. When this water filling method is used in the real case, all erosion is internal.

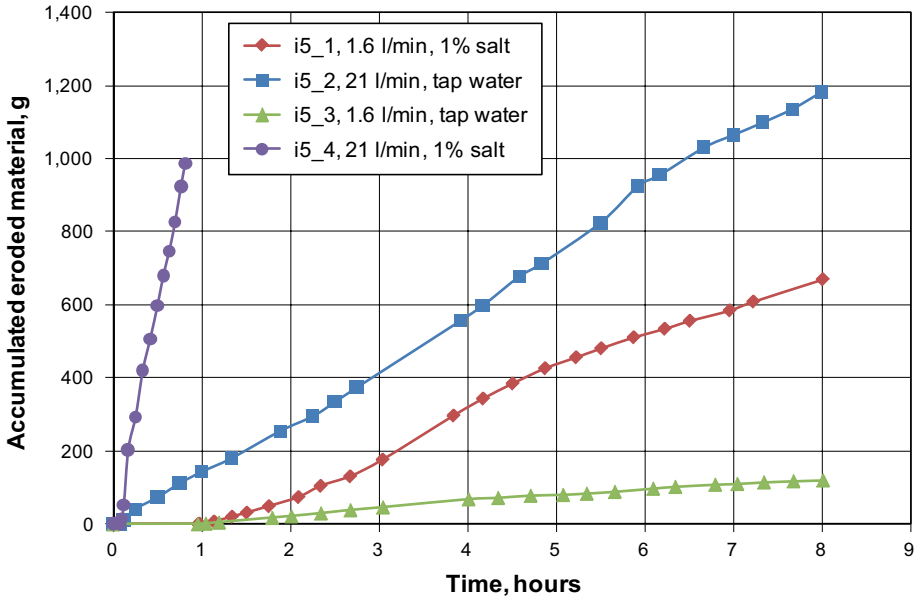

Figure 5-6. *The accumulated amount of eroded material plotted versus time.*

Erosion calculation with erosion model

Artificial water filling will take place through a plug placed in the drift compartment with the maximum length of 150 m (i.e. a 300 m drift will be divided in two parts by a plug). The filling will be made through 3 tubes, which means that they either act separately or, if they are located close to each other, as one inflow point.

The total volume exposed to flowing water is the empty space in the 150 m long deposition drift compartment, which is about 40 $m^3 = 4.0 \cdot 10^7$ g. If the inflow acts as one inflow point the eroding mass of bentonite will, according to Equation 5-1 be (using $\beta = 0.02–2.0$), see Section 5.2.2.

$m_s = \beta \cdot (4.0 \cdot 10^7)^{0.65} = 1.75–175$ kg bentonite,

If the inflow acts as three different inflow points the total erosion will instead be

$m_s = 3 \cdot \beta \cdot (1.33 \cdot 10^7)^{0.65} = 2.57–257$ kg bentonite,

The difference is caused by the reduction in erosion rate, which will be lower when the inflow is via a single point as opposed to three points. The total mass of eroded bentonite for a given inflow volume is therefore greater when there are multiple inflow points. Stronger when the inflow comes in one point than in three points. The total mass of eroded dry bentonite is for a certain inflow volume thus larger the more inflow points that are used.

However, this conclusion follows from the erosion model, which states that only the total volume and not the flow rate influences the erosion. The flow rates during water filling are, however, very high and it remains to be confirmed if the model is valid at those flow rates. The empty space is planned to be filled in 8 hours, which yields a water filling rate of 75.3 l/min or 1.3 l/s, which can be compared to the fastest inflow rate tested, which was 21 l/min.

Tests with very high inflow rates have been made for “Erosion by wetting in DAWE”. In these tests as described in Section 5.3 water filling according to DAWE was tested in scale ≈1:7 (diameter 28 cm and length 2.4 m) with water inflow rate of 1.7 l/min and 21 l/min. The layout of these tests also differed from the tests that Equation 5-1 was based on. In these new tests water flowed along an entire slot surrounding the bentonite, while in the previous tests the water flowed through a channel. Figure 5-7 shows results of the tests.

Figure 5-7 shows that the measured relations are independent of the flow rate and after a while also fell well inside the limits of Equation 5-1. However, the slope of the relations seems to differ from Equation 5-1 since α is larger than 0.65. The total erosion caused by artificial water filling with the

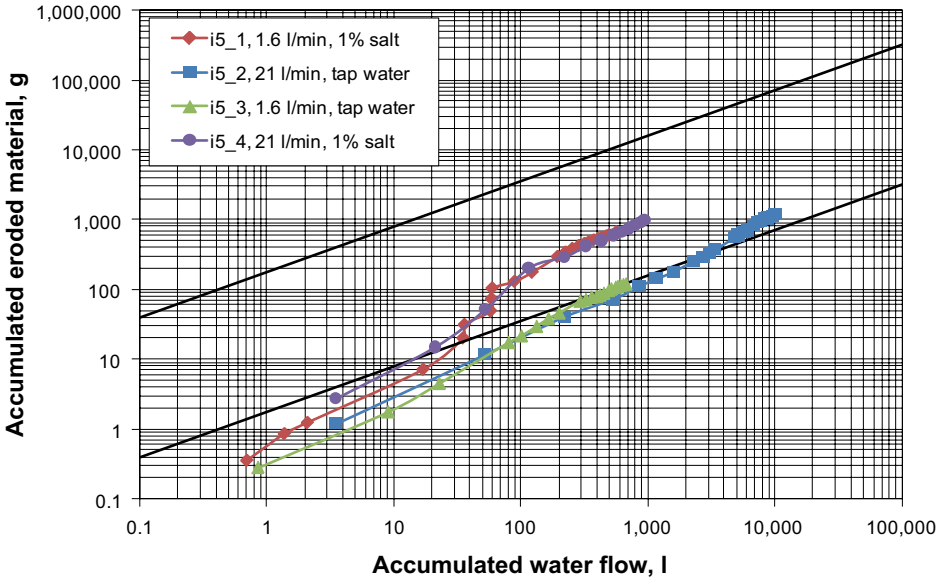

Figure 5-7. *The accumulated weight of eroded material plotted versus the accumulated volume of water. The black lines show the limits of Equation 5-1.*

salt content 1% in the water is expected to be about 40 kg if the measured relations are extrapolated. This is substantially lower than predicted from Equation 5-1 when using $\beta = 2$. It seems thus as Equation 5-1 overestimates the erosion when artificially flooding occurs. The total mass loss caused by erosion is apparently not critical since testing indicates that only a fraction of the total mass of bentonite in a Supercontainer section is lost.

Equation 5-1 describes the total mass of eroded bentonite as a function of the total mass of eroding water; it is derived from empirical results and used to estimate the erosion of the bentonite in deposition drift for different water filling cases. The results of the estimation showed that up to 257 kg of dry bentonite can be lost during artificial water filling via three injection points just inside the plug within the transition zone, see Figure 5-5, in which the test set-up is presented. The figures derived from Equation 5-1 are considered as guidance for design and are of course associated with uncertainties. The largest uncertainty is that the relationship used in the equations is derived under somewhat different conditions than those that will prevail during water filling for KBS-3H.

In the case of KBS-3H and artificial water filling through pipes led into the bottom of the deposition drift the results from tests made specifically for erosion with water filling in DAWE indicate that the estimated figures using Equation 5-1 overestimate the mass of erosion. Regardless of that, the overall conclusion was that erosion is not a problem at artificial water filling in DAWE.

5.3.3 Conclusions

The following conclusions have been drawn from the test results:

- **Influence of salt in the water**. There was a very clear impact of the water type (salt content) on mechanical erosion and redistribution properties of the bentonite within a compartment. The advantage with using fresh-water compared to formation water seems to be very significant. Since only salt-free water and water with salt content 1% have been used in those tests the conclusion is that salt-free water should be used if salt content in the groundwater is higher than 1%.
- **Erosion**. The empty space to be filled in a compartment is about 36.2 m^3 (150 m long compartment). If the limits of the suggested erosion model are used, see Figure 5-7, this flow could cause a total amount of eroded material between 1.64 kg and 164 kg, however, in this special case with water filling through the compartment plug, no material will leave the compartment, but it will just be redistributed within the compartment. In the performed test (see Figure 5-7) the total amount of eroded material using fresh water followed the lower limit of the erosion model.

- **Redistribution of bentonite**. When terminating the tests it was possible to see that a certain redistribution of bentonite had occurred. In the two tests performed with salt water, material had come loose from the block surface during the wetting and settled to the drift floor. The material seemed, however, to be distributed rather evenly along the test tube. In the two tests performed with fresh-water almost no material could be seen on the "drift" floor.
- **Local erosion close to the inflow points**. Careful examination during dismantling of the four laboratory tests did not show that erosion had occurred locally anywhere.
- **Pellets filling**. It was observed that some pellets installed at the inflow part of the test, had swollen into the slot between block and "rock" but there were no signs that pellets had eroded away. The pellets filling was in all tests completely wetted i.e. the voids between the pellets were filled with water.
- **Influence of water flow rate**. In order to fill a 150 metre long compartment in eight hours, a water flow rate of 75.3 l/min is needed. In the performed laboratory tests two different water flow rates were tested, 1.67 l/min and 21 l/min. The lower flow rate was chosen in order to achieve the same filling rate of the drift as in the real case and the higher flow rate, 21 l/min, was the maximum flow rate that could be achieved with available pumps and with the rather high flow resistance in the pipes leading water into the compartment. No difference in erosion rate (amount of eroded material per litre injected water) or buffer behaviour (such as localized erosion) between the two tested water flow rates was detected; see Figure 5-7. This behaviour is used to conclude that 75.3 l/min (the actual filling rate during artificial wetting) would not cause increased erosion rate.
- **Total weight of eroded material**. Since the results did not show any influence of flow rate the results may be extrapolated to the total volume 36.2 m^3, which yields the expected eroded mass of about 4.5 kg when fresh water is used and about 40 kg when water with 1% salt content is used. Using the erosion model given in the Equation 5-1 the maximum eroded dry bentonite mass lost in a deposition drift during artificial water filling using three discharge points just inside the plug would be 257 kg.
- **The buffer mass loss** by erosion relative to total mass in one compartment and effect on total density in one compartment is very small.

5.4 Erosion in DAWE due to detachment of bentonite particles from Supercontainer

5.4.1 General

With the DAWE design, Supercontainers, distance and filling components will be installed in a deposition drift, allowing water to flow along the drift floor until the compartment plug is installed as described in Section 4.3.1. During this time, up to about one and a half weeks for a 150 metre long drift, the buffer blocks that were installed first will be affected by the high relative humidity in the drift. They will start to swell and crack with flakes of bentonite from the Supercontainer detaching from the blocks and dropping onto the drift floor. The ring shaped buffer blocks inside the Supercontainer will have a low inital water content, about 11% (in order to have a high enough dry density) and they will be more sensitive to high relative humidity than the solid Supercontainer blocks with about 17% water content and distance blocks withe an initial water content of 20–22% (Sandén et al. 2006).

A possible scenario within the drift is that the bentonite blocks inside the Supercontainer will crack and material (dropped bentonite particles) falls onto the drift floor where it is moved away by the water flowing down the drift. In addition the bentonite on the floor will swell in contact with the flowing water and may after some time come in contact with the bentonite blocks and thus lead water to the bentonite block. This may lead to increased cracking rate and enhance the rate of bentonite spalling, a process that may be significant. if this process continues for some time. This erosion will contribute to a loss of material or its redistribution within a deposition drift.

The main objectives of the test were the following:

- Study the influence of a high relative humidity on the bentonite blocks inside a Supercontainer, especially related to block cracking and subsequent loss of material into the slot between the blocks and drift floor.
- Measure the erosion rate of the material lost into the block-drift floor gap by applying an axial flow in the “drift”.
- Earlier tests (Sandén et al. 2008a) have shown that this problem is insignificant at the distance blocks sections since those blocks will be made with a higher water content, which will prevent this type of cracking.

5.4.2 Description of work and results

To study the issue of bentonite erosion and redistribution, tests were performed at intermediate scale using a test chamber known as Big Bertha (BB). In this test, the longer segment of the outer tube was used; see Figure 5-8 for test set-up, together with the simulated Supercontainer. Three buffer blocks with an outer diameter of 705 mm were used in the test. The blocks had an initial gravimetric water content of 9.5%.

The size of the BB test equipment was originally chosen so that the slot width and thickness of the bentonite are at full-scale without a canister in the middle. This means that the width of the slot (42.5 mm) between Supercontainer and “drift surface” is the same as in full-scale as well as the perforated holes with the diameter 100 mm in the Supercontainer. Therefore the most important features were studied at full-scale although the diameter of the test cylinder was not at full-scale.

Laboratory tests performed previously have shown that bentonite blocks of the quality used (water content of about 10%) will crack and fall apart with time when they are exposed to high relative humidity. If this happens during the installation phase, bentonite pieces or fragments may fall to the drift floor and be eroded away from the compartment. In order to prevent bentonite fragments from falling to the floor it may be possible to wrap the blocks in a thin steel net with a mesh size of about 1 cm, but this remediation approach was not investigated in this study.

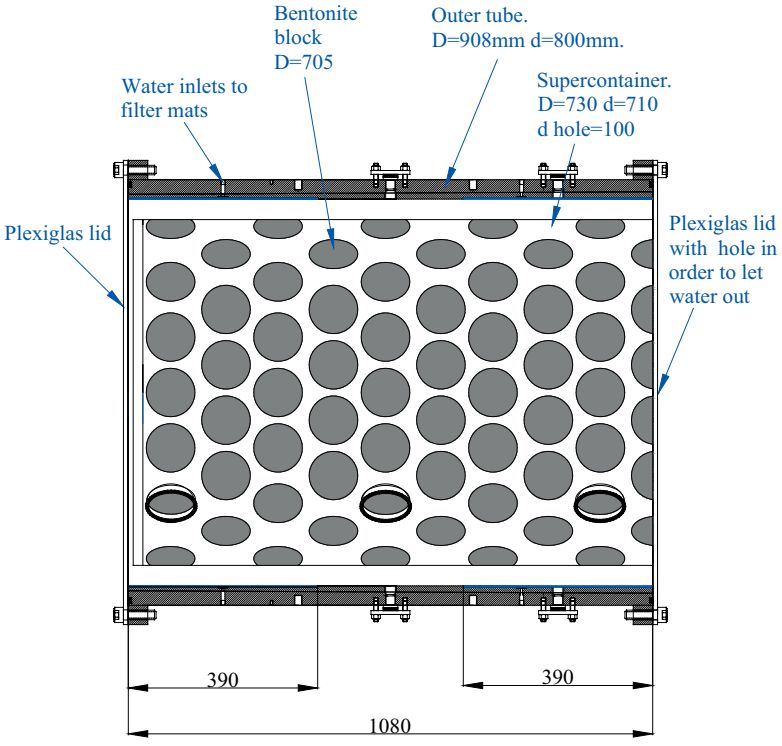

Figure 5-8. *Schematic diagram of the Supercontainer test set-up.*

Figure 5-9 shows the process used for installing the simulated Supercontainer. After installing the bentonite in the Supercontainer shell and placing the Supercontainer simulator in the outer tube, which simulates the deposition drift, lids of Plexiglas were placed at the ends for visual monitoring of the processes. The drift walls were partly covered with filter mats, see Figure 5-10. In these filter mats water was circulated continuously in order to keep the relative humidity on the walls close to 100%. One of the Plexiglas lids had an outlet present in its base in order to allow for seepage water to escape.

Figure 5-9. *Installation of Supercontainer simulator. (Left: The open end of the Supercontainer was covered with plastic to minimize atmospheric interactions. Right: Plexiglas lids mounted in the ends to allow visual monitoring of bentonite block behaviour.*

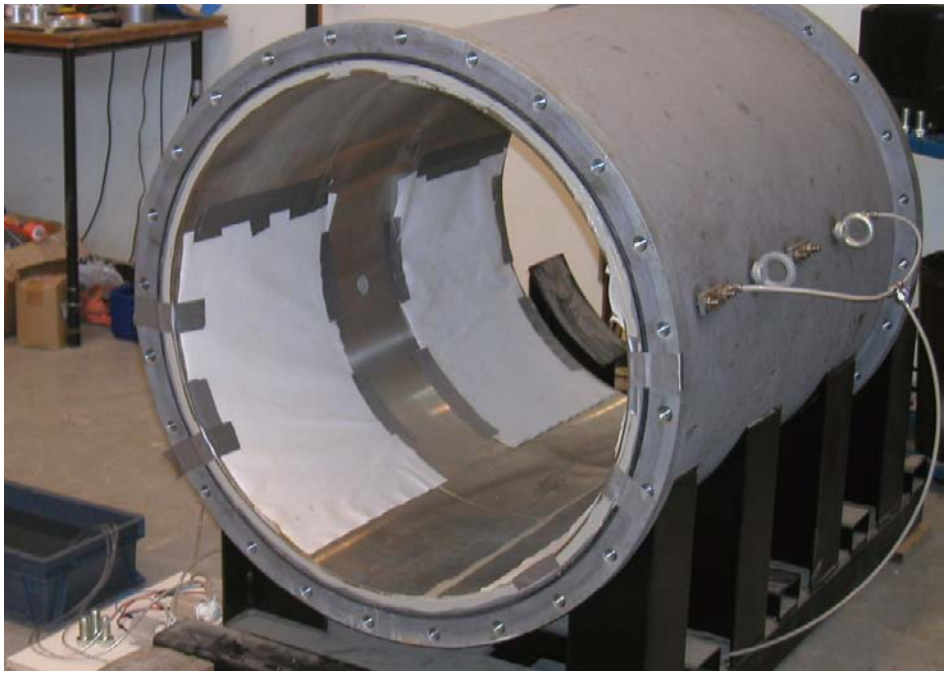

Figure 5-10. *Four filter mats were positioned on the simulated drift surface. Each of the filter mats was connected to a tube into which a constant flow was applied.*

Relative Humidity measurements

The total length of the test apparatus was 1,080 mm. Four filter mats, each with a width of 390 mm, were placed inside this steel "drift" with the filter mats only covering about half of the periphery in order not to have water dripping down onto the bentonite from the top of the drift, Figure 5-10. In a repository situation leakage water would be prevented from contacting the bentonite through the use of special drip or spray shields. The bottom (floor) part of the test cell was also left without a filter in order to perform erosion measurements along the length of the cell. A tube was connected to each of the filter mats in order to apply a constant water flow. At the point of inflow, located behind the filter mat, the water was distributed by a steel filter with a diameter of 20 mm. The water was then spread through the whole filter mat surface by capillary forces. In the described test tap water was used.

Three days after buffer emplacement the circulation of water was started. Small electric pumps were used for circulating a certain amount of water, about 10 litres. The water was pumped through the filters, then it was pouring down along the "rock" wall and then out through a hole at the bottom of the Plexi-glas disc covering the end of the test tube. The flow was set at 0.2 l/min divided between four inlet points. Water was circulated in the filters throughout the entire test period, except for the time when an axial flow was applied in order to measure the erosion rate. The amount of clay observed in this water (settled in the vessel containing the water), the main purpose of which was to set the relative humidity, was small.

The "drift" had an inclination of 2° in order to simulate the condition expected in a repository deposition drift.

Figure 5-11 shows the measured relative humidity (RH), present in the system during testing. The RH and temperature were measured at two points within the test assembly. One sensor was positioned on the top of the Supercontainer and one was positioned in the lower part. Each sensor was fixed in one of the perforated holes in the Supercontainer, as close as possible to the bentonite block surface. The initial RH measured before wetting was about 50%, see Figure 5-11, which corresponds well to the RH in the bentonite blocks (Sandén et al. 2008a). The RH measured during the water circulation period was between 70–85% with the higher values at the upper position. The reason for not measuring higher RH values for the air is because the bentonite absorbed water faster than the diffusion across the air gap.

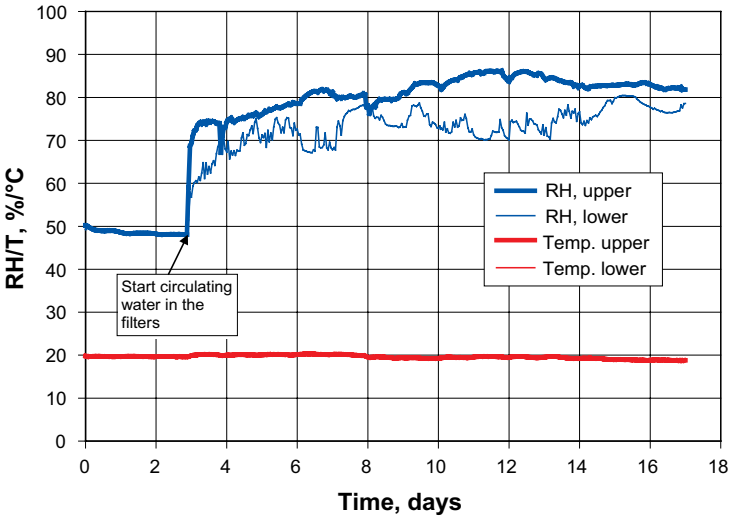

Figure 5-11. *Temperature and relative humidity measured during Supercontainer simulation. The measured temperature in the upper RH sensor is the same as in the lower (the curves are overlaying each other).*

Bentonite block behaviour

Blocks made of MX-80 Wyoming bentonite with a gravimetric water content of 9.5% and with a dry density of 1,989 kg/m^3 were used in this test. This water content and density are probably very close to what the blocks inside the Supercontainer have at the time of installation. Three days after emplacement in the "drift" the water circulation in the filter mats started. By measuring the amount of water consumed it was possible to make a rough calculation of the amount of water taken up by the bentonite during the first days of water circulation (days 2.8–5.2) shown in Figure 5-12.

The high relative humidity surrounding the bentonite and its water uptake strongly affected the blocks, see Figure 5-13. The bentonite block surface cracked and flakes of bentonite fell down on to the drift floor, but it was noted that no large pieces fell, only flakes.

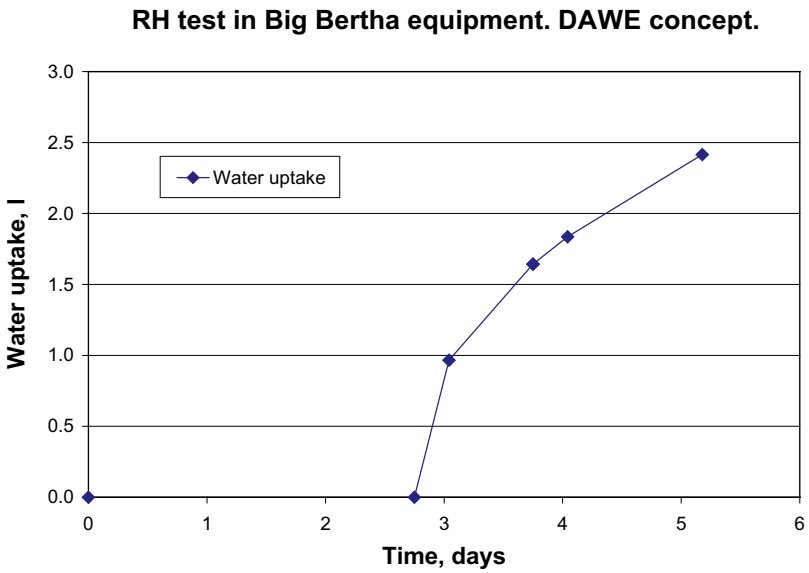

Figure 5-12. *Estimate of the water uptake during the first 2.5 days of water circulation through filter mat.*

Figure 5-13. *Flaking and accumulation of flakes of bentonite from the Supercontainer on the test cylinder floor. The pictures show the situation three days after starting the water circulation.*

Erosion measurements

During the test period, water flow into the filters was intentionally interrupted on a number of occasions, and during these periods an axial flow through the test cylinder was applied along the bottom to measure erosion of the material that had fallen from the Supercontainer. The results of these tests are shown in Figure 5-14. The amount of eroded material was very small. A discernible increase in the erosion rate was noticed when the water was changed from fresh water to a water with a 3.5% salt content, but after a few hours, the erosion rate also decreased to very low values for this water type.

A large number of erosion tests have been performed within other projects e.g. the Baclo project (Sandén et al. 2008b). With these earlier tests as a basis, a model describing the accumulated amount of eroded material as a function of the accumulated water flow in a double logarithmic diagram has been suggested as described in Section 5.2.2. An important finding was that the erosion decreases by time. In Figure 5-15 the data from the tests made in the BB equipment has been plotted in such a diagram together with the limits of the suggested model. The diagram shows that the erosion measured in the BB tests is much lower than the earlier measurements setting the limits of the model. One measurement is in the middle part of the model but with strongly decreasing erosion rate. The main reason for the low erosion rate is of course that the water is flowing on the drift floor and not directly on the material.

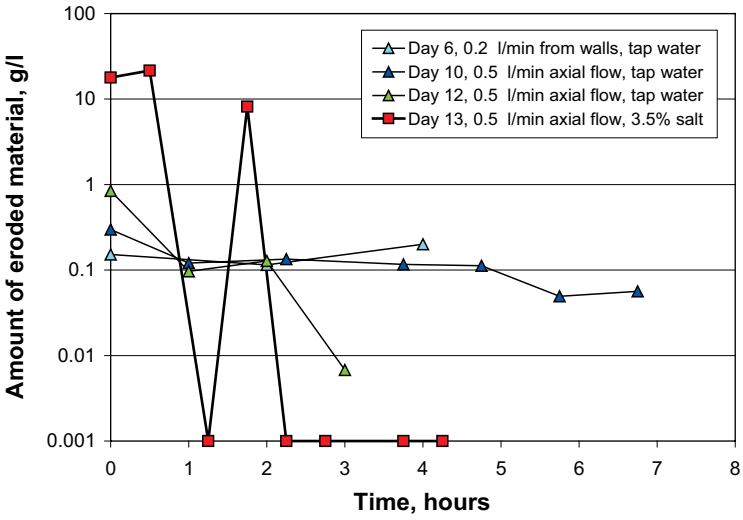

Figure 5-14. *Erosion along the floor measured on four occasions during Supercontainer test.*

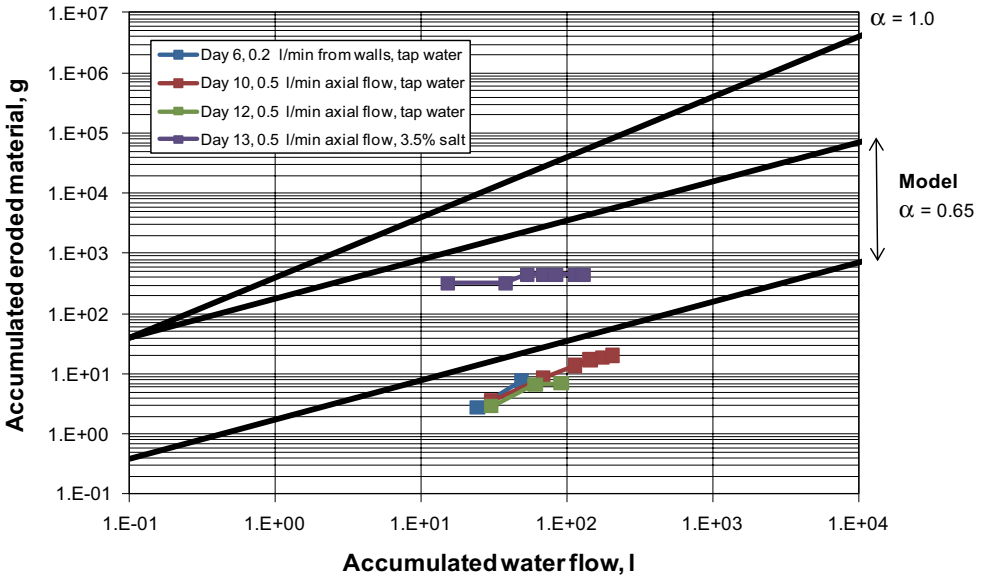

Figure 5-15. *The accumulated amount of eroded material plotted versus the accumulated water flow.*

After about two weeks, so much material had fallen down to the floor and subsequently swelled that it filled the gap between Supercontainer and bottom of experimental cylinder. The swollen clay clogged the gap and outlet pipe and water moving along its upper surface reached the base of the Supercontainer, as can be seen in Figures 5-16 and 5-17 setting the time limit for the deposition of a compartment.

5.4.3 Conclusions

Some key conclusions regarding the cracking and dropped/detached bentonite material drawn from the BB test were:

- The surface of buffer blocks was strongly affected by the high relative humidity. Flakes of bentonite were formed on all exposed bentonite surfaces (except in the joints between the blocks). The smaller amount of flaking in the region adjacent to the joints was probably due to the greater ability of these less constrained regions to strain without having to fail locally (2 D shrinkage perpendicular to the gap).
- The flakes from the lower part of the Supercontainer were detached and fell to the "drift floor" by gravity. This process started 2–3 days after the filters were wetted and after two weeks in an environment with a high relative humidity, less than 1% of the bentonite component was lost to "flaking". Even less than that would therefore be lost from an individual Supercontainer as the result of water flowing along the drift floor.
- In the full-scale in-situ case, it is expected that two or three Supercontainers will be installed every day. The process involving the formation of bentonite flakes seems to be rather slow (2–3 days before the first flakes fell down on the drift floor). Therefore it is not expected that flaking will be a problem during the transportation of Supercontainers into the drift and their subsequent installation but only after installation and before water filling of the drift.
- After about two weeks, so much material had fallen down to the floor and subsequently swollen so that it filled the slot between Supercontainer and bottom of experimental cylinder. This sets the approximate time limit for deposition of one compartment since direct water-Supercontainer interaction begins to dominate the system. With this comes interference with deposition activities and the risk of increased buffer erosion.

Figure 5-16. *View of the slot between Supercontainer and "drift" after nine days of testing (note the large amount of material that had fallen into the slot.*

Figure 5-17. *Picture taken before termination of the test. View from the water inlet side. The amount of bentonite on the drift floor had increased after two weeks so much that the outlet pipe was clogged and the water level rose above the Supercontainer base.*

5.5 Homogenization of cavities caused by erosion

5.5.1 General

The effect of homogenization of the bentonite after erosion in KBS-3H is of crucial importance for the long-term safety in the KBS-3H design. It is important to be confident that the buffer will not lose so much density that advective rather than diffusion contaminant transport conditions prevail around the canister.

In addition to loss of bentonite by erosion mechanisms given in Section 5.1 also, in rare cases, bentonite blocks may be incorrectly installed in the deposition drift as the result of mistakes in the installation process, e.g. when a distance block or Supercontainer is not been installed far enough into the drift, resulting in a gap left between neighbouring blocks.

The homogenization of the buffer under these latter situations and the effect of missing bentonite blocks have been investigated for KBS-3V and those results may be applied also for KBS-3H (Åkesson at al. 2010).

In order to assess the potential for the buffer material to seal the openings resulting from erosion processes (see Section 5.1) a series of scoping analyses have been completed. The homogenization of the bentonite under the situation with erosion caused by the artificial water filling, has been the primary erosion mechanism investigated for KBS-3H.

5.5.2 Description of work and results

The critical issue of homogenization of bentonite after erosion has been investigated for KBS-3V for SR-Site with FEM-calculations (Åkesson et al. 2010). The same calculation technique using the finite element code Abaqus has been used and adapted to the geometry of KBS-3H.

Geometry of the element model

The shape of the void caused by water inflow-driven erosion is not known but will probably be either half a sphere caused by point erosion, a half cylinder-shape or a half-doughnut shape caused by erosion along an intersecting fracture. If flow takes place along a flow path inside the bentonite it may of course also be in the form of a whole cylinder.

For a given mass of eroded material the most severe effect of material removal on the density distribution is where point erosion has occurred since it will generate the lowest clay density at the rock surface as shown in the modelling results of KBS-3V (Åkesson et al. 2010).

The hole can be located at different positions but by assuming symmetrical erosion a simplified geometry model with the lowest number of elements can be used as shown in Figure 5-18.

In order to simplify and understand more about the process a similar axi-symmetric model was used in most of the analyses, see Figure 5-19.

Applying the average density at saturation ρ_m = 2,000 kg/m^3, which corresponds to the dry density ρ_d = 1,570 kg/m^3, and the volume of a half sphere, the total loss of dry mass of bentonite can be calculated for different radiuses of the half sphere.

For the 3D cases shown in Figure 5-18 the following three cases have been analysed:

M_{loss} = 274 kg with the radius 0.447 m
M_{loss} = 800 kg with the radius 0.697 m
M_{loss} = 2,740 kg with the radius 1.010 m

The drift in this model has a radius of 0.925 m and a length of 5.0 m.

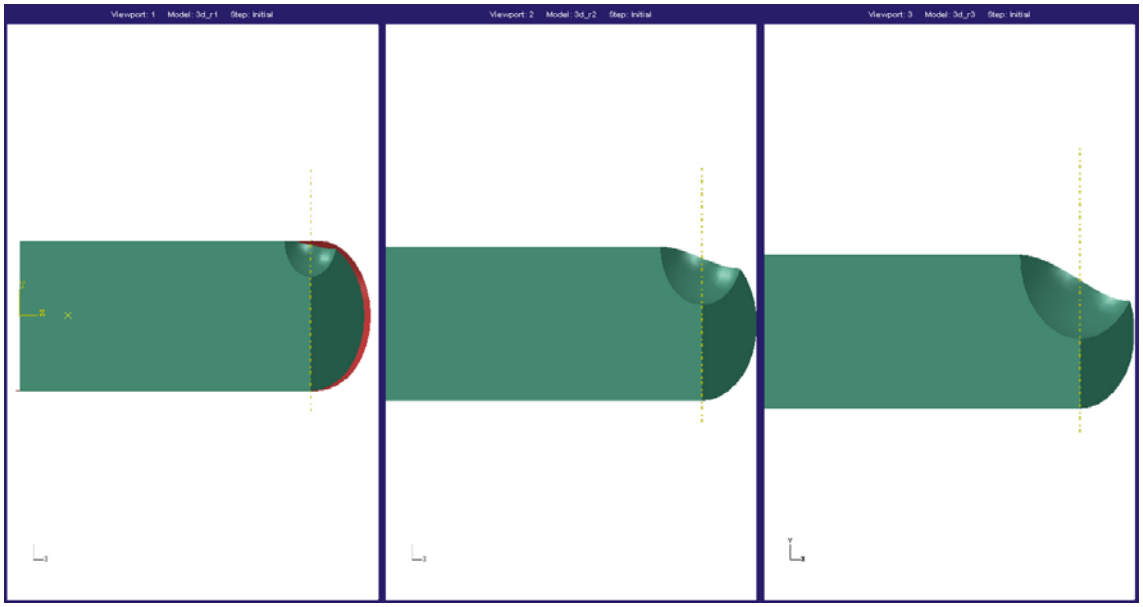

Figure 5-18. *Bentonite geometry showing the assumed eroded hole for three different bentonite mass losses (274 kg, 800 kg and 2,740 kg). The two vertical boundaries of the model are symmetry planes.*

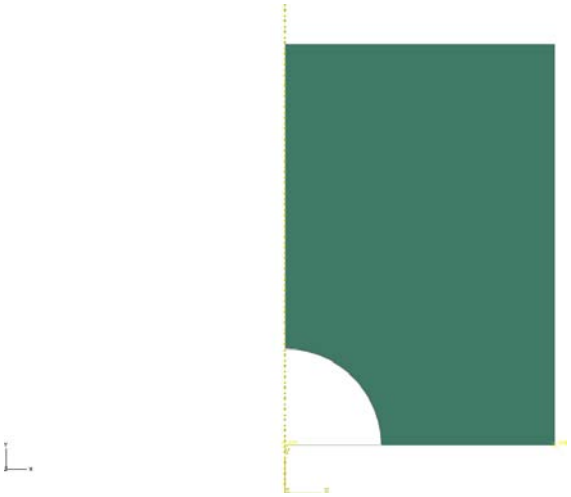

Figure 5-19. *Simplified axi-symmetric model. The horizontal bottom boundary is the symmetry axis.*

The simplified axi-symmetric model shown in Figure 5-19 has a hole with radius 0.447 m, outer radius 1.25 m with modelled axial length of 1.85 m.

The elements used in the analyses have pore-pressure and displacements as degrees of freedom using first order interpolation.

Material model

The bentonite has been modelled as completely water saturated at the start of erosion. This is for some scenarios a potentially non-conservative simplification, since erosion may occur before closure of the repository takes place and before full saturation of the buffer. The results of these analyses will, however, provide an indication of the potential significance of erosion on system equilibration. The motivation for assuming full water saturation is outlined in the points below:

- The mechanical models of unsaturated bentonite are very complicated and not sufficiently good for modelling the very strong swelling that takes place after such large loss of bentonite.
- The models for water saturated bentonite are much simpler and well documented.
- The stress path and time schedule will differ if saturated instead of unsaturated bentonite is modelled but the final state will be very similar.

The mechanical properties of the buffer controlling the swelling and consolidation phase are based on the models and properties derived for MX-80 by Börgesson et al. (1995). Porous Elasticity combined with Drucker Prager Plasticity has been used for the swelling/consolidation mechanisms, while Darcy's law is applied for the water flux and the Effective Stress Theory is applied for the interaction between pore water and structure. The density of the buffer at saturation is 2,000 kg/m^3.

Mechanical properties

When using Abaqus the model may be defined by pressure-dependent elasticity, *Porous Elastic*, combined with a pressure dependent plasticity, *Drucker-Prager*.

The *Porous Elastic Model* implies a logarithmic relation between the void ratio e and the average effective stress p according to Equation 5-2.

$$\Delta e = \kappa/(1+e_0)\Delta \ln p \qquad (5\text{-}2)$$

where κ = porous bulk modulus, e_0 = initial void ratio.

Also Poisson's ratio ν is required.

$\kappa = 0.21$ and $\nu = 0.4$

The *Drucker-Prager Plasticity* model contains the following parameters:

β = friction angle in the p-q plane
d = cohesion in the p-q plane
ψ = dilation angle
$q = f(\varepsilon^d_{pl})$ = yield function

The yield function is the relation between Mises' stress q and the plastic deviatoric strain ε^d_p at a specified stress path. The dilation angle determines the volume change during shear.

The following data has been derived for the *Drucker-Prager Plasticity* model (Börgesson et al. 1995):

$\beta = 17°$, $d = 100$ kPa, $\psi = 2°$

The yield function is shown in Table 5-2 (Börgesson et al. 1995).

The material model has been modified for a few analyses. Mainly the cohesion and yield surface for the Drucker-Prager model have been modified in order to improve the results.

Table 5-2. Yield function.

q (kPa)	ε_{pl}
113	0
138	0.005
163	0.02
188	0.04
213	0.1

Hydraulic properties

The hydraulic conductivity is a function of the void ratio, as shown in Table 5-3 (Börgesson et al. 1995).

Interaction pore water and structure

The effective stress theory states that the effective stress (the total stress minus the pore pressure) determines all the mechanical properties. It is modelled by separating the function of the pore water and the function of the particles. The density ρ_w and bulk modulus B_w of the pore water as well as the density ρ_s and the bulk modulus of the solid particles B_s are required parameters. The following parameters are used for modelling Na-bentonite (Börgesson et al. 1995):

Porewater

ρ_w =1,000 kg/m^3 (density of water)

$B_w = 2.1 \cdot 10^6$ kPa (bulk modulus of water)

Particles

ρ_s = 2,780 kg/m^3 (density of solids)

$B_s = 2.1 \cdot 10^8$ kPa (bulk modulus of solids)

Table 5-3. Relationship between hydraulic conductivity and void ratio.

e	*K* (m/s)
0.45	$1.0.10^{-14}$
0.70	$8.0.10^{-14}$
1.00	$4.0.10^{-13}$
1.5	$2.0.10^{-12}$
2.00	$1.0.10^{-11}$
3.00	$2.0.10^{-11}$
5.00	$7.0.10^{-11}$
10.00	$3.0.10^{-10}$
20.00	$1.5.10^{-9}$

Contact surfaces

The buffer is surrounded by rock, modelled as a rigid contact surface. The coefficient of friction 0 and 0.1 has been used, which correspond to the two extreme conditions of no friction and the same friction as in the bentonite itself (representing that the shear takes place in the bentonite).

Initial conditions

All calculations were done with the same initial conditions of the buffer. The buffer is completely water saturated and is assumed to have an average density at saturation of ρ_m = 2,000 kg/m^3 or the void ratio e = 0.77 corresponding to the average density in the deposition hole. The swelling pressure at this density is about 7 MPa so the pore pressure is set to u = –7 MPa in order to correspond to the effective average stress p = 7 MPa that yields zero total average stress according to the effective stress theory. With these initial conditions the clay is in mechanical equilibrium before starting the calculation. The required initial conditions of the buffer are thus:

u = –7 MPa
p = 7 MPa
e = 0.77

Analysis set-up

Several different strategies for simulating the swelling process have been used but the most successful strategy seems to be:

- starting with initial stress conditions for the buffer as total stress equal to zero,
- defining pore pressure as a boundary condition at the free surface (the spherical surface). The pore pressure is defined as being equal to the value specified as initial condition,
- gradually decreasing the pore pressure at the free surface over a reasonable time (as required by the definition for permeability used). However, since in this study only the final state is of interest, permeability and time scale for the changing of this value are not sensitive parameters.

5.5.3 Calculations of homogenisation

A number of element meshes with increasingly refined mesh were tested. For the final model the cohesion has been decreased substantially, cohesion 0.1 kPa instead of 100 kPa (this is realistic at very low densities. In fact the failure envelope is not a straight line but curved to the cohesion 0. The cohesion value of 0.1 kPa corresponds to a friction angle of 5.7 degrees), and the strain hardening has been neglected. Furthermore the coefficient of friction has been changed from 0 to 0.1 for the contact surface between the bentonite and the surrounding rock. This model seems to have an almost completely closed void and captures the expected results. Laboratory tests have shown that holes in highly compacted MX-80 bentonite will seal but remain at a lower density. A solution that results in an unfilled hole can thus not be expected to be correct.

The mesh used is shown in Figure 5-20. About 32,000 elements are included in the model and the smallest element has the size of about 0.878·0.036 mm^2 corresponding to the fraction 0.0000015% of the entire mesh. The results after completed calculation are shown in Figures 5-21 to 5-24. Figure 5-21 shows the Mises stress, Figure 5-22 shows the effective pressure, Figure 5-23 shows the void ratio and Figure 5-24 shows the pore pressure.

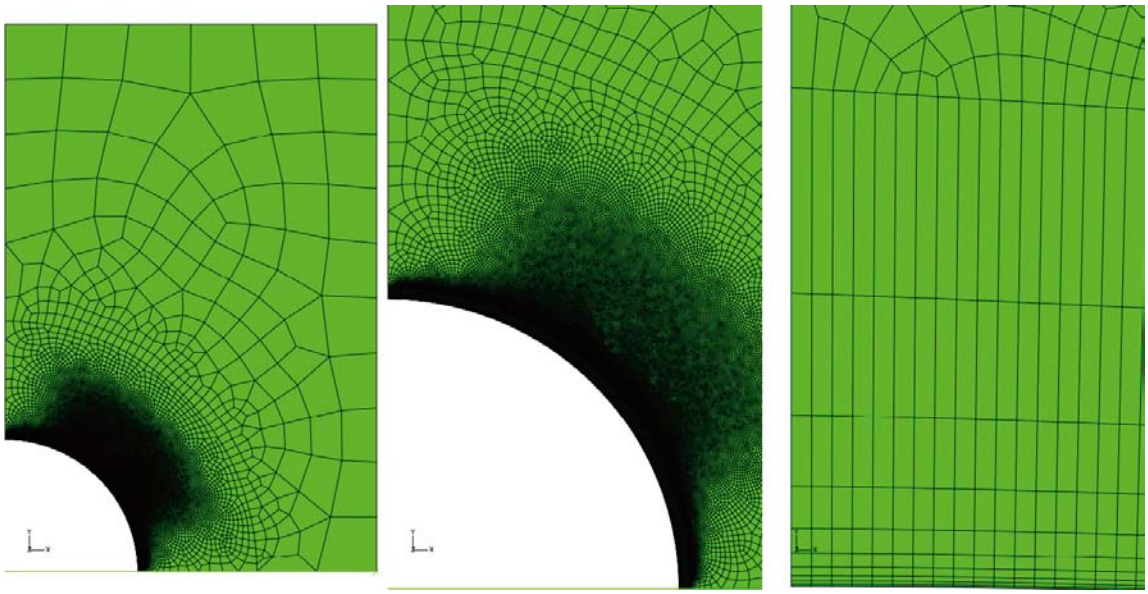

Figure 5-20. *The mesh with very dense element distribution; whole model (left), detail (mid) and lower left corner (right).*

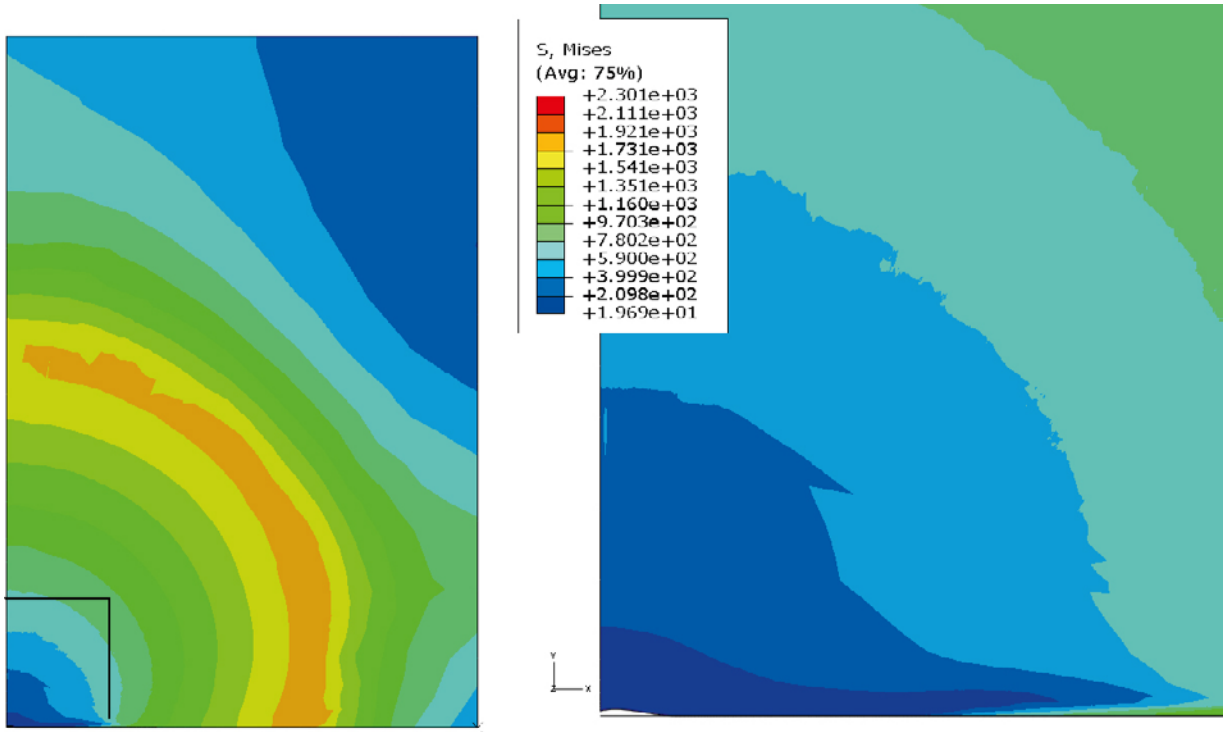

Figure 5-21. *Mises stress (kPa) at completion. The right figure is a magnification of the framed area in the left figure.*

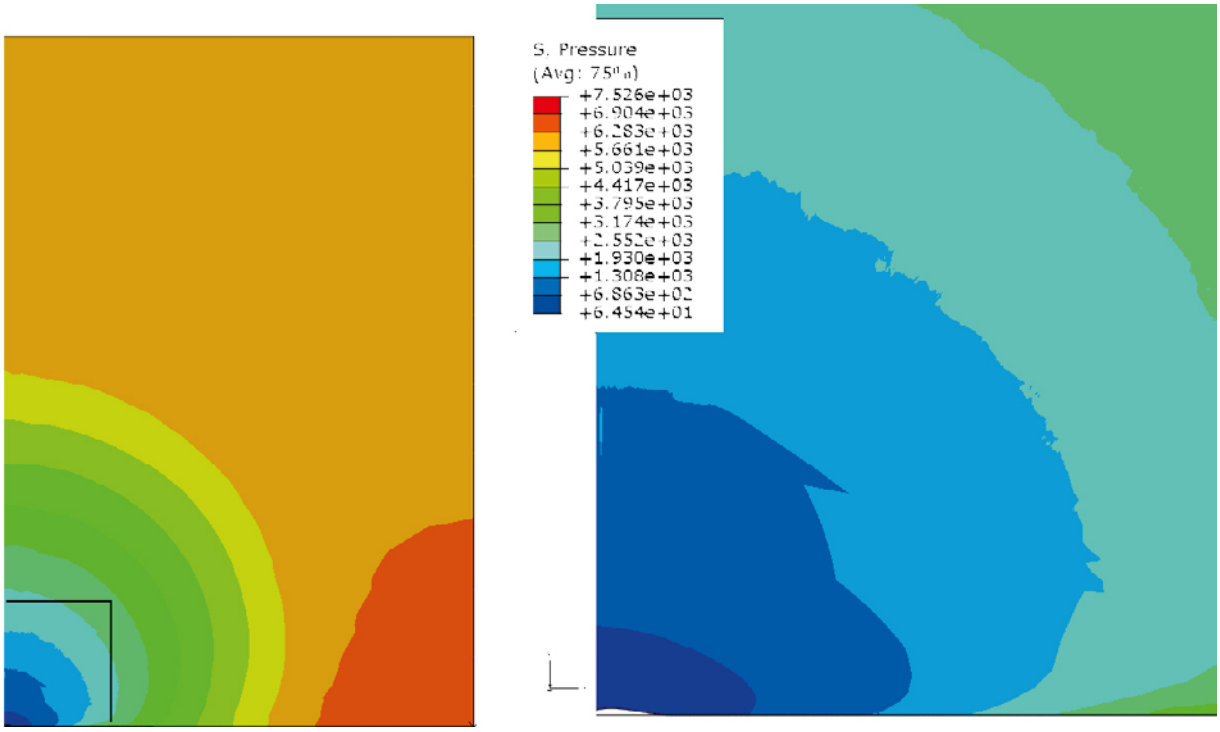

Figure 5-22. *Effective pressure (kPa) at completion. The right figure is a magnification of the framed area in the left figure.*

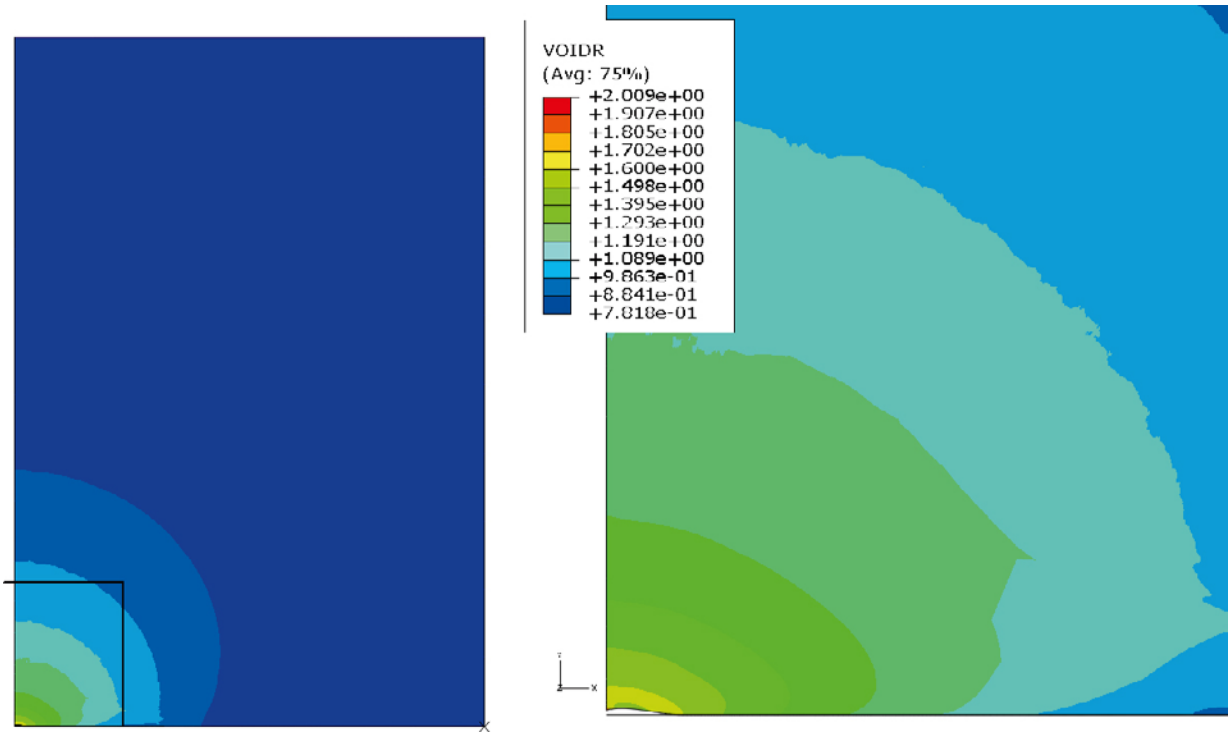

Figure 5-23. *Void ratio at completion. The right figure is a magnification of the framed area in the left figure.*

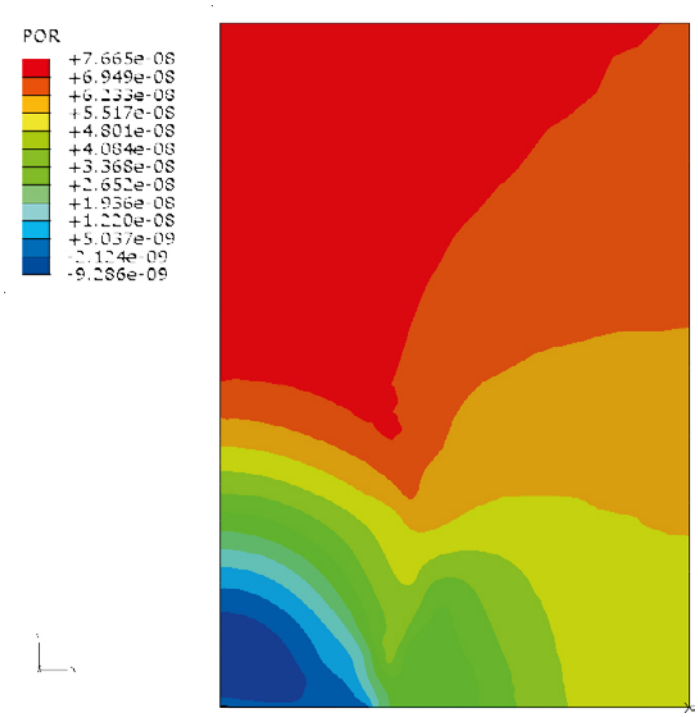

Figure 5-24. *Pore pressure (kPa) at completion illustrating that the pore pressure equalization is completed*

The results reveal that a very dense element mesh is required in order to realistically simulate the evolution of clay swelling into an erosion-induced void. Not even the element size of 0.878·0.036 mm^2 used in this calculation was small enough to completely close the void. The average swelling pressure at the gap boundary is about 65 kPa and the corresponding void ratio 1.7 (ρ_m = 1,660 kg/m^3).

Due to the problems with the remaining presence of an open void, even after pore pressure equalisation was achieved and the requirement of extremely small elements, the 3D-models shown in Figure 5-18 could not be run to describe the swelling process. Extension of the model to the 3-D case would have required too many elements to run on the available computer platform.

5.5.4 Conclusions

Although the results are unsatisfactory in the sense that the swelling was not shown as being completed, some tentative indications can be drawn from the results. The results are not representative at the location close to the remaining small open space where the largest deformations occur. The distribution of stresses and void ratios a relatively short distance away seems to comply with observations on material behaviour and appear to be more realistic. For example at the initial surface of the void at the radius 0.447 m, the swelling pressure is about 3 MPa and the void ratio about 1.0. Swelling pressure below 1 MPa exists inside about ¼ of the initial void volume (0.477 m). There is thus only a small isolated part of the initial void that may indicate the potential for unfavourable swelling conditions to exist, but the properties of that region cannot be assessed using the calculations performed.

The expected erosion caused by the artificial water filling the 150 m long compartment is less than about 250 kg (conservatively used as an upper limit). This corresponds to a half-sphere void with radius about 0.45 m. Since the bentonite loss due to artificial water filling is expected to be much localized (in fact in the transition block/filling component adjacent to the plug and not in buffer component), the effect on the buffer is not expected to be substantial.

A more realistic calculation yields an eroded value of about 40 kg in the drift due to artificial water filling. Approximately 40 m^3 of water will be pumped into the drift compartment during the artificial water filling (DAWE) and erosion models estimate erosion in the range of 0.1–1 g/litre, see Section 5.3.2 and Figure 5-7. This would yield a maximum erosion of about 40 kg in a drift. In

SR-Site (SKB 2011) for KBS-3V design it was concluded that about 100 kg could be lost between the rock surface and the canister in a deposition hole without jeopardizing the buffer function. If this figure is used for KBS-3H the conclusion would be that there is a large margin for material loss by erosion in the Supercontainer section. This is associated with the expectation that there will be very little water entering the deposition drift after water filling.

The overall conclusion is that the results reached from the homogenization modelling are uncertain and more work is needed in order to improve the material behaviour models and the calculation technique.

The results shown here should be considered examples of results and illustration of the difficulties in these calculations. Experimental studies are needed to support and to confirm the modelling results. Homogenisation is a prioritised research subject in the coming years.

5.6 Buffer swelling and sealing in heterogeneous inflow conditions

5.6.1 General

In a deposition drift it is possible that there will be relatively tight sections of rock next to wet sections intersected by water-leaking fractures. As a result there will be a situation where there will be full hydrostatic pressure in wet sections and absence of swelling pressure and buffer desiccation in dry sections, see Figure 5-25. This may result in the following features which were evaluated under this issue:

- Flow inside the drift from wet to dry sections resulting in erosion and redistribution of buffer.
- Uneven saturation which may cause unbalanced forces resulting in linear displacement of buffer.

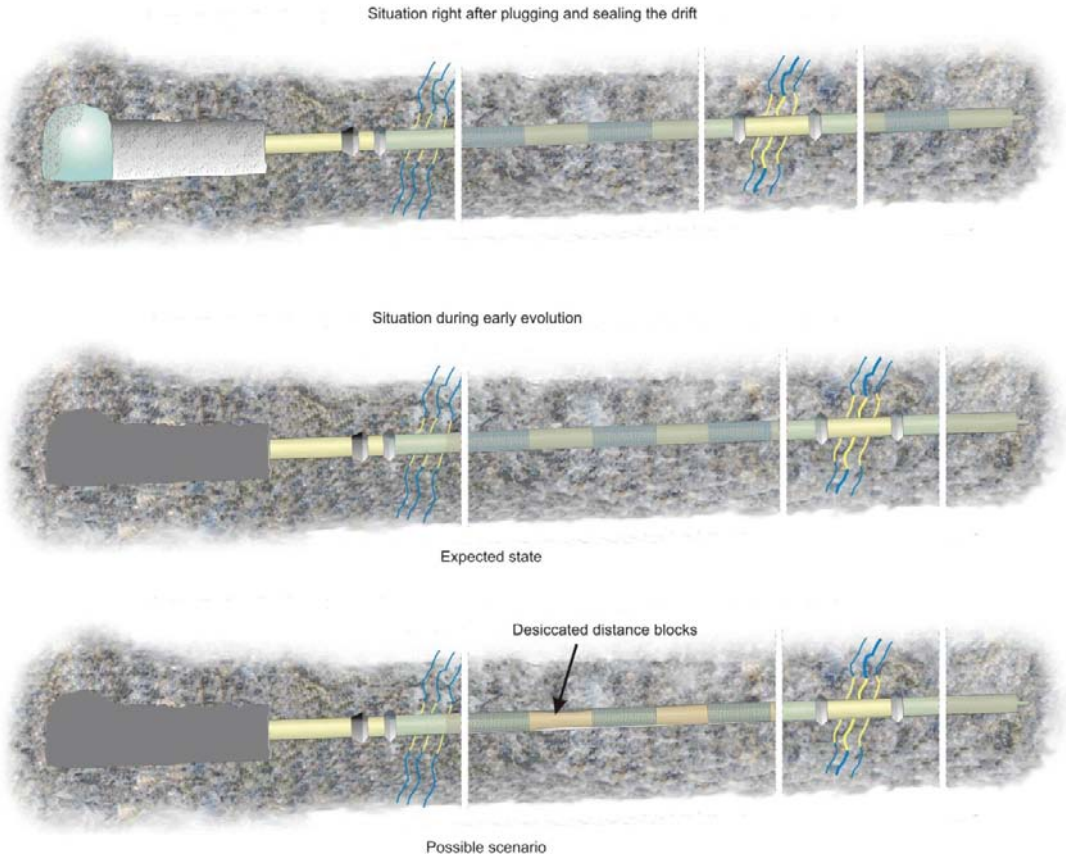

Figure 5-25. *Picture showing the ideal state after drift plugging and sealing the drift when buffer has been fully saturated (top). If there is a very dry section in the drift, it could be possible that some of the buffer in the dry section desiccate as water migrates towards the inner parts of distance blocks. The migration is caused by gradient in water content, i.e. water will migrate from wet parts to dry parts. The buffer starts to desiccate as the amount of water becomes smaller.*

The objective of the work was to evaluate these different features in order to define the uncertainties and need for further studies and possible experimental work in more detail. The work was based on using information available from other relevant studies in KBS-3H project and no modelling or experimental work was included in the scope. This evaluation does not address effects of erosion.

The issue has been presented by Autio et al. (2008) and it is also noted with respect to previous BD alternative" in Gribi et al. (2007), Chapter 4 "Tight drift section adjacent to less tight drift section". The axial displacement was addressed in Section 4.6.1 of the same report. The behaviour of buffer immediately after artificial wetting was different in the earlier BD alternative when compared to present DAWE design alternative, however, since roughly 50% of the porosity is located inside the buffer, there are some similarities in longer time perspective. The issue and the need for additional tests have been uncertain and were therefore discussed with long-term safety experts in early 2009. As a result of the discussion no clear detrimental effects were identified and the importance of the issue was lowered at the time. The evaluation of the issue and conclusions are discussed below.

The volume of open void space around a Supercontainer, which is artificially flooded is about 1.5 m^3 and the void space inside the buffer in a Supercontainer is roughly 1.2 m^3 (Autio et al. 2008). The latter value is the maximum volume of void space left in the Supercontainer after water filling. In Posiva's design the corresponding volumes for the distance block are roughly the same, which gives total pore volume of about 2.4 m^3 in buffer including both Supercontainer and distance block. Heterogeneous wetting situation may result in a (very) slow internal flow from wet sections to dry sections the volumes of which are at maximum 2.4 m^3 per Supercontainer unit. The maximum flow volume depends on the number of "dry" Supercontainer units where water is flowing from "wet" drift sections. This is based on the assumption that the drift plug seals the drift and there are no flow paths and hydraulic gradients between bedrock and drift that might affect the flow inside the drift.

5.6.2 Description of work and results

Buffer swelling and sealing in heterogeneous inflow conditions is caused by the fact that evidently there can be wet drift sections next to very dry sections in a deposition drift. This leads to a situation where after some time water has been redistributed and absorbed inside buffer and especially in distance blocks because the Supercontainer shell and temperature gradient inside Supercontainers reduces the water absorption in buffer inside Supercontainers with respect to distance blocks. In the absence of additional water after wetting distance blocks in dry sections may desiccate (see Figure 5-26) as shown in the BB experiment (using buffer with 10% water content, which is lower than nominal value for distance blocks) and studies related to swelling pressure (see Section 5.8) whereas distance blocks in wet section keep on absorbing water and swelling further. The result is that in dry sections there is no hydrostatic pressure and in wet sections next to leakage from transmissive fractures there is full hydrostatic pressure. The present estimate for the longest possible dry drift section is not fully known – but most likely several tens of metres or even more.

Internal piping from wet to dry sections driven by pressure gradient may cause some erosion. The pore volume in buffer (2.4 m^3 in Supercontainer section consisting of distance blocks and buffer inside a Supercontainer) is only 20% smaller than the open volume around the Supercontainer section (about 3 m^3) and therefore the mass of water to be transported in the pore space in buffer after wetting is roughly of the same order of magnitude than that used for wetting. The erosion has been studied as part of other buffer issues (see Sections 5.2 and 5.3). However, the flow rates used in the tests may not describe the internal piping since the flow characteristics in internal piping are not known, e.g. the flow is limited by the water absorption capacity of buffer but the process of water transport from wet to dry sections by piping is not fully understood and may happen in steps with higher flow speeds.

Moreover, the results of experiments concerning swelling pressure of the buffer in dry drift sections, effect on spalling of rock, as presented in Section 5.8, indicated that the possible redistribution of water from wet sections to dry sections occurs stepwise as internal piping, which is seen in tests as steps in flow pressure (Sandén et al. 2008a). Similar indications were obtained in the earlier experiments in 1:10 scale reported in Sandén et al. (2008a). The flow rates during internal piping may vary. In erosion tests (see Section 5.2 and Sandén et al. 2008a) the erosion rates have been higher during a short period of 24 hours in the beginning of tests. If internal piping occurs in short steps, it is possible that the erosion rates correspond to the higher erosion rates during the beginning of erosion experiments.

Figure 5-26. *Desiccation of distance block in the BB experiment simulating the behaviour of distance block (using buffer with 10% water content, which is lower than nominal value for distance blocks) in a dry drift section. Photo shows one side of BB test set-up immediately after removing the lid. The radial desiccation cracking is seen clearly adjacent to the surface of the steel cylinder corresponding drift surface. Note that the block in this figure has first swollen and then desiccated when the water has been absorbed into the block. This has led to reduced water content at the periphery with cracking as a result.*

This means that the flow path is changing as water is being slowly redistributed, the flow rate being limited by the absorption capacity of buffer. The channels that have been active swell and seal and new channels are formed. The channelling is likely to merge partly with the possible desiccation cracking. Therefore the possible flow path changes gradually and the possible erosive effect of flow is distributed evenly. The total volume of flow from wet to dry section depends on the expected length of dry section and is roughly 2.4 m^3 for a drift length of 10 m. If the dry section would be 40 m long, the flow from both sides of the section would total in roughly 9.6 m^3. If the flow is divided between two sides (flow in the dry section coming from two directions), it would result in maximum inflow of 4.8 m^3 over one distance block. Present estimates for erosion rates would result in erosion of 0.5–50 kg from one distance block which would be settled in the dry drift section. The flow rates during internal piping are not fully understood. Therefore the present estimates for erosion rate may not represent adequately the erosion in the case of internal piping. The result may be lower or higher erosion.

The results from studies on swelling pressure, especially BB experiments show that after the initial swelling caused by artificial wetting, the buffer fills the gaps and even during the possible desiccation the gaps remain filled and exert swelling force of 300 kPa. This information was, however, based on using buffer material with 10% water content which is lower that the distance blocks nominal design gravimetric water content 20%. Therefore the development of swelling pressure in BB experiment is likely to have been more rapid than if buffer with design water content would have been used. The possible axial displacement of buffer was studied earlier in Gribi et al. (2007) in the Section 4.6.1 for BD. The result of scoping calculations was that the effect of displacement on buffer density was not significant assuming that: a) the linear compaction per Supercontainer section is based on present estimates of gap size and b) the number of Supercontainers affected is limited. That is the density, for the calculated cases of 2 cm or 10 cm linear compaction, remained almost within the specified maximum density that is less than 2,050 kg/m^3. However, in the present DAWE alternative the movements (displacements) of buffer components after artificial wetting in DAWE design are smaller because the distance blocks are in contact with rock and there is a frictional force that resists movement as well as the gaps between distance blocks and Supercontainers have swollen and there is a contact force of the order of 300–500 kPa quite rapidly after wetting.

5.6.3 Conclusions

The issue of internal piping needs further evaluation but is considered further constrained on the basis discussed below. Some features have also been identified, which may be very beneficial to the buffer behaviour.

There are uncertainties related to erosion caused by internal piping induced by heterogeneous water inflow conditions which are discussed below, some of which are related to fundamental understanding of the issue, some related to hydraulic environment and some related to acceptability**.**

The mechanical erosion has been addressed in other studies (see Sections 5.2 and 5.3). However, the mechanical erosion at very low flow rates due to internal piping is not well known and still requires information on the expected length of dry drift sections. The process of piping is not well understood and therefore the transient flow conditions for evaluating erosion are uncertain and should be defined. The possible process of long lasting pulsating flow seems to be unique to KBS-3H when compared to KBS-3V alternative.

The effect of buffer axial displacement on buffer density is not assessed as being significant. The result of scoping calculations by Gribi et al. (2007) was that the present DAWE design provided the most suitable behaviour. However, the conclusion was based on assumption of the compaction forces and number of affected Supercontainer sections. In order to make more accurate estimates, more detailed data of length of dry drift sections and mechanical behaviour of desiccated buffer is needed. This would require more detailed geohydrological information, additional laboratory determinations on properties of desiccated buffer and likely experimental work. This is related to the process of water transport along the drift, which should also be addressed in the future work, see Section 5.9

Internal piping may have very favourable impact on the saturation of buffer and development of swelling pressure and therefore, instead of being an issue, it might be a positive factor which improves the behaviour by making the saturation and development of swelling pressure more rapid than in the absence of this process. Internal piping may enable transport and redistribution of water from wet sections to dry sections and enable swelling of distance blocks and Supercontainers in dry drift sections more rapidly than in the case of only advective transport of water through buffer.

The process of water transport and possible internal piping in desiccated buffer is not understood since the transport of water to dry drift sections is affected by the desiccation of buffer. The effect of desiccation is unclear; however, it might have positive effect on buffer behaviour since it keeps the buffer in contact with drift rock surface even in very dry drift sections. The contact pressure evidently seems to be roughly in the range of a couple hundred kilopascals, which reduces the rock failure by spalling. It may also enhance water transport from wet drift section to dry drift section. Water transport and buffer swelling are fundamental features in buffer behaviour and therefore there is a clear need to develop understanding with respect to buffer desiccation, saturation times, and development of swelling pressures. However, these are not deemed critical for the fulfilment of the requirements for KBS-3H design. Note that desiccation refers here to cracking, which is caused by water transport and redistribution from outer buffer section radially inwards. The water transport is a fundamental process, which may have a positive impact on development of swelling pressure (mitigating spalling of rock). The process of water transport from wet to dry section could be studied experimentally e.g. in experimental pipe set-up, which enables having heterogeneous buffer structure with dry and wet sections next to each other.

The ability to estimate the swelling of buffer in Supercontainers is poorly understood with respect to timeframes and mechanical evolution. Therefore the results from studies of the behaviour of distance blocks may not be representative of what is occurring in the Supercontainer section. It should also be noted that information from BB tests was based on using buffer material with 10% water content, which is lower that the distance block nominal design gravimetric water content 20%. More detailed data is needed in order to evaluate the effect of heterogeneous wetting and piping more adequately. The issue could be addressed by experimental work focused on assessing the swelling of buffer inside and outside of a Supercontainer.

The heterogeneous saturation of the system may have significant effect on flow of gases (e.g. air trapped in the system), since the desiccation cracking of the bentonite can form a natural pathway for gas flow. This is not considered a problem and may be beneficial by allowing high gas pressures to be released. This could be further evaluated by experimental work supported by scoping calculations focused on gas transport in dry desiccated buffer.

5.7 Impact of rock shear on canister

5.7.1 General

Existing fractures intersecting a deposition drift in the KBS-3H repository alternative may be activated and sheared by an earthquake. The effect of a rock shear through a canister position is of crucial importance for the long-term safety since damage to the canister may ruin the isolating function of the canister. The probabilities of various fracture plane orientations acting as potential shear planes vary from site to site. Applying the RSC criteria in the construction of the repository will reduce the risk of shearing canisters.

The buffer material surrounding the canister in a deposition drift shall not harm the canister in the event of rock shear across the deposition drift. However, at the high buffer density required for a repository the stiffness of the buffer is rather high and may allow transfer of large forces to the canister. The stiffness increases with increasing rate of shear, which means that there may be substantial damage to the canister at very high shear rates.

The effect of rock shear through a deposition hole in KBS-3V has been extensively investigated for SR-Site by Börgesson and Hernelind (2010). The purpose of the work undertaken to address the buffer issue related to rock shear is to model one of the worst cases with respect to stress transfer and to compare the results obtained for the KBS-3H and KBS-3V geometries. The KBS-3V finite element model has been used as the basis for modelling but the geometry is changed for the KBS-3H orientation and the Supercontainer has been included. One of the worst cases previously identified for KBS-3V has then been modelled for KBS-3H and the results compared. The analyses of Börgesson and Hernelind do not take any opinion on the statistical possibility of the postulated rock shear plane orientations. Börgesson and Hernelind only analyses a set of shear plane orientation variations and uses the worst orientation as a dimensioning base.

The risk caused by even larger rock movements, which may occur during the melting phase of a major continental ice sheet, is minimised to an acceptable level by locating the disposal gallery within justified distances outside major fracture zones in the bedrock, and by locating the deposition holes in such a way that they are not intersected by fractures with the potential to undergo damaging shear movements, for Olkiluoto site see (Hellä et al. 2009).

The compressional shear type, which is specific to the KBS-3H geometry has not been studied in this work but will be addressed in the future work, see Section 5.9.

5.7.2 Description of work and results

The rock shear has been modelled with finite element calculations with the code Abaqus. A three-dimensional finite element mesh of the buffer, the Supercontainer and the canister has been created and simulation of a rock shear has been performed.

The rock shear has been assumed to take place perpendicular to the canister at the quarter point of the canister as shown in Figure 5-27. The shear calculations have been driven to a total shear of 10 cm, although 5 cm corresponds to the reference and dimensioning case. Finally the results have been compared with the results of an identical rock shear through a KBS-3V deposition hole with identical properties and conditions.

Geometry of the mesh

The Supercontainer with the buffer blocks and the canister will be placed sequentially in the 300 m long drift starting from the inner end of the drift. After completed installation of all Supercontainers and distance blocks a tight plug will be built in the outer end of the drift. The geometry of the mesh is the following:

- Drift diameter: 1.850 m.
- Supercontainer length: 5.696 m.
- Supercontainer diameter: 1.765 m.
- Thickness of Supercontainer shell: 8 mm.
- Canister length 4.835 m.

- Canister diameter 1.05 m.
- Distance block lengths: 2.305 m and 2.295 m – total 4.6 m.

The lengths of the Supercontainer and the distance blocks may differ slightly from the reference dimensions but this difference does not substantially alter the results obtained.

Finite element model

The geometry used for the earthquake induced rock shear consists of the insert (made of iron), the insert lid (made of steel) and the copper canister surrounded by buffer material (bentonite) and the Supercontainer. The geometry is based on CAD-geometries received from SKB (Leskinen 2009).

Due to symmetry only one half has been modelled. The mesh is then generated by 3-dimensional solid elements, mainly 8-noded hexahedral (most of them using full integration technique) and a few 6-noded wedges.

The problem size is defined by about 173,000 elements and 203,000 nodes (total number of variables about 730,000).

The entire element mesh and a detail are shown in Figure 5-27. The property areas (different materials) are shown in Figure 5-28.

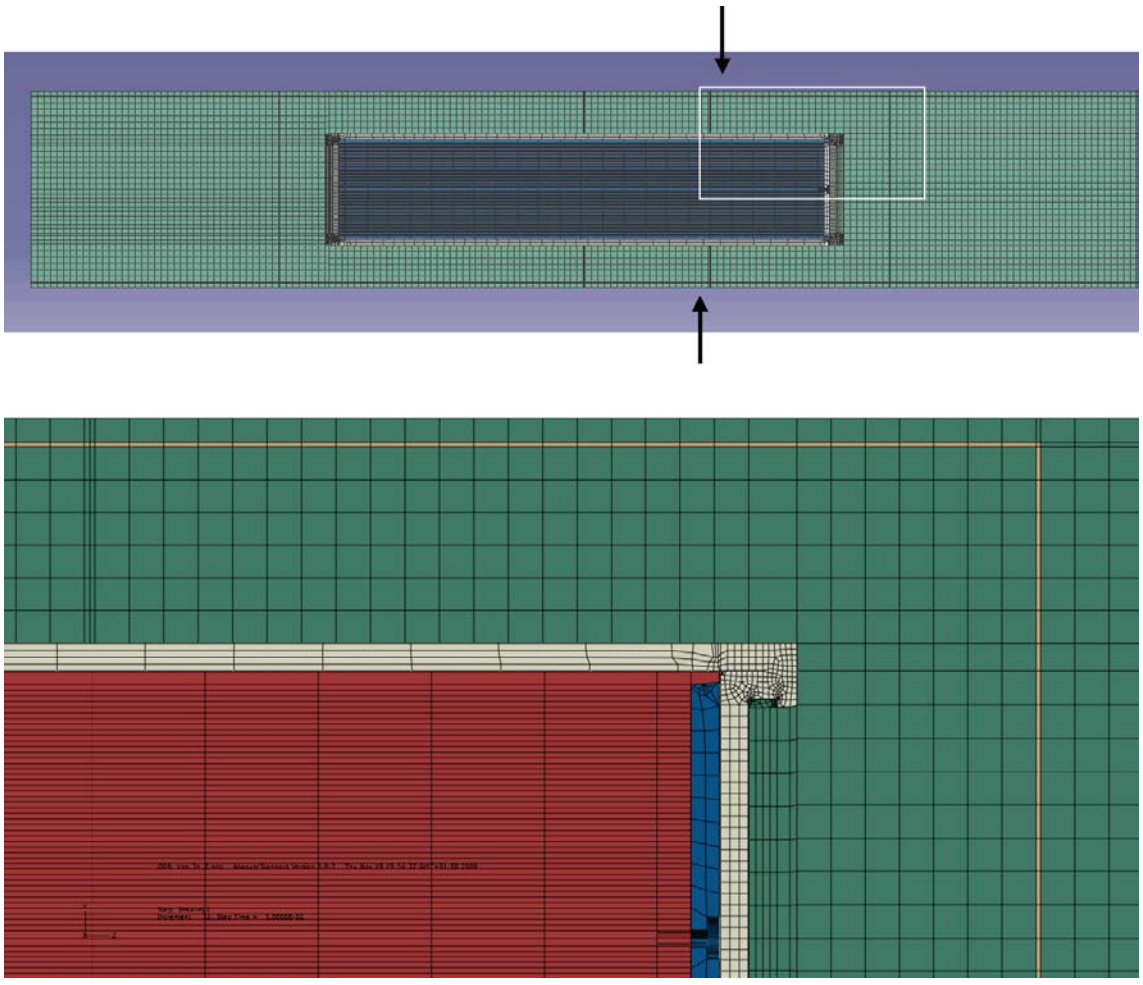

Figure 5-27. *Entire element mesh and indication of the location of the shear plane (upper) and a detail of the framed area.*

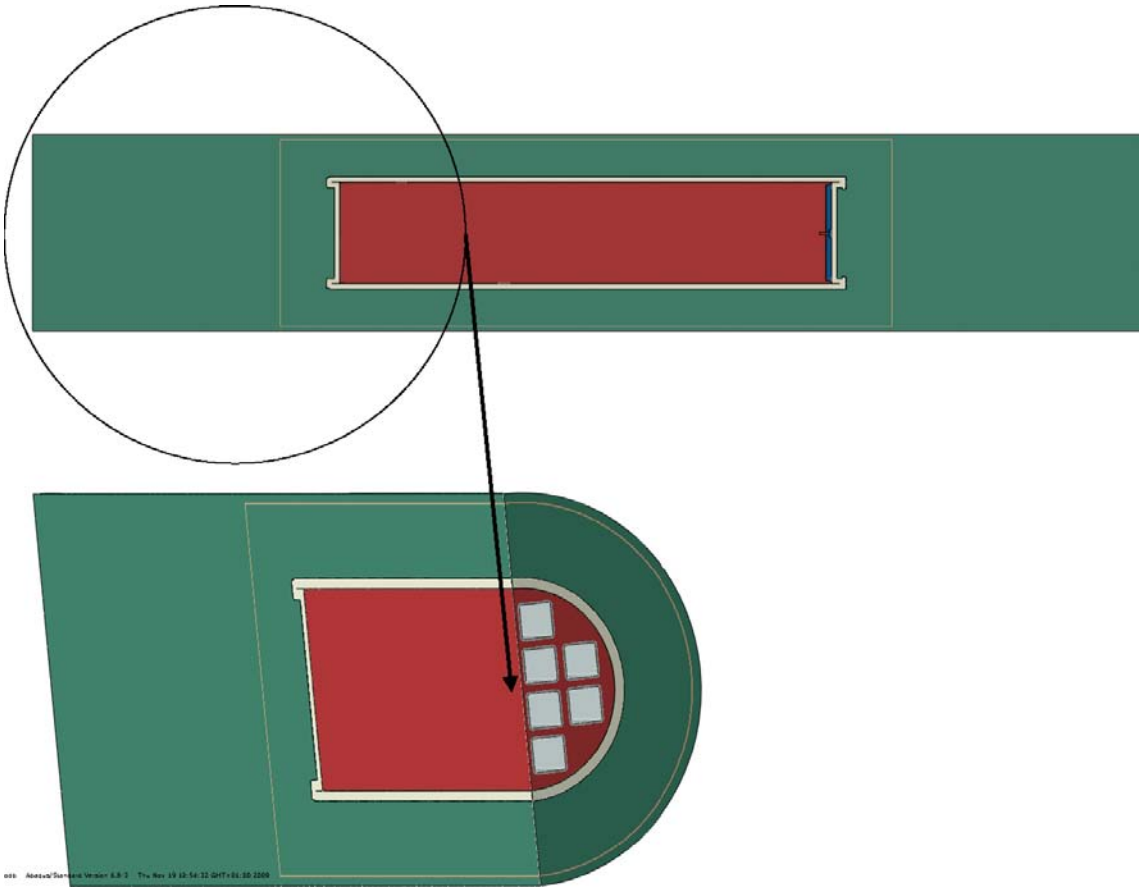

Figure 5-28. *Picture of the entire model and a detail cut to illustrate the third dimension.*

Material models

There are seven different materials included in the model. The properties of these materials are described in detail by Börgesson and Hernelind (2010) and will only be briefly described here.

The iron insert

The iron in the insert is modelled as a linear elastic material combined with von Mises plastic hardening. The plasticization starts at 0.17% strain at the Mises stress 293MPa and the maximum Mises stress 480 MPa is reached after 15% plastic strain whereupon the Mises stress is constant at zero strain rates. The yield surface will then increase proportional to the strain rate up to 0.5 1/s where the multiplication factor is 1.08.

The insert channels

The insert channels are modelled as a linear elastic material combined with Mises plastic hardening. The plasticization starts at 0.2% strain at the Mises stress 412 MPa and the maximum Mises stress 613 MPa is reached after 18.2% plastic strain whereupon the Mises stress is constant.

The insert lid of steel

The insert lid is modelled as a linear elastic material combined with von Mises plastic hardening. The plasticization starts at 0.16% strain at the Mises stress 335MPa and the maximum Mises stress 564MPa is reached after 18% strain whereupon the Mises stress is constant.

The copper shell of the canister

The copper shell is modelled as a linear elastic material combined with von Mises plastic hardening. The plasticization starts at 0.06% strain at the Mises stress 72 MPa and the maximum Mises stress 300 MPa is reached after 50% strain whereupon the Mises stress is constant.

The perforated Supercontainer shell

The Supercontainer shell used in the model is made of 8 mm thick perforated steel (study done prior to selecting titanium). The degree of perforation is 62%. Since the perforation cannot be included in the model the degree of perforation has been smeared out on the entire surface and the properties of the steel have been changed to correspond to a perforated shell by reducing the stiffness by about 60 %. Since the membrane stiffness probably is most important the perforation will reduce the average cross-section by about 60%, which also means that for a given in-plane deformation the force will be only 60% of the force corresponding to a non-perforated shell. The same discussion is also valid for pure bending and thus the actual stiffness will be reduced by 60%, if the structure with perforation, is treated as a continuum.

The Supercontainer shell is thus modelled as a linear elastic material combined with von Mises plastic hardening. The plasticization starts at 0.2% strain at the Mises stress of 165 MPa and the maximum Mises stress of 245 MPa is reached after 20% strain whereupon the Mises stress is constant. The plastic limit and the strength correspond to a reduction of corresponding values for steel by 60%.

The bentonite buffer

The bentonite model is in detail described by Börgesson et al. (2010) and the application for the modelling is described by Börgesson and Hernelind (2010). The most important properties of the bentonite for the rock shear are the stiffness and the shear strength. These properties vary with bentonite type, density and rate of strain. Ca-bentonite has higher shear strength than Na-bentonite and the shear strength increases with increasing density and strain rate. Since it cannot be excluded that the Na-bentonite MX-80 will be ion-exchanged to Ca-bentonite after a long time period, the properties of Ca-bentonite are used in the modelling. The result is a slightly conservative starting point, but the difference between these materials is rather small. Since the acceptable density at saturation of the buffer material is 1,950–2,050 kg/m^3 the highest density 2,050 kg/m^3 is used in the modelling, again providing a conservative basis for the analysis.

The bentonite is modelled as linear elastic combined with von Mises plastic hardening. The plastic hardening curve is made a function of the strain rate of the material. The reason for the latter relation is that the shear strength of bentonite is rather sensitive to the strain rate. It increases by about 10% for every 10-fold increase in strain rate. Since the rock shear at an earthquake is estimated to be 1 m/s the influence is strong and the resulting shear strength will be different at different parts of the buffer. Figure 5-29 shows the material model. The stress-strain relation is plotted at different strain rates.

Contact definitions

All the boundaries of the buffer, copper canister, insert and the insert lid interact through contact surfaces allowing finite sliding. All contact surfaces have friction at sliding along the elements with no cohesion and with the friction coefficient 0.1, i.e. the friction angle and cohesion are:

$\phi = 5.7°$
$c = 0$ kPa

The contact is released when the contact pressure is lost.

The interaction between the buffer and the rock (not modelled) is assumed to be linked through prescribed boundary conditions and will not allow for opening/closing or sliding.

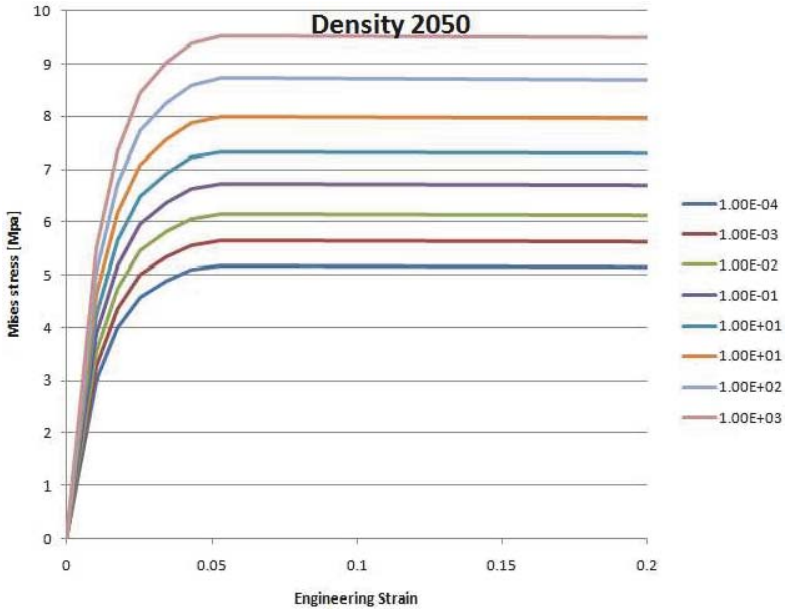

Figure 5-29. *Material model of the bentonite buffer at density of 2,050 kg/m³ at different strain rates.*

Calculation

Only one calculation has been performed for KBS-3H. For KBS-3V a large number of calculations have been performed with variation of bentonite properties, geometry, shear plane location etc. (Börgesson and Hernelind 2010). One of the cases that gave the highest stresses in the canister was the case that has been modelled for KBS-3H. By comparing the results of the two calculations the need for additional calculations for KBS-3H can be evaluated. As will be shown the difference between these calculations is so small that there is no need for further modelling.

The calculation done for KBS-3H corresponds to the KBS-3V calculation named *model6g_normal_quarter_2050ca3* in the report by Hernelind (2010), which is also the reference model. The calculation is done in two steps. At first the effect of the pore water pressure and the swelling pressure on the canister is simulated by applying an initial stress in the buffer. Then the actual shear takes place by moving the boundary on the right side of the shear plane at a constant rate of 1 m/s until the total displacement is 10 cm.

Results

Almost all results will be shown together with the results of the corresponding calculation for KBS-3V (Börgesson and Hernelind 2010).

The bentonite buffer

The bentonite buffer is strongly plasticised during the rock shear. Figure 5-30 shows the plastic strain after 10 cm shear. Figure 5-31 shows the same data but a level of detail that highlights the most affected part.

The shear resistance in the buffer is constant at plastic strains larger than 5% (ideally plastic) at identical strain rate, which means that all bentonite with colours other than the three darkest blue shades are ideally plastic. However, the Mises stresses are not the same since the strain rate differs which can be seen in Figure 5-32. The stresses are higher close to the shear plane due to the higher shear rates there.

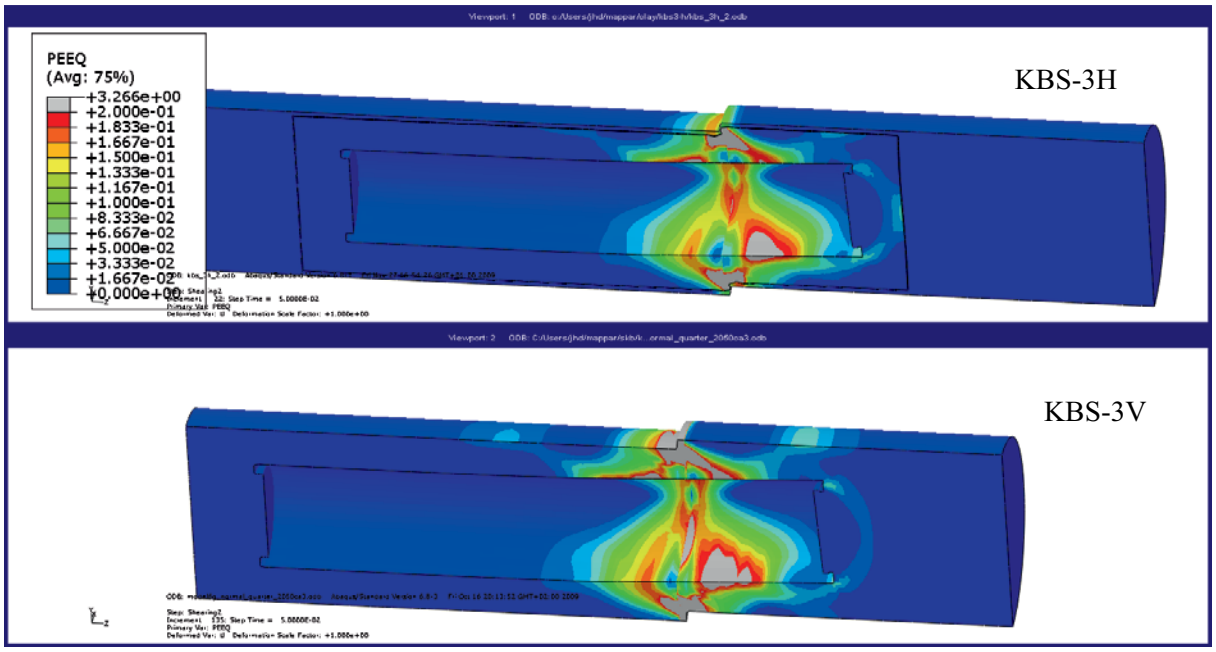

Figure 5-30. *Plastic strain in the entire bentonite buffer after 10 cm rock displacement.*

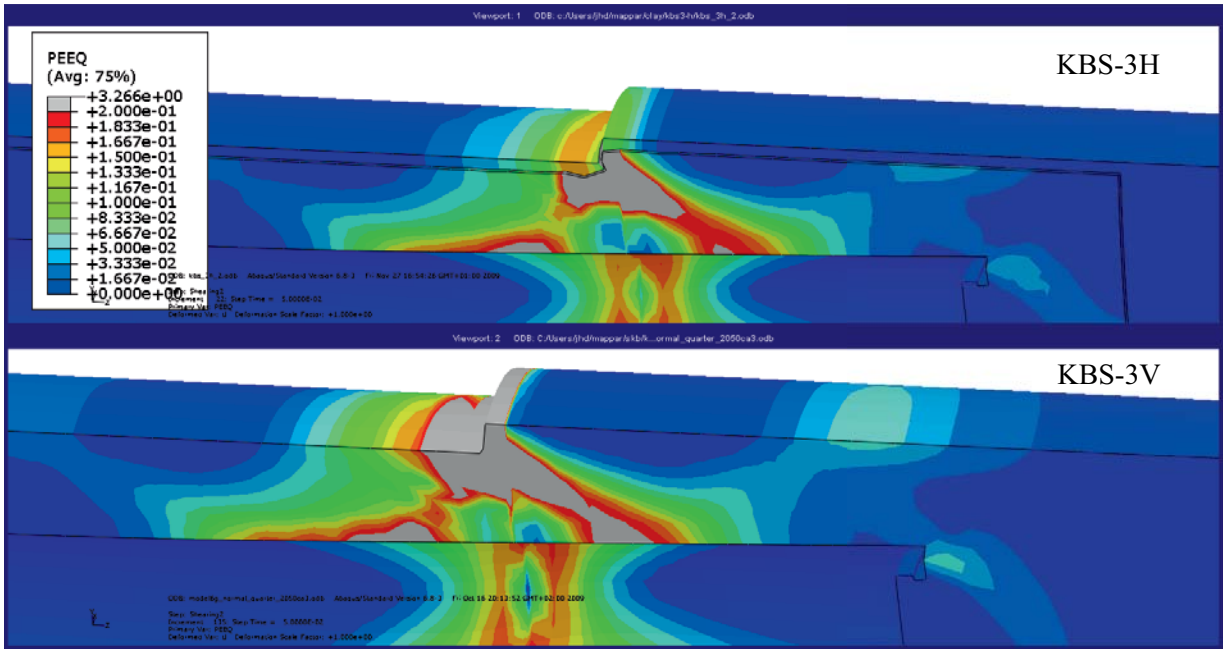

Figure 5-31. *Plastic strain in the bentonite buffer after 10 cm rock displacement – detail of Figure 5-30.*

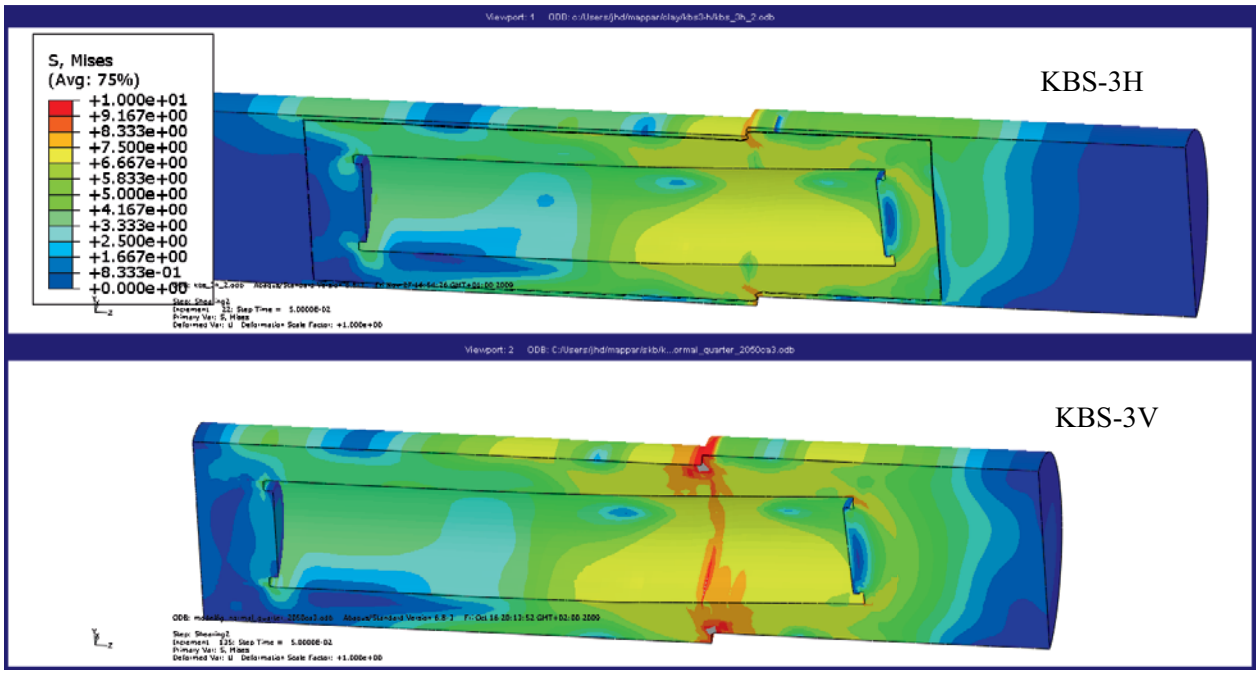

Figure 5-32. *Von Mises' stresses in the bentonite buffer after 10 cm rock displacement.*

Figures 5-30 to 5-32 clearly show that the difference in the results obtained for the two concepts is very small. The small difference in the two analyses generally implies smaller stresses and strains in KBS-3H than in KBS-3V. The difference is most likely caused by the extra 5 cm buffer that exists outside the canister in the Supercontainer in KBS-3H compared to KBS-3V, since the buffer is 5 cm thicker in KBS-3H.

The copper shell in the canister

The plastic strain in the copper shell of the canister is illustrated with two figures. Figure 5-33 shows the overall plastic strain in the entire shell, while Figure 5-34 shows a detail of the lid. There are stress concentrations in two quite different locations. As seen in Figure 5-33 the plastic strain is rather high in the centre of the copper shell with 1–2% plastic strain in a large part of the shell. Figure 5-34 shows that the plastic strain locally in the copper lid is higher than 10%.

Both figures clearly demonstrate that the effect of a rock shear on the stresses in the copper shell for these two concepts is essentially identical.

The iron insert

The plastic strains in the iron insert are shown in Figure 5-35. The figure shows that the plastic strain is up to about 1.5% in the periphery of the centre of the insert and that the difference between KBS-3H and KBS-3V is insignificant.

The perforated steel shell of the Supercontainer

The perforated steel shell of the Supercontainer is, as expected, strongly deformed close to the shear plane but otherwise rather unaffected. Figure 5-36 shows the plastic strains in the deformed Supercontainer shell. The plastic strains are so large (20–200%) that the Supercontainer shell would be broken close to the shear plane. This is not modelled but the effect of breaking is not expected to affect the results. Since the modelling work the shell material has been changed from steel to titanium, see Section 7.5.7.

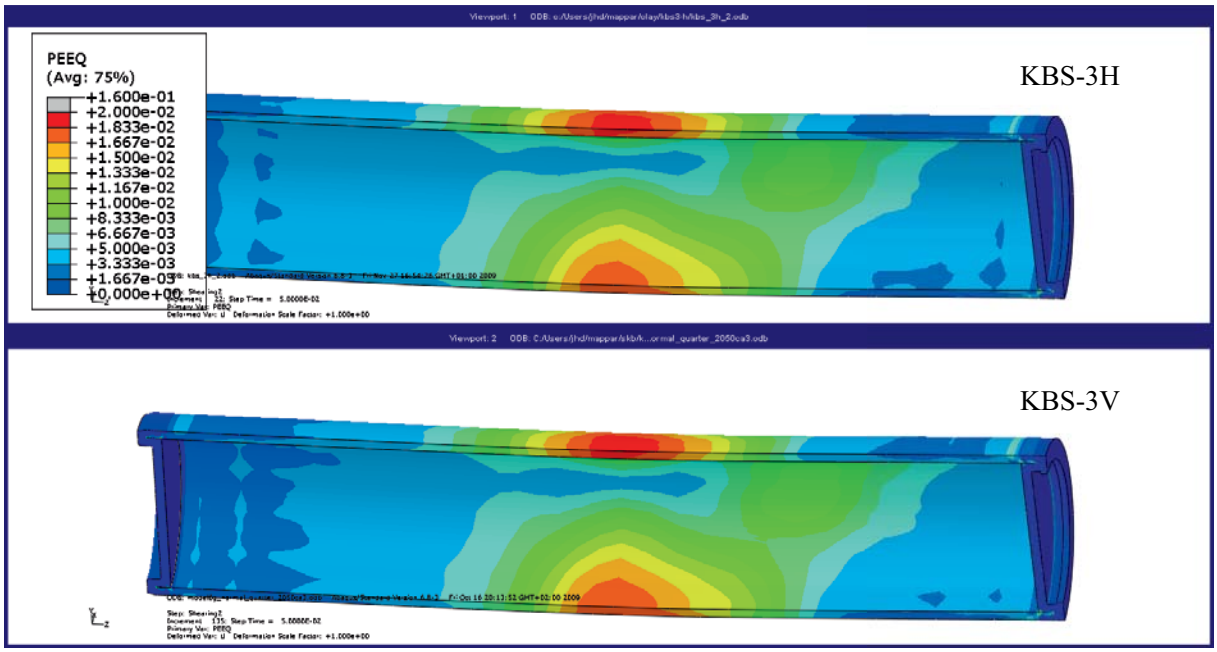

Figure 5-33. *Plastic strains in the copper shell of the canister after 10 cm rock displacement.*

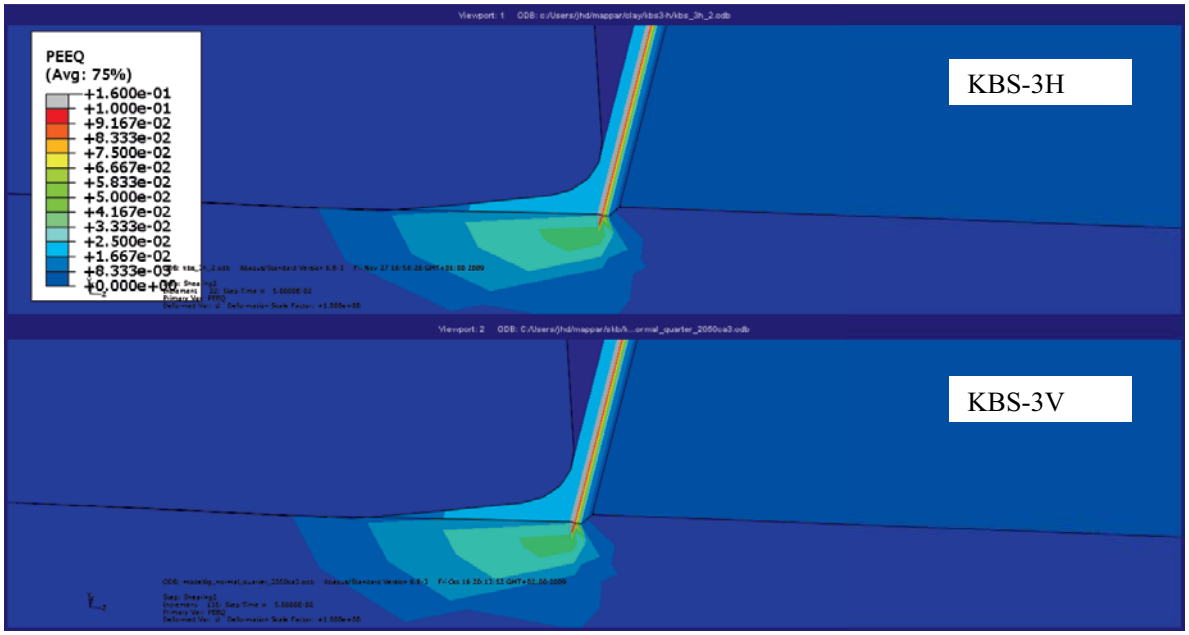

Figure 5-34. *Locally high plastic strains in the bottom of the copper shell of the canister after 10 cm rock displacement.*

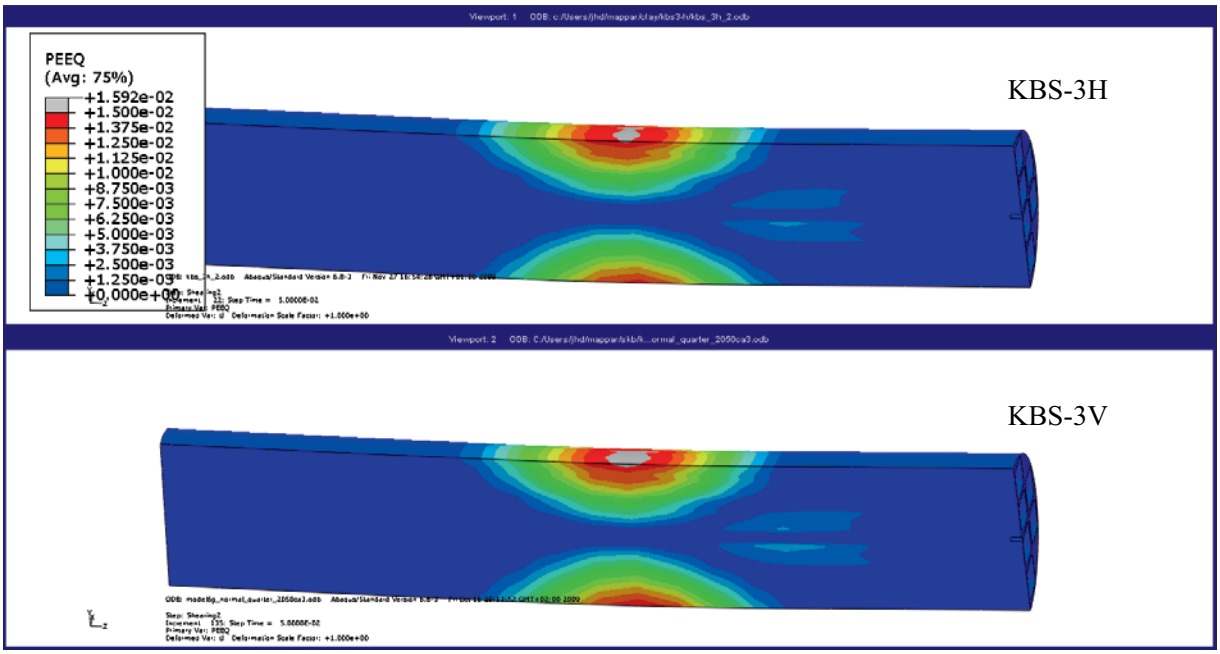

Figure 5-35. *Plastic strains in the iron insert of the canister after 10 cm rock displacement.*

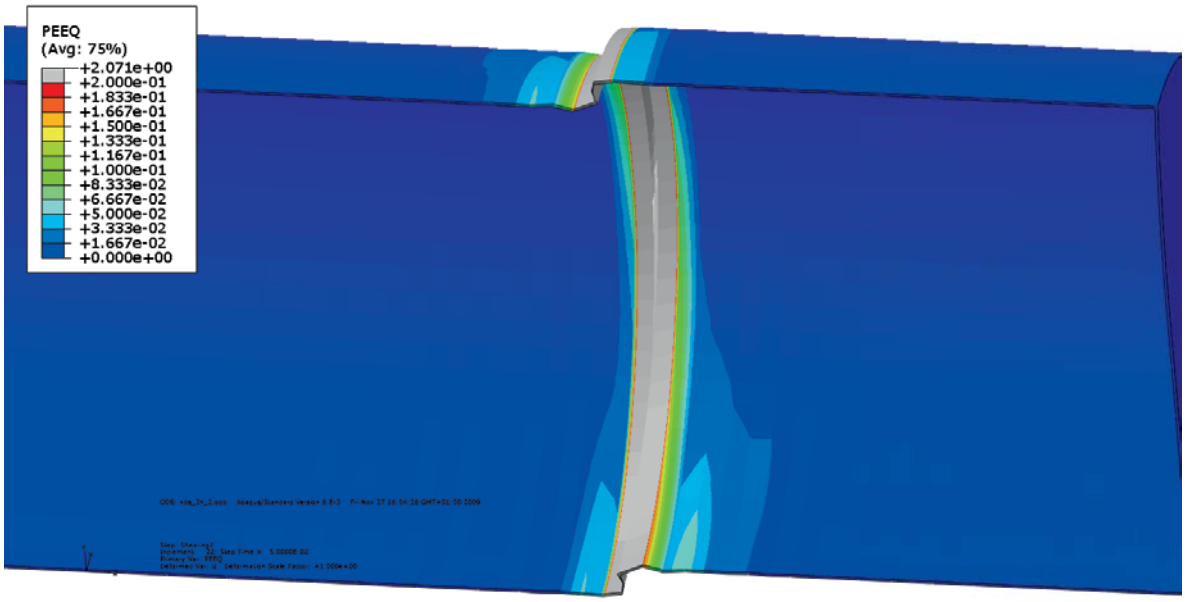

Figure 5-36. *Plastic strains in the Supercontainer shell after 10 cm rock shear.*

5.7.3 Conclusions

One of the most severe rock shear cases has been modelled for KBS-3H at Forsmark with identical element mesh, material models and modelling technique as was used for KBS-3V. The only substantive difference in these two models was the difference in geometry that exists between the two designs and the Supercontainer that is present in KBS-3H. The comparison shows that the Supercontainer shell is so strongly deformed close to the shear plane that it would probably break and that otherwise the difference between the effects of a rock shear in the two designs is very small for the stresses in the bentonite and negligible for the stresses in the canister. The very small difference in the behaviour observed seems to favour KBS-3H since in the Supercontainer there is an extra 5 cm thickness of bentonite buffer outside the canister, and secondly, the thick distance blocks between the consequent Supercontainers decrease the load effects of rock shear on the copper lids of the canister.

The reasoning of this conclusion is given next. The copper shell gets the highest strains in lid area (bottom or top lid) due to postulated rock shear load case. The highest strains are resulted in case the rock shear plane is 22.5 degrees inclined from the canister axis. The calculated maximum strain in copper lid is somewhat lower in 3H case when compared to respective 3V case. This is reasoned to be consequences of the fact that in 3H we have thicker bentonite buffer outside canister bottom and top lid in case of 3H than in case of 3V, in which we have only 0.5 m thick buffer between the bottom end of the canister and the solid rock bottom of the deposition hole. The buffer is more flexible material than solid rock and thicker layer of buffer is more flexible than a thinner.

The Supercontainer can therefore be assumed to be capable of withstanding a 5 cm rock shear of the type evaluated for the KBS-3V canister according to the supplementary analyses made.

There are uncertainties in the material models of the buffer and the canister materials as well as the finite element mesh of the canister. However, these uncertainties are common to those identified for the KBS-3V analyses and are treated by Börgesson and Hernelind (2010).

The material model of the Supercontainer does not include breakage of the steel (that was used as the material for the shell in the analysis) and the very large plastic strains (20–200%) imply that the Supercontainer shell would break. However, the effect of this is considered negligible since the Supercontainer shell is strongly deformed and follows the contours of the rock and thus acts as if it was broken.

The bentonite buffer is modelled with equal density inside and outside the Supercontainer and no consideration has been taken to the deformation of the Supercontainer shell during the water saturation and swelling process. In reality it is probable that the density will be lower outside the Supercontainer and that the distance between the Supercontainer and the rock surface will be reduced due to the expansion of the bentonite inside the Supercontainer. However, this is judged not to affect the results significantly since the difference between model and the expected real geometry is smaller than the difference between the model of KBS-3H and the model of KBS-3V and this difference had no influence on the stresses in the canister.

The Supercontainer shell is modelled as a steel cylinder without the 10 cm diameter holes that imply 62% perforation. However, since properties that should yield the same average behaviour have been applied to the steel and since the effect of the steel cylinder anyway is so small the conclusion is that this simplification is of no consequence. A change of shell material to Ti is not considered to have any influence on the conclusions.

The conclusions of the performed modelling of one of the most severe cases of rock shear through KBS-3H are that the difference in consequences of the rock shear between KBS-3H and KBS-3V repository design alternatives is insignificant. It has also been concluded that the consequences of the uncertainties regarding the differences between the two models are also insignificant. This means that the results and conclusions of the extensive investigations and modelling exercises of a rock shear in KBS-3V can also be used for KBS-3H.

Further work is needed to address the compression shear type, which was not covered in the calculation described above. The compression shear is a KBS-3H-specific issue.

5.8 Development of DAWE-specific swelling pressure of the buffer with special reference to ability to prevent spalling of rock

5.8.1 General

The host rock is one of the main components in a KBS-3H design that together with buffer and canister will ensure isolation of the spent fuel. After deposition of canister and buffer, it is possible that the emitted heat from the canister could together with the in situ and excavation induced stresses cause a thermally-induced spalling of rock. Rock spalling is a brittle failure induced by thermally-induced tangential stresses occurring in the drift walls; see Section 9.2.3 for rock spalling studies. This process can result in detachment and accumulation of loose rock fragments between the buffer components and drift surface and a damaged zone in rock adjacent to drift surface resulting in higher hydraulic conductivity than in the sound rock close to the buffer. This could affect the buffer and could result in loss or redistribution of bentonite mass.

Earlier investigations have shown that thermally induced spalling of the rock surface could potentially be prevented or at least mitigated with application of counter pressure (Glamheden et al. 2010, Andersson 2007). There are still significant uncertainties concerning both the magnitude and the development rate of the buffer swelling pressure needed to eliminate spalling of rock and also regarding the presence and magnitude of buffer swelling pressure in dry drift sections. There are clear indications from previous work that sufficient buffer swelling pressure to prevent spalling of rock could potentially be obtained in a KBS-3H geometry, which provides the motivation for continuing to examine this emplacement option. Additionally the importance and consequences of thermally induced spalling of rock for long-term safety will be studied in the next project phase.

The investigations regarding the development and the magnitude of the buffer swelling pressure (counter pressure) have been continued with different laboratory tests in different scales during the recent project phase. Some of the tests related to the swelling pressure that were completed earlier have been reported by Sandén et al. (2008a). One of the completed tests was the study how the buffer swelling pressure developed in dry drift sections. This test is also briefly described in the next section together with the tests that were completed during the recent project phase.

5.8.2 Description of work and results

Previous testing with 1 metre long test set-up

The test layout shown in Figure 5-37 was designed in order to study the mechanical interaction between the distance block and the simulated rock surface when no additional water is available. The bentonite blocks used in the test had an initial water content of 17% and a dry density of 1,790 kg/m^3. The bentonite blocks were centred by means of steel "feet" and the radial slot width between the blocks and the rock was set at 10 mm. The water used had a salt content of 3.5% (50/50 NaCl/$CaCl_2$). The space around the blocks was pre-wetted and de-aired. A total volume of 5.5 litres was injected over a period of 30 minutes. Once the slot between the bentonite blocks and the rock had been filled, the inlet valve was closed and the specimen had no further access to additional water.

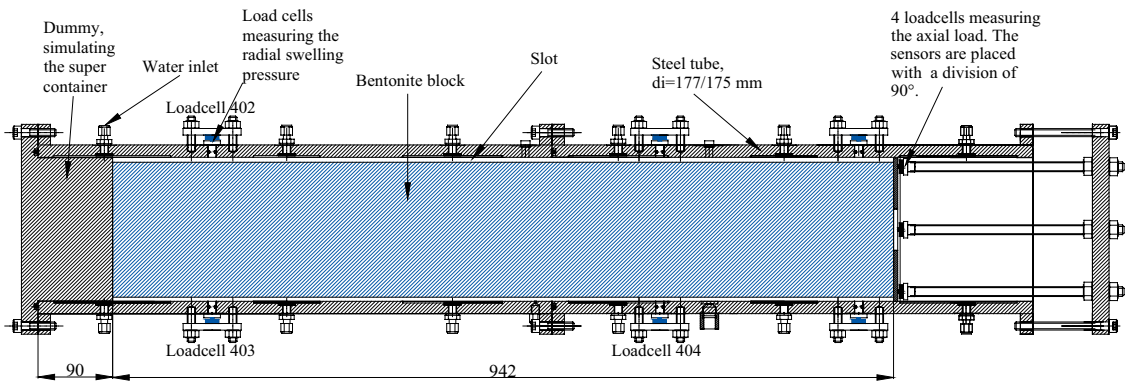

Figure 5-37. *Schematic drawing showing the test equipment used (dimensions in mm). The equipment has a radial scale of 1:10.*

The specimen was left for 112 days with no further access to additional water. The assumption was that the water in the slot would be drawn deeper into the buffer blocks resulting in clear reduction of swelling pressure and possible desiccation and cracking of the bentonite in the outer parts. This phenomenon has been previously noticed in similar tests performed in another project e.g. LASGIT, Large Scale Gas Injection Test, and have also been investigated within the KBS-3H project (Sandén et al. 2008a). The results of these tests showed that there are clear indications of desiccation and cracking of the surface, but also that a swelling pressure will still be acting on the walls. The radial pressure measurements in this test, Figure 5-38, showed similar behaviour.

A mechanical pressure from the clay was still acting on the cylinder surface after 112 days test duration. In the final stage it was tested how well the section had been sealed. Two different methods were used. Air pressure was applied in the section simulating the Supercontainer in the first method and the result showed that the section seemed to have been sealed. In the second method a water pressure ramp of 1 MPa/h was applied, Figure 5-39. After a certain amount of internal piping, the bentonite could withstand a water pressure of 5 MPa. During the applied pressure ramp, internal piping occurred several times. The amount of water injected was fairly large, which showed that a lot of empty voids had been formed. 24 hours after starting the pressure ramp, the maximum pressure, 5 MPa, was reached. The dip in the pressure after about 8 hours is a result of the fact that the pressurizing device ran out of water in the middle of the night.

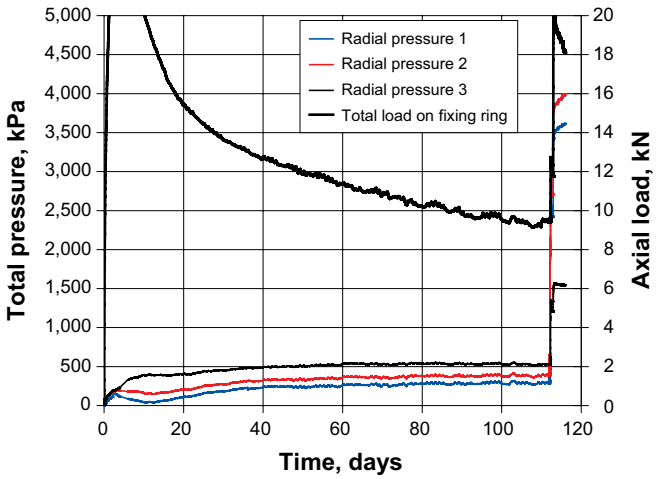

Figure 5-38. *Graph showing the axial load on the fixing ring (in BD) and the radial swelling pressure measured at three points as a function of time.*

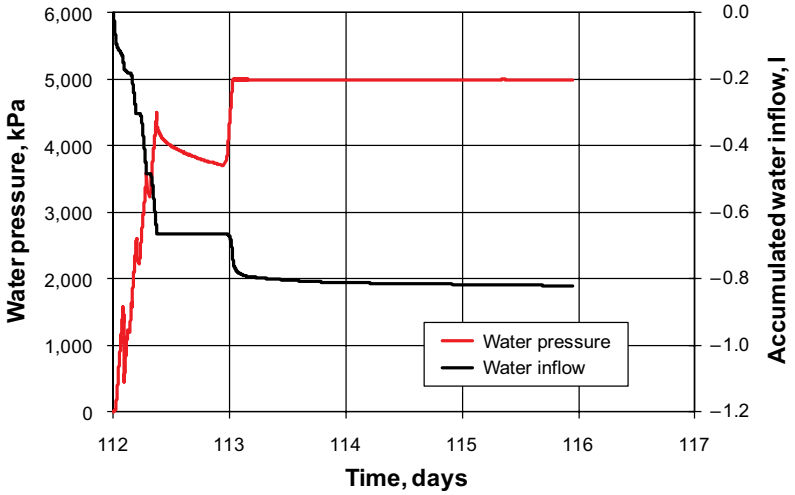

Figure 5-39. *After 112 days without access to additional water, a water pressure ramp was applied.*

5.8.3 Small-scale tests on artificial wetting of distance blocks

Artificial water filling of the gap between the rock and the distance block is the main option in the DAWE design. In the DAWE design, the entire drift compartment will be filled with water after plugging in order to accelerate system swelling and sealing. The initial water filling of the slot means that water is immediately supplied to the bentonite, thereby resulting in water uptake, clay swelling and filling of the slot. However, with time, the water will be drawn deeper into the bentonite and there may be a reduction in the water content of the low-density bentonite in the slot, resulting in desiccation and cracking unless additional water is available. This phenomenon was observed in tests carried out for the LASGIT project and was investigated in a scale of 1:10 by Sandén et al. (2008a) (Test III-13).

It has been assessed as being possible that the sealing ability of the distance blocks may be lost with time if the natural water supply is too low to satisfy the water uptake demands of the buffer thus resulting in desiccation, especially if the swelling pressure is reduced significantly. This subsequent desiccation of the perimeter region is not necessarily a long-term or system performance problem, but it is important to understand how much of the effect is left and how fast the process is. The possible reduction of swelling pressure may result at worst in rock spalling, which is likely to have impact on long-term safety. The main objectives of the tests were to find out for how long a slot will remain filled with bentonite and remain sealed under different conditions, and to find out how much the slot may be re-opened under conditions of dry rock.

Two types of tests were run in the laboratory (Test Type 1 and Test Type 2) representing different scales. All specimens were made of the commercially available sodium bentonite MX-80 (trade name for a Wyoming bentonite product from American Colloid Co.). The powder is delivered with a water content of 10%. Higher water contents were produced by adding water during mixing.

Test Type 1

Different conditions of initial gravimetric water content (10%, 20%, 22% or 24%); slot width (5 mm or 8 mm) and salt content of the added water (1% or 3.5%) were investigated. Seven different combinations were tested.

The specimens were enclosed in stiff swelling-pressure oedometers. Above each specimen a slot was left which was initially filled with water. Axial stress, radial stress and *RH* were all measured during the tests.

All specimens were compacted by applying a uniaxial compaction pressure of 50 MPa. The specimens with prescribed water content were compacted to a height of 25 mm. The initial gravimetric water content used was 10%, 20%, 22% or 24%, according to the test matrix. With the compaction pressure of 50 MPa the corresponding dry densities were between 1,650 and 1,830 kg/m^3. To obtain a total height of 50 mm including a slot of 5–8 mm, one of these specimens was sawn to a height of less than 25 mm. The two specimens were then placed on top of each other in the equipment shown in Figure 5-40. This type of equipment had previously been used in the LASGIT project. The device was sealed and RH measurement was performed for a period of 1–2 days to determine the initial RH value.

Then the lid was removed and the slot above the bentonite specimen filled with water with a prescribed salt content (1% or 3.5%). The lid was put back on, the device was sealed and no additional water was added. Radial and axial stresses were measured by load cells installed in the top lid and in the wall of the oedometer. The moisture redistribution was monitored by the RH sensor. In the first tests the load cell was pre-stressed to assure that it remained in its position. However, to be able to measure also a small load the load cell was fixed by means of an adhesive in the majority of the tests. The inner side of the steel equipment, i.e. the ring and the lids, were not lubricated.

After approximately 2 months, the test was terminated, the upper lid lifted and photos taken of the upper surface. The bottom plate was then removed and the specimen was pushed out of the ring. The total mass, height and diameter were measured and the specimen was then cut into 4-6 slices and for each slice the water content and density were determined.

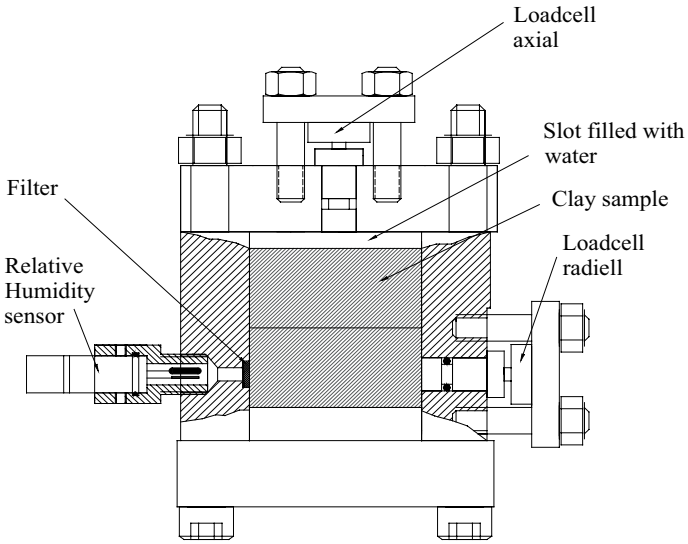

Figure 5-40. *Schematic diagram of the test equipment used for Test Type 1.*

Test results

The results are represented by stresses (measured as forces on a piston) on the clay-piston boundary with time and cracking observed at the end of the test. The gradients in water content and density over the specimen height and radius were determined after the test.

The measured relative humidity, axial stress and radial stress vs time are presented for two tests in Figures 5-41 and 5-42. The two selected specimens had initial water contents of 10% and 24%. In all test results the specimen names are denoted showing *initial water content, slot width, salt content in the added water (e.g. 10_5_3.5 in Figure 5-41)*. In each diagram the time when water was added is marked with a cross on the x-axis.

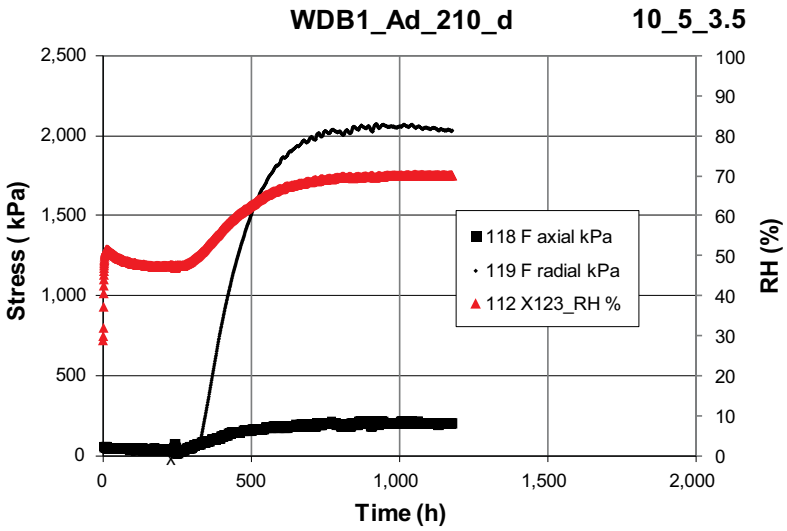

Figure 5-41. *Relative humidity, axial and radial stresses vs time from test W210 (Initial water content 10%, the slot width 5 mm and a salt content of 3.5%.)*

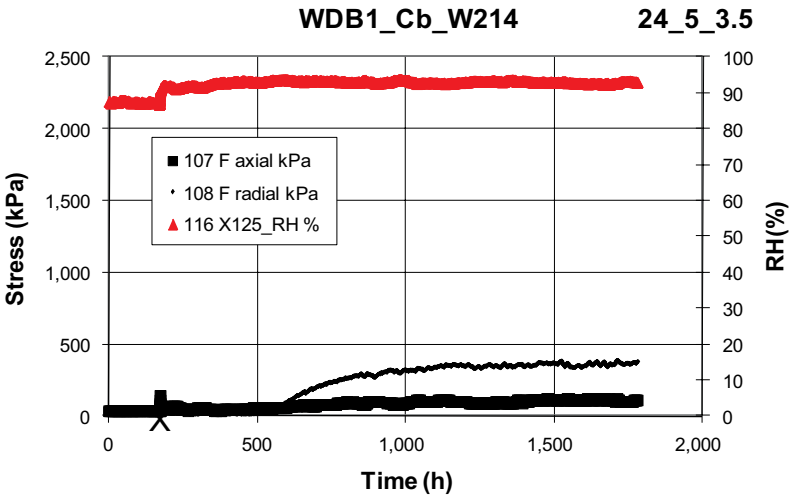

Figure 5-42. *Relative humidity, axial and radial stresses vs time from test W214 (Initial water content 24%, slot width 5 mm and a salt content of 3.5%).*

In the following graphs, the colours (blue, green, orange and red) denote the initial water content (10%, 20%, 22%, 24%) for which a maximum stress is associated. The specimen names with (t) or (p) at the end indicate that a shorter period of time (t) or a lid of acrylic plastic (p) was used.

The radial (Figure 5-43) and axial stresses for all tests were plotted vs final dry density. In the diagram the average stress for saturated conditions from a model by Börgesson et al. (1995) is also shown. The solid line represents model with de-ionized water and the broken line represents water with 3.5% salt content. In Figure 5-43 each radial stress from a specimen is presented twice, i.e. with two different dry densities. The value to the left is the average dry density over the specimen and to the right is the dry density at the level where the radial stress was determined, i.e. at the bottom of the specimen. The measured stresses are logically lower than the theoretically expected stresses after full saturation, since the tests have not reached full saturation.

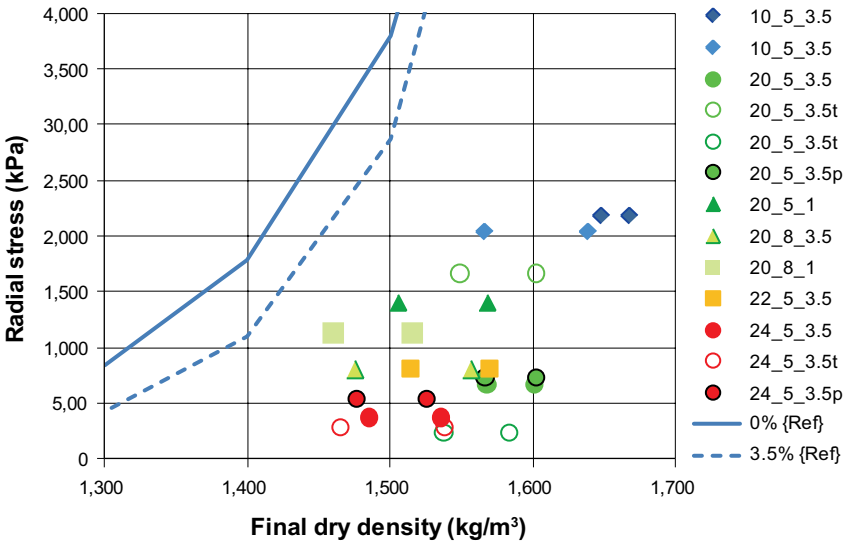

Figure 5-43. *Radial stress vs final dry density in the artificial wetting tests. Each test result is presented twice, to the left with the average dry density and to the right with the density at the level where the radial stress was determined. The lines represent relations for the average stress at saturated conditions presented by Börgesson et al. (1995) denoted {Ref} in the diagram. The solid line represents de-ionized water and the broken line represents water with 3.5% salt content.*

The axial stress was in some tests measured on a pre-stressed piston, i.e. an axial stress was applied at the start of the test. There is an uncertainty in the final axial stress when this axial stress is of the same size as the initially applied pre-stress. Especially in one of the tests no increase from the pre-stress was seen. However, the axial stress in all tests was lower than the radial stress, and for all tests the axial stress was lower than 600 kPa.

Gradients in water content and dry density are shown for selected samples in Figures 5-44 and 5-45, respectively.

The water content increased in all parts of the specimen in all tests. The dry density decreased in all parts of the specimens.

All specimens showed cracking in their upper surfaces at the time of test termination, despite there being contact between the lid and the bentonite. A photo of specimen W212 taken after lifting the lid is provided as Figure 5-46.

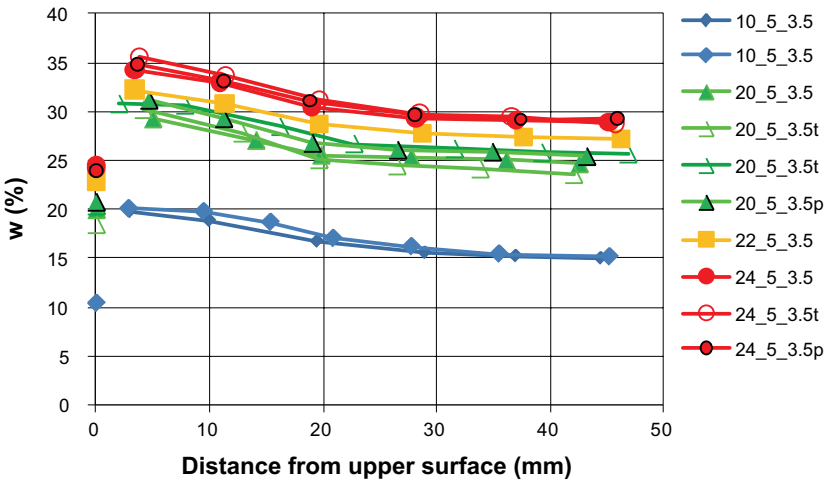

Figure 5-44. *Profiles of water content after the completed tests. (The initial gravimetric water content for each sample is marked on the y-axis as distance equal to 0 mm).*

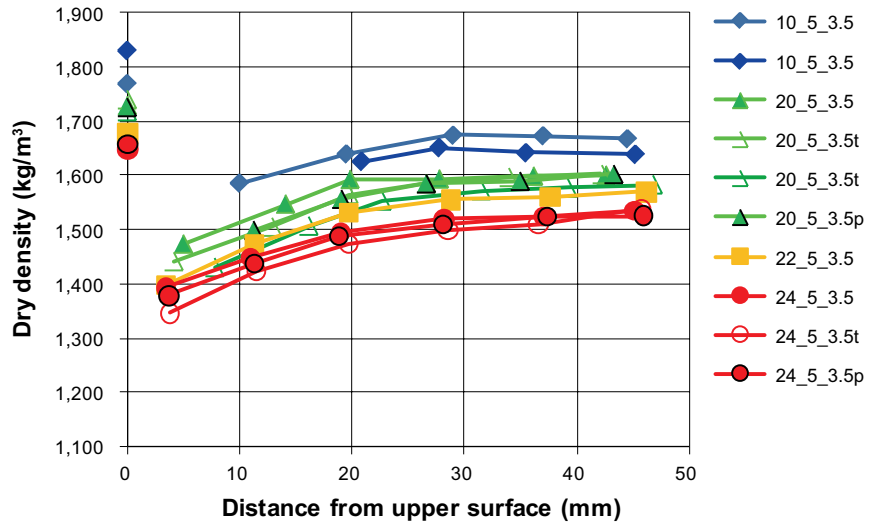

Figure 5-45. *Profiles of dry density after the completed tests. (The initial dry density for each sample is marked on the y-axis as distance equal to 0 mm).*

Figure 5-46. *Photo taken after lifting the lid but with the specimen still inside the oedometer ring. (Initial water content 20% in the bentonite, slot width 5 mm and a salt content of 3.5% in the added water).*

Test type 2

A test cell similar to the apparatus in Test Type 1 was also used in Test Type 2, but the length of sample was increased in order to reduce the effect of the bottom boundary condition. A 270 mm-long cylindrical specimen with a diameter of 100 mm was sawn and trimmed out of a larger bentonite block with initial gravimetric water content of 22% and dry density of 1,710 kg/m^3. The specimen was mechanically pushed into the steel cylinder in the device shown in Figure 5-47. The inner wall of the cylinder was not lubricated. Two specimens were performed. Both specimens had initial water content of 22% and slot width of 30 mm. The two salt contents used in this test series were 1% (specimen W313) and 3.5 % (specimen W323).

The 30 mm slot on top of the specimen was initially filled with water of the prescribed salt content. The device was then sealed and no additional water was added. During testing, only the axial stress was measured on top of the specimen. A pre-stress of approximately 50 kPa was applied on the piston where the upper part of the piston was pressed against the steel ring. The testing time was approximately 6 months for each specimen. After the test, the lid piston in Figure 5-47 was removed and the upper surface observed to detect bentonite cracking.

At 50 days before termination of the test the stresses were released by loosening the upper hexagonal nut. However, a full recovery of the originally measured axial stress was not observed. No additional water was added.

Profiles of water content and density determined over the specimen height are shown in Figures 5-48 and 5-49.

In all parts of both specimens, higher water content was measured at the end of the test than was present at the start of testing. In the upper part, 4 mm from the lid, the water content was lower than was observed 12 mm from the lid in both specimens. Photos of the specimens, W313 and W323, still inside the equipment and immediately after lifting the lid are shown in Figure 5-50. In Figure 5-51 these specimens are shown after dismantling.

The main region that experienced cracking in specimen W313 was seen in the cross section of the specimen and in specimen W323 the greatest degree of cracking was seen at the boundary close to the steel cylinder.

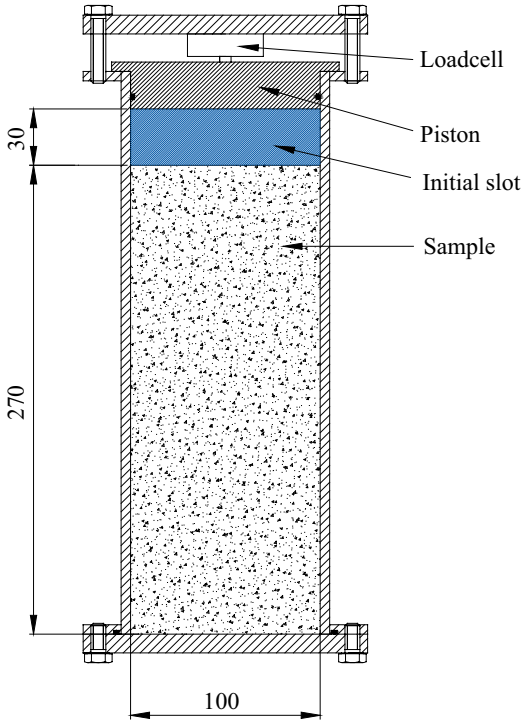

Figure 5-47. *Schematic diagram of the test equipment used for Test Type 2.*

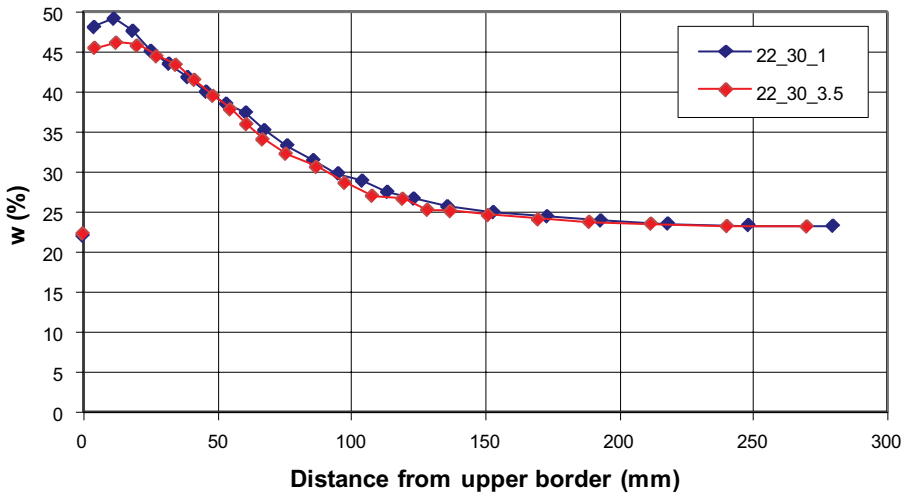

Figure 5-48. *Profiles of gravimetric water content for specimens W313 (blue) and W323 (red). (The initial water content for each specimen is marked on the y-axis as a distance equal to 0 mm.)*

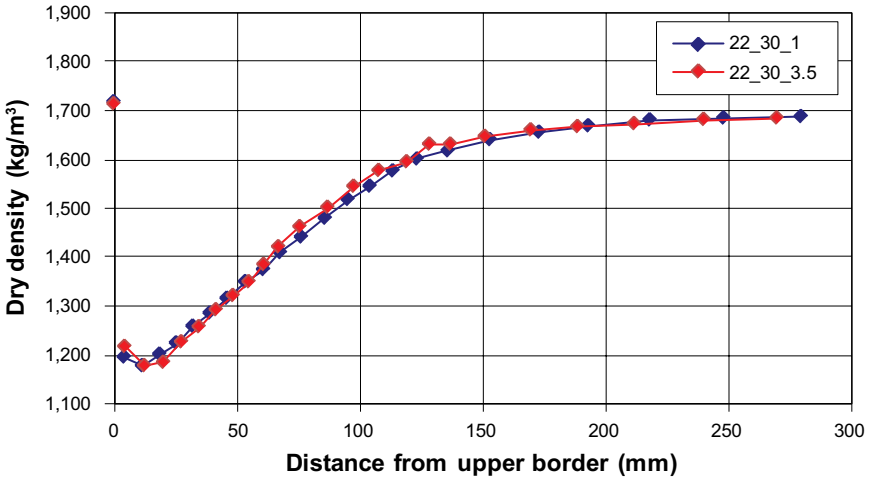

Figure 5-49. *Profiles of dry density for specimens W313 (blue) and W323 (red). (The initial dry density for each specimen is marked on the y-axis as a distance equal to 0 mm).*

Figure 5-50. *Photos of specimens W313 and W323 after lifting the lid.*

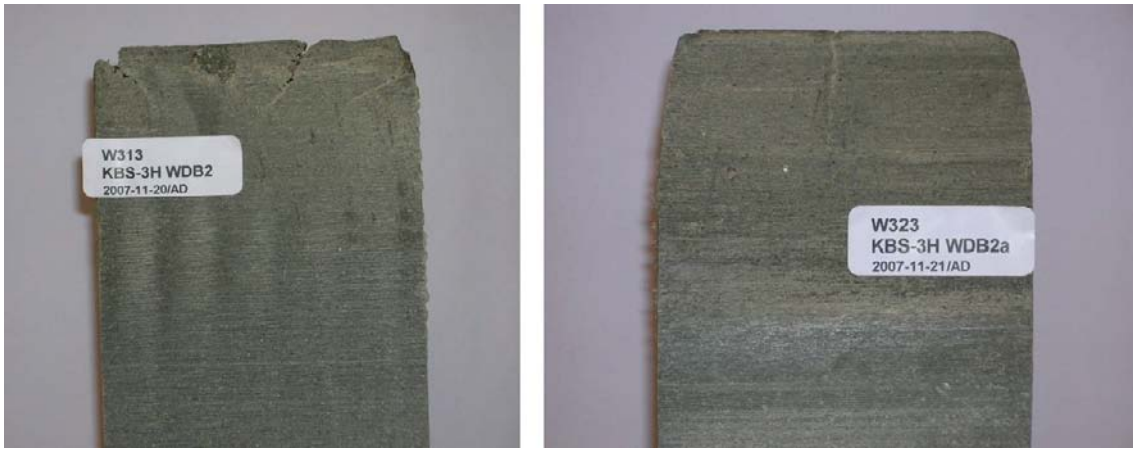

Figure 5-51. *Photos of one half of the upper parts of W313 and W323.*

Large-scale laboratory test

The objective of the large-scale BB test was to simulate the situation in which distance blocks are installed in a dry drift according to the DAWE design. After the artificial wetting of the empty space between the distance block (with lower gravimetric water content compared to the nominal water content for distance blocks) and the drift walls, there was no further access to water in the test. The magnitude and development of the radial swelling pressure during the redistribution of the water in the bentonite was studied as a supplement to the small-scale tests described above. The mechanical interaction between the distance block and the simulated rock surface when no additional water is available is important in addressing the critical issue of thermally-induced rock spalling.

The large-scale BB test equipment used in this test has an inner diameter of 800 mm. It is possible to perform tests with a length of 350 mm and 1,050 mm by using separate sections of this two-segment equipment, or the full length 1,400 mm can be used. The original purpose of the BB equipment was to simulate a section of a Supercontainer, as shown in Figure 5-52, and to study the long-term homogenization process.

Blocks made of MX-80 Wyoming bentonite at a water content of 10% and with a dry density of 1,989 kg/m^3 were produced for previous tests carried out using this equipment. This water content and density is probably very close to what the blocks inside the Supercontainer will have to have in connection with installation while the distance blocks between the Supercontainers probably must have an initial water content of 20–22% and a dry density of about 1,710 kg/m^3. Since the objective of the test described in this section was to simulate a distance block section this means that the available bentonite blocks do not perfectly represent the initial conditions that we wish to test. The differences in scale between the BB test and a full-scale distance block section affects, however, the ratio between the initial slot volume and the volume of the installed block which means that the calculated final saturated density in the BB test (2,002 kg/m^3) is very close to the final saturated density in full-scale (2,000 kg/m^3).

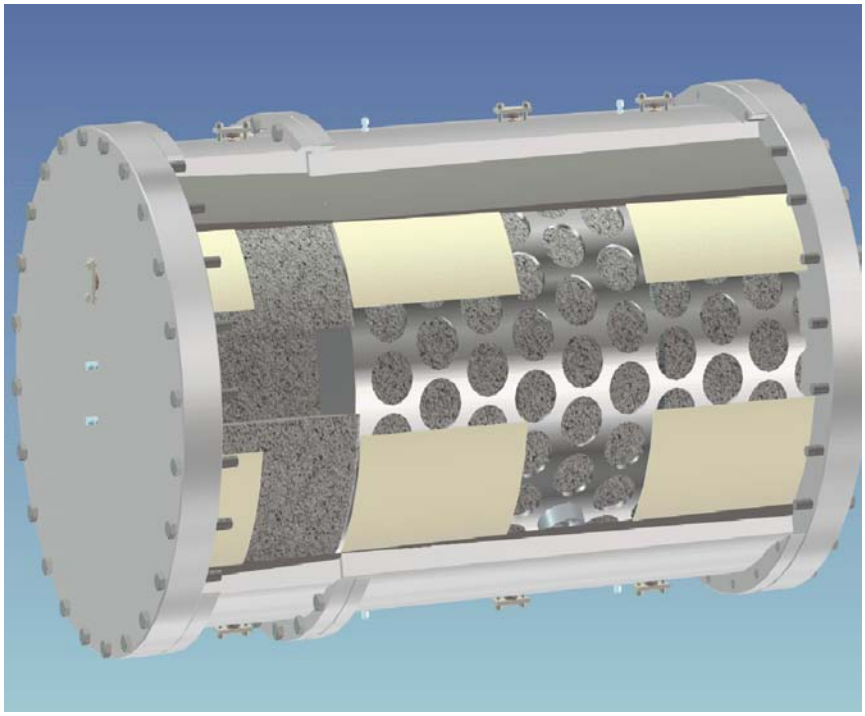

Figure 5-52. *Picture showing the BB test equipment at its full assembly length. The original purpose of this equipment was to simulate a section of a Supercontainer and to study the long-term homogenization process. The white partial covering that can be seen is filter sheets which were intended to be used in supplying the buffer with water.*

Only the shorter part of the "BB" test equipment was used, giving a test length of 350 mm (Figure 5-53). One of the 800 mm diameter blocks was machined down to a diameter of 715 mm, which gave a radial slot of the same width as in a full-scale installation (42.5 mm for the distance blocks). The bentonite block was centred in the "drift" by the use of bolts fastened into threaded holes in the block. This design also facilitated the adjustment of the block within the slot (Figure 5-54). After installation of the block, the steel cylinder was raised and the load cells mounted. After emplacement of the block, the radial gap was filled with water by the use of two tubes, one placed at the bottom and one at the top: The upper tube was used for de-airing while the lower one was used for filling. The water used in this test had a salt content of 1.2% (Na/Ca 50/50). This salinity was chosen since it is the concentration expected during operations in Olkiluoto.

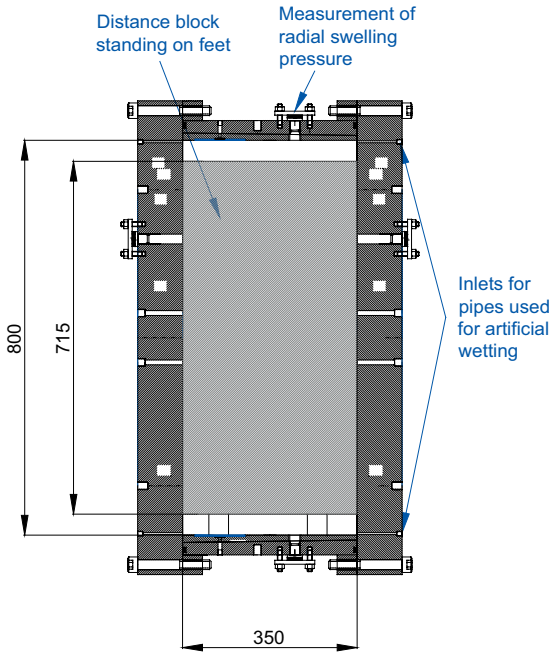

Figure 5-53. *Schematic diagram of the radial wetting test.*

Figure 5-54. *Bentonite block centred in the steel "drift" through the use of strong bolts.*

After finishing the initial water filling of the cell, there was no access to additional water. The development of the radial swelling pressure was measured continuously at two points within the system, one at the bottom and one at the top as can be seen in Figure 5-53.

The BB-test was started in October 2007 and the total test duration was almost 500 days. In Figure 5-55 the development of the radial pressure is plotted vs time. The pressure started to increase immediately after water filling was completed. Since the water-filled slot had a width of 42.5 mm, it was obviously not the swelling pressure from the bentonite that was being measured. When a bentonite block comes into contact with water it will start to swell, and if the system is closed, i.e. no water can leak out, the water pressure will start to increase and act on the pistons intended to measure the swelling pressure. In time, water will be sucked into the bentonite and the slot will be filled with clay. This means that the water pressure will decrease and go down to zero after a certain period of time. In order to verify whether it was water pressure that had been measured in the first early phase of the test, a pressure sensor was connected to the tube that initially was used for de-airing during the water filling stage. The sensor was installed after nine days of testing. A water pressure (100–150 kPa) was measured over a period of 50 days after commencement of the test, but was then found to decrease rapidly to zero, i.e. the earlier available water had been sucked into the bentonite block.

Since the start of testing, a continuously increasing radial swelling pressure has been measured. After about 500 days, a radial swelling pressure of between 450 (at the top) and 500 kPa (at the bottom) was noted, and the pressure at the top was still increasing.

The main reason for the deviation in pressure between top and bottom is probably that the centring of the bentonite block has not been perfect. If the block during installation was positioned a few millimetres closer to the bottom, it would result in the increase of swelling pressure starting earlier and reaching a higher level at the bottom than at the top position. The differences in pressure would, however, even out in time. The diagram gives a good picture of how the homogenization of buffer blocks in a deposition drift will proceed.

The test was terminated after almost 500 days of operation. The test cylinder was rotated so that one end was on the floor and the upper lid was then removed, see Figure 5-56. The region where the outer slot was originally present was completely filled with bentonite although some radial cracks could be seen here; see Figures 5-57 and 5-58.

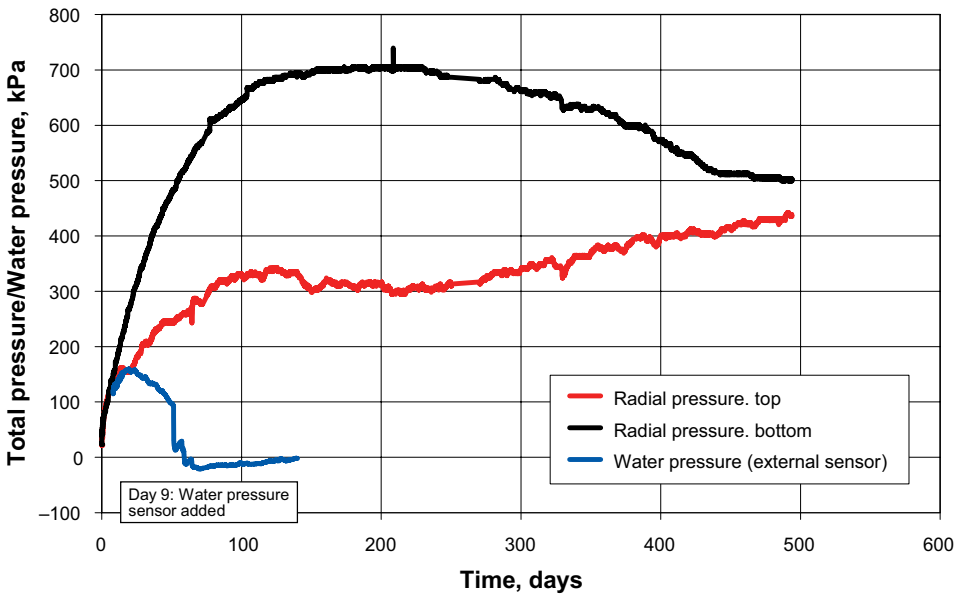

Figure 5-55. *Development of radial swelling pressure and porewater suction as a function of time.*

Figure 5-56. *Photo showing one of the sides of the distance block immediately after removing the lid. The former slot is completely filled with bentonite.*

Figure 5-57. *Close-up showing some of the radial cracks.*

Figure 5-58. *Photo of a sample showing the outer surface which has been in contact with the "rock". Some small cracks can be seen.*

Samples were taken from the bentonite at different radial distances from the "rock" surface at two levels:

1. **Surface closest to the lid**. Samples were taken from the location of the original slot at five distances from the "rock" and in four directions. For each position the water content was determined, see Figure 5-59.
2. **Fifteen cm down from lid surface**. Samples were taken from the location of the original slot and in to the centre of the block, in four directions. For each position the water content and bulk density were determined and then the dry density and degree of saturation could be calculated, see Figure 5-60.

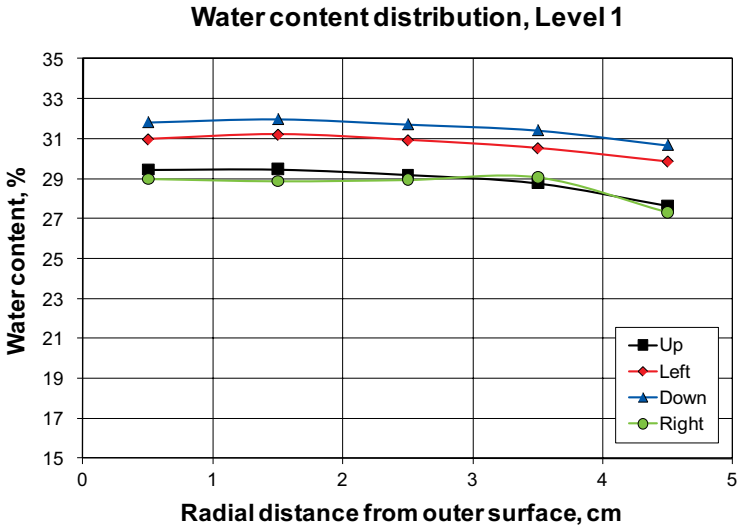

Figure 5-59. *Water content as function of distance from outer "rock" surface. The samples were taken from the surface closest to the lid.*

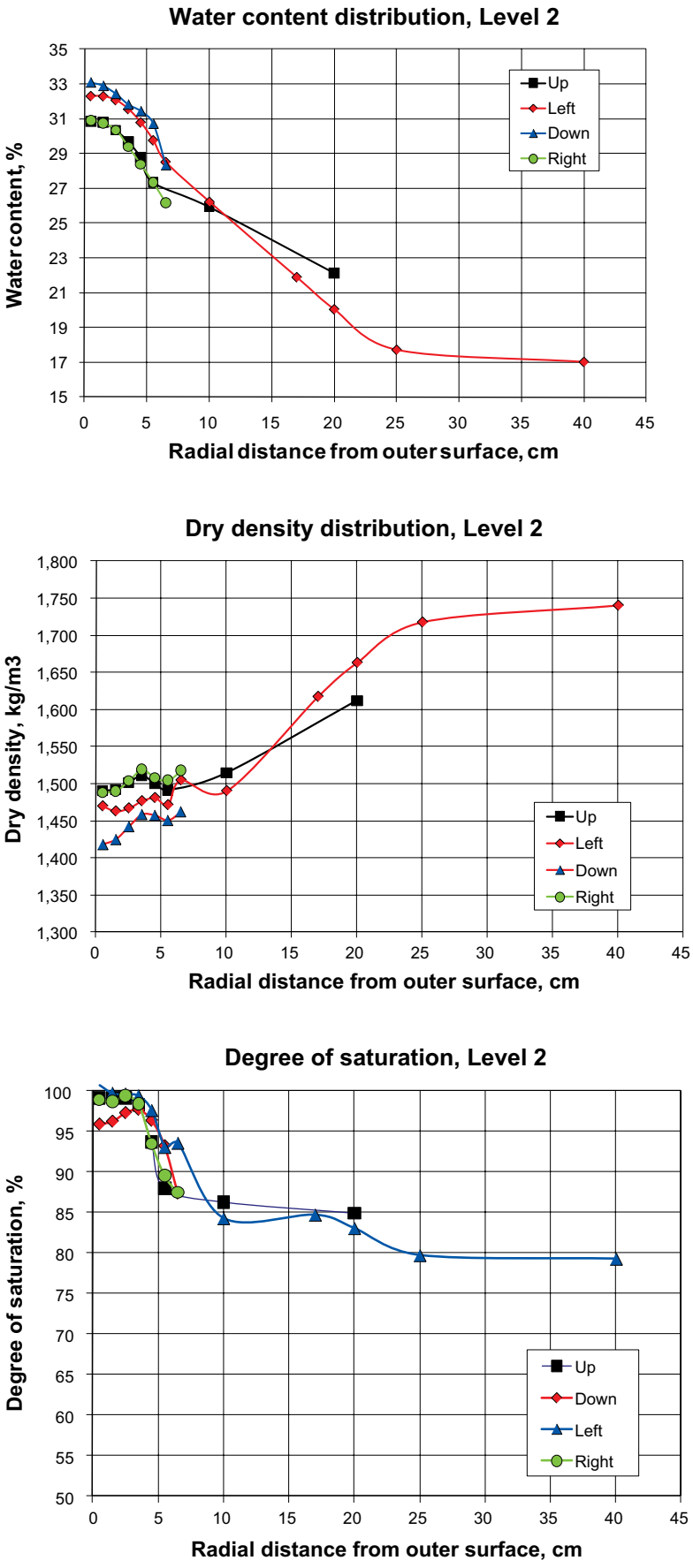

Figure 5-60. *Water content (upper), dry density (middle) and degree of saturation (lower) plotted as function of distance from outer "rock" surface. The samples were taken at a depth of about 15 cm from the surface closest to the lid.*

It was noticed that the contact between buffer and rock seemed to be very good at all positions in the test cylinder. Some small cracks could be seen, see Figure 5-58, but the main part of the "rock" surface was supported by swollen bentonite.

The diagrams show that the main part of the location of the original slot (not the cracks) was filled with material with rather high density (dry density of about 1,420–1,480 kg/m^3 at the outermost parts). The degree of saturation was high, 95–100%.

5.8.4 Conclusions

Discussion Test Type 1

- The measured stresses increased with time in almost all tests. The only test in which a very small decrease was seen in the axial stress with time was test W210. This test started with a water content of 10%. The salt content was 3.5%. The initial dry density was 1,770 kg/m^3 and the final average dry density was 1,650 kg/m^3.
- In all test results the axial stress was less than the radial stress. One reason for this might be the friction between the bentonite specimen and the steel ring. The axial stress in all tests was lower than 600 kPa.
- There is some scatter in the measured results. When compared to the relation representing saturated conditions there is no obvious influence of gap width and initial water content. However, regarding salt content there is an indication that increasing salt content gives less stress in both axial and radial directions. This corresponds to the relation by Börgesson et al. (1995).
- In all tests a gradient in water content and density was seen after completed tests although no large change in stress was seen during the last days of measurements.

Discussion Test Type 2

No decrease in stress with time was measured, but since the stress did not fully recover after a release of the vertical stress at the end of testing, the stress must be regarded as uncertain and in both cases lower than 60 kPa.

- The "recover" refers to that the vertical stresses were released by loosening the upper hexagonal nut 50 days before termination.
- Cracking was seen in both specimens (Test Type 2) at the end of testing, but the appearance of these two cracked regions was different.
- The final water content was larger and the final dry density lower, in the upper region of both specimens compared to a corresponding test of Test Type 1, e.g. W213 (22_5_3.5). The swelling pressure was also lower compared to the results from W213. One reason might be the larger slot width in Test Type 2 compared to the slot width in Test Type 1.

The results from the tests performed indicated the possibility of resolving the problem with thermally induced spalling of rock. The following conclusions have been drawn from the three presented test series:

- **Mechanical pressure against rock**. All three test types (different scales) have shown that in spite of no additional access to water, only what has been filled in the slot between rock and bentonite, a significant mechanical pressure (50–500 kPa) was acting on the "rock" surface throughout the entire test durations. One possible explanation proposed for the rather low swelling pressure observed in Test Type 2 (which was less than 50 kPa) is the friction on the surrounding steel surface which counteracts the swelling. This, however, is conservative with respect to consequences of resolving the issue since the expected swelling pressure in in-situ condition should be higher. The ratio between the free area with possible friction and the cross section of the swelling is largest in Test Type 2 and least in BB test, see Figure 5-53. The expected mechanical pressure from the distance blocks after wetting is probably a couple of hundred kPa but in order to be completely sure of the level, more tests are needed.

- **Time dependence**. There was no indication in any of the test types that the pressure would decrease markedly by time. However, in Test Type 1, W210, a very small decrease with time was seen. The BB test was running for about 500 days and during this time there were no evident indication that the pressure against the rock would decrease. The radial pressure was measured in two points, top and bottom which showed that there is some homogenization of the bentonite. The pressure measured at the bottom decreased during 300 days from a peak value of 700 kPa to 500 kPa but during the same time the pressure measured in the top increased from 300 to 450 kPa, see Figure 5-55.
- **Cracking**. The tests have also shown that there probably will be cracks present in the bentonite; see Figure 5-57. Especially in the small scale a lot of cracks have been seen. The cracking and desiccation can, however, be part of the process that generates mechanical pressure on the rock surface.

It is judged, that the test produces smaller swelling pressures than would be the case under in situ conditions. With access to additional water from the rock matrix, even small amounts, the swelling pressure or mechanical pressure from the bentonite will be guaranteed. A number of uncertainties regarding the issue are identified:

- **Time dependence**. The main uncertainty with the rock spalling issue is the time dependence. The laboratory tests have shown that using the technique with artificial water-filling of the slot in the DAWE design will give a mechanical pressure against the rock for a long time (500 days test duration) and there is no clear indication that the pressure would decrease with time. The problem with thermally induced spalling of rock will, however, be present for a very long time (Lönnqvist and Hökmark 2007). In order to better understand the bentonite behaviour during these special conditions i.e. a water-filled slot and no access to additional water, FE-modelling of the performed tests is desired.
- **Friction**. Friction seems to have influenced the test results. This makes the comparison between the different test series difficult. However, with no or less friction towards the boundary surfaces the measured stresses would probably have been the same or larger.
- **Swelling pressure**. The tests have shown that the method with artificial wetting will result in a swelling pressure of between 50–500 kPa against the rock. If this pressure is high enough to prevent rock spalling is, however, a rock mechanical issue.
- **Different sections**. The performed tests have simulated the sections with distance blocks. The buffer behaviour in Supercontainer has not been investigated.
- **Thermal effect**. The performed tests have been made without any increase of the temperature. An increase of the temperature will have an effect on the hydraulic conductivity but the effect on the swelling pressure is insignificant.
- **Salt content in water**. The performed tests have been made using water with a salt content between 1 and 3.5%. Salt in the water increases the hydraulic conductivity and also affects the swelling rate. At the same time it decreases the swelling pressure at low bentonite densities (which will occur during the swelling and filling of the empty slot). The erosion tests performed and reported during the project phase showed that regarding erosion and pipe removal issues it could be favourable to use fresh-water for artificial water filling. This may, however, delay the swelling pressure development. The final design of all components may be done when all critical issues are solved.

Test relevance with respect to the repository case

The laboratory tests have provided data concerning buffer behaviour like the evolution of buffer swelling pressures in different groundwater conditions – with different salt contents and with different slot dimensions. There are indications that the results are conservative due to the test arrangements like friction towards the boundary surfaces in the test cells affecting the swelling pressures. The results present the minimum magnitudes of the mechanical pressures against the drift wall. In the real repository case the magnitudes of the swelling pressures will be higher due to the smaller friction effect. The higher swelling pressures have positive implications on the friction against axial displacement but also on rock spalling.

Besides adding understanding about the buffer behaviour in the 3H variant the test results have given a basis for the design of the buffer components inside the Supercontainer and the distance blocks. The laboratory tests form a chain starting with small-scale tests before entering next phase with bigger scales, large scale and/or full scale, in a stepwise manner. Future tests are described in Section 5.9.

5.9 Remaining buffer/design issues and future buffer work

A number of critical issues have been investigated within the KBS-3H project. Some issues or uncertainties have been solved but there are still some issues that need to be addressed and new issues have been identified.

Remaining buffer issues including filling component issues that have been identified as important will be addressed in the next project phase with large- or full-scale tests but also with laboratory tests and scoping calculations.

Swelling pressure in dry and wet drift sections

Swelling pressure of the buffer exerted on drift surface has an important function to mitigate rock spalling. In dry drift sections and insections, where there is limited access to water to cause any additional swelling besides that created by the artificial water filling; water transport could affect bentonite saturation/swelling pressure. The understanding of drift system behaviour still needs efforts due to uncertainties involved in e.g. swelling of buffer and filling components to seal the voids in the drift and to prevent spalling of rock in dry sections.

In the current project phase BBtests using Supercontainer block type of bentonite have been performed simulating dry drift conditions. The magnitude of the swelling pressure and the time between the installation and when the buffer inside a Supercontainer generates a sufficient swelling pressure and tight contact against rock is still uncertain. This uncertainty applies particularly distance blocks, which have lower density and higher water content (c. 21%) than was used in the performed BB-test with Supercontainer type of bentonite (water content about 10%).

The identified studies that should be included in future studies are related to the performed tests in the current project phase and would complement them. Similar tests are planned to be carried out with Supercontainer type of bentonite both in dry as well as wet conditions including access to additional “inflow” water. These tests are of importance for the long-term safety to ensure the early evolution of the bentonite swelling towards the fulfilment of the performance requirements including both the rate of pressure increase and swelling of bentonite through the perforated Supercontainer shell and the pressure magnitude on the upper rock wall surface in the drift where rock spalling could occur. Additional test is planned using distance block type of bentonite to confirm the rate of swelling pressure increase in dry and wet conditions.

The early evolution of the swelling pressure will also be studied in the large-scale demonstration test called Multi Purpose Test, “MPT” included in the EC LucoeX project at the Äspö HRL during the next project phase, see Section 7.2.2. Besides the demonstration of emplacement of some drift components proposed as a part of an international project MPT includes several more detailed investigation objectives (e.g. homogenization of bentonite). This experiment has been proposed to be started by pre- modelling of some BB test that presents a well defined situation which will occur during the water filling process in DAWE design. This would increase understanding regarding swelling of unsaturated bentonite.

Spalling of rock

Evaluation of thermal spalling of rock for Olkiluoto will be updated with the input data from ongoing POSE-experiment at ONKALO. The rock spalling experiment (POSE) in the ONKALO is designed to establish the spalling strength of the *in situ* rock, in addition to a more reliable estimation of the *in situ* rock stress field and to understand the type of rock spalling that may occur in both designs (KBS-3V and KBS-3H).

POSE – experiment is similar to those rock spalling experiments performed earlier at Äspö (APSE and CAPS) and URL tailored to the Olkiluoto rock conditions.

Mechanical erosion of buffer

Mechanical erosion at very low flow rates in the form of internal piping is not well known and would also require information on the expected length of dry sections. The process of piping is not well understood and therefore the transient flow conditions for evaluating mechanical erosion are uncertain and should be defined. The possible process of long lasting pulsating flow seems to be unique to KBS-3H when compared to KBS-3V alternative.

Homogenization of buffer

The issue of homogenization of buffer after erosion must be considered as remaining unresolved. Efforts in terms of improving the material models and improving the calculation technique will need to be made in the coming years in order to address this issue conclusively.

Water transport

The transient behaviour, especially water absorption rates with respect to time is currently not well specified and there is no experimental information available on this. Main issues in the work are to increase understanding of the process of internal piping and erosion rates and to get representative estimates for the time period required to reach the fulfilment of the performance requirements. Improvement of conceptual understanding of the water transport process is required for the development of modelling techniques.

The issues will be addressed e.g. by small size experiments to study desiccation, piping and erosion followed by long experiment (8 m) at 1:10 scale representing heterogeneous inflow including erosion measurements. Whether buffer in a Supercontainer can “steal” water from distance blocks and would they then lose their function (support/counter pressure) will be addressed experimentally.

Impact of rock shear on a KBS-3H canister

The objective is to study the KBS-3H specific case of compression shear that has not been modelled before. An earthquake always means a shear direction that lifts the surface. This means that for KBS-3V one always gets “tension shear” for the canister, while in KBS-3H this corresponds to compression shear. The influence of this difference will be investigated by modelling and calculations. The Supercontainer shell of titanium will be used in the work.

Detailed studies on the impact of titanium on the buffer

The studies during the earlier project phase indicated that Ti would be the least harmful material for the buffer bentonite. Some preliminary tests with Ti confirmed that the reactivity will be low, though there were some technical problems in the set-up of the system studied. An improved set-up and more detailed analyses of possible reactions with clay is suggested for the next project phase in order to evaluate and confirm the possible interaction with the clay and formation of possible reaction products.

Chemical erosion (new issue)

The chemical erosion of buffer caused by dilute groundwater is an important process, which has been studied within KBS-3V project. Consequently this issue has not been covered in this report by KBS-3H project but due to its potentially significant impact on the design of KBS-3H repository system it will be addressed in the next project phase by both projects in co-operation.

The studies also include the impact of post glacial erosion specifically on KBS-3H, but also in co-operation with KBS-3V project.

Self sealing of fractures (new issue)

Self sealing capacity of pellets using different fracture apertures will be addressed in a test that has been earlier used to study erosion and homogenization of filling components in case of a leaking fracture . This issue is related to erosive transport of buffer out from the drift system, which would be an issue if a leaking fracture leads from the drift into an open tunnel and self sealing of fractures with bentonite does not function as assumed. There are test results with the compartment plug and pellet filling on the sealed side of the plug from the current project phase that is in line with this assumption. This issue will be studied with laboratory tests.

The effect of buffer axial displacement on buffer density (new issue) has been assessed to have an insignificant impact. The result of scoping calculations by Gribi et al. (2007) was that this issue has less impact in the DAWE design, because all gaps are artificially filled with water, the gaps will be closed due to swelling of buffer so that there will be no empty space available for axial displacement. In addition there will be no axial forces due to simultaneous water filling in the whole compartment that could cause axial displacement. However, the conclusion was based on assumption on the compaction forces and number of affected Supercontainer sections. In order to make more accurate estimates, more detailed data of dry drift section lengths and mechanical behaviour of desiccated buffer is needed. This would require more detailed geohydrological information, additional laboratory determinations on properties of desiccated buffer and likely experimental work. This issue is related to the process of water transport along the drift.

Mechanical erosion and homogenization of filling components (new issue)

The design of filling components has been introduced in the current project phase. Issues regarding the erosion resistivity and homogenization will be addressed in the next project phase via modelling work, scoping calculations and experimental work. The studies on the erosion resistivity of the filling component material will be focussed on those components placed in the inflow points. The transition zone (see Section 4.6) behind the plugs will be tested in connection with the Multi Purpose Test at Äspö.

Rock mechanical analysis on drift plug (new issue)

In addition to the stress due to the drift plug, in situ and excavation (drift, V-shaped notch) induced rock stresses and thermally induced stresses have an impact on the adjacent rock mass. The impact of all loads acting on nearby rock will be studied in the next project phase with a rock mechanical analysis. The analysis will also be used to define the minimum distance between the plug and the drift entrance.

Properties of isostatically/uniaxially compressed blocks (new issue)

With reference to the Section 4.5 there is a need to optimise the size of buffer components with respect to compaction technique. Isostatic compaction technique enables manufacturing of larger buffer block sizes. There are also indications that the behaviour of the isostatically compacted blocks is different from that of uniaxially compacted blocks and should therefore be studied. This may be caused e.g. by internal stresses induced by compaction. The objective is to determine the possible differences in the block properties using standard tests. This issue is common for KBS-3V/KBS-3H and the work will be carried out in co-operation between the projects.

Design basis or design premises

A report will be compiled to include the design basis and justifications for the set design basis for the KBS-3H design. This document should specify all the requirements related to the design that should be taken into account in the planning of experiments and evaluations of the performance of the drift. The design basis refers to the current and future environment-induced loads and interactions that are taken into account in the design of the disposal system, and, ultimately, to the requirements that the planned disposal system must fulfil in order to achieve the objectives set for safety and other factors. As part of the work, the viability of "one compartment plug" vs double compartment plug section concept should be assessed from safety point of view. The design of filling components is based on assumptions on buffer homogenization and mathematical calculations. These include uncertainties, which need to be resolved.

Performance of the whole drift (new issue)

There is a need to evaluate the behaviour and performance of the whole drift system including all functional components. This would be accomplished by considering the inflows along the drift and the total inflow into one drift and by assessing how the system performs and evolves at drift-scale from the initial state until the desired fulfilment of the performance requirements have been reached. This means a performance assessment should be done by taking into account the evolution of system during transient phase and THMC processes acting in the drift and based on the latest design and layout. This should be based on information available for the design, design basis/design premises and all results of the buffer and filling component studies on laboratory and field scale, and modelling of the processes affecting the evolution of the system.

Drift utilization degree based on site-specific fracture data will be evaluated (new issue)

Drift utilization degree was studied merely qualitatively in the Section 4.6 "Conceptual design of filling components" and in the future work this issue will also be addressed quantitatively.

6 Selection of main design alternative

The decision for the reference design was needed to define a clear way forward for the KBS-3H development. The selected design alternative, the reference design, will be used as the basis for further technical development, planning, safety analysis, radiation protection and work on environmental influence. Eventually a detailed comparison and selection between the selected KBS-3H design and KBS-3V will be made.

Two designs have been evaluated in the current project phase, STC and DAWE. When comparing the two designs, their respective ability to fulfil the requirements has been evaluated.

6.1 Requirements specific to the buffer

The requirements specific to the buffer have been presented in Section 3.3.4 and 3.3.5. In the following the evaluation is given how the two design alternatives meet the requirements.

The requirement of buffer to reach the target density with the allowed density range being 1,950–2,050 kg/m^3 is the most central requirement in the comparison between the two alternatives. The risks mainly concern loss and redistribution of buffer mass due to mechanical erosion caused by inflow water, internal piping and buffer exposure time to high humidity. Too low buffer density at the buffer-rock interface will also result in a low counter pressure against spalling of rock.

6.1.1 STC design

For STC design the most significant uncertainties are related to the potential loss and redistribution of buffer mass by mechanical erosion. The processes such as piping and erosion related to water inflow into a Supercontainer section may lead to unacceptable reduction in buffer density during the installation and water filling and saturation phases. During the water filling period, the length of which depends on the inflow rate into the drift and on the locations of the inflow points, water will flow from wet sections to dry sections. A dry section is defined as a section where the inflow is equal or less than what the buffer can absorb over the length of a Supercontainer section. The inflow criteria is not known quantitatively but estimated roughly to be of orders of 24 ml/min (equal to 1.4 l/h). Any eroded material will thus be transported from the wet parts to the dry parts. An extreme situation is if all water flow enters only one section and the other sections are dry, which yields a rather significant flow and erosion from the wet section. This could lead to unacceptable amount of eroded bentonite in a Supercontainer section and to the rejection of the drift. Since water inflow cannot be stopped, but piping always occurs with channel formation and subsequent erosion of bentonite in the channel, water inflow and erosion will continue until the empty slot between the rock and the bentonite is filled with water.

An obvious problem was detected in the bentonite block behaviour during a test with water filling of a Supercontainer section. The test was performed using water with a salinity of 3.5%. The water flow rate was set to 0.002 l/min in order to fill the section in 10 days. During the erosion test of STC it was found that at slow inflow rates gel could be formed that stopped piping and instead caused separation of water and gel, creating a water filled pockets and squeezing of the gel between different Supercontainer sections leading to a redistribution of the installed bentonite, which can be very large. This may lead to unacceptable reduction in buffer density during the installation and water saturation phases. The problems with bentonite block cracking and moving of gel were severe and are of course unfavourable for the STC design. The large cracking and the fact that the blocks fell apart will of course lead to a more inhomogeneous density distribution. Only one test was, however, performed and the uncertainties are still large regarding this issue. Erosion in STC caused by inflows has been described in Section 5.2.

In STC design alternative the buffer exposure time to high humidity with very little inflow can be very long resulting cracking of bentonite and redistribution of bentonite within the Supercontainer sections.

6.1.2 DAWE design

For DAWE design alternative the overall conclusion from the studies that have been carried out is that mechanical erosion of bentonite due to inflow is most likely not a problem when applying the artificial water filling. Artificial water filling after installation phase of a compartment provides development of full hydrostatic pressure in the entire drift compartment reducing the pressure gradient between rock mass and the drift and thereby limiting substantially the inflow into the drift. The artificial water filling of the compartment provides uniform and simultaneous bentonite swelling minimizing the risk of bentonite piping and erosion as well as displacement of distance blocks and Supercontainers.

Mechanical erosion of bentonite due to water filling process using short water filling pipes has been tested (Section 5.3) and the results show that the artificial water filling itself does not lead to critical erosion or subsequent redistribution of buffer within the drift compartments. This is due to the beneficial advantage with the artificial water filling that the salt content of the water that the compartment is filled with can be selected. The studies have shown that using fresh water (tap water) is favourable contributing to acceptable level of mechanical erosion during water filling of a compartment in DAWE design. It is preferred that fresh water is used since the erosion rate is lower and the internal redistribution of material is smaller compared to the case when salt water is used.

The main uncertainty regarding the erosion issue in DAWE is the buffer exposure time to high humidity. The rather short installation time, approximately one week, for filling one compartment with Supercontainers and distance blocks will most likely not affect the buffer in a critical way. However, if problems would occur during the installation phase the amount of eroded material will increase due to the prolonged exposure to high relative humidity.

The ring shaped buffer material in Supercontainers will have water content of about 11% and the solid blocks about 17%. The buffer blocks (mainly the ring shaped ones) inside the Supercontainer surrounded by perforated shell will absorb water rather fast and the surface of the blocks will start to crack. To mitigate cracking the section should be water filled as soon as possible, which can be accomplished with certainty only with artificial water filling according to DAWE design alternative.

6.2 Requirements on the buffer/rock interface

An important requirement deals with the development of sufficient buffer swelling pressure in the distance blocks and Supercontainer sections after installation phase. A sufficient swelling pressure to prevent the rock surrounding the deposition drift from spalling due to increased temperature must be established sufficiently promptly, see Section 3.3.4. This design requirement that is supporting the long-term function has been studied in different scales in laboratory conditions to determine the early evolution of buffer swelling pressure and the conclusions are given below.

The main uncertainty that is not fully solved is how high the counter pressure must be in order to prevent spalling of rock but also how fast the counter pressure has to be reached to prevent/to mitigate thermal spalling of rock. The consequences of rock spalling extending over several Supercontainer sections was not studied with safety assessment but it will be addressed in the future work.

The strict requirement for very limited disturbance to the buffer/rock interface adjacent to the distance blocks, which have the safety function of separating the Supercontainers hydraulically, in addition to the other safety functions of the KBS-3H buffer, is also affected by the bentonite swelling process. There is also a requirement that disturbances to the buffer in the vicinity of the Supercontainers should extend to only a limited radial distance inwards towards the canisters from the buffer/rock interface, such that the remainder of the buffer between the canister and the rock continues to perform its safety functions, and has a thickness of at least a few decimetres. In the current design, the distance from the canister surface to the drift wall is about 0.4 m, see Section 3.3.5.

6.2.1 STC

Thermally-induced spalling of the rock during the thermal period may take place in dry deposition drift sections in all design variants, but especially in the case of the STC design alternative in drift compartments that are relatively dry. This is due to the slot between the drift wall and the buffer being open for a very long time in dry conditions.

With the maximum allowed water inflow into one Supercontainer section (0.1 l/min) the filling time of the empty space would be about 20 days. After this time the water/gel will start to leak over to the next section. In dry drift sections the filling time could be much longer than 20 days depending on the flow rate. Due to uneven distribution of inflow locations in a drift especially those sections situated upstream behind the inflow points (the drift descends slightly towards the entrance) can remain unsaturated and the buffer swelling against the drift wall develops very slowly. There is a concern that thermally-induced spalling of rock at the top of the drift could lead to connected pathways for flow and mass transport along the drifts extending over several Supercontainer sections, which is considered as a critical factor against STC design alternative.

6.2.2 DAWE

The results from the tests carried out (Section 5.8) indicated that the thermally induced rock spalling issue can be mitigated or limited with DAWE design due to accelerated swelling after artificial water filling of the open slot between the rock surface and the buffer components simultaneously in the whole compartment.

All three test types (in different scales) carried out have shown that in spite of having no access to additional water, only what has been filled in the slot, a significant mechanical pressure (50–500 kPa) was acting on the “rock” surface throughout the entire test durations. A negative factor for the swelling in the laboratory tests is the friction on the surrounding steel surface which counteracts the swelling. This, however, is conservative with respect to consequences of solving the issue since the expected swelling pressure in in-situ condition should be higher. A significant mechanical pressure (400–500 kPa) was developed on the “rock” surface after a 500 day long test. The BB-studies have so far been done with Supercontainer block type of bentonite without perforated shell but similar tests are planned to be conducted in the next phase with the distance block type of bentonite, see Figure 5-51. The expected mechanical pressure from the distance blocks after water filling is estimated to be a couple of hundred kPas.

What was also demonstrated in the tests was that in DAWE design the swelling pressure of the buffer cannot only provide significant mechanical pressure (50–500 kPa) acting on the drift wall throughout the entire test duration but also that there was no clear indication that the pressure would decrease with time. It is judged, that the test produces smaller swelling pressures than would be the case under in situ conditions with access to additional water from the rock matrix, even small amounts, the swelling pressure or mechanical pressure from the bentonite will be guaranteed.

The performed tests have been made without any increase of the temperature. An increase of the temperature will have an effect on the hydraulic conductivity but the effect on the swelling pressure is insignificant.

The performed tests have been made using water with a salt content between 1 and 3.5%. Salt in the water increases the hydraulic conductivity and affects also the swelling rate. At the same time it decreases the swelling pressure at low bentonite densities (which will occur during the filling and swelling of the empty slot). Only DAWE design alternative enables the selection of water type for the artificial water filling phase where one alternative is to use fresh water. The use of fresh water increases swelling pressure at low bentonite densities like in the slot between buffer and the drift wall.

6.3 Additional requirements from an operational point of view

6.3.1 STC

In STC sealing rings will be placed for each Supercontainer section during the installation phase. The wetting of buffer will take place by natural groundwater inflow into the deposition drift. However, before full water saturation has occurred the inflowing water may cause detrimental effects on the buffer material especially in the case of large water inflow rates into a Supercontainer section. The water inflow into the Supercontainer section and past the distance block cannot be stopped due to the high water pressure, which means that water will continue to fill up the section and also the other sections in the drift until either a high swelling pressure or a high water pressure is formed that can prevent further water inflow.

The sealing technique (sealing rings) has not yet proven to be feasible from both operational and functional point of view. It may introduce operational risks such as uncontrolled water flows past the seals, which may cause additional operational actions such as rapid plugging. Additionally the behaviour of the sealing ring design component and the possibility of encountering detrimentally high hydraulic pressures because of rapidly sealing distance blocks have not been evaluated.

In STC the criterion for allowable flow from the inner Supercontainer sections to the section under installation has been set to zero, i.e. no outflow is allowed during installation. Knowing the inflow distribution, the geometry and the installation rate the time and location where this occurs can be calculated and a temporary plug installed if the water filling rate is higher than installation rate. This alternative does not allow very much of disturbance in the installation timetable and there remains a risk that the water flows into a section that is under installation.

Additionally trapped air inside the system could potentially have severe implications on the feasibility of the STC design.

6.3.2 DAWE

For DAWE design alternative water inflow during installation does not cause problems due to drainage along the drift floor, which descends slightly towards the entrance.

In DAWE a new water filling technique with short pipes was developed and found feasible. This would leave just one long pipe, the air evacuation pipe, to be removed, which would speed up the pipe removal process considerably. The pipe removal of artificial wetting and air evacuation pipes is of critical importance to the DAWE design. Due to long-term safety reasons the pipes cannot be left in the drift. The conclusion from the performed studies is that both the short wetting pipes as well as the long air evacuation pipe can easily be removed in a feasible timeframe i.e. within the first day after wetting. Pipe removal is deemed not to be a critical issue, see Section 4.3.5.

6.4 Initial state

For the safety assessment it is vital that the initial state of the engineered barriers is well defined and that the evolution after the transient phase reaches the fulfilment of the performance requirements. The initial state in time may differ for different locations (drift compartments) of the system and there is no obvious definition for the system as a whole. Deposition and building of the drift plug may be the natural starting point for the engineered barrier system, and in DAWE the subsequent artificial water filling ends the man-made actions. With this definition, at least for a comparison point of view, it is clear that DAWE presents a better defined initial state than STC which fully relies on natural inflows for both initial and long-term buffer saturation. For DAWE initial swelling of the buffer is guaranteed by the artificial water filling, the buffer and canisters are locked in place and axial displacement and significant buffer erosion can be avoided. Altogether DAWE is a more robust design with very much lower risk of problems resulting in an initial state outside the design requirements. This is very important regarding the evolution after the transient phase and reaching the fulfilment of the performance requirements.

6.5 Selection of DAWE as main design alternative

The design alternatives are equal in many aspects but that DAWE has important advantages in some important aspects.

When summarising the aspects presented above it is clear that DAWE presents a robust design with very much lower risk of problems resulting in an initial state outside the design requirements. The evolution of DAWE alternative from initial state to fulfilment of the performance requirements is adequately understood to ensure that the fulfilment requirements will be attained with high confidence. Both of these issues are opposite for STC alternative. Therefore the clear recommendation can be made that DAWE would be the KBS-3H reference design. The reference design is valid from the time when decision is taken until it is superseded by a future design option.

Table 6-1 Comparison between DAWE and STC based on the critical design and long-term requirements.

Requirement	Alternative 1 DAWE	Alternative 2 STC
Requirements on rock volumes for drift construction and canister emplacement. See Section 3.3.1.	Requirements expected to be fulfilled at both Forsmark and Olkiluoto. See Section 3.3.1.	Requirements expected to be fulfilled at both Forsmark and Olkiluoto. See Section 3.3.1.
Requirements common to all engineered components. See Section 3.3.2.	Requirements expected to be fulfilled; DAWE has the addition of leaving an end section of the evacuation pipe in the rear part of each compartment, which is deemed to be insignificant. See Section 3.3.2.	Requirements expected to be fulfilled; STC has the addition of leaving the sealing rings. See Section 3.3.2.
Requirements specific to the canister. See Section 3.3.3.	Requirements expected to be fulfilled (The same canister design as in 3V). See Section 3.3.3.	Requirements expected to be fulfilled (The same canister design as in 3V). See Section 3.3.3.
Requirements specific to the buffer. See Section 3.3.4.	Requirements expected to be fulfilled. See Sections 5.3, 5.4 and 6.1.2.	Could have difficulties in fulfilling the requirements. Cracking and moving of bentonite together with erosion cannot be excluded. See Sections 4.1.2, 5.2 and 6.1.1.
Requirements in the buffer/rock interface. See Section 3.3.5.	Requirements expected to be fulfilled. Counter pressure obtained by artificial wetting preventing/mitigating spalling of rock. Initial state better defined. See Sections 3.4.4, 4.10, 5.8, 6.2.2, 6.4 and 9.2.3.	Could have difficulties in fulfilling the requirements. In long and dry drift sections rock spalling could be continuous through several Supercontainer sections. See Sections 4.1.2 and 6.2.1.
Requirements on auxiliary components. See Section 3.3.6.	Requirements expected to be fulfilled; DAWE has the addition of leaving the drift end pipe, which is deemed to be insignificant. See Section 4.10.3.	Requirements expected to be fulfilled; STC has the addition of leaving the sealing rings. See Section 4.1.2.
Requirements from an operational point of view. See Section 3.4.	Requirements expected to be fulfilled; DAWE has the additional work with pipe removal. See Sections 3.4.2, 4.9. and 6.3.2.	Requirements expected to be fulfilled; STC has the additional work with sealing rings. See Sections 4.1.2 and 6.3.1.

7 Assessment of long-term material-buffer interactions

7.1 Introduction

Different structural components are planned to be used in the KBS-3H deposition drift (see Chapter 4). Early in the KBS-3H development programme, it was already recognised that the physical and chemical effects of the corrosion products of the Supercontainer made of carbon steel need to be evaluated. The main issue noted was the possible alteration of bentonite and loss of boundary transfer resistance between the buffer and the fracture in the host rock due to the interaction of iron from the Supercontainer with the bentonite buffer (Smith et al. 2007a). One of the main concerns noted by the authorities, STUK and SSM, in their review of the KBS-3H safety assessment was the impact of iron and its corrosion products on the performance of the buffer.

Several metallic materials could be used to replace the steel in Supercontainers with the presupposition that they comply with the required strength and long-term safety requirements. The first preliminary evaluation of the long-term safety aspects of nickel and titanium based alloys done during the earlier project phase indicated that both of the alloys considered appear to have advantages with respect to carbon steel in terms of lower corrosion rates and lower production of hydrogen gas. Of these alloys the greatest probability of bentonite alteration appears to result from Ni (II) whereas the impact of titanium on bentonite is expected to be minimal and it was recommended that titanium should be considered further as an alternative material for the Supercontainer and associated metal components. Further evaluation on the long-term impact of titanium is, however, warranted. Copper was also considered and it was concluded that copper alloys would require redesign of the Supercontainer and definitely increased material thicknesses due to the limitations in strength compared with the existing material. Copper was also considered not to be a potential alternative for other design components such as the compartment plug. However, it was suggested later on in the Complementary studies of horizontal emplacement KBS-3H 2008–2010 phase to include copper as an alternative material and summarise the current knowledge about the corrosion and migration properties of Cu and its corrosion products and also the potential impacts on the performance of the buffer.

The objectives of this chapter are:

- to present the main findings based on the long-term studies on iron-clay interaction and updated reactive transport modelling of iron-clay interaction,
- to summarise the information available on copper corrosion and possible interaction with bentonite,
- to present the main findings from first Ti-clay studies,
- to evaluate the consequences for long-term safety of the hydrogen gas produced in corrosion of the materials, and
- evaluate the consequences of a perturbed buffer-rock interaction on the long-term safety.

Finally the pros and cons of the alternative materials with focus on long-term safety aspects are summarised and a suggestion for the material to be used in future design is made.

The evaluation presented in this chapter focuses on the Supercontainer since it is the KBS-3H specific component (compared with the reference design, KBS-3V) which will have the greatest influence on long-term safety in a KBS-3H repository. It is closest to the canister and will also represent the main part of the KBS-3H additional components.

There is no required safety function of the Supercontainer shell and therefore the only assessment that needs to be made is related to how the Supercontainer shell affects the bentonite with respect to its desired long-term performance (see chapter 4).

7.2 Evaluation of materials

7.2.1 Studies of Cu-clay interactions

In this chapter, a review study (King and Wersin 2013) on interactions between a copper Supercontainer shell and the bentonite buffer is summarized. Moreover, copper corrosion rates derived from Cu profiles in a long-term experiment (Kumpulainen et al. 2011) are reported.

Review study

In the first part of the study, the corrosion behaviour of the Cu shell is presented and discussed. The second part focuses on Cu-clay interactions and their potential effects on the bentonite buffer. The overall effects are then discussed and compared with the behaviour expected for the copper canister.

It has to be noted that the boundary condition for the copper corrosion of the Supercontainer shell is different from the canister surrounded by the high density bentonite buffer. The corrosion agents such as sulphide in the groundwater have a much easier access to the Supercontainer shell than to the canister.

Copper corrosion strongly depends on the redox conditions in the near-field. Initially, *oxic conditions* will prevail and the Cu material will corrode to Cu (II) species due to reactions with residual molecular O_2 trapped in the pores of the buffer and the gap between the buffer and the rock. The corrosion rates will be rather high (of the order of 10's of μm/yr initially) and depend, besides O_2 levels, on chloride concentrations in the groundwater decreasing with increasing Cl concentrations. The total amount of corrosion during the aerobic phase is determined by the amount of atmospheric O_2 trapped initially in the repository. During the oxic period the initial oxygen present in the buffer surrounding the canister and in the gap between the shell and rock will corrode a maximum of 70 mol of copper (0.4% of the total mass of the shell). Upon depletion of the residual O_2, anaerobic conditions will be established leading to an entirely different corrosion behaviour. The corrosion rate will decrease and in the reducing conditions the main corrosion agent will be sulphide derived from the groundwater or from the buffer. High chloride concentration in combination with very low pH could cause copper corrosion in oxygen-free water. However, since deep groundwaters are neutral or slightly alkaline, and the buffer capacity of the bentonite and the rock counteracts acidification, dissolved sulphides are, in practice, the only corrosive substances that can react with the copper shell after the oxygen in the repository has been consumed. Moreover, a further sulphide source induced by microbially-driven sulphate reduction at the buffer/rock interface cannot be ruled out. Under these conditions, copper sulphide (Cu_2S) will be formed and Cu (I) species will predominate, and also hydrogen gas is formed.

Microbial activity in the buffer will initially be limited by the availability of organic material in the buffer and when this is depleted, by the availability of methane, hydrogen, etc, in the groundwater. The availability of methane, hydrogen, etc, in the groundwater will also limit the microbial reduction of sulphate outside the buffer. Thus the hydrogen produced by corrosion of the Supercontainer Cu shell may act as a source for microbial reduction of sulphate (see also section 6.4).

On the basis of literature data and site-specific information corrosion rates for Olkiluoto and Forsmark conditions for the *anaerobic conditions* after oxygen depletion were estimated as summarized in Table 7-1. This highlights that initially Cu shell corrosion rates at closure after oxygen depletion are estimated to be similar for both sites. At the sulphide level expected at Forsmark the corrosion rate for the Cu shell is low. But due to the conservatively estimated higher sulphide levels at Olkiluoto, higher long-term corrosion rates are expected. The pessimistic highest corrosion rates would occur for the sulphide concentrations of about 12 mg/l based on the highest sulphide concentration measured at Olkiluoto (Posiva 2009).

In SR-Site it is assumed that corrosion of the canister by sulphide is *instantaneous*, which means that corrosion is entirely determined by the i) content of sulphide in the groundwater and ii) the transfer (mass balance) of sulphide from the groundwater to the canister surface. In case the buffer is intact, mass transfer is by diffusion and the resulting corrosion will never lead to canister failures, regardless of the sulphide levels. However, in SR-Site it is concluded that for high flowing canister positions loss of buffer due to dilute groundwater composition cannot be excluded. In this case mass transfer is determined by groundwater flow in the deposition hole (deposition location for KBS-3H)

Table 7-1. Estimated upper Cu shell steady-state corrosion rates for realistic (high) buffer density and conservative (low) buffer density.

	Olkiluoto		Forsmark	
	At closure after oxygen depletion	After 10,000 yr	At closure after oxygen depletion	After 10,000 yr
HS^- concentration (mol/L)	$2 \cdot 10^{-5}$	$3.6 \cdot 10^{-4}$	10^{-5}	10^{-5}
Total steady-state sulphide corrosion rate of copper Supercontainer shell (µm/yr) at buffer density 2,000 kg/m^3	$6.4 \cdot 10^{-4}$	0.0085	$4.1 \cdot 10^{-4}$	$4.1 \cdot 10^{-4}$
Total steady-state sulphide corrosion rate of copper Supercontainer shell (µm/yr) at very low buffer density	0.10	1.8	0.058	0.058

and the sulphide content in the groundwater. Furthermore, since the origin of elevated sulphide levels in some groundwater samples is unclear (both at Forsmark and Olkiluoto) the sulphide levels are uncertain.

The corrosion behaviour of copper can be interpreted in terms of thermodynamic relationships in the Cu-Cl-S-CO_3-H_2O system. As indicated from the stability diagram (Eh-pH diagram) shown in Figure 7-1, under oxic conditions both Cu(I) species, in the form of Cu_2O and dissolved $CuCl_2^-$, and Cu(II), in the form of solid CuO or $CuCO_3$ and dissolved Cu^{2+}, are thermodynamically stable at various pH and redox potentials. Under anoxic conditions, metallic Cu is stabilized, except in the stability field of copper (I) sulphide (Cu_2S). In this stability domain, the concentration of soluble Cu (I) sulphide is low.

The higher calculated corrosion rate at Olkiluoto is caused by a much higher assumed sulphide content at Olkiluoto compared to Forsmark.

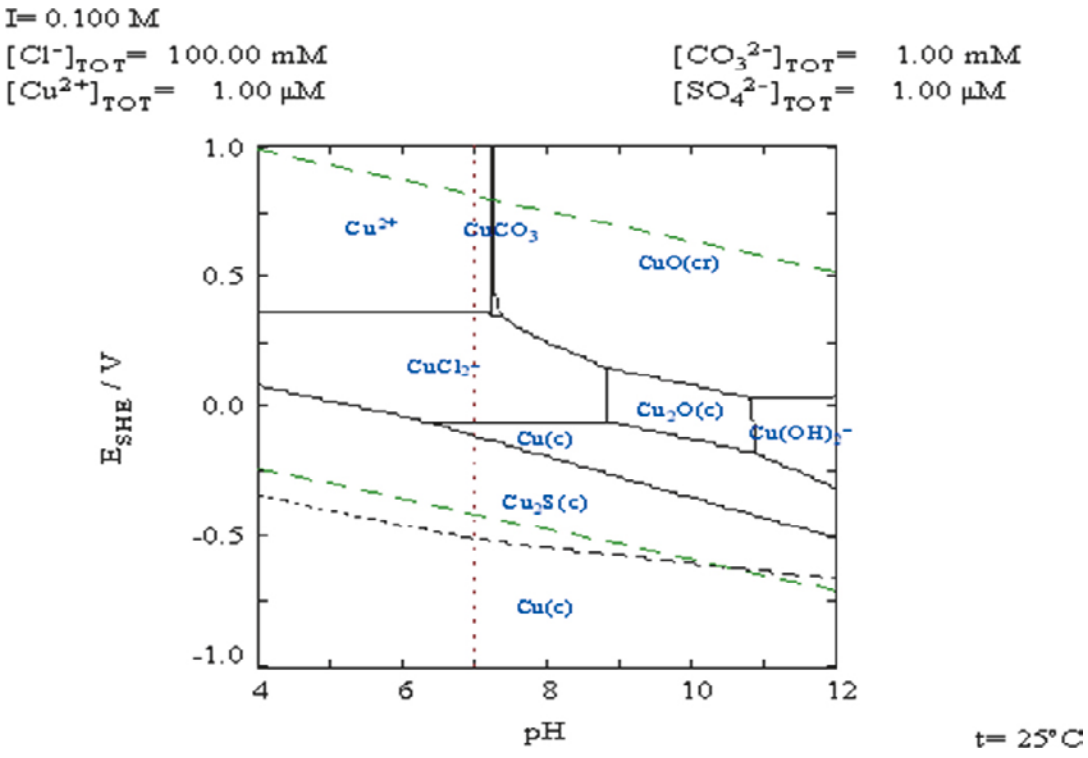

Figure 7-1. *Pourbaix diagram for the Cu-Cl-S-CO_3-H_2O system constructed with the program MEDUSA and HYDRA (database for Cu species from Puigdomenech and Taxén 2000).*

The interaction processes between corrosion-derived Cu and the bentonitic clay can be assessed by various means. From the evaluation of diffusion-type studies a contrasting behaviour for Cu (II) and Cu (I) can be deduced as illustrated schematically in Figure 7-2. At high dissolved O_2 concentration and/or low Cl^- concentration, dissolved copper exists primarily in the Cu(II) oxidation state. Cupric species are strongly adsorbed by the clay, resulting in high interfacial total copper concentrations and short, steep concentration profiles. The total copper concentration shown in Figure 7-2 is the sum of the dissolved, precipitated, and adsorbed copper. Conversely, at low $[O_2]$ and/or high $[Cl^-]$, the Cu (I) oxidation state is stabilised, in the form of dissolved $CuCl_2^-$ species. Being an anion, the $CuCl_2^-$ is not strongly adsorbed and diffuses relatively rapidly through the bentonite, resulting in the extended copper concentration profiles in Figure 7-2 (b).

The strong affinity of Cu (II) to the smectite mineral surface is confirmed by numerous sorption studies. Spectroscopic data indicate covalent binding of Cu (II) at edge surface sites. Under thermal treatment (T > 200°C) Cu(II) is incorporated in the interlayer structure (mainly in hexagonal cavities) which, at high Cu(II) loadings has a strong impact on the bulk properties of bentonite and leads to significantly reduced swelling capacity. The relevance of this process for KBS-3H type conditions is considered to be small in spite of remaining uncertainties with regard to long-term effects. The impact of Cu (II) on the buffer was estimated from simple diffusion-retardation considerations and the total amount of available residual O_2. Thus, a diffusion distance of 2–6 cm into the buffer was deduced. The amount of Cu(II) taken up by the clay in this zone was estimated to be rather small compared to its cation exchange capacity.

The interactions of Cu (I) with the clay are much weaker than those of Cu (II) species. This is indicated from diffusion profiles as schematically indicated in Figure 7-2. However, a systematic investigation on potential uptake of Cu (I) to clay surfaces is lacking so far.

From the above considerations it can be inferred that the main process affecting the buffer is corrosion resulting from interaction of the Cu surface with sulphide and leading to an insoluble Cu_2S layer of approximately 2–3 times the volume of the original shell. Bentonite within a few cm of this layer may also contain a small amount of copper sulphide due to the conversion of aerobic corrosion products that had diffused away from the shell prior to the onset of anaerobic conditions. There is no evidence that bulk properties of the bentonite e.g. swelling pressure, hydraulic conductivity or sorption capacity would be adversely affected by interaction with copper corrosion products. In addition, because of the very low solubility of Cu_2S, dissolved Cu porewater concentrations will be very low ($< 10^{-9}$ M). The possible changes in bulk properties are thus limited to an interfacial zone of < 3cm enriched in Cu_2S between the Cu source and bentonite source. The extent of this zone is estimated from the assumption of complete corrosion of the Cu shell and accounting for the molar volume of Cu_2S. The hydraulic properties of this zone are uncertain.

Because of its exposure closer to the rock, the Cu shell may corrode at a higher rate compared to the Cu canister, in particular if microbial activity were to occur in the rock/shell region. The Cu shell will moreover limit the flux of HS^- to the canister by the corrosion process until it has completely corroded. The period for this corrosion process depends on HS^- groundwater concentrations and buffer density and is estimated to be between 2'800 and $2.7 \cdot 10^7$ years (for a Cu shell of 8 mm)

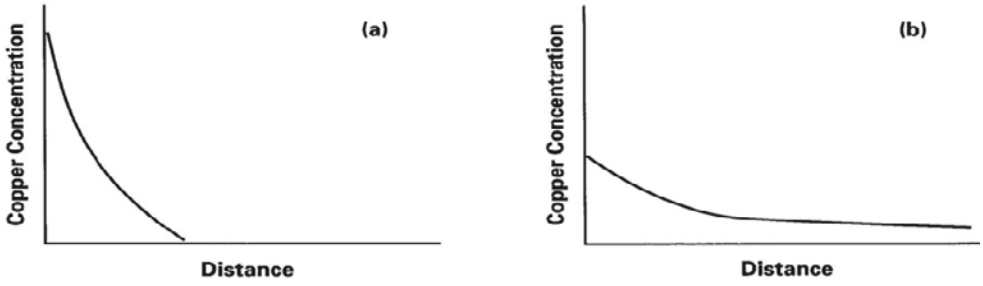

Figure 7-2. *Schematic diffusion profiles observed in compacted bentonite in contact with corroding copper under conditions where (a) Cu(II) and (b) Cu(I) are stable.*

In summary, the impact of Cu derived corrosion from the shell on the buffer's performance is expected to be very limited from the review study. The main uncertainties derived from this assessment include potential interaction processes between Cu(I) and the clay, such as for example the possibility of oxidation to Cu(II) by structural Fe(III) and simultaneous reduction of Fe(III) to Fe(II), as well as the bulk properties of the copper sulphide corrosion layer.

Copper corrosion in compacted MX-80

In the long-term experimental study reported by Kumpulainen et al. (2011), compacted saturated bentonite samples partly containing a cast iron cylinder in the centre were in contact with copper vessels. The main focus was the study of iron-bentonite interactions which is presented in more detail in the following section. A side aspect of the study was the analysis of copper profiles in the bentonite samples extracted after 8.2 years of reaction time in order to estimate Cu corrosion rates. For this purpose, four profiles were analyzed with aid of acid digestion of the slices cut perpendicular to the Cu source followed by ICP-OES analysis.

The results are summarized in Table 7-2. These show consistent corrosion rates for all four samples, with an average corrosion rate of 0.035 μm/yr. It should be noted that these calculated corrosion rates omit possible precipitated corrosion products at the metal surface. From visual inspection (shiny surface), however, the amount thereof is presumably small. The time-averaged corrosion rate is likely due to some initial oxygen present in the system and is likely to continue to decrease; because of that corrosion stops. This experiment thus represents early transient phase of evolution of the system going from oxic to anoxic conditions. No analysis of sulphide was performed, and thus it is not known if there is a supply of sulphide for long-term corrosion.

These corrosion rates are somewhat lower than those reported from the LOT A2 experiment at Äspö (Karnland and Birgersson 2009) who estimated rates of 0.14–1.8 μm/yr. A further corrosion study in compacted Ca bentonite (Kim et al. 2007) reported a corrosion rate of ~0.2 μm/yr. In both of these studies, conditions evolved from aerobic to anaerobic conditions, thus reflecting a "mixed" corrosion rate. The comparison of corrosion rates suggests that conditions in the study of Kumpulainen et al. (2011) were more reducing than the two other ones although also in this case initially conditions were oxic, thus, causing higher corrosion rates until oxygen was consumed from the system.

Table 7-2. Calculated Cu corrosion rates from Cu concentrations in study of Kumpulainen et al. (2011). For all calculations background in MX-80 Cu concentration conservatively assumed to be zero.

Sample	Cu conc. background (wt%)	Cu conc. interface layer (wt%)	Thickness of layer c (mm)	Cu corrosion rate (μm/yr)
6c	< 0.04	0.12	1.5	0.036
19c	< 0.04	0.09	2	0.034
20c	< 0.01	0.09	2	0.038
29b	n.m.*	0.08	2	0.03

* Not measured.

7.2.2 Studies of Fe (carbon steel)-clay interactions

In this chapter, a new reactive transport modelling exercise (Birgersson and Wersin 2013) and a long-term experimental study (Kumpulainen et al. 2011) are summarized. The general focus of these studies was to (1) to improve process understanding of Fe (carbon steel)-clay interactions within the KBS-3H framework and (2) decrease quantitative uncertainties with regard to the extent of alteration of the bentonite buffer.

Reactive transport modelling

This modelling exercise was based on the preliminary reactive transport modelling study with the CrunchFlow code carried out in 2006/2007 (Wersin et al. 2007). Recent advances in experimental, modelling and thermodynamic data were taken into account for this update. A particular aspect was the consideration of the potential effect of pH increase during corrosion. Without the clay, the anoxic corrosion reaction is commonly perceived as being pH neutral (e.g. Grauer 1984), as depicted for the reaction to magnetite and hydrogen:

$$3Fe(0) + 4H_2O \text{ à } Fe_3O_4 + 4H_2 \quad (7\text{-}1)$$

However, in the presence of clay, an increase in pH could in principle occur by slow precipitation of corrosion products and concomitant scavenging of Fe(II) by the clay surface (e.g. by cation exchange reactions):

$$Fe(0) + 2H_2O + 2NaX \text{ à } FeX_2 + H_2 + 2Na^+ + 2OH^- \quad (7\text{-}2)$$

The extensive thermodynamic database THERMODDEM (Blanc et al. 2007) established rather recently by the French Geological survey (BRGM) was applied. For the purpose of reactive transport modelling, the mineral data was critically evaluated by conducting thermodynamic calculations representative for Olkiluoto-type conditions. Thereof a selection of minerals, including corrosion products, clays, CSH phases, zeolites, hydroxides and carbonates was made.

The scope of the 1D transport model was to simulate the Fe (carbon steel)-clay interactions and accompanying geochemical reactions in the buffer as a result of the corrosion of the steel. The buffer with an assumed width of 40 cm was split into 20 cells, with an open boundary to the groundwater side and a closed to the canister side. The initial geochemical conditions are presented in Table 7-3.

Table 7-3. Initial geochemical conditions in the calculations. The groundwater used was the limiting dilute water and calculated bentonite porewater (Tables 3-2 and 3-3 in Wersin et al. 2007), Due to clogging of the outer cell with gypsum a lower sulphate content was used in the waters (for details, see Birgersson and Wersin 2013).

	Groundwater/initial bentonite pore water	Initial bentonite composition	
		Mineral	Volume%
pH	7.391	Na-mont.	30%
Al^{3+}	10^{-12} M	Ca-mont.	12%
Mg^{2+}	$1.65 \cdot 10^{-4}$ M	Quartz	9.6%
Ca^{2+}	$1.045 \cdot 10^{-2}$ M	Calcite	0.6%
Fe^{2+}	10^{-15} M	Gypsum	0.2%
Na^+	$1.668 \cdot 10^{-1}$ M		
		Physical properties buffer	
Cl^-	Charge	Dry density	1,570 kg/m^3
SO_4^{2-}	$7.42 \cdot 10^{-3}$ M	Porosity	0.43
SiO_2(aq)	10^{-15} M	Eff. diffusivity* (all species)	$4.5 \cdot 10^{-11}$ m^2/s
PCO_2	$10^{-3.5}$		

*The value given is for pore diffusivity. This value is scaled with the porosity to give an effective diffusivity. I.e. the effective diffusivity changes with precipitation/dissolution.

CrunchFlow (Steefel 2006) is a powerful and versatile code specifically aimed at reactive transport modelling in porous media. It considers coupling of porosity and diffusivity (porosity update feature) and has well-established kinetic dissolution/precipitation rate formulation based on the transition state theory implemented in the code. For this application, mineral reaction rates were formulated according to the following rate expression for near-neutral conditions:

$$\text{Rate} = \frac{dm}{dt} = S \cdot k_n^{T_0} \cdot \exp\left(\frac{-E_n}{R}\left(\frac{1}{T} - \frac{1}{T_0}\right)\right) \cdot \left(1 - \frac{Q}{K}\right) \quad (7\text{-}3)$$

where dm/dt is the rate (mol/s), S is the surface area (m^2), E_n is the activation energy (kJ/mol) and T_0 is the temperature at 298.15 K, Q is the activity product and K is the equilibrium constant. Similar rate expressions are given for acidic and alkaline conditions.

For all calculations, a temperature of 25°C was assumed because temperatures close to the shell are not expected to exceed 50°C (Ikonen 2003).

The mineral rates were taken from Palandri and Kharaka (2004) and various other sources as outlined in Birgersson and Wersin (2013). As highlighted also in other modelling studies on Fe(carbon steel)-clay interactions (e.g. Marty et al. 2010), the precipitation rates of many of the potentially forming mineral phases are poorly constrained. In particular this includes precipitation of corrosion products, such as magnetite or mixed Fe(II)/Fe(III) hydroxide (green rust). Therefore, a major aspect in this modelling exercise was to analyze the effect of different precipitation rates of potentially forming corrosion products (magnetite, green rust, goethite, FeS and pyrite). Different test cases, a base case and alternative cases were defined. These cases differ in the precipitation rates assumed for the corrosion products (Table 7-4). In the base case (A0), green rust was the main corrosion product to form, due its lowest solubility for the conditions of interest. Two alternative test cases (A1 and A2) considered magnetite and goethite as corrosion products respectively. A further test case assumed very slow precipitation of Fe (hydr)oxides thus favouring the precipitation of berthierine. In the final case, sulphate reduction was assumed to occur thus enabling the precipitation of pyrite or FeS (test case B1).

Results

The results for the base case after 5,000 years of interaction time are illustrated in Figure 7-3. At this time, the iron shell has completely corroded. The predominant sink for corroded Fe is green rust and very little interaction of Fe(II) with the clay has occurred. Thus montmorillonite remains virtually unaffected by the corrosion reaction. After this time period, very little further alteration takes place, because of the low solubility of the corrosion phase (data not shown).

Assuming magnetite or goethite to form as main corrosion product (cases A1 and A2) yields a very similar picture, thus showing little Fe(carbon steel)-clay interaction and very restricted alteration of montmorillonite (not shown). A somewhat larger effect is obtained if no precipitation of Fe (hydr)oxides is assumed (case A3). Released Fe(II) reacts with the clay and forms predominantly berthierine (Figure 7-4). The extent of the altered zone is about 2 cm. As for the other cases, not much interaction occurs once the zero-valent iron has been corroded.

Table 7-4. log (rate constant, mol $m^{-2}s^{-1}$) of selected minerals for the different calculated cases. Because there was no kinetic data for green rust available, the same data as for magnetite was assumed.

Case	Pyrite	FeS(am)	$Fe_3(OH)_7$	Magnetite	Goethite
A0	–	–	–11	–10.78	–7.94
A1	–	–	–31	–10.78	–7.94
A2	–	–	–31	–30.78	–7.94
A3	–	–	–31	–30.78	–27.94
B1	–5.0	–5.0	–11	–10.78	–7.94

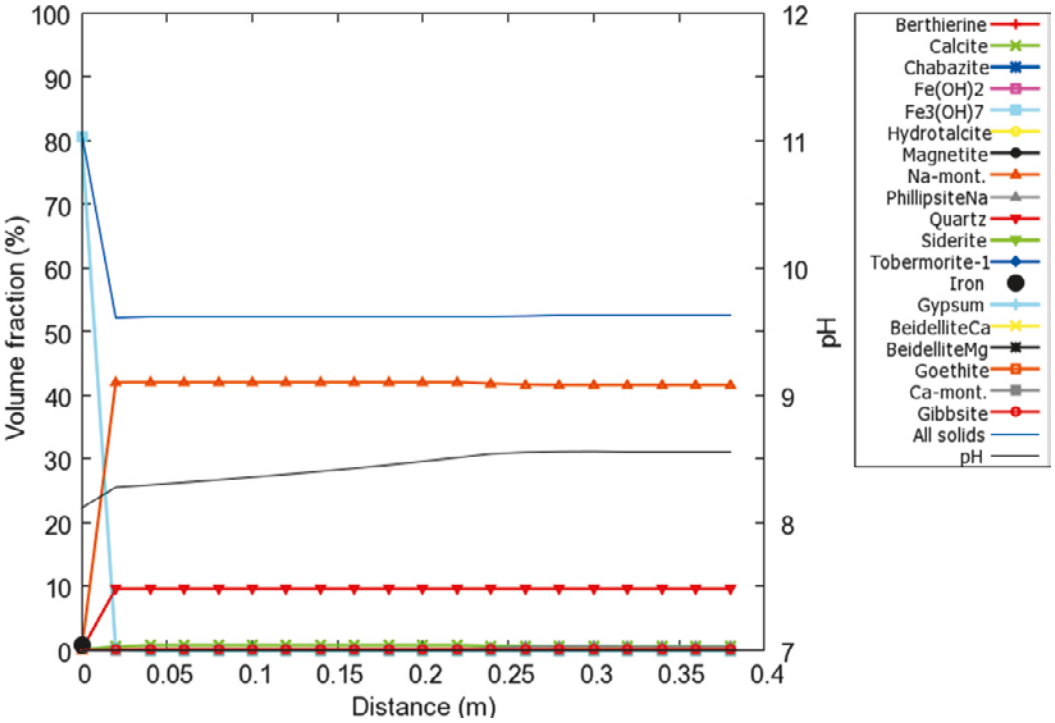

Figure 7-3. *Results for the base case (A0) after 5,000 years: x-axis: distance from the rock surface; left y-axis: volume fraction of minerals; right y-axis: pH. In this case log K=5 for the berthierine precipitation reaction was used.*

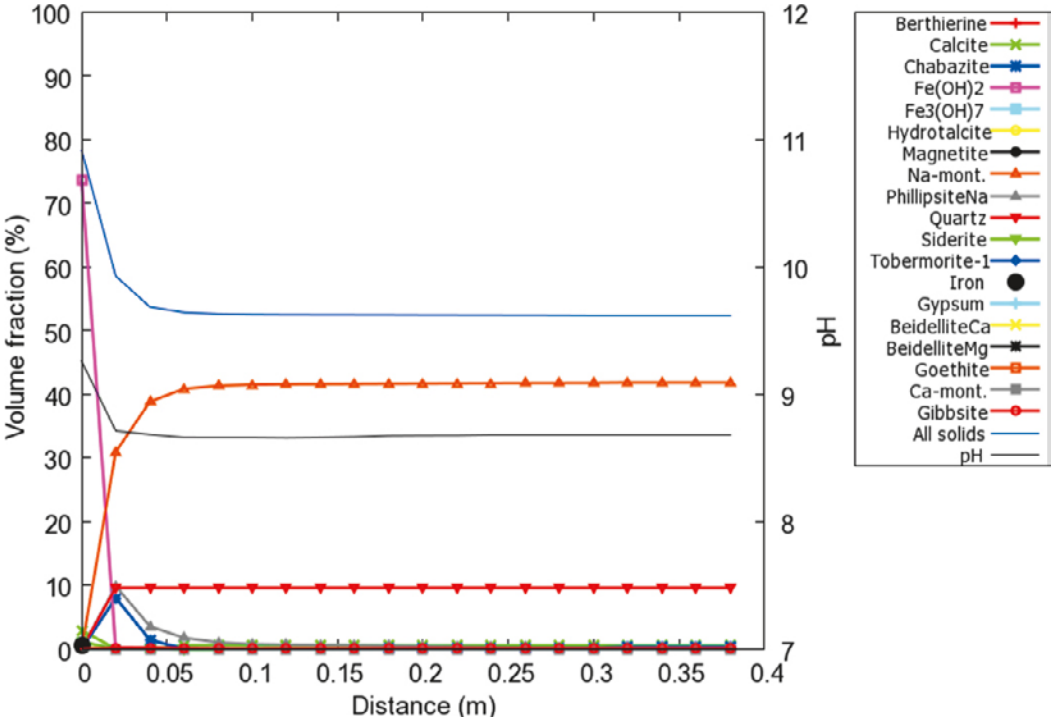

Figure 7-4. *Results assuming slow precipitation of iron oxides and berthierine as main corrosion precipitate (case A3) after 5,000 years: x-axis: distance from the rock surface; left y-axis: volume fraction of minerals; right y-axis: pH. In this case log K=5 for the berthierine precipitation reaction was used.*

The largest effect on montmorillonite alteration is predicted for the case where sulphate reduction is included (case B1). This is because of the induced increase in pH from this redox reaction:

$$4Fe + 10H^+ + SO_4^{2-} \text{ à } FeS(s) + 3Fe^{2+} + 4H_2O \quad (7\text{-}4)$$

This pH increase which cannot be fully compensated by the formation of corrosion products leads to the dissolution of montmorillonite and subsequent precipitation of the zeolites (Figure 7-5). The extent of the altered zone after 5,000 years is somewhat larger, about 5 cm. As with the other test cases, no significant further alteration occurs once the corrosion reaction has ceased.

Additional tests have been run with varied groundwater composition (more sulphate, more/less pCO_2). These cases results in bentonite alteration which is very similar to the base case. Further, a case has been run where chlorite phases are allowed to precipitates. This results in minor chamosite precipitation and a slightly increased damage of the buffer.

Finally, a test case has been run in which the THERMODAT database value for the log K for berthierine precipitation has been used. This leads to a larger transformation of montmorillonite to berthierine during the corrosion phase. However, the resulting pore water concentration of Fe^{2+} is unrealistically low (10^{-29} M). The impact on the buffer is, however, not severe also in this case and is limited to the first few cm:s.

Conclusions drawn from the reactive transport modelling exercise

The results confirm previous ones in that the extent of montmorillonite alteration is predicted to remain spatially limited to a few centimetres from the iron source. The largest impact occurs during the initial corrosion reaction where clay dissolution may be triggered by the generation of OH^-. The pH buffering reaction in the clay as well as from carbonate reservoir in the surrounding host rock will limit the increase in pH. The largest effect predicted from reactive transport modelling is the case where (microbially-induced) sulphate reduction would occur. Because of hostility of the compacted clay environment towards microbial activity, sulphate reduction will be limited, if occurring at all, to the interface zone between the host rock, shell and the clay buffer.

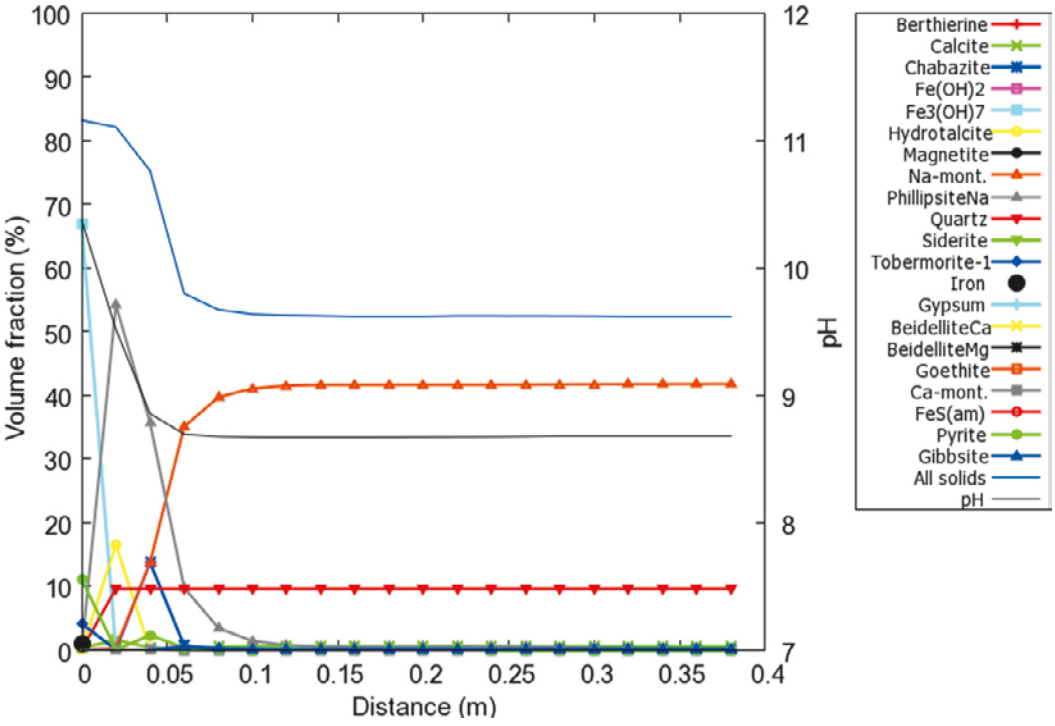

Figure 7-5. *Results assuming sulphate reduction and slow precipitation of iron oxides (case B1) after 5,000 years: x-axis: distance from the rock surface; left y-axis: volume fraction of minerals; right y-axis: pH*

The modelling exercise highlights that the main uncertainties are reaction kinetics of minerals and thermodynamic data of clays. In spite of these uncertainties, the results are robust with regard to predicting the extent of montmorillonite alteration. The main factors limiting this process are: the diffusional constraints, the effective pH buffering processes in the EBS system and the low solubility of corroded iron products.

Long-term experimental studies

Reliable predictions for iron-bentonite interactions and their effects on the buffer's long-term performance hinge on reliable experimental data. Long-term studies are very valuable in this regard, because, if performed under consistently anoxic conditions, are more representative of processes occurring in the EBS after repository closure. Within the KBS-3H programme, solid and liquid samples from two entirely different types of long-term experiments were analyzed: batch experiments carried out at JAEA in Japan and diffusion-type experiments carried out at VTT in Finland.

Batch experiments (JAEA)

These experiments included Kunipia bentonite and iron powder suspensions in different anoxic (N_2) electrolyte solutions which were left to react in glovebox for a period of about ten years. Five of the samples were sent to B+Tech/VTT for liquid and solid phase analysis. The conditions of these samples are summarized in Table 7-5 (right column). Note the high Fe/clay ratio (1:1 mass ratio) in these experiments.

The solution composition after exposure for four samples is illustrated in Table 7-6. This shows for all samples a significant increase in pH and strongly reducing conditions. The increase in pH is most likely explained by the corrosion reaction and the concomitant scavenging of Fe(II) by the clay (see eq. 7-1).

The solid phase analysis also revealed significant changes. These were already visible after opening of the samples, where the H_2O dist. and $NaHCO_3$ exposed samples were thick grey pastes whereas the sulphate and chloride exposed samples occurred as bluish-green slurries. The visual differences were confirmed by XRD analysis (Figure 7-6) which indicated very little transformation of montmorillonite for the H_2O dist. and the 0.05 M Na_2SO_4 samples but substantial transformation for the NaCl and $NaHCO_3$ exposed samples. Thus, XRD indicate partial to complete loss of montmorillonite and formation of a 1:1 clay, possibly berthierine. FTIR data (not shown) confirmed this finding.

Diffusion-type experiments (VTT)

The configuration of these tests is illustrated in Figure 7-7. A cast iron cylinder surrounded by saturated compacted MX-80 bentonite was contacted by 0.5 M NaCl solution via a porous steel filter. The samples were held in a copper vessel which was placed in a nitrogen-filled glovebox. In addition "reference" samples with the same configuration but without the iron cylinder were exposed to the same conditions.

Table 7-5. Experimental set-up and conditions of long-term Fe-bentonite experiments.

	8 y old VTT's samples	10 y old JAEA's samples
Bentonite composition	Bulk MX-80	Purified (clay fraction) Kunipia-F
Clay to solution ratio	Compacted, 30 g solids with 100 mL of external water	Batches, 25 g solids with 250 mL of solution
Reactive surface area of iron to clay	One cast iron cylinder (surface area 14 cm^2)	Fine iron powder, 25 g (surface area 82,500 cm^2)
Initial solution composition	0.5 M NaCl-solution	Distilled water or synthetic water with 0.3 M NaCl, 0.6 M NaCl, 0.1 M $NaHCO_3$, or 0.05 M Na_2SO_4

Table 7-6. Water compositions of JAEA samples after 10 years of reaction time. All concentrations are given in mg/L. Alkalinity is given in mmol/L.

sample no.	62	63	65	68
Initial electrolyte	0.3 M NaCl	0.6 M NaCl	0.1 M $NaHCO_3$	0.05 Na_2SO_4
pH	12.7	12.8	12.6	11.1
Eh (mV)	-446_{Pt}	-584_{Pt}	-565_{Pt}	-250_{Pt}
	-443_{Au}	-614_{Au}	-611_{Au}	-250_{Au}
Na	10,700	19,300	6,200	3,900
Mg	< 0.05	< 0.05	< 0.1	< 0.5
Ca	0.94	0.81	1.5	16
Si	6.0	3.7	14	14
Al	< 0.5	< 0.5	< 1	< 5
K	84	84	92	150
Fe_{tot} (ICP analysis)	0.14	0.35	0.13	< 0.2
Fe_{tot} (colorimetry)	0.11	0.35	0.12	0.02
Fe^{2+}	0.05	0.10	0.04	0.01
Fe^{3+}	0.06	0.25	0.08	0.01
Cl^-	12,200	24,300	160	210
SO_4^{2-}	460	480	240	8,000
Alkalinity	80	135	245	4

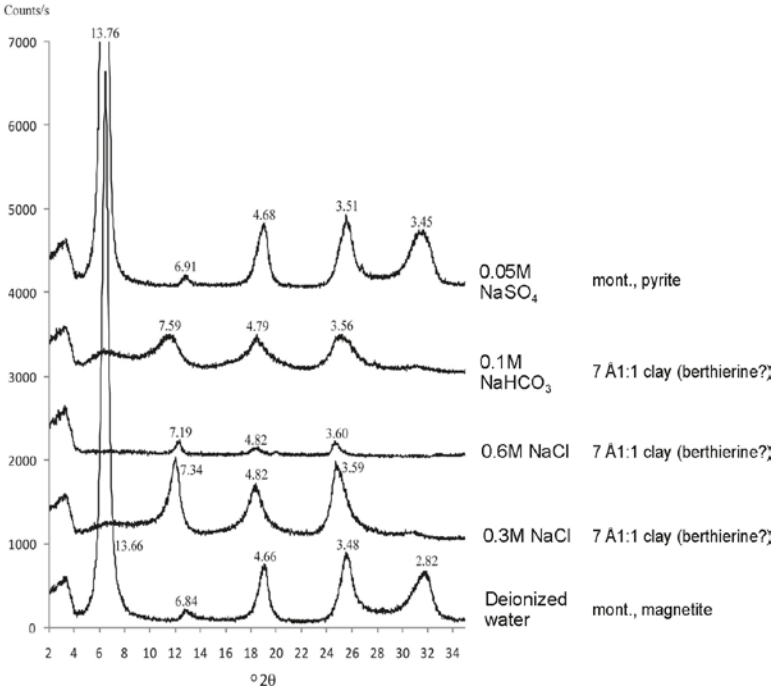

Figure 7-6. *XRD spectra of JAEA samples.*

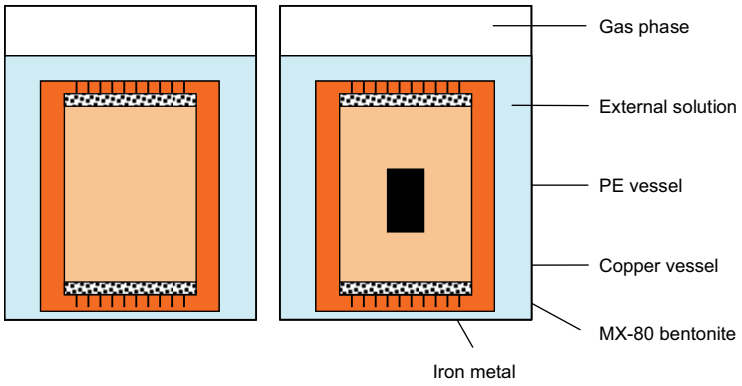

Figure 7-7. *Experimental set-up of experiment of VTT, left: "reference" sample, right: sample with iron source.*

After eight years of exposure time a pair of samples was dismantled and both solution and solid analyses were conducted. A brownish iron front extending up to 7 mm into the bentonite could be visually observed. SEM-EDX and ICP analysis confirmed that the iron concentration in the clay close to the metal source had increased. From the Fe analyses (by ICP) of two separate profiles an average corrosion rate of about 1.5 µm/yr could be deduced. The speciation of the reacted iron in the clay was studied both by Mössbauer and XANES (Figure 7-8) analysis. These data indicated a clear increase in Fe(II) content of the clay relative to the reference sample and also an increase towards the iron source. The combined analysis from XRD, SEM, and Mössbauer indicates that no new Fe-rich clay had formed. It rather suggests the formation of an X-ray amorphous mixed Fe(II)/Fe(III) hydroxide phase close to the metal source. This is supported by geochemical modelling (see below).

In general, the clay showed little changes in contact with the cast iron. From SEM, precipitation of $CaCO_3$ was observed in the contact area, suggesting that some cementation had occurred therein. A slight decrease in swelling pressure, but no change in hydraulic conductivity for material from the contact was indicated, but because of the small sample size, no clear conclusions in this regard could be drawn.

The data of the contacting external solution (initial composition 0.5 M NaCl) after 8.2 years of contact time revealed changes in composition, thus showing increase in Ca, Mg, K, SO_4, Alk, Si, Fe, a decrease in Eh, while for Na, Cl and pH little or no changes were observed (Table 7-7). It is noteworthy that compositions for the reference sample and Fe sample were very similar except that the Fe sample showed lower Eh. The changes in water chemistry were simulated by applying an equilibrium model for bentonite (Wersin et al. 2004). This thermodynamic model considers cation

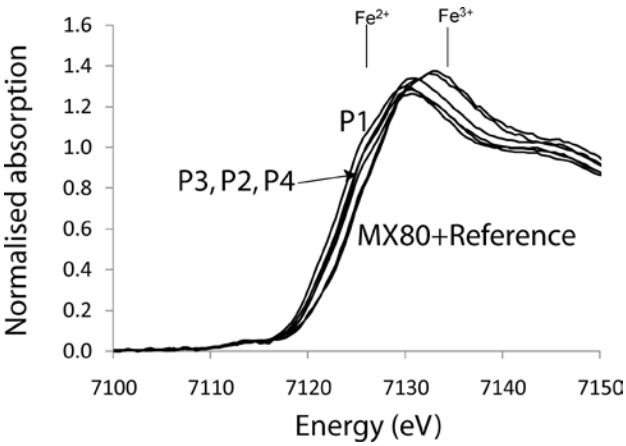

Figure 7-8. *XANES spectra of MX-80 samples at different distances from iron metal source: P1 directly at contact.*

exchange at interlayer sites, surface complexation at edge sites and dissolution/precipitation reactions of accessory minerals (calcite, gypsum, quartz). For the Fe sample, iron corrosion was included by a zero-order kinetic reaction taking corrosion rate of 2μm/a. The simulated concentrations (Table 7-7) show good agreement with the measured ones, and hence support the validity of the simple modelling approach. Thus, main reactions occurring in both samples are cation exchange, dissolution of gypsum and of calcite. In the case of the Fe sample, the most likely corrosion product is a mixed Fe(II/III) hydroxide phase (green rust) with a Fe(II)/Fe(III) ratio of ~2. This is compatible with findings from spectroscopic analysis (see above).

Conclusions from experimental studies

The batch experiments, albeit representing extreme and unrealistic conditions, enabled relevant process understanding on montmorillonite transformation. Thus, bentonite in (direct) contact with a large source of zero-valent Fe induces high pH and low Eh conditions as well as transformation to a non-swelling 1:1 clay (presumably berthierine).

Diffusion-type experiments, representing more-realistic repository conditions, revealed very limited changes in the clay fraction and a very limited zone affected by cementation (< 2 mm), but no effect with regard to clay alteration. The corrosion rate of iron was estimated to be about 1.5 μm/yr, in agreement with previous corrosion studies in compacted bentonite (e.g. Smart et al. 2004). The corrosion reaction generated an increase in iron (predominately Fe(II)) in the clay close to the contact. The most likely form of this Fe-pool is a mixed Fe(II/III) hydroxide green-rust type phase. Results confirmed the large pH buffering capacity of the bentonite which helps to counteract the alkalinity generated by the corrosion reaction.

7.2.3 Study of Ti-clay interactions

Titanium alloys exhibit a range of corrosion and physical properties that make them suitable for numerous applications. Commercially pure Ti (Ti Grade 2) exhibits excellent corrosion resistance to a wide range of environments, but is suspectible to localised corrosion, such as crevice corrosion (under aerobic conditions) and many of the alloys are also suspectible to hydrogen induced cracking. Crevice-corrosion resistant materials have been developed through the addition of e.g. Pd (grades 6, 11, 16 and 17) (Schutz 2005). The absorption of hydrogen in titanium can be enhanced through galvanic coupling of Ti to a more active material such as C-steel, therefore this should be prevented by avoiding steel in contact with Ti.

Table 7-7. Comparison between measured water compositions and modelled compositions of VTT samples. All concentrations are given in mmol/l.

	Ref sample 8.6 years	Model	Fe sample 8.6 years	Model
pe	–3.56	–3.71	–8.27	–8.93
pH	8.0	7.97	8.0	7.95
Alkalinity	3.5	2.54	2.9	3.7
Na	543.7	456.6	526.3	469.3
Ca	13.0	18.4	14.5	12.9
Mg	7.8	4.1	11.1	4.2
K	2.2	1.6	1.5	1.5
Fe_{tot}	3.04E–03*	4.53E–03	7.0E–03*	3.2E–03
Cl	573.0	484.1	561.7	484.3
HCO_3^-	2.65	1.95	2.17	2.9
SO_4^{2-}	12.5	8.28	10.4	8.4

* Total of measured Fe(II) and Fe(III) concentrations.

Titanium metals display very low uniform corrosion rates (< 1 nm/yr) over a large range of pH and Eh conditions. The corrosion behaviour is governed by the low solubility of tetravalent TiO_2 which forms a passive surface corrosion layer under both oxic and reducing conditions. The dependence of the composition and properties of the titanium oxide film on electrochemical potential have been extensively studied. The different factors controlling film growth are understood, as are the associated corrosion processes (Shoesmith 2006). Amongst all the common engineering alloys, Ti is perhaps the only one believed to be immune to microbially-induced corrosion (Little et al. 1991).

The low content of other metals in the Ti alloys restricts any impact of these, e.g. the recommended Ti alloy material Ti grade 2 alloy has such a low content of other metals in the alloy (0.3% Fe and 0.1% C) that the impact of these will be negligible.

The interactions between titanium and clay have been barely studied so far. Preliminary long-term data obtained by Prof. Olefjord and co-workers from Chalmers (S) in the 1980^{ies} (as part of SKB's canister programme) indicates similar corrosion rates in compacted bentonite compared to those measured in water, i.e. ≤ 1 nm/yr. So far, no work on reaction products from this interaction process has been carried out. Even the speciation of Ti in natural clays is uncertain. In principle, five possible reaction products resulting from Ti-clay interactions are possible: (i) Ti sorbed to the clay surface via cation exchange or specific adsorption, (ii) Ti incorporated in the octahedral or tetrahedral clay structure, (iii) Ti precipitated as separate TiO_2 or mixed (Fe, Ti) oxide, (iv) Ti precipitated as separate silicate phase and (v) polymerized as cross-linked TiO_2 units in the interlayer (Ti pillared clay). The latter two transformation products would have the strongest impact on the buffer, but are improbable on the basis of current knowledge. The geochemistry of Ti, its behaviour in natural environments, with a particular focus on clay-rich ones, and possible interaction processes with clays are outlined in detail in Wersin et al. (2011).

Preliminary batch study on Ti-clay interactions

The scope of this preliminary and pioneering study was to shed more light on Ti-clay interaction processes and on the Ti species resulting from these interactions. Because of the known very low corrosion rates of Ti alloys, a main focus was to analyze the reacted clay materials with advanced spectroscopic techniques. Synchroton-based x-ray absorption spectroscopy (XAS) and μ-XRF were the main tools applied for this purpose.

Two series of batch experiments have been conducted, the results of which are summarized below. Currently a third series of batch tests is foreseen.

1st series of batch tests & spectroscopic baseline study:

In these tests, purified MX-80 powder (2g) was reacted with Titanium nanopowder (2g) or with Ti foil in 0.1 M NaCl solutions (100 mL) previously purged with N_2 at room temperature. The Ti nanopowder was contained in a dialysis bag (Spectropore 7) in order to facilitate separation of the two solid materials after reaction. The samples were centrifuged after about 4 months of reaction time and both solution and solid were analyzed.

The XRF bulk analysis of the raw and purified MX-80 showed a Ti content of about 0.1 wt%, in agreement with previous studies. This indicates that Ti is not removed by the purification procedure. Rokle bentonite (raw) showed a considerable higher content (~2.5 wt% Ti).

The results from solution analysis are shown in Table 7-8. As expected, Ti concentrations remain low, even for samples adjusted initially to extreme pH conditions (pH 2 and pH 12). The measurable Fe concentration (expect for the high pH sample) indicates that in fact anoxic conditions were achieved.

Table 7-8. Solution data for MX-80 samples from 1st series in contact with Ti for about 4 months.

					ICP-AES		
Sample number	**Description**	**Initial pH**	**Final pH**	**EC (mS/cm)**	**Fe (mg/l)**	**Na (mg/l)**	**Ti (mg/l)**
1.	pur. MX-80, Ti powder	~8.7	7.9	1.35	1.84	282	0.06
3.	pur. MX-80, Ti powder, adj. to pH 2	2.1	2.8	2.95	3.10	438	< 0.02
4.	pur. MX-80, Ti powder, adj. to pH 12	12.4	12.2	6.34	< 0.3	1,510	0.02
6.	pur. MX-80, Ti powder, no dialysis bag	~8.7	6.7	1.39	nd	nd	nd
10.	pur. MX-80, Ti foil, no dialysis bag	~8.7	7.4	1.32	nd	nd	nd

nd: not determined.

XAS analysis on clay reference samples and selected reacted batch samples was carried out at the Swiss Light Source (SLS), Paul Scherrer Institute (Switzerland). The reference samples included purified MX-80, raw Rokle bentonite, Opalinus Clay, illite du Puy as well as Ti standard minerals rutile, anatase and titanate ($CaTiSiO_5$). The XANES spectra for Rokle bentonite and Opalinus Clay are depicted in Figure 7-9. These reveal the same spectral features as for anatase, thus indicating that Ti in these clay materials occurs predominately as small TiO_2 particles. A different result was obtained by illite du Puy and MX-80 bentonite which show similar spectra as that of $CaTiSiO_5$ (Figure 7-10). This suggests that Ti in these latter clay materials is bound in the clay structure (presumably in the octahedral layers).

The XAS analysis of the reacted MX-80 samples indicated no difference with regard to the unreacted material. From the obtained XANES and EXAFS spectra in combination with the XRF results it could be concluded that the amount of Ti that reacted from the corrosion process was too small to yield any information on Ti speciation. This was true for all studied samples, including also the high and low pH ones.

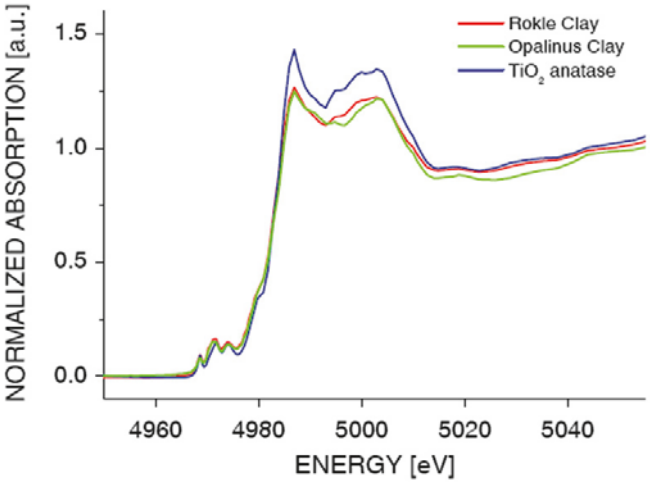

Figure 7-9. *Ti XANES spectra of two natural Ti-clay materials (Rokle Clay, compared to anatase TiO_2. Note the close match of the pre-edge features.*

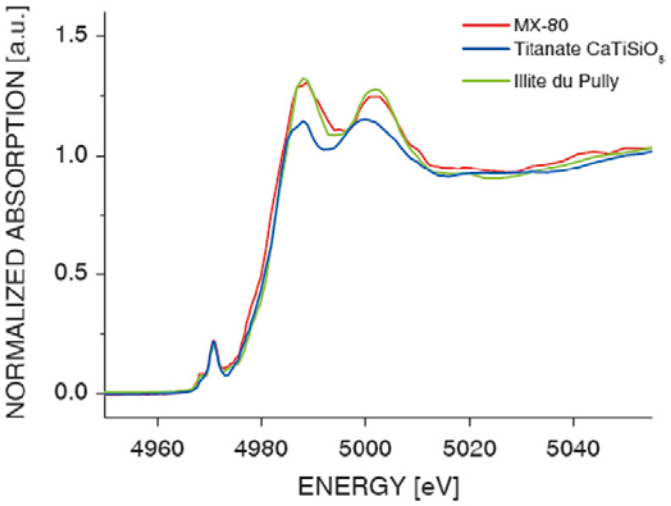

Figure 7-10. *XANES spectra of MX-80 and Illite du Puy, compared to that of titanate.*

2nd series of batch tests:

The main scope of these series was to enhance Ti transfer from the metal to the clay, thus to enable spectroscopic analysis of the Ti released from corrosion and taken up by the clay. For this purpose, synthetic "Ti-free" montmorillonite produced by hydrothermal synthesis was used as starting material. From elemental analysis (determined by XRF) and thermal gravimetry analysis (TGA), the following structural formula could be derived: $Na_{0.34}[Al_{1.64}Mg_{0.37}f_{0.99}][Si_{4.00}]O_{10}(OH_{1.95}F_{0.05})$ $4.0H_2O$, where *f* stands for vacancy. This confirms that the synthesized product is dioctehedral smectite. A further difference with regard to the 1st series is the higher temperature (80°C) at which experiments were conducted, in order to increase corrosion and transfer rates to the clay. Other than that, the experimental procedure was very similar: the synthetic montmorillonite was contacted with Ti nanopowder and foil in 0.1 M NaCl solutions in a N_2 purged glovebox for about four months.

The results from solution analysis are shown in Table 7-9. For all samples with synthetic montmorillonite, Ti concentrations are very low (< quantification limit). On the other hand, the sample with purified MX-80 exposed to Ti nanopowder for 17 months revealed higher Ti concentrations of about 5mg Ti/L. Note that these concentrations are higher than were determined for the samples from the first series. The same trend is observed for Fe, where the purified MX-80 sample displays a Fe concentration of about 200 mg/l, or about 3.5 mM. The initial pH of the synthetic montmorillonite exposed to 0.1 M NaCl was rather low (~5.1) which is explained by the preparation behaviour of this material (Wersin et al. 2011). At the end of the experiment, however, all samples showed pH values close to 7.

Table 7-9. Solution data for samples from 2nd series at 80°C after about four months and sample 2 from 1st series after 17 months of reaction time.

					ICP-AES		
Sample number	**Description**	**Initial pH**	**Final pH**	**EC (µS/cm)**	**Fe (mg/l)**	**Na (mg/l)**	**Ti (mg/l)**
17.	synth. mont., Ti powder	5.13	7.01	1,366	0.03	244	< 0.02
19.	synth. mont., Ti powder, adj. to pH 2	2.00	4.73	2,520	< 0.03	289	< 0.02
20.	synth. mont., Ti powder, adj. to pH 12	12.01	10.34	2,320	< 0.03	643	< 0.02
21.	synth. mont., Ti powder, no dialysis bag	5.32	6.86	1,414	< 0.03	272	< 0.02
23.	synth. mont., Ti foil	5.19	7.33	1,306	< 0.03	240	< 0.02
24.	synth. mont., no Ti	5.13	7.24	1,327	< 0.03	234	< 0.02
2.	purif. MX-80, Ti powder, 17 months reaction time	nd	7.03	1,395	231	416	5.38
2.	see above	nd	7.03	1,395	174	798	3.67

Micro-XRF analysis, which was carried out with a focussed X-ray beam, revealed extremely low Ti concentrations for the synthetic montmorillonite, contrary to purified MX-80 (Figure 7-11), thus confirming the suitability of this material to study Ti-clay interactions.

Another result of this analysis was the identification of small Ti metal particles on the clay surfaces for samples with Ti nanopowder (emplaced in dialysis bags). The remaining surface did not show any or showed only extremely low concentrations of Ti. This indicates that the samples were contaminated with metal Ti nanoparticles by the experimental procedure. The analyzed sample with bentonite exposed to Ti foil showed measurable Ti concentrations (sample 23), which is not attributed to any experimental artefact. This was confirmed by preliminary XAS analysis which indicated a different coordinative environment for Ti than that of Ti metal (Figure 7-12). In fact, the XANES spectrum is similar to that of titanate, thus suggesting that Ti occurs in the clay structure or is surface-bound. This result for one sample can only be regarded as preliminary at this point and needs to be supported by further data.

Conclusions from the preliminary Ti-clay study:

- Titanium forms a thermodynamically stable passive film of insoluble TiO_2 corrosion layer under both oxic and anoxic and reducing conditions and is therefore very inert. As revealed from previous studies, including a long-term study in compacted bentonite (Mattson and Olefjord 1984), the corrosion rate of Ti metals is very low, in the range of 1 nm/yr or lower. The inert layer can be disturbed and lead to crevice corrosion cracking, which is a drawback for its potential use as a canister material.
- Spectroscopic analysis on a number of natural and purified clay materials showed that Ti occurs either as small TiO_2 particles (e.g. Rokle bentonite) or is incorporated in the clay structure (MX-80). Differences in Ti concentration or speciation do not appear to affect the bulk properties of bentonite, as indicated from the study of Karnland et al. (2006).
- Because of the high Ti background concentration, meaningful experiments on Ti-bentonite interactions are difficult. The use of synthetic "Ti-free" montmorillonite yielded promising results in this regard. This material is recommended in future experiments to unravel the speciation of Ti transferred to the clay via the corrosion process.
- Preliminary data suggest that Ti released from corrosion is in fact transferred to the clay. This, however, needs to be supported by further data in order to allow for conclusive results. The experimental set-up with Ti nanopowder, however, proved not suitable because of experimental artefacts induced. Further batch tests with coarser grained Ti material are recommended.

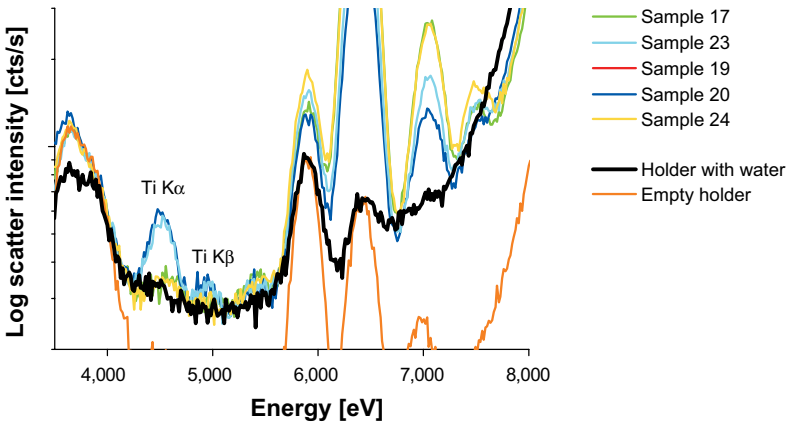

Figure 7-11. *Synchrotron-based XRF spectra showing the Ti content of different synthetic clay samples after exposure to Ti. For samples 20 and 23 the K_α and K_β emission lines of Ti are clearly visible. The other samples exhibit Ti contents at the limit of detection (less than two-fold the background count rate) and are statistically indistinguishable from blank samples.*

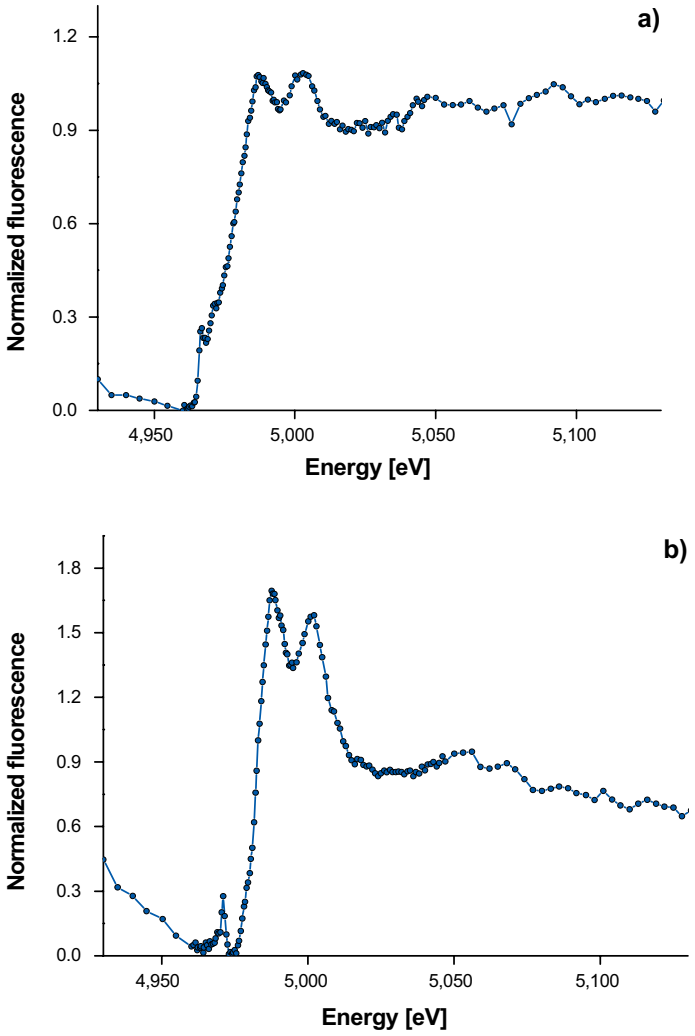

Figure 7-12. *MicroXANES spectra recorded for sample 23. a) microXANES of a localized contamination hot spot. Spectrum is indicative of metallic Ti. b) microXAS of the homogeneous Ti content induced by the corrosion exposure. Characteristic single pre-edge feature points towards a Ti speciation similar to the Ti coordination environment found in $CaTiSiO_5$ (titanite).*

7.3 Evaluation of consequences of disturbed buffer/rock interface

7.3.1 Overview of scoping calculations

This chapter presents scoping calculations to illustrate the impact of perturbations to the buffer/rock interface caused, e.g. by the presence of the Supercontainer and its corrosion products or by thermally-induced rock spalling, on flow around a deposition drift and mass transfer of the dissolved species between the KBS-3H buffer and flowing water. The species in question may, for example, be corrosive agents in the groundwater that could potentially degrade the canister. They may also be radionuclides that are released to the buffer subsequent to canister failure.

The calculations described in Section 7.3.2 illustrate the case of a single transmissive fracture that intersects the perturbed buffer/rock interface, introducing flowing water to the interface zone. On the upstream side of the fracture, water migrates along the interface zone in both horizontal directions away from the fracture. The water also flows around the tunnel and converges again towards the fracture, where it exists on the downstream side (see Figure 7-13). The flowing water within the zone is in contact with the buffer and there will be diffusive exchange of solutes between this water and the buffer pores. These calculations illustrate the impact of different degrees of hydraulic perturbation on the diffusive exchange of dissolved mass transfer across the interface. The analytical solution used in these calculations assumes that the perturbed interface zone is thin in the radial direction and that the fracture plane is normal to the deposition drift axis. The flow in the undisturbed rock is assumed to be confined to the fracture, consistent with the sparse nature of the rock fracturing at the Swedish and Finnish sites.

In Section 7.3.3, further analytical solutions are derived that illustrate the impact of the finite thickness of the interface zone and of ambient groundwater flow that is parallel to, rather than perpendicular, to the drift axis. In these calculations, the rock is treated as a homogeneous porous medium, and the calculations are thus rather far removed from the actual system of interest. They can, however, be seen as giving a tentative and preliminary indication of the significance of interface zone thickness and flow direction when considering a perturbed buffer/rock interface.

It is assumed throughout that the total flow through the perturbed interface zone controls the rate of solute mass transfer across the interface. This will be the case if solutes entering the zone are well mixed, such that there are no concentration gradients within the region. This will be the case, for example, it fracturing in the disturbed region causes significant radial mixing by transverse dispersion. The analysed situation might not occur in reality, but was selected as a means to bound the impact of e.g. corrosion products or extensive rock spalling.

Finally, conclusions from the scoping calculations are compiled in Section 7.3.4.

The following notation is used in the analysis:

b[m]: Fracture half aperture.

i: Undisturbed hydraulic gradient in the rock.

l[m]: Length of perturbed interface zone, or major axis of ellipsoid representing perturbed buffer/rock interface.

q[m s^{-1}]: Darcy velocity through section of the drift with the perturbed buffer/rock interface treated as homogeneous slender ellipsoid.

q_x[m s^{-1}]: Darcy velocity of ambient flow through host rock treated as porous medium, with flow parallel to drift axis.

q_z[m s^{-1}]: Darcy velocity of ambient flow through host rock treated as porous medium, with flow normal to drift axis.

r[m]: Radial coordinate, centred on drift axis.

r_0[m]: Drift radius.

s [m]: Minor-axis of the ellipsoid representing perturbed buffer/rock interface.

x[m]: Cartesian coordinate.

z[m]: Cartesian coordinate.

A[m^2]: Constant.

B[m]: Constant.

D [m^2 s^{-1}]: Diffusion coefficient of dissolved species in water.

K [m s^{-1}]: Hydraulic conductivity of perturbed interface zone.

K' [m s^{-1}]: Hydraulic conductivity of section of the drift with the perturbed buffer/rock interface treated as homogeneous slender ellipsoid.

K_{HR} [m s^{-1}]: Hydraulic conductivity of host rock treated as porous medium.

Q [m^3 s^{-1}]: Amount of water passing through the interface zone.

Q_{eff}[m^3 s^{-1}]: Effective flowrate in the boundary layer.

Q_r[m^3 s^{-1}]: Radial outflow from a small segment of cylinder.

Q_x[m^3 s^{-1}]: Flow along a cylinder due to outflow/inflow from a row of sources/sinks.

T [m^2 s^{-1}]: Fracture transmissivity.

Δr [m]: Thickness of perturbed interface zone.

ζ[m]: Hydraulic potential in the interface zone.

ζ_f [m]: Hydraulic potential in the fracture.

ζ_{HR} [m]: Hydraulic potential of host rock treated as porous medium.

ϕ [m^2 s^{-1}]: Velocity potential due to a source.

θ: Polar coordinate.

σ [m^2 s^{-1}] Source strength of small segment of cylinder.

7.3.2 Calculation of single fracture intersecting the perturbed interface zone

Mathematical model

The calculations in this section consider the simplified model system shown in Figure 7-13.

An annular perturbed interface zone is taken to exist between the undisturbed buffer and the rock. It has a thickness Δr [m] that is small compared to the buffer thickness and has a hydraulic conductivity K [m s^{-1}] that is elevated compared with the adjacent buffer and the rock matrix. The interface zone thus conducts flowing water, and also perturbs the ambient flow in the rock around the drift. The zone is assigned a length l [m], which would, for example, correspond roughly to the length of the Supercontainer if the perturbation is due to the interaction of Supercontainer corrosion products with the buffer. Ambient flow in the fracture occurs in the x-direction, and the fracture intersects the interface zone at its mid-point.

Flow in both the fracture and in the interface zone is described by a hydraulic potential, governed by Laplace's equation. Because it is assumed that both the fracture and the interface zone are thin, the 2-D form of Laplace's equation can be used in both regions.

If the hydraulic potentials in the fracture and the interface zone are denoted by ζ_f [m] and ζ[m], respectively:

$$\nabla^2 \zeta_f = \nabla^2 \zeta = 0. \tag{7-5}$$

If the undisturbed hydraulic gradient is i, then:

$$\frac{\partial \zeta_f}{\partial x} \to i \quad \text{as} \quad r \to \infty. \tag{7-6}$$

If the z-direction is along the drift, assuming there is no flow along the drift beyond the ends of the disturbed interface zone:

$$\frac{\partial \zeta}{\partial z} = 0 \quad \text{at} \quad z = \pm \frac{l}{2}. \tag{7-7}$$

The hydraulic potential is continuous at the intersection between the fracture and the disturbed region:

$$\zeta_f = \zeta \quad \text{at} \quad r = r_0; \quad z = 0. \tag{7-8}$$

where r_0[m], is the drift radius.

Finally, the rate at which fluid passes across the interface between the fracture and the disturbed zone is continuous:

$$T \left. \frac{\partial \zeta_f}{\partial r} \right|_{r=a} = -2K\delta r \left. \frac{\partial \zeta}{\partial z} \right|_{z=0}, \tag{7-9}$$

where the factor of 2 arises because fluid may pass into the interface zone in either the positive or negative z directions.

Laplace's equation for flow in the fracture, with the boundary condition given by Eq. 7-6, has a solution:

$$\zeta_f = ix + \frac{A}{r^2} x = \left(ir + \frac{A}{r} \right) \cos\theta, \tag{7-10}$$

where A is a constant and (r,θ) is a polar coordinate system in the fracture plane, with its origin at the point where the plane intersects the drift axis.

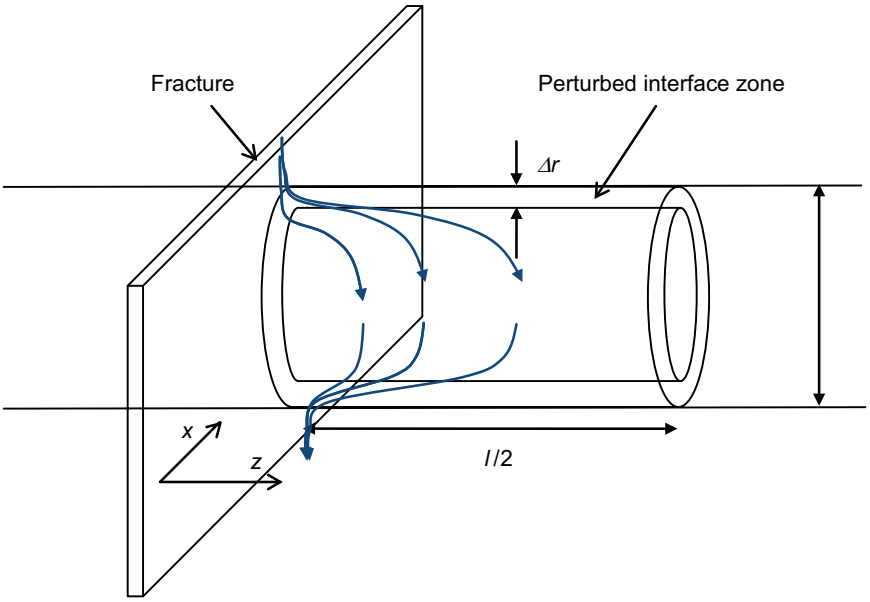

Figure 7-13. *Problem geometry for the case where a fracture intersects the disturbed interface zone. Flowing water is shown by blue arrows.*

Laplace's equation for flow in the interface zone, with the boundary condition given by 7-7, has a solution:

$$\zeta = B\left(e^{-z/r_0} + e^{(z-l)/r_0}\right)\cos\theta\,, \tag{7-11}$$

where B is a constant.

Substituting Eq. 7-10 and Eq. 7-11 in Eq. 7-8:

$$ia + \frac{A}{a} = B\left(1 + e^{-l/r_0}\right). \tag{7-12}$$

Substituting Eq. 7-10 and Eq. 7-11 in Eq. 7-9:

$$T\left(i - \frac{A}{r_0^2}\right) = 2\frac{K\delta r B}{r_0}\left(1 - e^{-l/r_0}\right). \tag{7-13}$$

From Eq. 7-11 and Eq. 7-12:

$$A = ir_0^2 \frac{T - 2K\delta r \tanh\left(l/2r_0\right)}{T + 2K\delta r \tanh\left(l/2r_0\right)}. \tag{7-14}$$

Finally, from Eq. 7-14 and Eq. 7-10, the hydraulic potential in the fracture is given by:

$$\zeta_f = ix\left(1 + \frac{r_0^2}{r^2}\cdot\frac{T - 2K\delta r \tanh\left(l/2r_0\right)}{T + 2K\delta r \tanh\left(l/2r_0\right)}\right). \tag{7-15}$$

This reduces to:

$$\zeta_f \approx ix\left(1 - \frac{r_0^2}{r^2}\right) \text{ for } 2K\delta r \tanh\left(l/2r_0\right) >> T, \tag{7-16}$$

which implies a constant potential at the interface, would be the case of an infinitely conductive disturbed zone, and

$$\zeta_f \approx ix\left(1+\frac{r_0^2}{r^2}\right) \text{ for } 2K\delta r \tanh\left(l/2r_0\right) << T. \tag{7-17}$$

Q [m^3 s^{-1}],the amount of water passing through the interface zone, is given by:

$$Q = r_0 T \int_{-\pi/2}^{\pi/2} \left.\frac{\partial \zeta_f}{\partial r}\right|_{r=r_0} d\theta\,. \tag{7-18}$$

Using Eq. 7-10:

$$Q = 2r_0 T\left(i - \frac{A}{r_0^2}\right) \tag{7-19}$$

and, from Eq. 7-14:

$$Q = 8r_0 Ti\left[\frac{K\Delta r \tanh\left(l/2r_0\right)}{T + 2K\Delta r \tanh\left(l/2r_0\right)}\right] \tag{7-20}$$

Note that:

$$Q \to 4r_0 Ti \quad \text{as} \quad \frac{K\delta r}{T} \to \infty. \tag{7-21}$$

which is the "mixing tank" flow rate assumed in the recent KBS-3H safety assessment in cases where the buffer/rock interface is assumed to be significantly perturbed (see Eq. 6.7-3 of Smith et al. 2007b).

Impact of the interface zone hydraulic properties on mass transfer

Q, the flow passing into and out of the interface zone is a key determinant of radionuclide releases from the zone in all cases where complete mixing of radionuclides with water passing through the zone (by diffusion and/or transverse dispersion) can be assumed, and if advection in flowing water can be assumed to be the dominant transport process moving radionuclides out of this well-mixed interface zone into the rock.

Figure 7-14 shows Q plotted against the lumped parameter $K\delta r$ assuming example fracture transmissivities of $5\cdot10^{-10}$ m^2 s^{-1} and $5\cdot10^{-9}$ m^2 s^{-1}. Other data used here and in later scoping calculations are:

r_0 = 0.925 m (Börgesson et al. 2005)
l = 5.525 m (Johansson et al. 2007)

As the value of $K\delta r$ is increased, Q tends towards a limiting value that is equivalent to the "mixing tank" flow rate assumed in the KBS-3H safety assessment in cases where the buffer/rock interface is assumed to be significantly perturbed. Using this flow rate in a safety assessment is always conservative, since it is never exceeded by Q. For the higher transmissivity value of $5\cdot10^{-9}$ m^2 s^{-1}, this limiting value is about an order of magnitude higher compared with the lower transmissivity case. For low values of $K\delta r$, the flow in the interface zone becomes insensitive to fracture transmissivity.

Cases where flow in the interface zone is so slow that diffusion is the dominant transport process are not covered by the present model. Rather, mass transfer across the interface zone is better described using the "boundary layer" mass transfer typically assumed in Posiva in SKB safety assessments for undisturbed buffer cases, where the effective "boundary layer flowrate" is:

$$Q_{eff} = 4\sqrt{2br_0 DTi}. \tag{7-22}$$

Here, D [m^2 s^{-1}] is the diffusion coefficient of dissolved species in water and $2b$ [m] is the fracture aperture.

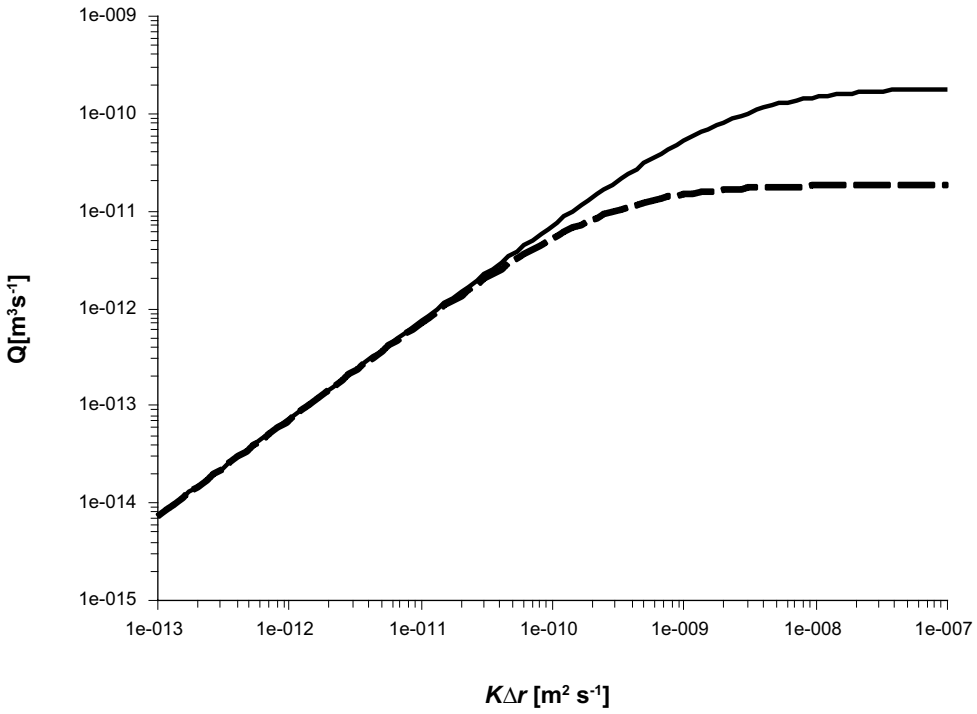

Figure 7-14. *Flow in the interface zone for ambient flow normal to the drift axis with the host rock modelled as a fractured medium and as an equivalent porous medium. Solid curve: fracture transmissivity = $5 \cdot 10^{-9}$ m^2 s^{-1}. Dashed curve: fracture transmissivity = $5 \cdot 10^{-10}$ m^2 s^{-1}.*

The effect of perturbation on the mass transport resistance of the interface is illustrated in Table 7-10, which shows the ratio of the flow in a perturbed interface zone, Q, to the boundary-layer flowrate, Q_{eff}, i.e. the ratio of the flow rates that controls mass transport across the interface in the presence and in the absence of perturbation. Additional parameter values used to generate the results are $2b = 10^{-4}$ m and $D = 2 \cdot 10^{-9}$ m^2 s^{-1}.

The table shows that, for the ranges of fracture transmissivity and interface perturbation ($K\delta r$) considered, perturbation of the interface can increase mass transport across the interface by a factor of as much as about 14. The increase is most pronounced in the case where the intersecting fracture has a transmissivity that is approximately equal to $K\delta r$.

Table 7-10. Ratio of the flow in a perturbed interface zone to the "boundary-layer flowrate", which controls mass transport across the interface in the absence of perturbation. × indicates that the boundary-layer flowrate exceeds the calculated flow in the interface zone, which indicates that flow and mixing in the perturbed interface zone has negligible impact on diffusive mass transfer to the boundary layer.

Fracture T [m^2 s^{-1}]	Perturbation to interface zone ($K\Delta r$) [m^2 s^{-1}]					
	10^{-13}	10^{-12}	10^{-11}	10^{-10}	10^{-9}	10^{-8}
10^{-11}	×	×	×	×	×	×
10^{-10}	×	×	×	1.4	2.0	2.1
10^{-9}	×	×	×	1.1	4.5	6.5
10^{-8}	×	×	×	×	3.6	14
10^{-7}	×	×	×	×	1.3	11
10^{-6}	×	×	×	×	×	4.2

7.3.3 Effects of flow direction and interface zone thickness

The further calculations described next illustrate the impact of the finite thickness of the interface zone and of ambient groundwater flow direction with respect to the drift axis. To allow analytical solutions to be derived, the calculations treat the rock as a homogeneous porous medium, rather than as a fractured medium. The modelled systems are in this respect rather far removed from the actual system of interest. They do, however, give a tentative and preliminary indication of the significance of interface zone thickness and flow direction to mass transfer across a perturbed interface zone, which is not possible with the solution presented in the previous section.

Mathematical model: finite-thickness interface zone

First, consider the system shown in Figure 7-15. As before, flow is described by hydraulic potentials, governed by Laplace's equation. If the hydraulic potentials in the host rock and in the interface zone are denoted by ζ_{HR} [m] and ζ[m], respectively:

$$\nabla^2 \zeta_{HR} = \nabla^2 \zeta = 0 \tag{7-23}$$

If undisturbed flow in the host rock is in the z-direction and the undisturbed hydraulic gradient is again i, then:

$$\frac{\partial \zeta_{HR}}{\partial z} \to i \quad \text{as} \quad r \to \infty, \tag{7-24}$$

Where z is the flow direction and r is radial distance, measured from the drift axis.

The hydraulic potential is continuous at the intersection between the host rock and the disturbed region:

$$\zeta_{HR} = \zeta \text{ at } r = r_0. \tag{7-25}$$

The rate at which fluid passes across the interface between the host rock and the interface zone is continuous:

$$K_{HR} \left. \frac{\partial \zeta_{HR}}{\partial r} \right|_{r=r_0} = K \left. \frac{\partial \zeta}{\partial r} \right|_{r=r_0}. \tag{7-26}$$

and the buffer inside the interface zone is taken to be impermeable:

$$K \left. \frac{\partial \zeta}{\partial r} \right|_{r=r_0-\delta r} = 0. \tag{7-27}$$

Here, K_{HR} is the hydraulic conductivity of the host rock and K is the hydraulic conductivity of the perturbed interface zone.

Eq. 7-23, with the boundary conditions given by equations 7-24 to 7-27, has the solution:

$$\zeta_{HR} = iz + \frac{A}{r^2} z = \left(ir + \frac{A}{r} \right) \cos\theta, \tag{7-28}$$

where A is given by:

$$A = ir_0^2 \frac{\dfrac{r_0^2}{(r_0 - \delta r)^2}\left(K_{HR} - K\right) + K_{HR} + K}{\dfrac{r_0^2}{(r_0 - \delta r)^2}\left(K_{HR} + K\right) + K_{HR} - K} \tag{7-29}$$

and (r,θ) is a polar coordinate system in the plane normal to the drift axis, with its origin at the point where the centre of the drift is located.

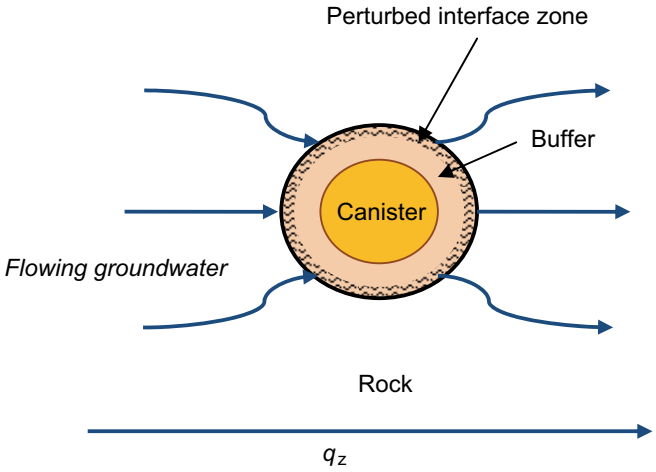

Figure 7-15. *The case in which ambient flow in the host rock is directed normal to the deposition drift axis.*

Note that:

$$A \to -ir_0^2 \quad \text{as} \quad \frac{K}{K_{HR}} \to \infty. \tag{7-30}$$

Q [m^3 s^{-1}],the amount of water passing through the interface zone, is given by:

$$Q = K_{HR} r_0 l \int_{-\pi/2}^{\pi/2} \left. \frac{\zeta_{HR}}{\partial r} \right|_{r=r_0} d\theta = 2 q_z r_0 l \left(1 - \frac{A}{r_0^2 i} \right). \tag{7-31}$$

where q_z[m] is the Darcy velocity of the ambient groundwater flow.

$$Q \to 4 q_z r_0 l \quad \text{as} \quad \frac{K}{K_{HR}} \to \infty. \tag{7-32}$$

Results

Figure 7-16 shows Q plotted against $K\delta r$ for different values of interface zone thickness δr (note that δr = 0.4 m corresponds to an interface zone spanning the entire buffer thickness). A host rock hydraulic conductivity of $K_{HR} = 9.0 \cdot 10^{-11}$ m s^{-1} is used, based on data used for equivalent porous medium modelling of sparsely fractured rock at the Olkiluoto site in the depth range 400–2,000 m (Table 2-2 in Löfman and Poteri 2008). An ambient Darcy velocity $q_z = 9.0 \cdot 10^{-13}$ m s^{-1}is also assumed, being the product of the hydraulic conductivity and a hydraulic gradient of 0.01, as given by Löfman (1999). The results show that flow in the interface zone is insensitive to the assumed thickness of the zone, δr.

To quantify the impact of treating the host rock as an equivalent porous medium, the result from Figure 7-14 for a fracture transmissivity = $5 \cdot 10^{-10}$ m^2 s^{-1} is also shown in Figure 7-17. This fracture transmissivity is also equivalent to a host rock hydraulic conductivity $K_{HR} = 9.0 \cdot 10^{-11}$ m s^{-1} if the fracture spacing is set equal to l. For high values of $K\delta r$, the limiting value of Q for the fracture case is the same as for the equivalent porous medium case. For low values of $K\delta r$, irrespective of transmissivity, the amount of water passing through the interface zone is lower by a factor of about 3 in the case that the host rock is treated as a fractured medium compared with the value for an equivalent porous medium.

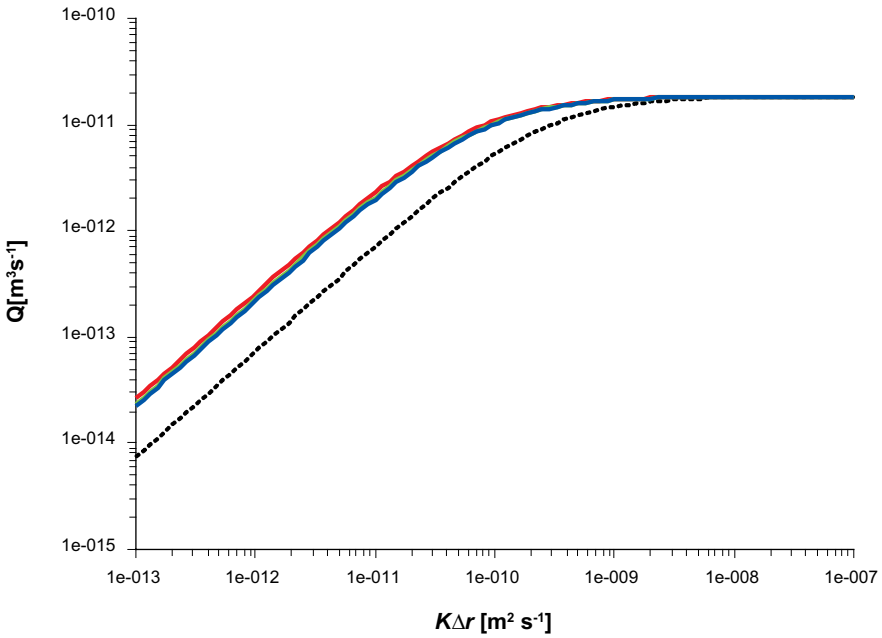

Figure 7-16. *Effect of interface zone thickness on flow in the interface zone. Red line: interface zone 0.4 m; green line: interface zone 0.1 m; blue line: interface zone 0.01 m. The dashed line is the result from Figure 7-14 for a fracture transmissivity = $5 \cdot 10^{-10}$ m^2 s^{-1}.*

Mathematical model: ambient flow parallel to the drift

Next, consider the system shown in Figure 7-17, in which ambient groundwater flow is parallel to the repository drift, and has a Darcy velocity of q_x [m s^{-1}].

There is no general solution to this problem. However, if the section of the drift with the perturbed buffer/rock interface is treated as homogeneous slender ellipsoid of hydraulic conductivity K' [ms^{-1}], then an approximate solution for steady-state Darcy flow, q [m s^{-1}], through the drift section is given on p. 428 of Carslaw and Jaeger (1959):

$$q \approx q_x K' \left[K_{HR} + (K' - K_{HR}) \frac{4b^2}{l^2} \cdot \left[\ln\left(\frac{l}{s}\right) - 1 \right] \right]^{-1}. \qquad (7\text{-}33)$$

Here, s [m] is the radius of the minor-axis of the ellipsoid. It can be assumed that:

$$\pi r_0^2 K' \approx 2\pi r_0 \Delta r K; \quad \text{i.e. } K' = 2\frac{\Delta r}{r_0} K \qquad (7\text{-}34)$$

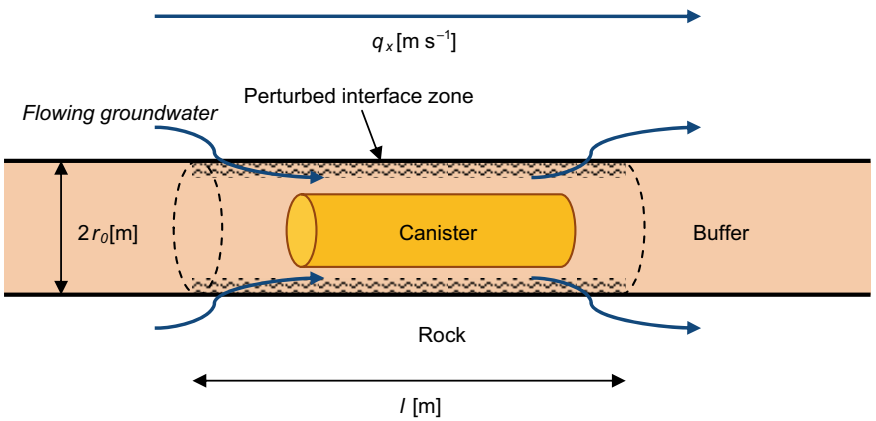

Figure 7-17. *The case in which ambient flow in the host rock is directed parallel to the deposition drift axis.*

For high *K'*, the limiting form of this solution is:

$$q \approx \frac{q_x l^2}{4b^2\left[\ln\left(\frac{l}{s}\right)-1\right]} \tag{7-35}$$

Alternatively, a solution for this limiting case can be obtained by analogy with the case of a long cylindrical electric conductor in an electric field solution, as considered by Taylor (1966). Under the assumption of Darcy's law, flow may be described by a hydraulic potential, governed by Laplace's equation. Similarly, an electric field may be expressed in terms of an electric potential, also governed by Laplace's equation. If the electrical potential is analogous to the hydraulic potential, the charge distribution in a conductor is analogous to a distribution of sources/sinks of water in a high-*K* hydraulic medium. Taylor gives a first approximation to the charge distribution in long cylindrical electric conductor in an electric field and the electrical potential around the conductor (see Taylor 1966, p 151). By analogy with this approximation, the source strength $\sigma\delta x$ [$m^3\ s^{-1}$] in a segment of the cylinder of length δx a distance x from the mid-point of the cylinder is given by:

$$\sigma\delta x \approx -\frac{q_x x\delta x}{2\ln[l/(2r_0)]}. \tag{7-36}$$

The velocity potential at a distance r from the segment, ϕ [$m^2\ s^{-1}$] is given by:

$$\phi = -\frac{\sigma\delta x}{r} \approx \frac{q_x x\delta x}{2r\ln[l/(2r_0)]} \tag{7-37}$$

The radial outflow form the segment, Q_r [$m^3\ s^{-1}$], is given by:

$$Q_r = 4\pi r^2 \frac{d\phi}{dr} \approx -\frac{\pi q_x x\delta x}{\ln[l/(2r_0)]}. \tag{7-38}$$

The flow along the cylinder due to outflow/inflow from the sources/sinks, Q_x [$m^3\ s^{-1}$], is given by:

$$Q_x = \int_{-l/2}^{x} Q_r dx' \approx -\frac{\pi q_x}{\ln[l/(2r_0)]}\int_{-l/2}^{x} x'\delta x' = \frac{\pi q_x\left(l^2/4 - x^2\right)}{2\ln[l/(2r_0)]} \tag{7-39}$$

Thus, in this case, the flow in the interface zone varies strongly with the position along the drift axis, and is highest at the mid-point ($x = 0$), where:

$$Q \approx \frac{\pi q_x l^2}{8\ln[l/(2r_0)]} \tag{7-40}$$

and

$$q \approx \frac{q_x l^2}{8r_0^2\ln[l/(2r_0)]}. \tag{7-41}$$

In Eq. 7-35, if we set

$$s = r_0\sqrt{2}, \tag{7-42}$$

in which case r_0 is, to a reasonable approximation, the average radius of the ellipsoid:

$$q \approx \frac{q_x l^2}{8r_0^2[\ln[l/(2r_0)] - 0.6534]}\ . \tag{7-43}$$

There is thus some discrepancy between the flow obtained treating the drift section as an ellipsoid (Eq. 7-43) and as a circular cylinder (Eq. 7-41) which disappears for $l >> r_0$ (the slender body approximation), but gives an error in calculated flow of a factor of a little over two in the present

application (see Figure 7-18). Nevertheless, the ellipsoidal approximation is retained here for the purpose of scoping calculations, allowing use of Eqs. 7-33 and 7-34, which give flow as a function of interface zone hydraulic conductivity.

Results

The solution given by Eqs. 7-33 and 7-34 is plotted in Figure 7-18, with Q obtained from q by multiplying by πr_0^2. The limiting solutions (Eqs. 7-43 and 7-41) are also shown, as is the result from Figure 7-14 for ambient flow normal to the drift axis assuming the same magnitude of ambient flow Darcy velocity in both cases.

The results show a rather limited impact of ambient flow direction on the results. For low values of $K\Delta r$, the flow in the interface zone is higher by a factor of about three in the case of an ambient flow normal to the drift compared with the case when ambient flow is parallel to the drift. The difference is less for high values of $K\Delta r$ where the limiting value of Q is approached, with ambient flow normal to the drift giving somewhat lower flow in the interface zone.

7.3.4 Conclusions

The preceding sections have presented scoping calculations to illustrate the impact of perturbations to the buffer/rock interface caused, e.g. by the presence of the Supercontainer and its corrosion products or by thermally-induced rock spalling, on flow around a deposition drift. The main conclusions from the scoping calculations presented above are as follows.

- The effects of perturbation to the buffer rock interface on mass transfer are described in terms of the lumped parameter KΔr.
- For the ranges of fracture transmissivity and interface perturbation (KΔr) considered in the scoping calculations, perturbation of the interface between the buffer and the rock can increase mass transport across the interface by up to about a factor of 14.
- The increase in mass transfer across the interface is most pronounced in the case where the intersecting fracture has a transmissivity that is approximately equal to KΔr.
- For higher values of transmissivity the impact of the interface zone on mass transfer across the interface is small, allowing the" boundary layer" approach to be used.
- The limiting rate of mass transfer at high values of KΔr is equivalent to that obtained using the "mixing tank" flow rate assumed in the KBS-3H safety assessment in cases where the buffer/rock interface is assumed to be significantly perturbed.
- This limiting "mixing tank" flow rate is always conservative.
- The equations presented in the present analysis could potentially be used as a basis for a more realistic treatment of mass transfer across the interface zone in future safety assessments should reliable estimates of the hydraulic properties and physical extent of the disturbed zone become available.

The problem of a disturbed buffer rock interface is also considered in an earlier report by Neretnieks (2006). The main difference is that, in the present study, migrating solutes entering the disturbed zone are assumed to be well mixed, such that there are no concentration gradients within the region. This will be the case, for example, if fracturing in the interface zone causes radial mixing by transverse dispersion. Neretnieks (2006), on the other hand, assumes that the radial distribution of radionuclides within the interface zone is determined by diffusion. It is not currently possible to state which approach is more realistic, as this will depend on the detailed properties of the disturbed zone. This is acknowledged, for example, in the discussion of mass transfer from a damaged rock zone to the buffer in Section 4.5 of Neretnieks et al. (2010).

"*Although there are many large rock fragments, which can lead to few mixing locations and strong channelling it cannot be ruled out that transverse dispersion can be considerable and can dominate over molecular diffusion*."

The solutions in the present analysis are, however, expected to be the more conservative.

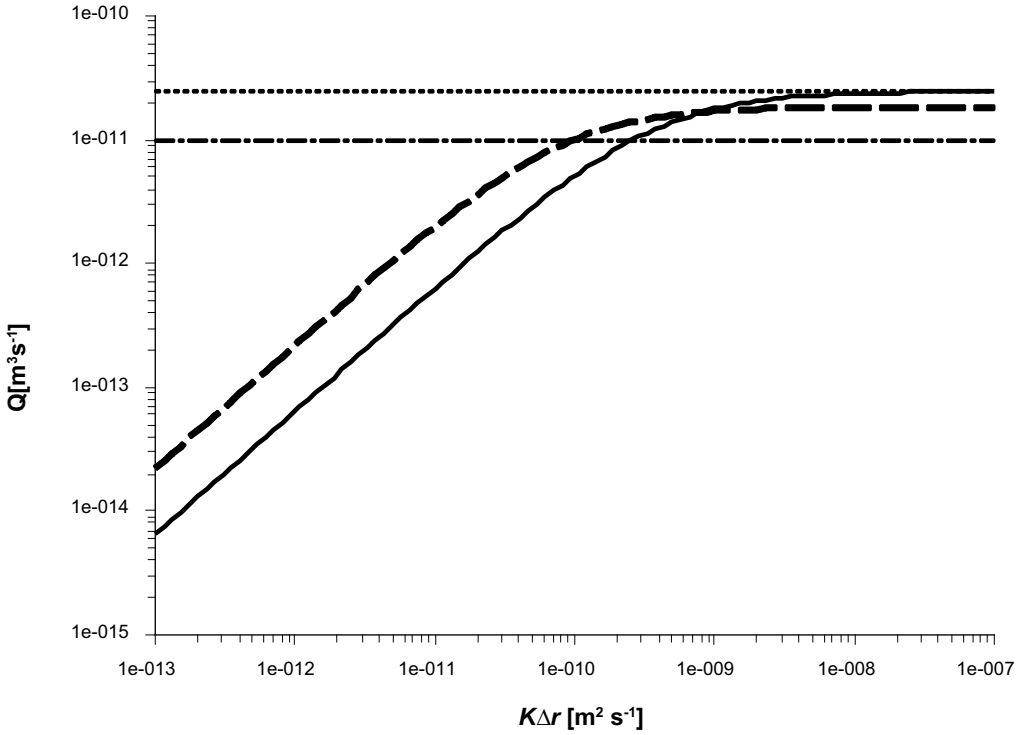

Figure 7-18. *Effect of ambient flow direction. Flow in the interface zone for the case that ambient flow is parallel to the drift axis (solid line) and limiting solutions for high-K, approximating the geometry either by an ellipsoid (dotted line) or by a circular cylinder (dot-dash line). The dashed line is the result from Figure 7-14 for flow normal to the drift axis.*

7.4 Hydrogen impact on porewater chemistry

General considerations

Hydrogen is generated by the corrosion of all potential shell materials. Due to its very low corrosion rate Titanium will release only minor amounts of H_2 which will dissipate via diffusion. Copper corrosion in the presence of sulphide will produce H_2, but the rates of H_2 production will generally be small, such that H_2 will be transported away in dissolved form. Only under very conservative assumptions (i.e. large HS^- fluxes, and low buffer densities), H_2 generation may be sufficiently high in the tighter sections of Olkiluoto for copper, such that a separate gas could form (King and Wersin 2013). In the case of iron, the highest hydrogen fluxes will be induced (e.g. King 2008), which may lead to a separate gas phase and large hydrogen partial pressures, depending on the hydraulic properties of the surrounding rock.

High partial pressure of hydrogen gas, pH_2 may also potentially affect the porewater chemistry. In a review comment to the assessment of iron-bentonite interactions by Wersin et al. (2007), the possibility of acidification by shifting the sulphide equilibria at high hydrogen partial pressure (pH_2) was put forward:

$$HS^- + H_2 \text{ à } H_2S + H^+ + 2e^- \quad (7\text{-}44)$$

This representation omits that the oxidation half reaction 7-44 needs to be balanced by a corresponding reduction half reaction, as for example:

$$0.25SO_4^{2-} + 2.5H^+ + 2e^- \text{ à } 0.25H_2S + H_2O \quad (7\text{-}45)$$

Combining half reactions 7-44 and 7-45, the opposite effect results, namely an increase in alkalinity rather than in acidity.

Furthermore, the iron corrosion reaction and release of Fe (II) needs to be considered:

$$Fe + 2H^+ \text{ à } Fe^{2+} + H_2 \quad (7\text{-}46)$$

which may react with H_2S and precipitate Fe(II) sulphide:

$$Fe^{2+} + H_2S \text{ à } FeS + 2H^+ \quad (7\text{-}47)$$

Combining eqs. 7-46 and 7-47 results in a pH neutral reaction.

Considering the "classical" anaerobic corrosion reaction with iron corroding to magnetite and hydrogen (eq. 7-1, see Section 7.2.2), no change in alkalinity is induced. However, Fe (II) released by corrosion may also be scavenged by the clay via cation exchange, as schematically represented by eq. 7-2 (see Section 7.2.2), and this leads to an increase in pH.

From these qualitative considerations it can be inferred that high pH_2 conditions in combination with the iron corrosion reaction does not lead to acidification but rather to an increase in alkalinity. This is supported by preliminary scoping calculations and results from reactive transport modelling (Section 7.2.2), as will be outlined in the following section. It should be noted, however, that in these considerations potential microbially-mediated reactions with H_2 acting as electron donor (thus leading to a consumption of H_2) are not accounted for.

Results from preliminary scoping calculations

Preliminary scoping calculations using the PHREEQC code were carried out to evaluate the effect of iron corrosion and hydrogen production on porewater composition and pH in the buffer. The recently updated thermodynamic model for compacted bentonite (Wersin et al. 2004) was applied (cf. Wersin et al. 2012). The iron corrosion reaction was considered as zero-order rate with 1 µm/yr for a time period of 100 years. Saline-type Olkiluoto groundwater was assumed to be in contact with the buffer. No microbiological processes, such as sulphate reduction were considered. A closed system was conservatively assumed, thus no buffering from the rock via exchange of CO_2 was taken into account. The thermodynamic database was THERMODDEM, provided by the French Geological survey (BRGM).

Selected results of different test cases are listed in Table 7-11. These show a comparison between results obtained for the corrosion in saline groundwater (no buffering from minerals) and for corrosion in the bentonite buffer. Various tests cases with different corrosion products (green rust, magnetite, $Fe(OH)_2$) are presented. Only small amounts of FeS are formed because of the limited amount of this compound in the groundwater, since sulphate reduction is assumed not to occur. For all cases, strong lowering of Eh (pe) and increase in pH_2 results from the corrosion reaction. The pH in bentonite is in the range of 7.9–8.8, depending on the corrosion products formed. Compared to the clay-free case, pH values are slightly higher because of the buffering reactions in the clay (cation exchange and surface proton reactions).

Table 7-11. Selected results from scoping calculations on effect of corrosion on porewater composition and pH (see text). $logpCO_2$ and $logpH_2$ refer to log of partial pressure of these gases (bar).

Test cases	Main corrosion products	pH	pe	$logpCO_2$	$logpH_2$
No clay					
a0	Green rust, FeS, (siderite)	7.32	-8.61	-2.96	2.61
b0	Magnetite, siderite, FeS	8.57	-9.90	-5.46	2.66
Bentonite					
Base line	No corrosion reaction	7.93	-2.53	-3.72	-10.8
a1	Green rust, FeS, (siderite)	7.93	-9.31	-3.73	2.76
b1	Magnetite, siderite, FeS	8.82	-10.22	-5.51	2.81
c1	$Fe(OH)_2$, siderite, FeS	8.72	-10.06	-5.31	2.80

The preliminary scoping calculations indicate that pH in compacted bentonite in contact with a corroding iron source will be buffered to slightly alkaline values by surface reactions in the clay, the carbonate system and the precipitation of corrosion products. High pH_2 does not affect pH under these conditions.

Support for these findings is given by reactive transport calculations carried with the CrunchFlow code, presented in Section 7.2.2. These indicate similar porewater compositions and pH values as found by the scoping calculations. In all the test cases considered, except for those including sulphate reduction, no large variations in porewater compositions and pH values resulted. Thus, the overall results indicate that under conditions of no or limited microbial activity, no important changes by the corrosion reaction and the generation of H_2 are induced – except for the lowering of the redox potential.

Microbial processes and uncertainties

Microbial processes generating or consuming H_2 occur in deep groundwaters and are relevant at Olkiluoto, where at repository depth and below sulphate reducing bacteria (SRB), methanogens, iron reducers, acetogens, nitrate reducers and manganese reducers have been identified (Pedersen 2008). As highlighted by a recent status report on microbiological processes of Olkiluoto groundwater (Pedersen 2008), the following two microbially-mediated processes with H_2 are potentially relevant:

Acetate production: $H_2 + CO_2$ à acetate (7-48)

Methane oxidation: $CH_4 + 2H_2O$ à $4H_2 + CO_2$ (7-49)

Both processes may induce sulphate reduction, thus SRB may utilize acetate or H_2 for the sulphate reduction reaction and release hydrogen sulphide. Thus, high hydrogen favours sulphate reduction, which at low H_2 levels occurs mainly from the oxidation of dissolved organic matter (DOC).

The impact of microbially-mediated processes involving H_2 on porewater chemistry has not been yet assessed. It depends on the interplay of kinetically-controlled microbial redox reactions and iron corrosion, mineral dissolution/precipitation (e.g. calcite) and diffusional processes. Moreover, the geochemical conditions in the rock surrounding the buffer will strongly affect the extent of microbial activity. Assessing the microbial-induced effects including H_2 on both groundwater and porewater composition by bounding calculations in future modelling exercises is recommended.

7.5 Conclusions

7.5.1 Evaluation of long-term safety impact of Cu, Ti and Fe on bentonite

Iron has been the reference Supercontainer shell material in earlier studies of the KBS-3H variant. Key long-term safety issues for a steel Supercontainer shell are the uncertain impacts of the Fe(II) and hydrogen that will be released as the shell corrodes on the bentonite buffer. In the Complementary studies of horizontal emplacement KBS-3H 2008–2010, copper and titanium have also been studied as alternative materials. Studies have addressed their corrosion rates and the impacts of their corrosion products on the buffer. Studies of iron-clay interactions have also continued.

7.5.2 Copper corrosion and interaction with bentonite

Copper corrosion strongly depends on the redox conditions of the near-field. Initially, while oxic conditions prevail, rather high corrosion rates are expected (of the order of 10's of μm/yr initially). Soluble copper oxide corrosion products (mainly Cu_2O) will be formed and dissolved Cu(II) chloride and carbonate species will predominate. The corrosion rate will be substantially lowered once anoxic conditions are established, with sulphide derived from the groundwater being the only corrosive agent. An insoluble copper sulphide corrosion layer will form on the copper surface some 2–3 times the volume of the original shell, and some soluble Cu(I) sulphide species will slowly be released to the bentonite buffer. A Supercontainer copper shell is expected to corrode at a somewhat quicker rate than the copper canister because of the larger sulphide flux induced by its proximity to the rock and the possibility of microbially-induced sulphate reduction at this interface. The trapping of sulphide

by the copper shell will limit the sulphide flux to the canister surface until corrosion of the shell is complete. A long-term (8.8 years) laboratory study has been conducted, indicating a corrosion rate under predominately anoxic conditions of 0.035 μm per year. This rate would be expected to decline as corrosion products build up at the metal surface. The time-averaged corrosion rate is likely due to some initial oxygen present in the system and is likely to continue to decrease, and because of that corrosion will stop. This experiment thus represents the early transient phase of evolution for the system going from oxic to anoxic conditions. No analysis of sulphide was performed, and thus it is not known if there is a supply of sulphide for the long-term corrosion.

On the basis of literature data and site-specific information, it is concluded that rates of copper corrosion will be similar at the Olkiluoto and Forsmark sites during the oxic phase but due to the estimated higher sulphide fluxes the steady-state corrosion rates are expected to be higher for Olkiluoto than for Forsmark in the anoxic conditions.

The impact of Cu(I) on the performance of the bentonite buffer is expected to be very limited. Diffusion experiments reveal that the interactions of Cu(I) with the clay are much weaker than those of Cu(II). Further support for weak or no uptake of Cu(I) is provided by chemical analyses of natural bentonites. Some interaction processes between Cu(I) and the clay, e.g. the possibility of oxidation to Cu(II) by structural Fe(III) and the concomitant reduction of Fe(III) to Fe(II), cannot be ruled out. There are also uncertainties in the bulk properties of the copper sulphide corrosion layer and of a few centimetres of bentonite adjacent to this which may contain a small amount of copper sulphide, produced from aerobic corrosion products that had diffused away from the shell prior to the onset of anaerobic conditions. The consequences of a disturbed buffer/rock interface for long-term safety are discussed later in this section.

7.5.3 Titanium corrosion and interaction with bentonite

Titanium forms an insoluble TiO_2 passive corrosion layer on its surface under both oxic and anoxic conditions and over a wide pH range. The passivity will be maintained during the evolution of the repository environment in the abscence of localised corrosion (see section 7.2.3). Thus a titanium shell will corrode and release titanium to the bentonite buffer only slowly (at 1 nm of corrosion per year or lower). The limited studies that have so far been performed indicate that this titanium will not affect the bulk properties of the buffer. The speciation of titanium transferred to the clay by corrosion is, however, difficult to determine. This is because significant amounts of titanium are naturally present in bentonite, e.g. in the form of small TiO_2 particles (Rokle bentonite) or incorporated in the clay structure (MX-80). In a first series of batch experiments, MX-80 powder was reacted with titanium nanopowder, or with titanium foil, in 0.1 M NaCl solutions. Titanium concentrations remained low, and spectroscopic analysis showed no difference between the reacted and unreacted clay. In order to overcome the masking effects of the titanium background concentration, a second series of batch experiments used synthetic "Ti-free" montmorillonite. Preliminary results based on one single sample indicate that titanium from corrosion is incorporated into the clay structure or is surface-bound.

7.5.4 Iron-bentonite interaction

Iron corrosion products have a low solubility under expected repository conditions, but will nevertheless slowly dissolve, releasing Fe(II) to the buffer porewater, where it may subsequently react with montmorillonite and lead to montmorillonite alteration. Batch experiments by JAEA performed over a ten year period show that a large source of zero-valent iron in direct contact with bentonite induces high pH and low Eh conditions, as well as transformation of montmorillonite to non-swelling clay in samples exposed to NaCl and $NaHCO_3$ solutions. The increase in pH is most likely explained by the production of OH^- ions by the cathodic corrosion reaction and the uptake of Fe(II) by the clay which prevents the hydrolysis of the dissolved ferrous species which would otherwise produce protons to neutralize the hydroxide ions formed from the cathodic reaction. The high pH was considered to be the factor that had the most influence on the transformation of montmorillonite to the non-swelling clay berthierine. The batch experiments represent extreme and unrealistic conditions. A closer approximation to repository conditions is obtained represented by diffusion-type experiments, consisting of a cast iron cylinder surrounded by saturated compacted MX-80 bentonite, contacted by 0.5 M NaCl solution via a porous steel filter. The corrosion rate of iron was estimated to be about 1.5 μm per year, in agreement with previous corrosion studies in

compacted bentonite. Material examined from near the iron-bentonite contact showed, based on swelling pressure measurement, a slight decrease in swelling pressure, but no change in hydraulic conductivity. However, because of the small sample size, no clear conclusions in this regard could be drawn. No measurable occurrence of alteration was found, although there was an increase in iron – predominately Fe(II) – in the clay close to the contact. The most likely form of this Fe-pool is a mixed Fe(II/III) hydroxide green-rust type phase. The results confirm the large pH buffering capacity of the bentonite, which helps to counteract the alkalinity generated by the corrosion reaction.

Reactive transport modelling using the CrunchFlow code has been carried out to examine montmorillonite alteration over longer time periods than those that can be studied experimentally. The results suggest that the part of the buffer affected by montmorillonite alteration will be limited to a region extending only a few centimetres inwards from the shell. The main factors limiting the extent of alteration are (i), diffusional constraints, (ii), pH buffering from reactions in the clay and from the carbonate reservoir in the surrounding host rock and (iii), the low solubility of iron corrosion products. These conclusions are insensitive to all identified uncertainties, the largest of which concern the reaction kinetics of minerals and the thermodynamic data for clays. Alteration is expected to be fastest during the initial corrosion reaction, where clay dissolution may be triggered by the generation of OH^-. The predicted extent of alteration is largest (about 5 cm in 5,000 years) in cases where microbially-induced sulphate reduction is taken into account. However, because of hostility of the compacted clay environment towards microbial activity, sulphate reduction, if it occurs at all, will be limited to the interface zone between the host rock, the shell and the bentonite buffer.

7.5.5 Impact of hydrogen on bentonite porewater chemistry

Hydrogen is generated by the corrosion of all potential shell materials, but only in the case of iron is the expected generation rate high enough to lead to the formation of a separate gas phase and, in relatively tight drift sections, potentially large hydrogen partial pressures may form that may affect bentonite porewater chemistry. Preliminary considerations of relevant chemical reactions, scoping calculations and the results from reactive transport modelling indicate that the presence of hydrogen, together with corroding iron, will render porewater more alkaline and lower the redox potential. Thus, analysis from a recently updated thermodynamic model for compacted bentonite (Wersin et al. 2012), and taking into account surface reactions in the clay, the carbonate system and the precipitation of corrosion products, indicate that porewater pH will be buffered to slightly alkaline values (7.9–8.8), and will be unaffected by large hydrogen partial pressures. These findings are further supported by reactive transport calculations using the CrunchFlow code. Microbial processes may also generate or consume hydrogen, and one important aspect is that SRB may use hydrogen for reduction of sulphate to sulphide. The impact of these processes on porewater chemistry has not yet been assessed, and is recommended as a topic for future bounding calculations.

7.5.6 Evaluation of the consequences of a disturbed buffer/rock interface

In the safety analysis of a KBS-3H repository (Smith et al. 2007a, b), radionuclide transport calculations were carried out in which the buffer/rock interface was considered to be significantly perturbed, e.g. by the presence of the Supercontainer and its corrosion products or by thermally-induced rock spalling. In these calculations, the interface zone was treated as a "mixing tank" of effectively infinite hydraulic conductivity, due to the absence of data on its likely spatial extent and bulk properties.

In the Complementary studies of horizontal emplacement KBS-3H 2008–2010, scoping calculations have been carried out to illustrate more realistically the impact of perturbations to the buffer/rock interface on flow around a deposition drift and mass transfer between the KBS-3H buffer and flowing water. The calculations have shown that use of the "mixing tank" flow rate is conservative in all cases considered. These include cases where flow is parallel to the deposition drift as well as perpendicular to the drift, and in which the host rock is treated as either an equivalent porous medium or as a fractured medium. It has also been shown that various more realistic approximations to the flow through the interface zone and to the consequent radionuclide release rates to the rock could be used if values for the quantity $K\delta r$ (the product of zone thickness and hydraulic conductivity) could be obtained experimentally. The most appropriate approximation will depend on whether diffusion or advection is the dominant process moving radionuclides out of the interface zone into the rock. The dominant transport process needs to be checked on a case-specific basis.

7.5.7 Selection of materials

Establishing evidence on the long-term performance of the buffer including interaction with other materials was one of the main objectives of the recent project phase. A decision on a reference material for the Supercontainer, plugs and other structural components is required for further technical development and evaluation of the KBS-3H design, critically, the decision will form a basis for coming safety evaluations.

Long-term safety will always be the critical aspect in a repository material selection process. In addition technical and cost aspects have also been evaluated and weighed in. Operational and worker safety aspects are expected to be similar for all materials and the environmental impact is not expected to be critical for any of the materials. All these questions will be further evaluated in coming development work.

Copper, titanium and steel alloys are the alternatives that have been studied and that are compared in the sections below.

Selection of Supercontainer material

From the safety perspective, the most important aspect is the Supercontainer shell- clay interaction, which also has been the focus of these studies. When comparing the metal-clay interactions (Table 7-10) a number of questions have been discussed related to the corrosion properties, solubility, diffusion and sorption properties, evidence from natural analogues and known impact on physical properties of the clay and finally also the remaining uncertainties.

Based on the summary table:

- The corrosion behaviour of all metals is well known. The corrosion rate and production rate of hydrogen is lowest for Ti and highest for Fe, for which the possible risk of formation of a gas phase in tight very dry drift sections is thus also the highest1. Solubility for all metals is low but lowest for Cu and Ti.
- Ti is present as TiO_2 and in the clay structure in bentonites in various amounts, but these clays do not show any differences in the physical properties.
- Fe is known to react with bentonite by forming non-swelling silicate phases. Cu as Cu(II) is very reactive at high temperatures, but Cu(I) reactivity towards the clay is low as indicated from diffusion profiles. Natural analogues also suggest a low reactivity for Cu(I).
- Reported impact on physical properties of bentonite is highest for Fe, but very little is known about the impact of Cu and Ti. The extent of impact seems to be limited for all metals, due to the low corrosion rate and solubility for Cu and Ti, low solubility and slow diffusion rate for Fe. The range of impact according to modelling studies is expected to be 3–5 cm for Fe(II) and 2–3 cm for Cu.
- For all materials (Cu, Fe and Ti) there remain a number of uncertainties related to process understanding, formation of phases, diffusion and sorption, and possible impact on the physical properties in relevant repository conditions.

This limited scope of evaluation did not consider items such as manufacturing aspects, and only preliminary cost estimates are presented in Table 7-12.

[1] The degree to which gas can accumulate in a given drift section, and hence the degree to which it affects groundwater inflow and drift saturation, depends strongly on the hydraulic properties of the adjacent rock, including the excavation damaged zone (EDZ) around the drift and transmissive fractures in the rock that intersect the drift wall. However, in tight very dry drift sections in which the average hydraulic conductivity of the rock is in less than about 10–13 m s-1, repository-generated gas from the corrosion of steel components in the drift is expected to hinder or prevent altogether the saturation of the buffer until gas generation by steel corrosion ceases and gas pressure falls, which, as noted above, is expected to take up to tens of thousands of years, assuming a rate of steel corrosion rate towards the low end of the range of uncertainty (Gribi et al. 2007).

Table 7-12. A summary of properties of the alternative Supercontainer shell materials.

Properties	Iron (carbon steel)	Copper	Titanium	Most favourable for long-term safety
General knowledge about material.	Well known corrosion behaviour.	Well known corrosion behaviour.	Well known corrosion behaviour.	
Corrosion rate (long-term anaerobic conditions).	1–2 µm/year.	< 0.01–0.03 µm/year (sulphide present).	< 0.001 µm/year.	
Hydrogen production rate.	High.	Low.	Very low.	Titanium lowest rate.
Risk for formation of a gas phase?	In tight very dry drift sections.	Very low.	Very low.	Low risk for titaniumand copper.
Solubility in anaerobic conditions.	10^{-5}M	~ 10^{-12}M	10^{-9}M	Low solubility of copper and titanium.
Present in clays.	In the structure and as hydroxide, pyrite and carbonates.	?	As microcrystalline TiO_2 and in structure.	
Reactivity with bentonite.	Known to react with bentonite by forming non-swelling silicate phases.	Cu(II) ions known to be reactive, strongly sorbed as inner sphere surface complexes; at high T (> 200°C) Cu(II) enters the structure Cu(I) shows lower sorption affinity towards bentonite.	Not studied so far according to our knowledge. TiO_2 is considered as one of the most inert materials on surface.	Low reactivity of titanium and copper.
Impact of redox conditions on mobility.	Under reducing conditions, Fe(II) stabilized, under oxidizing conditions formation of Fe(III) oxides.	Under reducing conditions Cu(I) stabilized, under oxidizing conditions more soluble Cu(II).	Insoluble Ti(IV) expected for both reducing and oxidizing conditions.	
Reported impact on bentonite/experimental and modelling studies.	Reduction of swelling pressure and increase in hydraulic conductivity has been reported (very few relevant studies though available). Also modelling studies have been performed. The modelling points towards an altered zone of 3–5 cm forming within 5,000 years.	Cu(II) at high temperatures (> 200°C) causes decrease in swelling pressure but this reaction is not likely at the temperature range of the repository. Some relevant experimental studies available but none on the potential physical impact on bentonite. Generally Cu(I) corrosion layer is estimated to be 2–3 cm.	No literature data available on the impact on bentonite. First results from the KBS-3H studies available, though only analyses of occurrence of titanium in clay and possible uptake of titanium in clay. However, bentonites containing different content of titanium do not show any differences in physical behaviour.	Low reported impact of titanium followed by copper.
Known factors affecting the extent of impact.	Fe(II) penetration into bentonite is expected to be diffusion-limited and also limited by low solubility.	Low corrosion rate and slow diffusion and low solubility of Cu(I).	Very low corrosion rate and solubility.	
Influence on the corrosion rate of the canister.	May reduce the corrosion rate of the canister due to consumption of sulphide.	May reduce the corrosion rate of the canister due to consumption of sulphide.	Probably none.	Copper and iron may consume sulphide.
Natural analogues.	There is little natural analogue data available. Analysis of ancient iron objects buried in clay sediments or iron-rich altered volcanic rocks might provide interesting information.	Some natural analogues available. Natural analogues suggest low reactivity of Cu(I).	Titanium in the natural clay materials Rokle bentonite, Opalinus Clay and Illite du Puy occurs as microcrystalline TiO_2 (presumably as anatase). Possible also as structural titanium in MX-80.	
Main known/remaining uncertainties.	Which phases will form and which processes take place, e.g. can reduction of structural iron take place? Also better data on Fe(II) diffusion in bentonite is needed (ongoing research at VTT). More experimental data is needed on impact of iron in relevant repository conditions.	May Cu(I) be oxidised to Cu(II) by structural Fe(III) in the bentonite? No available information on eventual changes in physical properties due to interaction in relevant repository conditions.	Very scarce data on possible reactivity with clay. Uncertainties in the technical set-up in 3H tests would need to start up new experiments. Could stiffness of titanium (TiO_2) have an impact on clays mechanical properties?	Still remaining uncertainties for all materials.

Properties	Iron (carbon steel)	Copper	Titanium	Most favourable for long-term safety
Ongoing activities related to metal/clay interaction.	French programme/ ANDRA. Some research starting up by Nagra. ABM-studies. SKB/Studies on structural iron. VTT/studies on diffusion and sorption of Fe(II).		Still ongoing accelerated titanium-clay tests within the KBS-3H project.	Still ongoing studies on iron and titanium interaction with clay.
Technical aspects Manufacturing*	Well proven manufacturing and installation procedures/experiences exist already.	New manufacturing and installation procedures must be established. Manufacturing and installation are more demanding than for carbon steel**	New manufacturing and installation procedures must be established. Manufacturing and installation are more demanding than for carbon steel.	Manufacturing and installation need to be established for copper and titanium.
Costs for manufacturing a SC shell*	150 kSEK	340 kSEK	310 kSEK	

* Both manufacturing estimates and costs are very preliminary as there is as yet no detailed design available for the Cu or the titanium SC shell. Estimated costs are considering serial production, why single prototypes will be considerably more expensive. Indicated costs are for manufacturing performed in work shop, which includes the material cost. The assembly of the SC which will be performed in the assembly hall at the repository is not included, however, these costs are assumed to be the same for titanium and copper.

** The statement is made with regards to welding aspects. Welding in steel is less demanding than titanium and copper, especially for titanium where shielding gas is extremely important.

As for the mechanical properties of the materials the load cases are exactly the same regardless of the material. However, the yield strengths for the materials differ and the allowable stress levels that can be accepted. The material thickness must therefore be increased for the weakest material (copper) not to exceed allowable stress levels.

When weighing up all the aspects presented above a recommendation to proceed with titanium as the reference Supercontainer material can be made. Titanium is expected to be the most inert, having lowest corrosion rate and lowest rate of production of hydrogen. In addition, this element is already present in various amounts in natural bentonites which have been shown to display favourable properties as buffer materials Titanium has been selected.

A steel based Supercontainer is not excluded entirely and if additional research verifies that its implications on long-term safety are within the requirements the selection should be re-evaluated).

Selection of plug and structural component materials

In addition to the Supercontainer itself, various other metallic components are left in the deposition drift after closure, including supports for the Supercontainer and distance blocks, and compartment and drift plugs. Based on the preliminary analysis, it is considered feasible to manufacture all of these components from the same materials, e.g. the use of steel tools in handling titanium components can lead to accelerated corrosion of Ti alloys if Fe particles become embedded in the oxide film. Dissolution of the Fe particles followed by hydrolysis of the resulting Fe (III) can lead to initiation of a form of localized attack. These problems can be prevented by avoiding galvanic couples and the use of steel handling tools for the emplacement of the Supercontainers and other metallic components in the deposition drift, such as compartment and end plugs, drip shields, air evacuation pipe, etc.

The reasoning presented above in the Supercontainer section is valid for the compartment and drift plug and other structural components as well. Copper is furthermore excluded as plug material for mechanical reasons. The material recommendations will hence be the same as for the Supercontainer and Titanium has been selected.

8 Layout adaptations

The scope of the Complementary studies of horizontal emplacement KBS-3H 2008–2010 phase included layout adaptations for KBS-3H at Forsmark and Olkiluoto. The main input in both cases was the latest layout work carried out for KBS-3V (SKB 2009c, Kirkkomäki 2009). For the Olkiluoto case basis is also found in layout adaptation work done in earlier project phases (Autio et al. 2008). The approach was somewhat different for the two sites. For Forsmark it was calculated whether a KBS-3H layout could host the required amount of canisters (6,000) in the same proposed layout and area as for KBS-3V, for the Olkiluoto case a certain number of canisters (2,820) was placed in a certain area and the outcome was the efficiency of the area used. The estimated excavated rock volumes between the two designs were also compared for both sites.

8.1 Layout adaptation at Forsmark

Two alternatives were modelled, one with 40 m and one with 30 m spacing between the deposition drifts. The 40 m spacing is equal to the original layout for the vertical emplacement and the 30 m spacing between the deposition drifts was selected to see if this could resulted in better utilization of the available deposition area. Figure 8-1 illustrates the underground layout with 30 m spacing between deposition drifts.

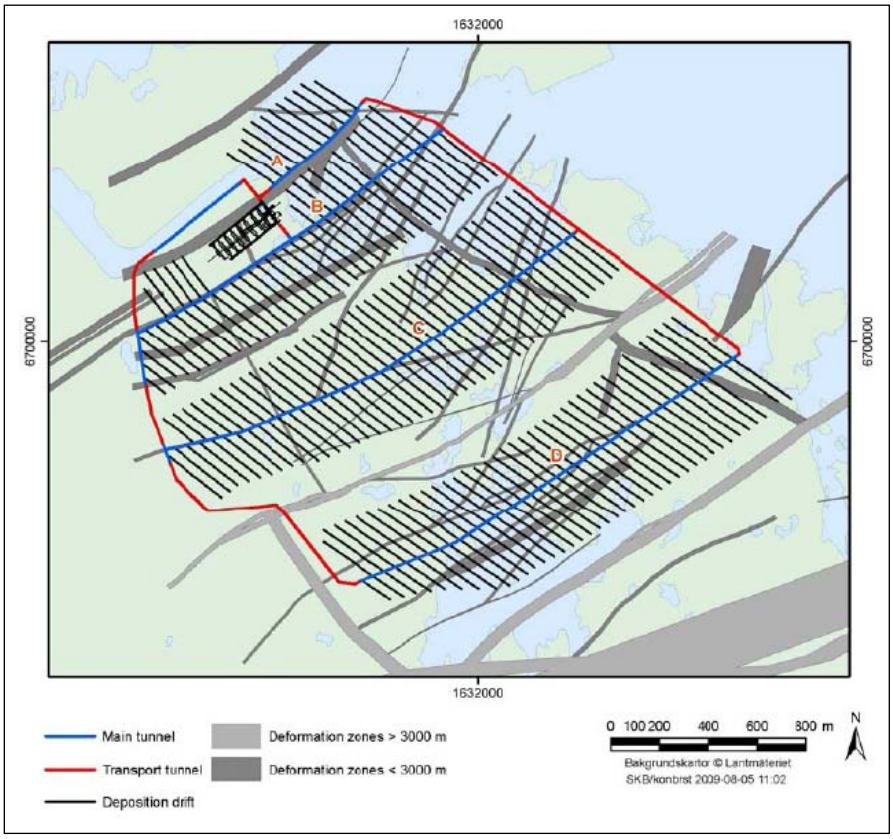

Figure 8-1. *Layout alternative with 30 m drift spacing. "A" to "D" stand for different main tunnels. Section at 470 m depth.*

8.1.1 Methodology and restrictions

The design methodology for the layout of KBS-3H was based on the design methodology for KBS-3V, which is described in SKB (2007). The relevant chapter concerning the layout in SKB (2007) denotes that a compilation of layout options with adequate capacity and with regard to conditions noted in SKB (2009a) should be carried out. Consequently and as mentioned earlier two layout options have been modelled, 40 m and 30 m. Other chapters in SKB (2007), concerning the initial study, functionality study, evaluation of constructability, and risk evaluation of proposed layout, were not included in the KBS-3H study. Some additional deviations from SKB (2007) are listed below.

- The dimensions of the deposition tunnels described in SKB (2007) are not relevant as the deposition drifts for the horizontal emplacement have specific dimensions.
- In KBS-3H the distance between two drift ends is allowed to be 10 m, rather than the 80 m stated in SKB (2007) for the KBS-3V layout, since drifts are drilled and not blasted.
- Drifts that are penetrated by investigation boreholes are supposed to be rejected. However, it is considered that a drift can be adjusted geometrically so that it is not penetrated by an investigation borehole. Consequently the drifts that seem to be penetrated by investigation boreholes have not been rejected in the KBS-3H layout.

The Site Engineering Report (SER) for Forsmark (SKB 2009a) is also based on vertical emplacement, a few recommendations and/or requirements in these report are hence not either applicable with horizontal emplacement. The following list describes the main deviations from SKB (2009a).

- Whenever a requirement is denoted for the layout of a deposition hole, considerations have been taken, and adjusted, to the emplacement of Supercontainers.
- In the vertical emplacement the distance between deposition holes is 6.0 and 6.8 m, respectively, depending on the thermal properties of the specific rock domain. These distances are not to be used in the horizontal design. Instead the distance between Supercontainers is to be used. Thermal dimensioning analyses for KBS-3H have only been carried out in Forsmark main rock domain RFM029, this data was used as basis to calculate the distances regardless of rock domain; results are presented in Table 8-1. The table presents the results for tunnel spacing 40 metres and 30 metres and with rock conductivity 2.9 and 3.57 W/mK. The lower value corresponds to the 0.1 percentile of the conductivity and the higher value is the mean conductivity value for the Forsmark main domain, RFM029. The layout is based on the values calculated for the 0.1 percentile conductivity, the shaded area in the table. Thus the distance between Supercontainers is dependent on the rock domains and the used drift spacing.
- According to SKB (2009a) the allowed inflow rate is 5 l/min per 300 m tunnel for the vertical alternative whereas the earlier value of 10 l/min for KBS-3H was used for the horizontal layout study.

  The reason of having higher inflow criterion in KBS-3H compared to KBS-3V is the fact that the 3H variant (DAWE design) will be drained during the installation phase (inclined drift) and the components composed of bentonite clay will be standing on feet forming a gap of 42.5 mm around the components. This allows the water to flow freely out of the drift without being in contact with the components which would cause mechanical erosion of bentonite. The components could allow a flow of several tens of litres per minute but the deposition machine based on water cushion techniques has to be modified if the inflow exceeds 7 l/min (i.e. inflow after the inflow sections (> 0.1 l/min) of the drift have been grouted).
- The degree of utilization was assumed to be the same as in the KBS- 3V design, where the main alternative assumes a 13% loss of positions due to large fractures. This assumption will require future investigation including definition of a criterion for KBS-3H when to abandon canister positions and which are the inflows accepted at different positions in the drift. The practicality of using the Full Perimeter Intersection Criterion (FPI) has still to be evaluated in terms of its consequences for unnecessarily discarding deposition holes in case they are intersected by an FPI fracture that in reality has a limited size and thus unlikely to undergo damaging shear movements and also not to form continuous type connections through fracture network. Even further using the Extended Full Perimeter Intersection Criterion (EFPC) in a similar way as in KBS-3V would likely mean a considerable increase in lost positions for KBS-3H.

Table 8-1. Canister spacing's depending on rock conductivity 2.9 and 3.57 W/(mK) and drift spacing. The lower value corresponds to the 0.1 percentile of the thermal conductivity and the higher value is the mean conductivity value for the Forsmark main domain, RFM029. The drift spacing assumes air in all slots and eccentric placed canisters.

Conductivity (W/mK)	2.9	3.57
40 m drift spacing (m)	7.9[1]	6.5[2]
30 m drift spacing (m)	8.6[3]	7.2[4]

[1] Correspons to a distance block with a length of 2.34 m.
[2] Correspons to a distance block with a length of 0.94 m.
[3] Correspons to a distance block with a length of 3.04 m.
[4] Correspons to a distance block with a length of 1.64 m.

8.1.2 Layout

The first model, a layout with 40 m spacing between deposition drifts, was done to best compare the possible number of positions with the vertical alternative which yields a gross capacity of 7,818 deposition positions. The second model, an alternative with 30 m spacing between deposition drifts, was completed to see what difference a layout with smaller distance does to the capacity in terms of number of deposition positions.

The gross capacity of the 40 m spacing alternative will be 5,922 canisters, while the 30 m spacing alternative yielded 7,215 canisters. This alternative allows for 17% loss of positions. Two reserve areas have been identified as a possible means of adding capacity. One area south of deformation zone ENE0062A which would yield 553 positions in the 40 m spacing alternative and 674 canister positions in the 30 m spacing alternative (~730 positions for KBS-3V). This area was excluded in the initial calculations since it was considered small in relation to the possible problems when passing zone ENE0062A. The other area is located underneath the nuclear power plant and it should be noted that this is outside the administrative boundary and is presently not allowed to be used. If this area can be allowed it would give space for some 243 canisters in the 40 m spacing alternative and 282 canister positions in the 30 m spacing alternative. Together these areas would yield 796 extra canister positions for the 40 m alternative and 956 positions for the 30 m spacing alternative. The gross capacity, including reserve areas, is thus raised to 6,718 canister positions for the 40 m spacing alternative, which allows for 11% of position loss to reach the limit of 6,000 net positions. The gross capacity of the 30 m alternative with reserve areas comes up to 8,171 canister positions, which allows for 27% loss. Several optimization alternatives have been proposed to possibly further raise the capacity of the horizontal alternatives:

- If drifts are allowed to be longer than the stipulated 300 m several canister positions can be gained.
- If the distance between the end of the niche and the drift plug is allowed to be a little flexible and go below the stipulated eight metres, further positions can be gained.
- Some flexibility regarding drift orientation may allow for more deposition positions.
- Some of the stochastically judged deformation zones are also included in the geological model, which has as consequence that deposition positions are lost twice.

8.1.3 Comparison between vertical and horizontal deposition

There are large differences between the two alternatives: vertical versus horizontal emplacement of canisters. Not only with respect to amount of possible canister positions but also regarding, for example, the excavated rock volume, costs and environmental effects. All of this was not within the scope of the KBS-3H Forsmark layout adaptation work; some comparisons of excavated rock volume were, however, made to facilitate further evaluation.

The "skeleton" of the underground facility, i.e. the main and transport tunnels, is largely the same for both KBS-3V and KBS-3H. Therefore, the excavated volume for these tunnels remains unaltered. Concerning the excavated volume for deposition tunnels and deposition drifts, respectively, the difference is, however, significant since the drifts in the KBS-3H alternative have a much smaller diameter than the deposition tunnels in the KBS-3V alternative. In addition, deposition holes are excavated in

KBS-3V. In Table 8-2 and Figure 8-2 a comparison of the excavated volume is shown. It is important to understand that the excavated volume has been calculated on the gross capacity for each alternative and not on the net capacity (6,000 positions). This is due to the complexity in predicting where the exact position of losses will occur and whether this will cause shortening of a deposition tunnel/drift or simply relocating canister positions. Therefore, the actual difference in excavated volume may be somewhat smaller but still significant. While this number may be subject to discussion the calculated excavated volume per canister is a relevant number to compare (see Figure 8-3).

Table 8-2 also shows the required area per canister which will be larger for the horizontal alternative; the figures have been estimated based on the area needed for the vertical alternative. While excavated rock volume is in favour of KBS-3H the larger footprint of a horizontal repository works in the other direction and must be closely considered when doing both safety assessments and cost comparisons.

8.1.4 Conclusions

The gross capacity of the layout using KBS-3V was 7,818 deposition positions. The horizontal alternative with 40 m spacing provided a gross capacity of 5,922 deposition positions, which is less than the required net capacity of 6,000. Adjusting the deposition drift spacing to 30 m increased the gross capacity to 7,215 deposition positions. If the two reserve areas are utilized using the 30 m horizontal alternative the gross capacity of the repository increases to 8,171 deposition positions. The layouts used to reach theses gross capacities were not optimized for horizontal emplacement and hence there may be more efficient layouts that can increase the gross capacity above these values. Nonetheless, it appears from these preliminary analyses that a horizontal alternative, which will provide the required capacity for deposition positions, can be achieved.

For future layout adaptations specific KBS-3H criteria for utilization will have to be developed (compare FPI and EFPC for KBS-3V) and evaluated in terms of its consequences for unnecessarily discarding deposition holes in case they are intersected by e.g. an FPI fracture that in reality has a limited size and thus unlikely to undergo damaging shear movements.

When looking at the deposition area, the calculations done on excavated rock volume shows that it is in the order of 1/3 for KBS-3H compared to KBS-3V. This will lower the cost for KBS-3H since every cubic meter of rock that is not excavated does not only lower the excavation cost but reduces the amount of backfill material and work required to place that backfill. A complete cost analysis taking care of all these aspects were, however, not included in the layout adaptation work.

Table 8-2. Comparison of estimated excavated volumes between different layout alternatives, calculated on gross capacities.

Layout alternative	3V	3H	3H
Distance between deposition tunnels/drifts	40 m	40 m	30 m
Excavated volume, m^3			
Access ramp and shafts	205,500	205,500	205,500
Rock loding station	7,100	7,100	7,100
Central area	111,500	111,500	111,500
Transportation tunnels	182,100	182,100	182,100
Main tunnels	384,100	384,100	384,100
Sum	**890,300**	**890,300**	**890,300**
Deposition tunnels and holes	1,287,900		
Drifts		317,300	426,800
Total	**2,178,200**	**1,207,600**	**1,317,100**
Number of canisters	7,818	5,922	7,215
Excavated volume per canister, m^3	279	204	183
Required area per canister, m^2	444	586	481

8.2 Layout adaptation at Olkiluoto

The updated layout adaptation to the Olkiluoto site was done using the same principles as in the KBS-3V adaptation (Kirkkomäki 2009) in 2009. The total amount of canisters was 2,820 and the total amount of canister positions were 10% bigger, i.e. 3,102. The spacing between deposition drifts was 25 m and the spacing between canisters varied from 7.2 m to 10.6 m depending on the canister and spent nuclear fuel type. As with the Forsmark layout, the layout was carried out assuming a one-storey repository design.

The bedrock model (Hellä et al. 2009) was the same as in the KBS-3V adaptation (Kirkkomäki 2009) (Figure 8-2). It is based on the data (Posiva 2009) that were available in 2009. The latest data and bedrock model is a little different, but in this work it was decided to use the same bedrock model so that the two adaptations were made comparable. The principle of having two parallel central tunnels used in the KBS-3V adaptation (Kirkkomäki 2009) was also used in this work. The deposition drifts are connected to the parallel central tunnels. The distance between the central tunnels is about 20 metres. The purpose of using the parallel tunnel principle is to ensure the maximum flexibility in construction and operation phases.

Parallel central tunnels provide also efficient emergency exit facilities. The central tunnels are separated in two different fire compartments. This allows quick movement from one fire compartment to another in the event of an accident.

The length of the deposition niche is about 23 metres. The distance between the central tunnels is about the same and the niches can be made between the central tunnels. This configuration gives the opportunity to operate two deposition drifts from one niche. This saves excavation volume and gives better efficiency of the use of the deposition area.

The KBS-3H layout adaptation to the Olkiluoto site is presented in Figure 8-3. There are 122 deposition drifts and the total length of those is 31.5 km. The total length of the central tunnels is 9.2 km. The total excavated volume of the disposal facility is 920,800 m^3. The volume of the deposition drifts is 84,800 m^3 and the central tunnels 441,000 m^3.

The total volume of the disposal facility is not going to be excavated at once. It has been divided into eight excavation phases (Figure 8-4). Building of the underground research facility ONKALO is the first one. It begun in year 2004 and should be completed in year 2011. ONKALO rooms will form the basis for the rest of the disposal facility.

The implementation of the disposal facility will commence with extending the ONKALO facility. Before the disposal of the canisters is started, the central tunnels and deposition drifts that are needed in the first deposition stage will be constructed. The total excavated volume of the preparation stage is 182,900 m^3. During the operational stage more central and deposition drifts are constructed in six excavation stages with an average excavating volume of about 52,500 m^3 (Table 8-3).

The largest open volume during the operation phase at a time in the disposal facility is about 695,700 m^3. That is 77 % from the total volume. Minimum open volume during the operation phase is 520,900 m^3, which is 58% from the total volume. The average open volume during the operation phase is 577,100 m^3.

Compared to the KBS-3V layout (Figure 8-5 and Table 8-4) the total volume of the central tunnels in KBS-3H layout is 135,600 m^3 bigger. For the KBS-3V layout the total volume of the central tunnels is only 287,200 m^3. The layout of KBS-3V is relatively uncomplicated to draw up, especially in northeast from the ONKALO. For KBS-3H the maximum length of deposition drifts is 300 metres, which is 50 metre shorter than the maximum length of the deposition tunnels in KBS-3V. This combined to the shape of the deposition area and the orientation of the deposition drifts makes it impossible to use efficiently the same layout in KBS-3H. To cover the deposition area efficiently the layout of the central tunnels has to be more complex.

Table 8-3. Excavation phases of the underground disposal facility excluding the volume of the deposition drifts (Kirkkomäki and Rönnqvist 2011). Phases 1 to 6 are shown in Figure 8-6.

Phase	Volume (m^3)
ONKALO	337,921
Preparatory phase	182,940
Phase 1	47,384
Phase 2	59,981
Phase 3	57,141
Phase 4	44,896
Phase 5	68,781
Phase 6	36,926
Total	835,970

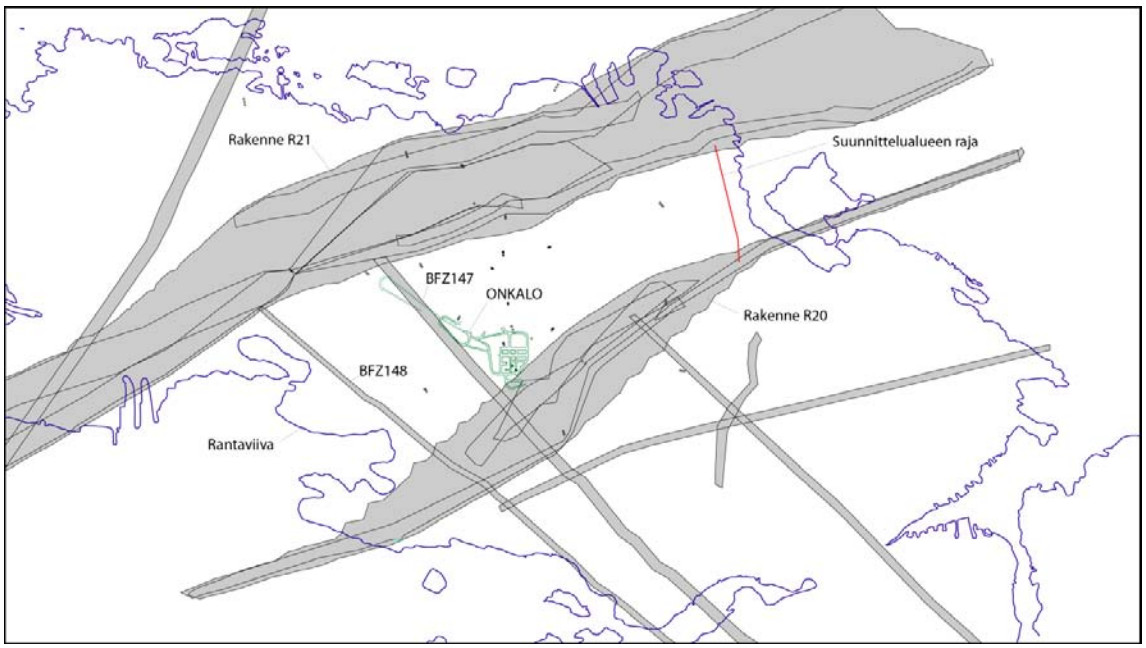

Figure 8-2. *Olkiluoto major fracture zones (gray) according to the 2009 research data, ONKALO (green) and coastline (blue)(Kirkkomäki 2009).*

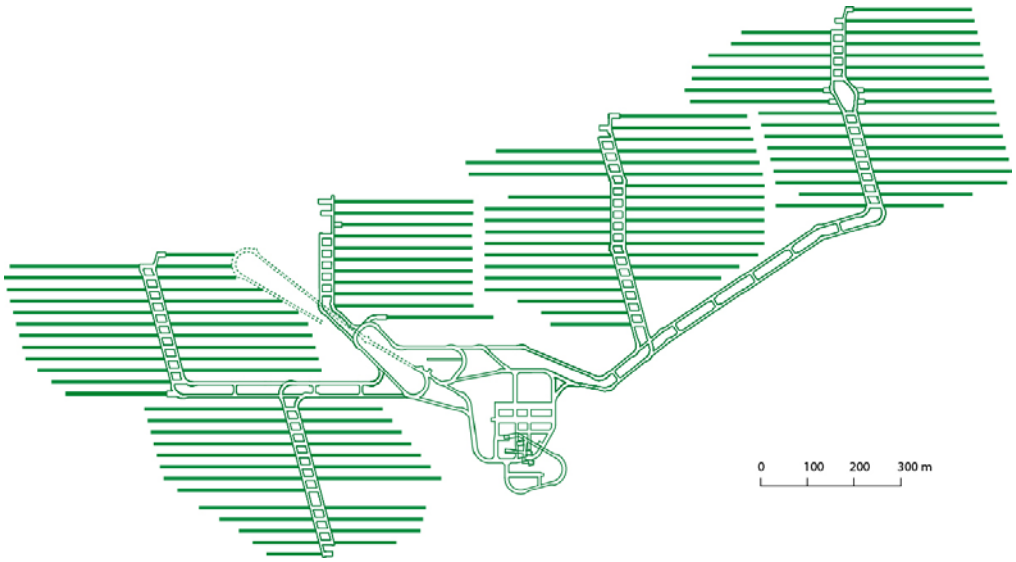

Figure 8-3. *KBS-3H layout adaptation to the Olkiluoto site (Kirkkomäki and Rönnqvist 2011). The layout area shown is between fracture zones R20 and R21, see Figure 8-4.*

Figure 8-4. *Construction phases of the underground disposal facility in Olkiluoto, a) ONKALO, b) preparatory phase and c) – h) excavation phases 1–6 (Kirkkomäki and Rönnqvist 2011).*

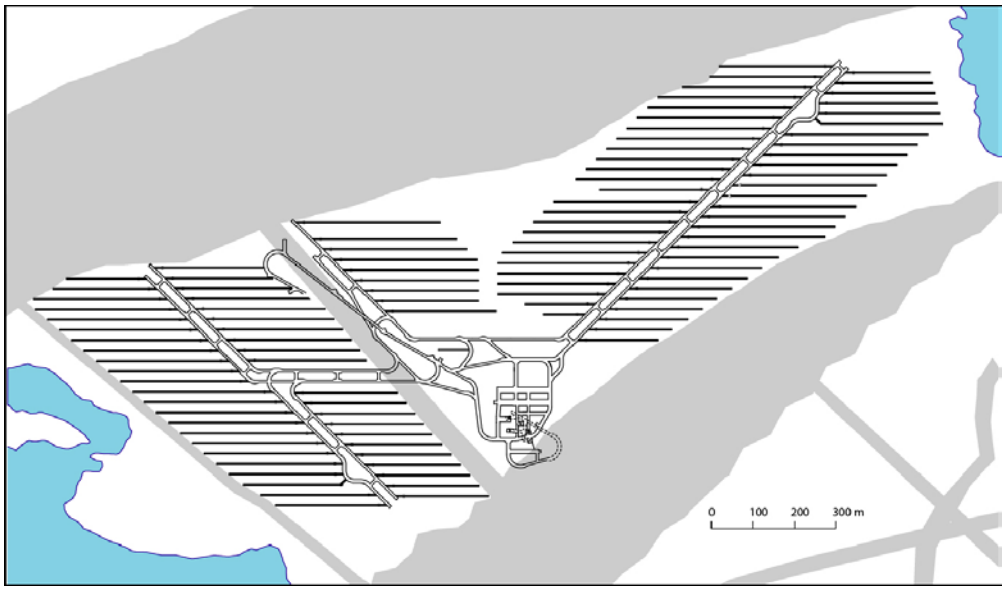

Figure 8-5. *Comparative KBS-3V layout adaptation to the Olkiluoto site (Kirkkomäki 2009).*

Table 8-4. Comparison between KBS-3V and KBS-3H layouts. (Kirkkomäki and Rönnqvist 2011).

	KBS-3H	KBS-3V
Number of deposition drifts/tunnels	122	105
Total length of deposition drifts/tunnels	31,547 m	31,244m
Average length of deposition drifts/tunnels	259 m	298 m
Maximum length of deposition drifts/tunnels	300 m	350 m
Total volume of the underground disposal facility	920,769 m^3	1,166,398 m^3
Excavation volume of the disposal facility **	835,970 m^3	1,114,301 m^3
Total volume of the deposition tunnels	–	436,661 m^3
Total volume of the deposition drifts/holes	84,799 m^3	52,096 m^3
Total volume of the central tunnels	440,976 m^3	287,201 m^3
Total volume of the access tunnel, shafts and shaft connections	280,216 m^3	280,216 m^3
Total volume of the technical rooms	78,284 m^3	73,730 m^3
Total volume of the repository for low- and intermediate-level waste	36,494 m^3	36,494 m^3
Maximum open volume of the disposal facility at once *, **	695,723 m^3	698,771 m^3
Minimum open volume of the disposal facility at once *, **	520,861 m^3	513,259 m^3
Average open volume of the disposal facility at once *, **	577,104 m^3	595,812 m^3

* During the operation phase.
** Excluding the volume of the deposition holes/drifts.

8.2.1 Conclusions

In the KBS-3H layout design for Olkiluoto the total number of the canisters was about 2,820. The layout adaptation for the KBS-3V made earlier for the same area using the same deposition tunnel/drift direction included the same number of canisters. In Olkiluoto's case the footprint is just slightly larger in KBS-3H design compared to KBS-3V. The same spacing (25 m) between deposition tunnels/drifts is used. In KBS-3H design the length of the drifts is limited to 300 m and in KBS-3V the corresponding maximum length of a deposition tunnel is 350 m.

The total excavated volume of the repository was about 921,000 m^3 for KBS-3H design and about 1,166,000 m^3 for KBS-3V. In both designs the utilization degree was estimated to be the same. The layout was designed for a number of canisters that is 10% higher than actually needed.

9 Construction and Operation

This chapter introduces the outlining of the preliminary production lines. They are followed by an account of the work carried out regarding the construction of drifts; drilling, measurement techniques and rock spalling. The characterisation and handling of water, grouting techniques, is then elaborated under the section on groundwater control.

There has been limited work carried out with the horizontal deposition machine and no work carried out concerning canister retrieval in the recent project phase, an account for the deposition technique and earlier retrieval work is, however, given to present the whole picture.

Operational and workers safety for drift construction and preparation, Supercontainer assembly and for the deposition work has also been addressed by preliminary safety analyses and are.

9.1 Outlined production lines for KBS-3H

The work on preliminary production lines during the project phase 2008–2010 aimed at defining the work with the compilation of the production line reports for KBS-3H to be performed within the next project phase. The production lines have mainly been structured in the same way as for the KBS-3V design (SKB 2010c). The work that shall be performed within the next project phase shall be based on the production reports compiled for the KBS-3 reference design. Some of these reports are more or less also valid or not relevant for KBS-3H design.

The production line reports, as illustrated in Figure 9-1, are part of the safety report for the KBS-3 repository and repository facility. The Production line reports will provide information on how to produce, handle and inspect the engineered barriers and underground openings within the facilities of the KBS-3 system. The so-called “Engineered barriers” includes the production of “Canisters”, “Supercontainer”, “Buffer and filling materials”, “Plug” and “Closure”. Further, they will provide information on acceptable impairments on the engineered barriers in order for them to be fit for deposition or installation.

It is important to recognize that the handling of the engineered barriers and construction of underground openings is a safety related quality assurance issue. Canister handling is also important from an operational safety point of view in the KBS-3 repository facility.

An overview of the KBS-3H system and the handling of spent fuel, production of the different technical barriers and the construction of the underground openings are illustrated in Figure 9-2.

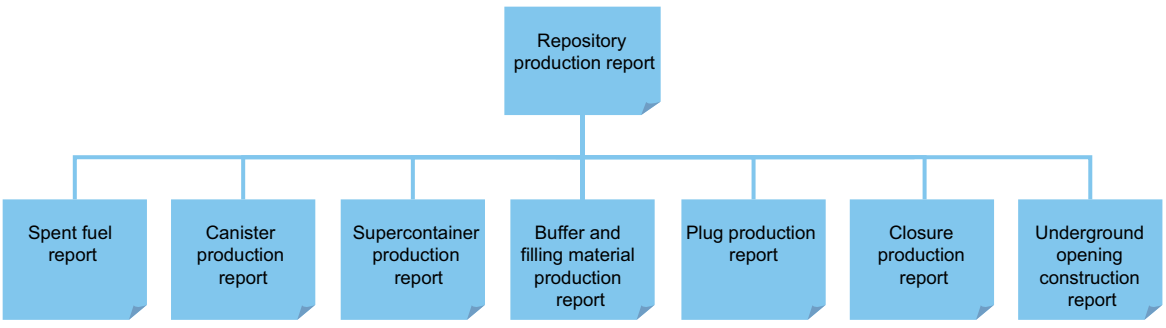

Figure 9-1. *Set of reports accounting for how the KBS-3H repository is designed, produced and verified.*

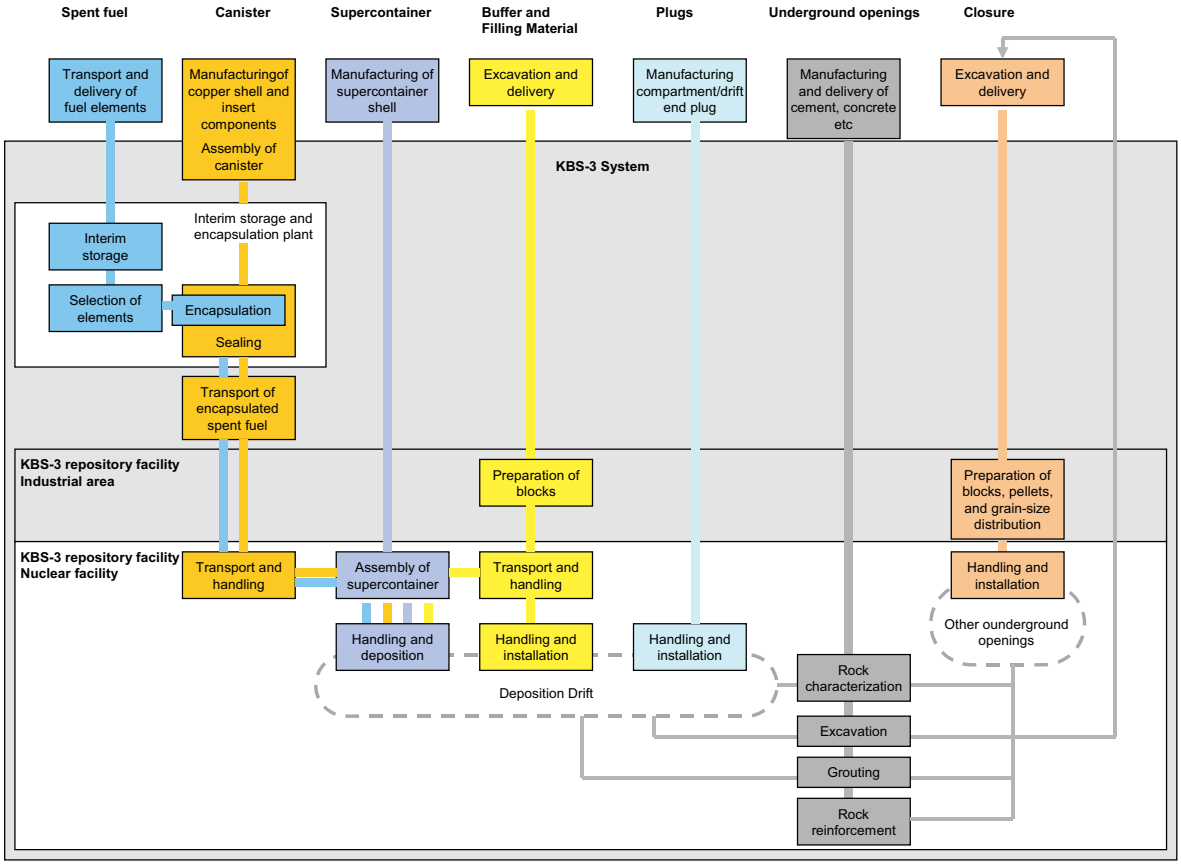

Figure 9-2. *Overview of the main parts of the production lines for the spent nuclear fuel, engineering barriers and underground openings of the KBS-3H repository and within which of the facilities of the KBS-3 system they are performed. Facilities marked with white colour are nuclear facilities.*

9.1.1 Purpose and Objectives

The purpose of the set of *Production line reports* is to account for how the spent nuclear fuel is handled and how the engineered barriers and underground openings of the KBS-3H repository are designed, produced and inspected in a manner related to their importance for the safety of the KBS-3H repository. With the *Production line reports* the next project phase intends to present the design premises for the KBS-3 repository and their sources, and demonstrate how the engineered barriers and underground openings can be designed and produced to conform to the stated design premises. The *Production line reports* shall present the current reference designs and production methods and summarise the research and development efforts that supports that the KBS-3H repository can be produced in conformity to the design premises.

The purpose with the – **Repository production report** – is to give an overview of the barriers and barrier functions of the KBS-3H repository and to provide the overarching design premises for their design. The report shall also provide an overview of the KBS-3H system and the production lines for the handling of the spent nuclear fuel, the production of the engineered barriers and construction of the underground openings.

The objectives of this report are to account for:

- the role of the *Production line reports* within the safety report,
- central concepts and their definitions,
- overarching design premises for the KBS-3 repository and its engineered barriers and underground openings,
- the methodology to derive and manage design premises,
- the KBS-3H repository, its barriers and their barrier functions,
- the KBS-3H system and the handling of the spent fuel and the production of the KBS-3H repository with focus on common aspects and interfaces and dependencies between the production lines,
- present the safety and quality classes for the different parts of the KBS-3H repository and introduce the quality assurance measures that are carried out before the production and construction is initiated and during the production and construction.

The purpose of the **Spent Fuel report** is to present the spent nuclear fuel to be deposited, provide the information about the spent nuclear fuel needed for **SR-Site,** to present the spent nuclear fuel to be handled and to give an overview of its way through the KBS-3H system.

The purpose of the **"Engineered barrier"** production reports and the "**Underground openings construction report"** is to provide information on design premises, design, production and construction and the resulting initial state as a basis for the safety assessment **SR-Site**. The"**Engineered barrier"** production reports and the "**Underground openings construction report"** shall also provide information to PSAR-operation concerning the handling, deposition and installation of the engineered barriers and construction of the underground openings.

The objectives of these reports are to account for:

- the design premises (SKB) or design basis (Posiva),
- the reference design,
- the conformity of reference design to design premises,
- the planned production,
- the initial state, i.e. the results of the production.

9.1.2 Content of work

Repository production report

This report is to be updated to reflect the new Engineered barrier reports that will be introduced for the KBS-3H design.

Spent Fuel Report

This report is valid also for KBS-3H. No update needed.

Canister Production Report

This report is to be updated with requirements and information that is specific for the KBS-3H design.

- Some load cases are different for KBS-3H.
- The handling in the reloading station is different.

Closure Production Report

This report is valid also for KBS-3H. The report to be updated with information regarding backfill of the KBS-3H niche.

Backfill and Plug Production Report

Backfill of the deposition tunnels are not needed for the KBS-3H design why this report will be deleted for the KBS-3H work. The plugs described in the report will be included in a new report called Plug production report. Backfill of the niche will be included Closure Production report.

Supercontainer Production Report

This is a new report that will include the following:

- Manufacturing of the Supercontainer shell in workshop.
- Transportation from workshop to the reloading station.
- Assembly of the Supercontainer in the reloading station including description of the shielded handling cell.
  - Handling equipment for shell and buffer.
  - Welding equipment.
  - Transportation tube (including gamma gates) for Supercontainer.
  - Handling equipment for transport tube.
- Transportation of the transport tube with Supercontainer from reloading station to deposition niche.
- Deposition of the Supercontainer, including description of the deposition equipment.
  - Set-up of equipment in the niche.
  - Operational aspects (deposition speed).

Buffer and filling material production report

This report shall be based on the buffer production report (SKB 2010e). The report shall cover:

- Manufacturing of blocks and rings (Supercontainer).
- Manufacturing distance blocks.
- Manufacturing filling material.
- Storage and transportation.
- Emplacement of distance blocks and filling material, including description of equipment for emplacement of buffer (distance blocks) and filling materials.
  - Set-up of equipment in the niche.
  - Operation aspects (emplacement speed).

Plug production report

This is a new report that will include the following:

- Manufacturing of compartment/drift end plugs.
- Transportation from workshop to the reloading station.
- Installation of compartment/drift end plug.
  - Operational aspects.
- Installation of air evacuation pipes and water filling pipes.
- Water filling.
  - Operational aspects.
- Removal of air evacuation pipes and water filling pipes.
  - Operational aspects.

Underground Opening Construction Report

This report is to be updated with information regarding excavation of the deposition drifts:

- Excavation of niche.
- Pilot hole drilling deposition drift.
- Reaming of the deposition drift.
- Excavation of notches for compartment/drift end plugs.
- Handling of excavated rock.
- Hydrological characterisation.
- Grouting techniques for the deposition drift (Mega-Packer).
- Installation of drip shields.
- Installation of docking flange.
- Aspects regarding construction and operation considerations (logistics).

The report will be based on the underground openings production report.

9.2 Deposition drifts

9.2.1 Drilling techniques

Geometrical requirements on the KBS-3H deposition drifts are high; cf. Section 3.4.1 and Table 3-3. The demands on the excavation method are therefore also high. The method should fulfil all quality criteria and at the same time be robust and industrial.

For excavation of the deposition drift a number of technologies are feasible, or expected to be feasible, and the sequence for the drift development can be arranged in several ways, Figure 9-3.

The use of a full face Tunnel Boring Machine (TBM) that excavates the drifts in one step and the cluster drilling technique have previously been ruled out. Mini-TBM-drilling has developed considerably in the last years and can possibly be evaluated again in coming project phases. Other alternatives explored were cluster drilling, or "horizontal push-reaming", i.e. to push a raise-boring head, rather than pull it. Both alternatives require a pre-existing pilot borehole, subsequently reamed to the final diameter of the drift.

Currently the option on how to proceed is to drill a pilot hole that is reamed to full drift size, possibly with an additional intermediate reaming step. The techniques considered applicable for drilling a pilot hole are core drilling and rotary crushing. Pilot holes can be drilled either with or without directional (steered) drilling. Further details on the drift excavation is found in Autio et al. (2008).

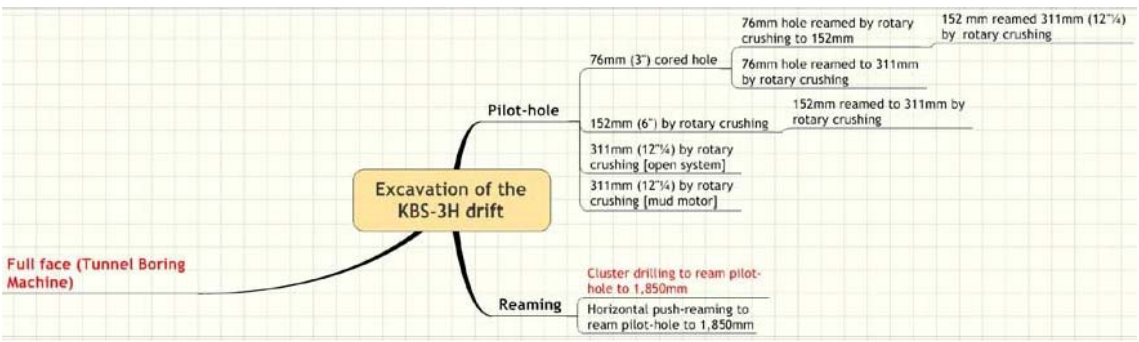

Figure 9-3. *Outline of options for deposition drift excavation. Alternatives in red font are disregarded.*

Pilot hole drilling

The pilot-hole can be bored either by directional core drilling, or rotary crushing as the main alternatives even if percussion drilling also should be feasible. A standard diameter used by SKB for coring is 3” (76 mm). This hole needs later to be reamed to the final pilot-hole diameter, here proposed to be minimum 311 mm (12” ¼). Another alternative is to drill the full diameter of the pilot-hole using rotary crushing techniques.

Guided directional drilling requires two main systems, one that establishes the position of the drill bit in space and a second system that guides the direction of the borehole based on the error in the bit position relative to the theoretical trajectory of the borehole.

Several options are currently available on the market for directional drilling. The systems are using different measurement techniques to establish the current drill bit position. The ability of these systems should be evaluated and in some cases verified before a decision on how to proceed is taken.

Apart from the technical aspects of the pilot hole excavation rock, characterisation aspects should also be taken into consideration since the ability to accurately characterise the pilot hole varies with the excavation method, e.g. core produced or not, availability of characterisation methods for the large diameter holes.

Reaming and completing the drift

Reaming of the pilot hole can be made by using slightly adapted equipment for conventional raise drilling, where the head is pushed and rotated. Stabilisers are necessary to stabilise the drill string, Figure 9-4.

The tests at the Äspö Hard Rock Laboratory, successfully demonstrated the feasibility of push-reaming (Bäckblom and Lindgren 2005). With respect to the geometrical requirements (see Section 3.4.1), a diameter change it is anticipated due to wear of the periphery cutters. For a 300 m long drift, it is envisaged that the demands placed on the minimum and maximum diameter of the drift will result in careful monitoring of the wear of the cutters and timely exchange of cutters during the course of reaming.

Concerning the smoothness of the drift, the reamer head manufacturers have no documented experience how it may be affected by the reamer head design, e.g. using six instead of four periphery cutters. Furthermore, there are no data available on the marginal extra overbreak that is generated beyond the periphery cutter. The reaming may also generate grooves and steps but it is not fully clear how to design the reamer head and how to operate the equipment to minimize generation of grooves and steps. Figure 9-5 illustrates the 95 metre full diameter drift at Äspö after reaming.

Conclusions

The studies of drilling methods led to the conclusion that the final selection of the drilling process can only be made after the KBS-3H programme for detailed investigations has been decided upon. Due to the extreme requirements on waviness/undulation, real-time directional drilling will most likely be difficult to use. Drilling without steering and employing a stiff drilling system remains a viable alternative despite the length of the pilot boreholes.

The push-reaming as the final reaming step worked out in the tests at Äspö, there was however the question of effectively removing excavated rock which was handled at Äspö but would require improvements for a more industrialised performance. TBM technology has been improving since it was excluded and could possibly be revisited at a later stage.

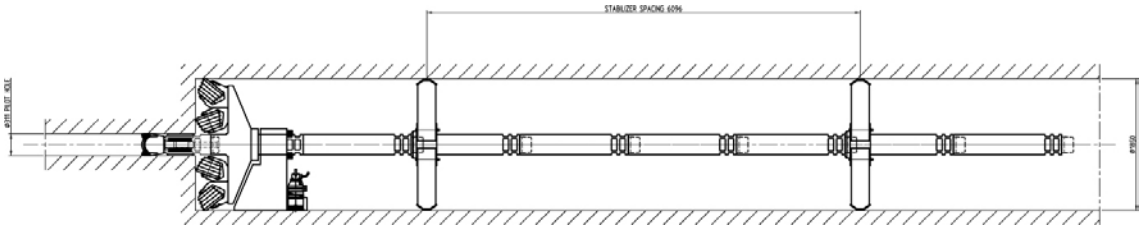

Figure 9-4. *Principal illustration of horizontal push-reaming, showing the reamer head to the left and stabilizers in the already excavated drift. Courtesy: Atlas Copco*

Figure 9-5. *The end of the 95 m drift at the Äspö HRL showing the final shape of the face and occasional grooves.*

9.2.2 Measurement techniques

Verification that the geometrical requirements have been met constitutes an important part of the drift excavation process. If the drift for some reason does not fulfil the requirements it could imply that deposition is not possible. The measurements should be done stepwise and using proven technology to the extent possible. Special measurement devices cannot be ruled out in future applications.

Drift inclination and direction can be measured by use of conventional techniques. During the excavation of the 95 metre drift at Äspö HRL during 2005, conventional survey techniques were used with good results. In order to accomplish this, a special device was manufactured to suit the conditions at hand, cf. Figure 9-6. The method, however, requires a direct line of sight and therefore does not allow for deviations of the hole larger than the borehole diameter. Therefore the method may not be useful when excavating a 300 metre drift where total deviation can be larger than the pilot borehole diameter. Other methods must therefore be at hand as well. There are a number of systems available on the market, each with its own limitations and special characteristics. Inclination and direction of the drift is best measured during the drilling of the pilot hole, where efforts can be made early to correct deviations that might lead to the drift not fulfilling the requirements.

Drift surface requirements, roughness, steps, diameter changes etc, were measured manually during the drift excavation at Äspö using a profiler as well as a Supercontainer dummy with sensors. The method is time consuming and there is a risk that all anomalies are not detected. Laser scanning of the drift was also tested and found feasible, the method generates huge amount of data from which the surface can be analysed.

Detailed information regarding the measurement techniques can be found in Bäckblom and Lindgren (2005) as well in Autio et al. (2008).

Figure 9-6. *Device used for measuring the straightness of the pilot hole in the demonstration at Äspö.*

Conclusions

Measurement of the drift geometry can in some cases be made using conventional techniques. Some parameters do, however, require further investigation of alternative techniques in order to have an efficient and robust method.

9.2.3 Rock spalling study

Rock spalling occurs when the concentrated rock stress around an excavation reaches the rock strength. There is a spectrum of such spalling, ranging from slight cracking through to complete failure of the excavation. Rock spalling can increase/occur due to the enhanced stress state resulting from thermal stresses (i.e. the thermal stresses around the deposition drifts added to the stress state resulting from the in situ and excavation induced stresses, which all contribute to total stress). The severity of the rock spalling may jeopardize/impact the long-term safety of the repository. For example, the spalled zone may create a hydraulic path along the length of the drift that may not be acceptable.

A study was carried out in the recent project phase with the aim of providing a preliminary estimate of the potential for rock spalling in the KBS-3H deposition drifts at the SKB's Forsmark site. Two-dimensional analyses using the stress magnitudes from mechanical analyses were combined with the thermal stress magnitudes adapted from the Forsmark KBS-3V analyses to provide a preliminary estimate of the potential and severity of rock spalling in the KBS-3H design at Forsmark

The potential for rock spalling was evaluated using the most likely and the unlikely maximum in-situ stress magnitudes and orientations given in SKB (2009a).

Input data and repository layout

The preliminary KBS-3H layout for Forsmark, see Chapter 8, was used in the study. The repository was assumed to be located at the depth of 470 m and the angle between the deposition drifts and the maximum horizontal *in situ* stress varies between 5° to 22°. The majority of the drifts will be situated in fracture domain FFM01 (rock domain RFM029), the rest will be in fracture domain FFM06 (rock domain RFM045), see Figure 9-7. Two inspection times were analysed; right after excavations and at maximum thermal loading, which corresponds to a time approximately 50 years after the deposition (Lönnqvist et al. 2010). The possible swelling pressure of buffer was not taken into account.

The rock spalling probability was studied for the rock types of the fracture domains FFM01 and FFM06, assuming rock spalling strength being 52% or 62% of the uniaxial compressive strength (UCS). The rock spalling strength range is based on results of Äspö (APSE) and URL in situ rock spalling experiments.

All calculations were based on the 2D-analyses of vertical cross-section of deposition drift, i.e. the combined effect of the main tunnel-drift intersection area was excluded. Based on the current KBS-3H layout the rock spalling probability of the first metres of the drift will be lower, because the main tunnel is perpendicular to major in situ stress, resulting lower stress state beside tunnel wall than the in situ stress. The in situ stresses and thermal stresses used in calculations were those acting on the analysed cross-section. The calculations were performed either using 2D-code boundary element code Examine2D or Kirsch equations assuming an elastic material. The remaining input data was taken from the reports Lönnqvist et al. (2010) and SKB (2008).

Key issues for the study was the orientation of the drifts compared to the maximum horizontal *in situ* stress and the location of thermal stress calculation models as in study by Lönnqvist et al. (2010). Using the same naming system as used by Lönnqvist et al. the drifts are divided into three groups; A, B and C&D (Figures 9-7 and 9-8). Axis of A-drifts deviates 22° from the orientation of maximum horizontal *in situ* stress, the corresponding angle for B-drifts is 5° and 18° for C&D-drifts.

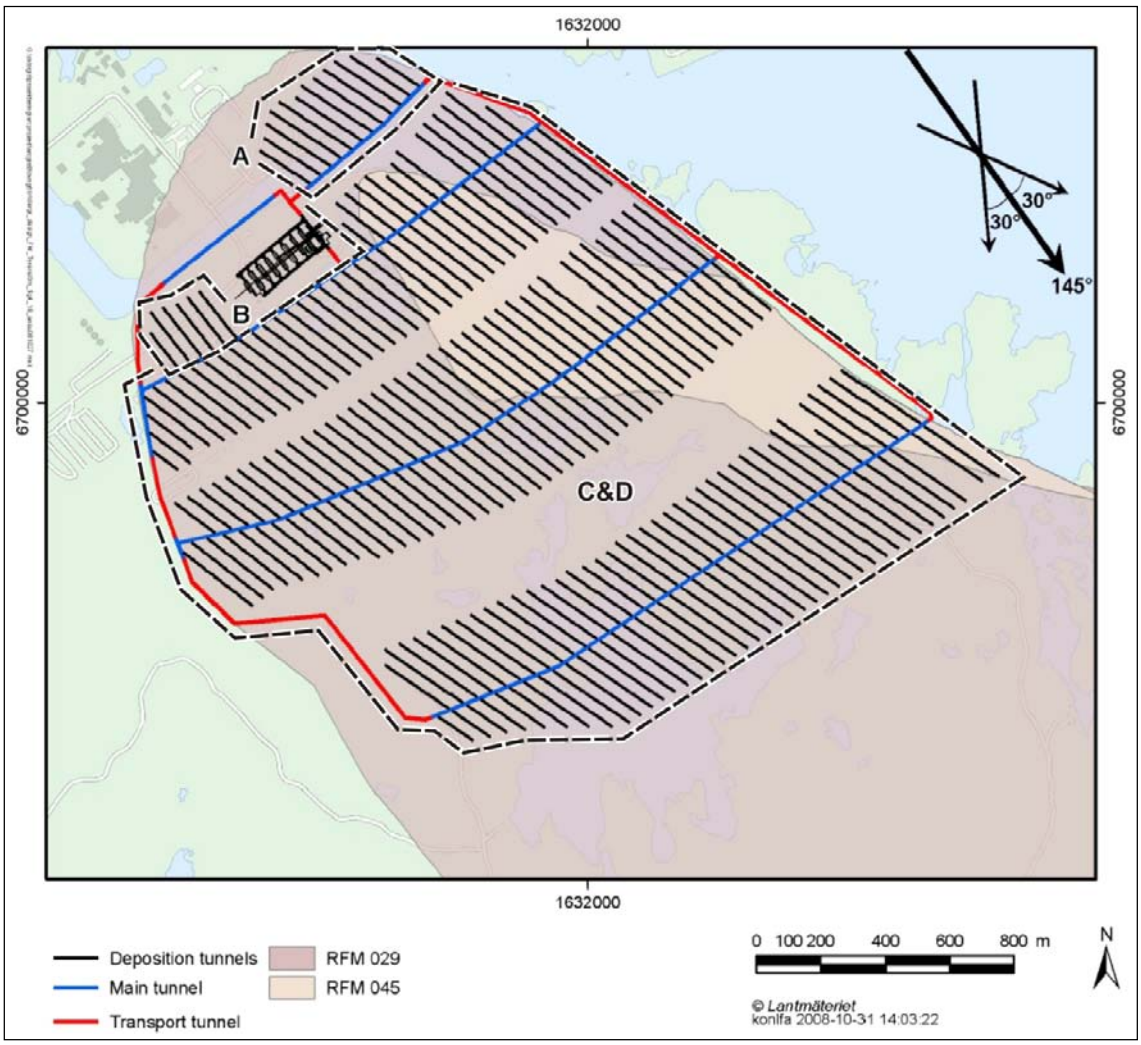

Figure 9-7. *Naming of the drifts to groups A, B and C&D based on their orientation compared to trend of maximum horizontal in situ stress.*

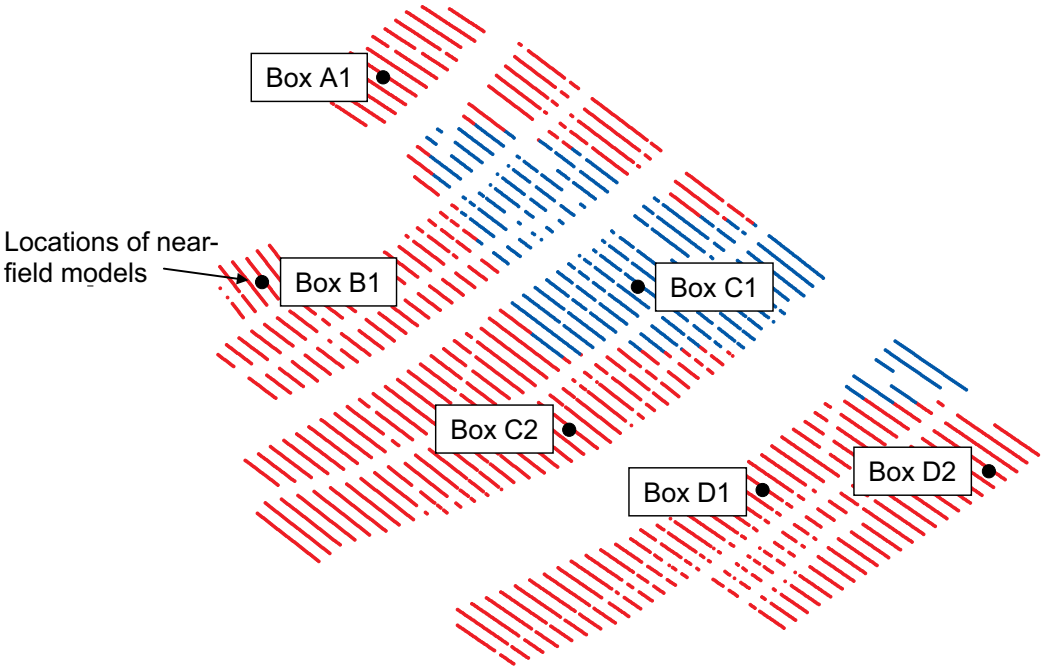

Figure 9-8. *Forsmark layout D2 and locations of near-field models. Red colour represents 6 m canister spacing (coincides with rock domain RFM029 and fracture domain FFM01) and blue colour represents 6.8 m canister spacing (coincides with rock domain RFM045 and fracture domain FFM06) (Lönnqvist et al. 2010).*

Concerning the material the mechanical properties of Glamheden et al. (2007), SKB (2008) and the thermally dimensioning properties of Back et al. (2007) and Sundberg et al. (2008) were used.

The studied in situ stress cases were the so called *most likely* (based on stress model for fracture domains FFM01 and FFM06) and *unlikely maximum* (proposed maximum stress model, upper limit) as presented by Glamheden et al. (2007) and SKB (2009a).

Instead of true thermal stresses, effective thermal background stresses were used, which will cause the same effect on the surface of the deposition drift. Thermal background stresses, called thermal stresses for the simplicity, are caused by thermal expansion and boundary conditions affecting around the hole of interest.

Thermal horizontal stresses were back calculated from the results presented by Lönnqvist et al. (2010). Lönnqvist et al.'s results assume the repository layout as presented in Figure 9-8. These results cannot be used to estimate vertical thermal stress fields; therefore a vertical-horizontal thermal stress ratio of 0.55 was used. This value was calculated from the thermal stress results presented for the Olkiluoto horizontal concept (Lönnqvist and Hökmark 2007). As long as the thermal effect of one hole is unaware of the other holes or other boundary conditions, the warming and the thermal stresses are more or less uniform, but when holes beside each other start to interact the horizontal components of thermally induced stresses increases more than the vertical one and later also the free rock surface increases this anisotropy.

The described approach is not accurate but serves as reasonable estimate in situation when thermal gradients are low. Lönnqvist et al. (2010) used two parameter sets to calculate thermal stresses, *the mean value material parameters* and *the dimensioning thermal properties;* these were both also adopted in this study. The dimensioning thermal properties resulted in higher thermal stresses.

Lönnqvist et al. (2010) present total stresses on walls of deposition holes at six repository locations, called "boxes" (Figure 9-8). The major principal stress curves from the depth of 5 m below the deposition tunnel floor were used because the effect of the disposal tunnel and the end of the deposition hole to principal stress magnitudes and orientations is at a minimum at this depth. The maximum and minimum differences at the same location were picked and the horizontal thermal stress field without

the effect of circular hole were back calculated using Kirsch equations (Table 9-1). The resulting horizontal thermal stress components are very close to each other resulting that the orientation of the drifts compared to thermal stress field can be neglected. For simplicity and as a conservative assumption, homogeneous horizontal thermal stress field were assumed. For the magnitude, higher values of back calculated components were selected. The vertical thermal stress is 55% of the horizontal thermal stress (Table 9-1).

Analyses

The analyses was divided into two main cases based on the *in situ* state of stress; being either the *most likely (Iss1)*- or *unlikely maximum (Iss2)*. Further, in case of both in situ stresses two different maximum thermal stresses were analysed, based either on *mean value material properties (Ths1)* or *dimensioning thermal properties (Ths2)*. These *in situ* stress and thermal stress field values vary slightly for the selected locations (boxes) A1, B2, $C\&D_{MIN}$ and $C\&D_{MAX}$, resulting six stress conditions for each box, i.e. totally 24 cases (Table 9-2).

In order to estimate the rock spalling potential, the resulting elastic tangential stresses around deposition drift perimeter in these 24 cases were compared to the lower and upper bound rock spalling strength for the two rock domains RFM029 (FFM01) and RFM045 (FFM06). Because the repository location has a minor effect on the rock spalling potential compared to rock spalling potential from the in situ stress and thermal stress magnitudes, the results of all locations are presented in the same figure with different line types.

Table 9-1 Maximum and minimum tangential thermal stresses on deposition hole wall at the depth of 5 m below the tunnel floor (columns 1–2), back calculated horizontal thermal stress field (columns 3–4) and estimated vertical thermal stress (column 5).

Thermal stresses calculated with mean value material parameters (MPa)					
Box	$\sigma_{\theta,th,max}$	$\sigma_{\theta,th,min}$	$\sigma_{H,th}$	$\sigma_{h,th}$	$\sigma_{v,th}$
A1	55	56	28	28	15.4
B1	54	47	26	24	14.3
$C\&D_{MIN}$	50	51	25	25	13.7
$C\&D_{MAX}$	53	57	28	27	15.4
Thermal stresses calculated with dimensioning thermal properties (MPa)					
Box	$\sigma_{\theta,th,max}$	$\sigma_{\theta,th,min}$	$\sigma_{H,th}$	$\sigma_{h,th}$	$\sigma_{v,th}$
A1	68	67	34	34	18.7
B1	66	59	32	30	17.6
$C\&D_{MIN}$	62	62	31	31	17.1
$C\&D_{MAX}$	69	69	34	34	19.0

Table 9-2. Analysed cases for Forsmark KBS-3H rock spalling analyses.

In situ stress	**Thermal stress**	**Location (box)**
Most likely (Iss1)	after excavation (–)	A1, B2, $C\&D_{MIN}$, $C\&D_{MAX}$
	mean mat. prop. (Ths1)	A1, B2, $C\&D_{MIN}$, $C\&D_{MAX}$
	dimensioning th. prop. (Ths2)	A1, B2, $C\&D_{MIN}$, $C\&D_{MAX}$
Unlikely max (Iss2)	after excavation (–)	A1, B2, $C\&D_{MIN}$, $C\&D_{MAX}$
	mean mat. prop. (Ths1)	A1, B2, $C\&D_{MIN}$, $C\&D_{MAX}$
	dimensioning th. prop. (Ths2)	A1, B2, $C\&D_{MIN}$, $C\&D_{MAX}$

The potential for rock spalling is assessed using factor of safety value (Equation 9-1) (Martin and Christianson 2009). Using statistical approach, rock spalling is more or less evident if the mean factor of safety is below 1.0 and mean factor of safety > 1.25 will reduce rock spalling probability to very low.

$$F.O.S. = \sigma_{SM}/\sigma_{\theta\theta} \quad (9\text{-}1)$$

where, $\sigma_{\theta\theta}$ = maximum boundary stress
σ_{SM} = rock mass spalling strength

The severity of the rock spalling is defined by the depth of spalling (Equation 9-2) (Martin and Christianson 2009).

$$S_d = a\,(\,0.5\,(\sigma_{\theta\theta}/\sigma_{SM}) - 0.52\,),\ \text{for}\ \sigma_{\theta\theta} > \sigma_{SM} \quad (9\text{-}2)$$

where S_d = rock spalling depth, measured from the boundary of the tunnel
a = tunnel radius

Because the presented rock spalling potential estimation method should be used with statistical approach, it can be applied for *most likely* in situ stress condition results but not for *unlikely maximum* case. In case of unlikely maximum in situ stress the probability of rock spalling is much less than indicated by factor of safety and the depth of spalling is just a hypothetical maximum.

Results

Most likely *in situ* stress

It is concluded that for the most likely in situ stress conditions no rock spalling is predicted due to the excavation induced stresses. For FFM01 rock type the factor of safety against spalling strength is between 1.9 and 2.6.

At the time of maximum thermal stresses rock spalling is possible in FFM01 rock type domain. Figure 9-9 illustrates the case of at the time of maximum thermal stresses. For lower rock spalling strength estimate (0.52 UCS) the factor of safety is between 0.8 and 1.0 and the depth of rock spalling is between 0 cm and 18 cm. In higher rock spalling strength estimate (0.62 UCS) spalling is very unlikely; factor of safety is between 1.0 and 1.2. In FFM06 rock type domain no rock spalling exists.

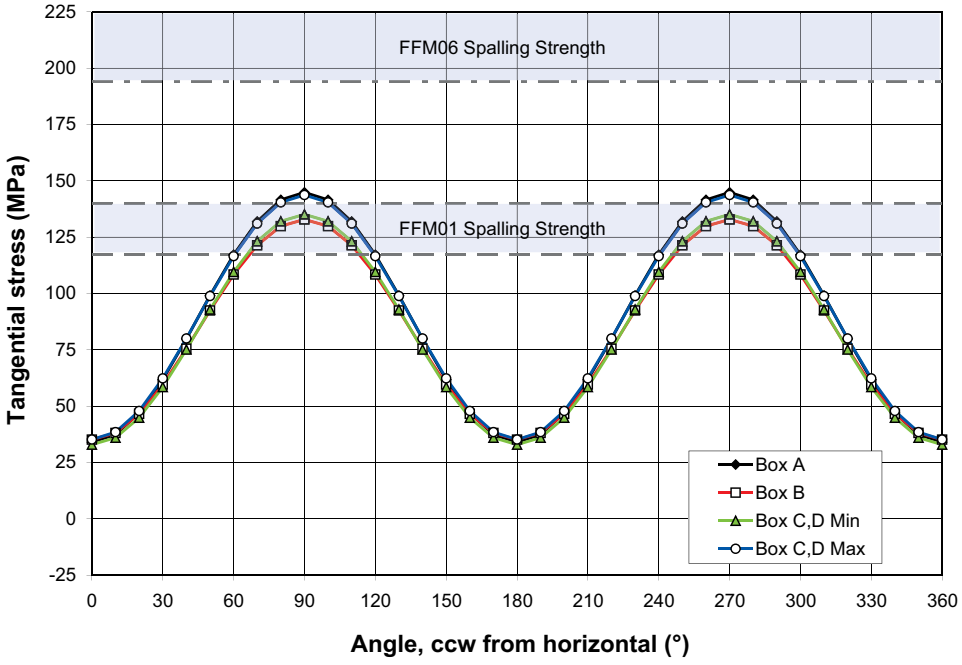

Figure 9-9. *Tangential stresses around the deposition drift at the time of maximum thermal stresses at four repository locations at 470 m level in case of most likely in situ stress and thermal stresses calculated using dimensioning thermal properties (Case i1,t2).*

Unlikely maximum *in situ* stress

In unlikely maximum in situ stress conditions rock spalling have very small possibility after the deposition drift excavation in FFM01 rock type domain. For lower rock spalling strength estimate (0.52 UCS) the factor of safety is between 0.9 and 1.1. In higher rock spalling strength estimate (0.62 UCS) no spalling exists.

At the time of maximum thermal stresses rock spalling is possible in FFM01 rock type domain and practically not in FFM06 domain. In FFM01 domain the factor of safety for lower rock spalling strength estimate (0.52 UCS) is from 0.6 to 0.7 and the hypothetical maximum depth of rock spalling is between 46 cm and 67 cm. With higher rock spalling strength estimate (0.62 UCS) the factor of safety is from 0.7 to 0.8 and the hypothetical maximum depth of rock spalling is between 23 cm and 41 cm. In FFM06 rock type domain the factor of safety against lower rock spalling strength estimate (0.52 UCS) is from 0.9 to 1.3.

Evolution of thermal stresses

Based on the results in Lönnqvist et al. (2010), the evolution of thermal stresses around vertical deposition hole (KBS-3V) is the following; 30% of maximum value takes place in 0.1a, 65% in one year and 92% in 10 years. Applying this to the results of the presented Forsmark horizontal concept (KBS-3H), this means that in case of most likely in situ stress conditions the rock spalling initiation would take roughly from 1 to 10 years depending on the parameter values used in thermal calculations. In case of the unlikely maximum in situ stress rock spalling can already initiate right after the drift excavation and any heating will increase the severity of rock spalling.

Conclusions

It can be concluded that for the most likely in situ stress conditions the excavation of the deposition drifts will not induce rock spalling. However, minor to moderate rock spalling will be encountered in the deposition drifts located in weaker rock domain RFM029 (FFM01) when the thermal stresses reach a maximum (about 50 years after deposition). The factor of safety for thermally-induced rock spalling ranges from 0.8 to 1.2 and the depth of spalling is less than 18 cm. In the stronger rock domain FFM06, no spalling is predicted.

For the unlikely maximum in situ stress conditions the excavation of the deposition drifts will induce minor rock spalling in weaker rock domain RFM029 (FFM01). When the thermal stresses reach a maximum (about 50 years after deposition) the maximum depth of rock spalling could range from 23 cm to 67 cm. There is also a very minor risk for thermally-induced rock spalling in the stronger FFM06 domain.

Based on the results of thermal stress evolution presented by Lönnqvist et al. (2010) the rock spalling initiation would take roughly from 1 to 10 years depending on the parameter values used in thermal calculations in case of most likely in situ stress conditions. In case of the unlikely maximum in situ stress rock spalling can initiate right after the drift excavation and any heating will increase the severity of spalling of rock.

Noteworthy is that all the results assume that there is no confinement pressure caused by the buffer material, which could mitigate the rock spalling. The Äspö rock spalling experiment (APSE) has shown that even relatively small confinement pressure, 150–250 kPa, could prevent rock spalling initiation (Andersson 2007). See also the buffer swelling results in Section 5.8.4.

The results from this study should be considered indicative, because no thermo-mechanical calculations were carried out. To confirm the preliminary results and to minimize the uncertainties full 3D thermo-mechanical analyses for the KBS-3H design should be carried out.

9.3 Groundwater control

Water inflows to the deposition drifts will have significant impact on the feasibility of the KBS-3H repository design, which is sensitive to groundwater inflows. Groundwater inflow into the deposition drift may cause e.g. piping and erosion in the various buffer components. The limits for acceptable inflows is being investigated further but given current knowledge the maximum allowed inflow is set to 0.1 l/min for a Supercontainer section, approximately 10 m in length (Supercontainer plus distance block) (Autio et al. 2008). It is therefore important to select suitable drift locations and for these locations assess the number of possible canister positions. The number of suitable canister positions is regarded as the utilization degree and optimisation of the utilization degree was identified as a critical design issue in earlier project phases (Autio et al. 2008).

9.3.1 Effects of conductive fractures and associated inflow requirements

Concerning deposition of canisters in horizontal drifts there are a number of aspects of the rock mass that need to be investigated and the properties of the rock mass hosting the deposition drift/-s must be accepted before deposition is allowed, see Table 3-1. Inflow of water to a deposition drift is of particular interest since:

- Inflow of water may erode the buffer material which may eventually entail a decrease in the required hydraulic separation of the canisters as initially defined by distance blocks and/or by decreasing locally the density of buffer sections in the drift.
- The water may introduce harmful components to the canister(-s), which may cause corrosion of the canister(-s).
- Conductive fractures contacting a canister position with surrounding fracture network may in the long-term perspective transport radionuclides away from a damaged canister.

To prevent or mitigate these adverse effects, it is important to verify that the inflows from the fractures in the deposition drift are sufficiently small and also that the overall total inflow into the drift is small.

The preliminary target values for acceptable inflows have recently been updated as new filling components have been developed, see Section 4.6, the updated inflow requirements are listed in Table 4-8.

Characterisation data from pilot boreholes and subsequent assessment using models form the basis for the predictions of the actual rock conditions and groundwater flow around and to the drift. The water inflow has to be measured before any disturbance of the natural inflow, such as grouting of the borehole section, is made since the inflow criteria (c.f Table 9-3) are based on natural conditions. The question arises how accurate this prediction can be made and how it should be used in decision-making. There is no problem as long as the actual conditions in the drift are within the acceptable bounds. The definition of an acceptance criterion links to the observational method where it is stated that design should be performed for the most probable conditions as well as for the most unfavourable deviation from these conditions. Grouting may be considered a contingency action using the nomenclature of the observational method. Expectations are that a conceptual basis for linking the inflow distribution to a pilot borehole with that to the excavated drift will successively be assembled during repository development, which will help make well-founded decisions regarding pre-grouting and/or reaming to full drift diameter. Important inputs to this conceptual understanding are expected from the planned development of a new experimental drift at Äspö HRL, cf. Chapter 10, “Future work”.

Hydrogeological characterisation methods commonly used by Posiva and SKB are described in Autio et al. (2008). These methods as well as different grouting methods applicable for horizontal drifts are presented in brief in the subsequent sections.

9.3.2 Hydrogeological characterisation

Hydrogeological characterisation associated with the canister position is very straightforward for KBS-3H since the investigated pilot borehole itself forms the deposition hole after reaming. Also, if post-grouting with the Mega-Packer could be used exclusively, which might be the case in the dry rock-conditions in Forsmark and Olkiluoto, KBS-3H could successively improve the conceptual basis for relating inflow to a characterisation borehole with data on inflow to the drift.

The following fracture related characteristics and properties govern the distribution of groundwater flow in fractures and fractured rock (and indirectly the transport of solutes):

Fracture geometrical properties

- Fracture geometry (strike/dip or equivalent).
- Fracture frequency (fracture intensity), obtained as linear intensity P10 along a borehole. Other area- and volumetric intensity measures are also used.
- Channelling (the area of a fracture that is available for flow). Not entirely a physical entity. In part governed by fracture roughness and fracture shear which defines physical conduits and contact areas where fracture surfaces mate. Superimposed are the effects of boundary conditions which activate or deactivate different parts of the fracture plane.
- Fracture size cannot be assessed from borehole data. The necessary statistics is inferred from fracture trace maps based on surface outcrops or underground openings.

Fracture hydraulic properties

- Transmissivity (inferred from various types of hydraulic tests). Mostly attributed to a test section of finite length. Can also be attributed to individual fractures.
- Hydraulic aperture (as inferred from transmissivity and frequency of potentially conductive fractures).

Fracture mineralogical properties

- Fracture filling.

Fracture mechanical properties

- Mechanical properties (shear strength and deformability).

The parameters transmissivity (hydraulic aperture), fracture frequency and fracture geometrical properties are measured according to commonly available characterisation methods. Channelling and area available to flow are difficult to measure directly and indirect inference through modelling is required. Fracture size data relevant to repository depth are expected to be obtained from measurements on underground openings. Below, a brief description is provided of the most commonly used methods to characterise the hydrogeological properties in boreholes.

Injection test

The short duration injection test involves injection of water into the rock at constant excess pressure. The injection can be made either in a packed off test section of finite length or in the complete hole. From the test, the transmissivity and the hydraulic aperture may be evaluated. It is also possible to evaluate the skin, or the inflow resistance from this test (Gustafson 2009).

Flow logging

A particular form of flow logging employed by Posiva and SKB is the so called differential flow logging which involves measurement of the attenuation of a thermal pulse in a section of a borehole (SKB 2010a). Generally the characterisation is made with a one metre section length. However, by employing overlapping measurements characterisation of conductive structures with a decimetre resolution can be achieved. The lower theoretical measuring limit for PFL is 6 ml/h (Öhberg 2006), which is well within the requirements for hydrogeological characterisation, according to Ludvigson et al. (2002).

Flow and pressure build-up test

The transient pressure recovery is measured after a flow period in a borehole or borehole section. In addition to transmissivity it is also possible to investigate the dimensionality of the flow. It is also possible to calculate the skin-factor and the specific storage from this test.

Geological information

In order to properly interpret and describe the hydrogeological situation it is important to incorporate a characterisation the geology with particular focus on the location and geometry of potentially conductive fractures along the borehole. A key investigation method is the Borehole Image Processing System (BIPS) which together with core logging provides the basis for the integrated geological and hydrogeological interpretation. A complementary method in this context is the acoustic televiewer.

9.3.3 Pre-grouting

The fact that grout injection boreholes are not allowed outside the contour of the drift (Autio et al. 2008) sets limit for the possibility to use pre-grouting. In addition, there are long-term safety requirements regarding e.g. injection borehole layout and the maximum pH of the grout.

Pre-grouting in investigation and pilot holes

Investigation holes (one or several) or the pilot hole for the drift are used to seal water-bearing fractures. Practically, a technique must be developed to handle grouting at repository depth and at potentially high groundwater pressure. A design must be developed that gives adequate sealing effect in the excavated drift. After grouting, the equipment in the borehole must be removed to facilitate re-drilling of the hole, hydraulic verification of grouting efficiency and reaming to full drift diameter.

Using one hole in the centre, the required grout penetration radius to reach the contour of the drift is approximately one metre. The degree of penetration, including penetration beyond the drift periphery is dependent on the transmissivity of the fractures being grouted. Low-transmissive fractures may theoretically be sufficiently sealed, and remain sealed, with a penetration length of c. one decimetre, if the fracture is completely and consistently filled with grout. High-transmissive fractures, connected to high groundwater pressure boundaries, are more difficult to seal and would therefore benefit from a longer grout penetration length.

Pre-grouting of the drift during reaming

Grouting during reaming of the drift must be made with grouting boreholes inside the contour to meet the long-term safety requirements. The required penetration length for a good sealing depends on how close to the contour the drill holes may be drilled. With the use of several boreholes less deep penetration is necessary.

If several holes are used instead of a single hole this increases the possibility of intercepting open parts of the fracture, which hence increases the possibilities to seal the fractures.

The selection of those sections to be pre-grouted is based on the information collected in the pilot boreholes. Irrespective of whether the whole drift is to be grouted using multiple holes (continuous pre-grouting) or whether only select sections need to be grouted, it affects the progress of the reaming since the excavation of the drift needs to be halted. Continuous pre-grouting means that the total amount of grouting material increases, as well as it prolongs the total excavation time.

9.3.4 Post-grouting

Post-grouting using the Mega-Packer

Since traditional post-grouting is not possible (since no boreholes are allowed outside the drift contour) the Mega-Packer system for sealing sections in the drifts after excavation was developed, see Section 4.9 for performance and a more extensive description.

If pre-grouting has not been employed, post-grouting using the Mega-Packer would also enable hydraulic characterisation of the fully reamed drift to complement the pilothole measurements. Since the Mega-Packer system is a post-grouting method there is a risk of by-pass and/or re-distribution of inflow positions in the fracture network along the drift due to differences in pressure beyond the packer (formation pressure) and outside the packer (atmospheric). However, these aspects will be dealt with in upcoming work, including e.g. use of several Mega-Packers in a series.

9.3.5 Theoretical grouting efficiency

Theoretical studies concerning requirements and sealing potential using different methods is reported in Design Description 2007 (Autio et al. 2008). In the report, three different grouting methodologies are compared, pre-grouting from a single borehole, pre-grouting from eight boreholes inside the drift and post-grouting with the Mega-Packer. These three different methods were theoretically evaluated for three different scenarios regarding the fracture frequency and hydraulic aperture. According to the study, the best effect is achieved with pre-grouting from 8 boreholes and post-grouting with Mega-Packer. However, for rock of low fracture frequency, with single fractures with apertures around 20 μm, the Mega-Packer showed the best projected efficiency and was hence identified as the most promising sealing method.

9.3.6 Summary

The parameters governing groundwater flow in fractures and fracture networks are transmissivity (hydraulic aperture), frequency of potentially conductive fractures, fracture geometry. By employing the catalogue of hydrogeological investigation methods available to Posiva and SKB a general characterisation of the hydrogeological conditions around the horizontal drift may be performed including parameterisation of the parameters of interest. However, improved assessments of fracture size at repository depth will emerge from mapping of exposed underground openings. Assessments of channelling (parts of fracture available to flow) will have to rely on indirect inference from modelling.

There are different grouting methods and strategies to seal inflow into the drift, either employed as pre- or post-grouting. Pre-grouting the drift from a pilot hole is the method that theoretically gives the lowest sealing efficiency, but it is possible that the method may be further developed but in relation to the other methods it will show a lower sealing effect. Pre-grouting the drift during reaming using conventional grouting is a possible method. The major drawback is the long-term requirement that the multiple injection boreholes must be kept inside the drift contour, which will set a high demand on the accuracy of drilling these holes.

Post-grouting with the Mega-Packer makes it possible to seal sections in the drifts after reaming. There are a limited number of tests performed but the method seems promising.

In previously performed theoretical study (Autio et al. 2008), the two most promising grouting methods were pre-grouting with multiple injection holes inside the drift contour and post-grouting using the Mega-Packer . The advantage of using of pre-grouting with holes inside the drift contour is that the grouting may be performed before the rock is excavated, enabling use of high grouting pressure. The main conclusion from the study was that the Mega-Packer showed the best theoretical sealing efficiency. This was also verified in full-scale tests at Äspö HRL, see Section 4.9.

Hydraulic characterisation and groundwater control will be rea dreesed in upcoming work when a KBS-3H specific detailed investigation programme is developed.

9.4 Deposition techniques

A KBS-3H repository requires a deposition equipment that can transport the Supercontainer, distance blocks and filling components for up to 300 m in the slightly inclined deposition hole. A deposition equipment has been developed and demonstrated in earlier project phases (Autio et al. 2008). The deposition equipment design is based on a transport principle where the Supercontainer is moved stepwise. The Supercontainer, which is provided with feet, as described in Section 4.4, is moved with help of a lifting cushion palette and a slide plate placed in the space between the feet underneath the Supercontainer. The lift cushions are standard air cushions for heavy load handling that have been adapted to run on a cylindrical surface with water as pressure medium. In Figure 9-10 the lifting technique is illustrated. The same principle is used for transport distance blocks according to the DAWE and STC alternatives.

The transport principle is chosen to reduce required forces needed to move the Supercontainer, which will minimize the risk for damage of the surrounding Supercontainer shell and the bentonite buffer. This lifting technique is implemented on the deposit machine slide plate, Figure 9-11.

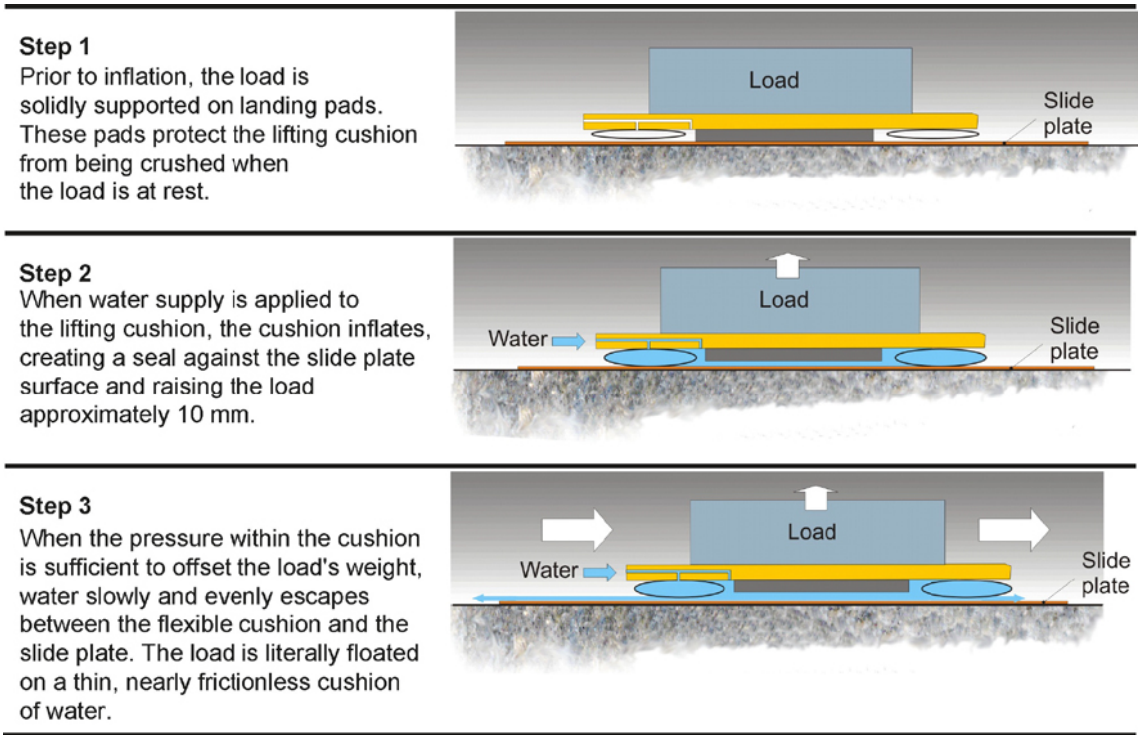

Figure 9-10. *Lifting cushion principle.*

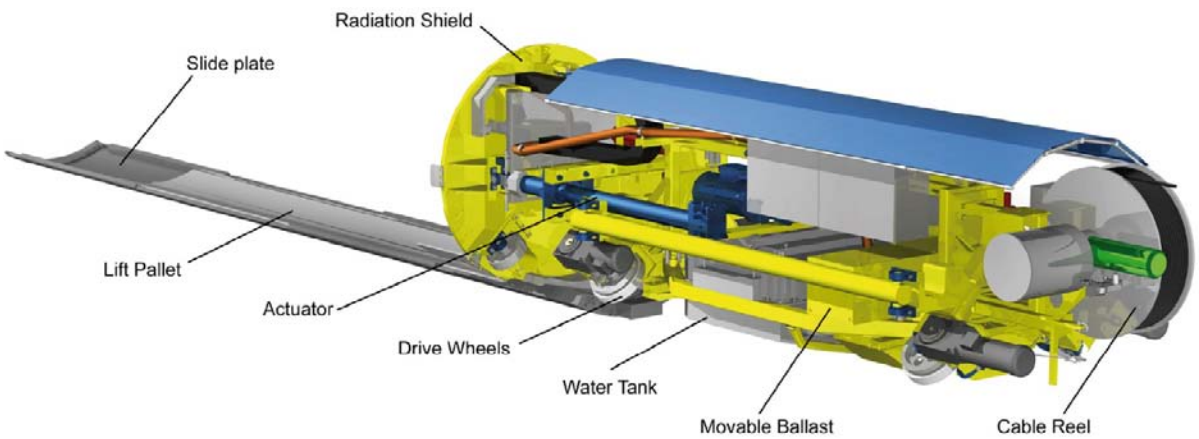

Figure 9-11. *Deposit machine 3D illustration.*

The deposit machine has been tested further and operated for maintenance reasons during the recent project phase. Work has been carried out on the control system and software updates now enables easier fault localization. A series of tests with the aim of identifying problems in the control system and then proposing solutions is carried out when this report is being compiled.

A Basic Design of a new sliding plate and palette has also been developed with the aim to improve the performance of the machine.

A detailed description of both the deposit technique and the equipment is found in Autio et al. (2008)

Conclusions

The method of deposition has showed to be functional and efficient; the deposition machine is, however, in need of updates to ensure increased reliability. Both soft- and hardware upgrades of the machine is in planning. When these upgrades have been carried out a test series will need to be set-up to further validate the function and reliability.

9.5 Retrivability and reverse operation

Retriviability was studied in the previous, Demonstration phase (Autio et al. 2008) and has not been studied further during the recent project phase. A brief presentation of the technique is, however, given here to include the whole picture.

It is assumed that, at any time during the operation period of the repository after disposal of Supercontainers or installation of other equipment in the drift, it should be possible to retrieve/ remove emplaced components from the drift due to the following considerations:

- The waste disposal process itself must be reversible in the event a serious error or accident takes place during emplacement.
- Supercontainer recovery could be necessary as a result of Supercontainer fault occurring during or after emplacement.
- Supercontainer recovery could be necessary if the repository does not function correctly.
- Retrievability is required by the licensing requirements in Finland.
- Future generations might have an interest in retrieving emplaced material.

There are two main scenarios, either the components have absorbed water and has started to swell or they are intact and not affected by water. For the case with no swelling, prior to the artificially wetting , the deposition machine can be operated in reverse (so-called “reverse operation”), this has also been successfully demonstrated at Äspö HRL using Supercontainer dummies.

In the case where the bentonite buffer has absorbed water, reverse operation may not function properly and other means will be required for Supercontainer recovery, i.e. retrieval.

Due to the different barriers (components/material) that will be introduced into the deposition drifts, a number of different techniques will be required for their removal and ultimate retrieval of the canisters.

The different techniques proposed for removal of these barriers include:

- Remove drift plug.
- Removal of filling materials.
- Removal of distance block, buffer materials.
- Cutting the Supercontainer end plate.
- Removal of bentonite inside the Supercontainer.
- Retrieval of the canister.
- Removal of steel shell (Supercontainer).
- Cleaning of the drift.

The removal of the various barriers will take place through a combination of different techniques. It is proposed that the concrete and titanium components are removed by means of hydro-demolition methods and water cutting. The removal of bentonite can be carried out using hydrodynamic/chemical methods, which have already been tested for retrieval of a KBS-3V canister. Alternatively, hydro-demolition methods can be used; however, this would require tests to verify that the method will not damage the copper canister. The work carried out during the Demonstration phase concluded that it is possible to remove the Supercontainer and other components after installation.

9.6 Operational safety

9.6.1 Performed analyses

A pre-study of a safety analysis for the operational safety was carried out during the Demonstration phase (Autio et al. 2008). This study was updated during the recent project phase with DAWE as the reference design. The analysis was again carried out as a What-if analysis with the objective to identify possible damage sequences for copper canisters of spent fuel which can give radiological consequences. The risks were analyzed and mapped in a matrix with consideration to the variables: event, consequence, cause, measure and detection. The analysis was a comparative study where only the operations that deviate from the KBS-3V method were analyzed.

The following steps in the deposition process were included in the analysis:

- Preparation of drift, when the main activites are: excavation, characterisation, sawing of plug notches and installation of fastening rings and the air evacuation pipe).
- The reloading station with the shielded handling cells for Supercontainer assembly).
- The deposition area and deposition work.

The sequence for these three working areas was studied in detail (the transport from the surface down to the reloading station was not analyzed since it is the same as for the KBS-3V alternative). A panel of experts on the KBS-3H design was formed and an analysis meeting was arranged in order to identify and discuss risks related to the KBS-3H design. The following conclusions were drawn from the different steps:

Preparation of drift

The following additional risks, compared to KBS-3V were identified for this part of the process:

- Too high inflows of groundwater to the drift will give problems with eroding buffer when the Supercontainers and distance blocks are deposited. It is important that the rock characterisation is made properly and that the zones with high water inflows are grouted.
- It is technically a more complex task to excavate a 300 m long drift and to manage the water inflows in it.
- During the preparation of a drift several components are installed; fastening rings for the plugs, an air evacuation pipe and spray and drip shields to block water from coming in contact with the buffer. If these are incorrectly installed and not identified by inspection it can affect the deposition process in a negative way.

The reloading station

The following additional risks, compared to KBS-3V were identified for this part of the process:

- Lowering of the copper canister into the Supercontainer.
- Lift of the transport tube used for Supercontainer transports.
- Longer exposure time. Though, the copper canister is always in the shielded handling cell when it is moved.
- The shielded handling cell contains equipment that may cause additional risks, e.g. increase the likelihood of fire.

The deposition area and deposition work

Compared to KBS-3V the following advantages were identified:

- During deposition the deposition machine lifts the Supercontainer with water cushions and the lifting height is very low. There is no risk for dropping the canister.
- The fire load on the deposition machine is less for KBS-3H. Fire cannot be spread to other material than the deposition machine and cables.

The following disadvantages from a safety/availability point of view were identified:

- It is not optimal to use the deposition machine for transporting distance blocks in the drift. The stepwise movement of the blocks might cause cracks in the bentonite near the feet attachment. Alternative machines should be considered. A KBS-3H machine inventory will be developed early in the upcoming project phase to clarify these potential needs. The implications in drift operation and costs should also be included in upcoming work.
- The air evacuation pipe can get stuck in the swelling buffer. The air evacuation pipe may act as flow path for water and might erode buffer in zones where it has not swollen yet.
- Compared to KBS-3V the KBS-3H alternative will probably have lower availability. The canisters are deposited in a sequence in the same drift, hence it will be a more complex task to correct a failure event, e.g. unwanted wetting of the buffer or mechanical failure to the deposition machine and buffer degradation.

9.6.2 Conclusions and recommendations

KBS-3H mainly differs from KBS-3V concerning the preparation of the drift, the reloading station and activities in the deposition area. And although separate risk were identified for the reloading station the controlled assembly of the Supercontainer in shielded handling cells (compared to the mounting of bentonite into the deposition hole in the KBS-3V method) is considered an advantage. The lower lifts of the deposition machine inside the drift is also favourable from a safety analysis point of view compared to the higher lifts with strict precision requirements of KBS-3V. The main disadvantage is that if a failure occurs in a deposition drift there is a higher probability that several copper canisters will be affected.

The deposition machine is primarily designed for optimal transport of Supercontainers but is also used for transport of distance blocks and filling components in the current design. It might be better to deposit the distance block with a different type of machine, e.g. designed like a forklift in order to avoid repeated lifting and lowering of the distance blocks and filling components during the transport in the drift. This issue will be addressed in the upcoming project phase by developing a KBS-3H machine inventory.

Several risks that were identified were connected to the power supply and function of water pumps and a clear recommendation for redundancy can be given.

The analysis that was carried out focused on the operational safety. However, some of the failure events could possibly influence the long-term safety; these were identified but were not systematically studied. In order to ensure that all aspects of the long-term safety have been covered it is necessary to consider all design premises and assess whether there are events during operation that could affect these, this will be done in the upcoming project phase.

9.7 Personnel safety

9.7.1 Performed analyses

A workers safety studied was carried out during the recent project phase; the objective was to identify potential personnel safety risks which can occur during each operation in deposition work with KBS-3H, DAWE. The analysis was performed using “what-if”-methodology where possible risk were identified and classified due to consequence and probability category 1 to 5.

The risk analysis highlighted the differences identified in KBS-3H compared to KBS-3V. This relates, for instance to fire and evacuation, welding in confined space, traditional personnel safety and radiological risks. The scope of the personnel safety analysis comprised the risks which can occur:

1. during preparation of the drift,
2. in the reloading station,
3. during deposition work when filling compartments with distance blocks and Supercontainers.

The study showed a number of identified events. Some of these were considered “unacceptable”, and require suitable safety measures to be reduced to an acceptable level. These are presented in Table 9-3 together with recommended safety measures in Table 9-4.

Measures were also suggested for lower graded risks. The main causes of potential risks are connected to the work in confined space:

1. Risk for falling rocks/stones during preparation of drift.
2. Fire in the deposition drift.
3. Risk for asphyxiation during arc welding.
4. Dust.
5. Loss of lighting.
6. High noise level.

9.7.2 Conclusions

For the risk areas fire, asphyxiation and dust, a well functioning ventilation system is the most suitable physical barrier. In the area of reloading station the work is fully automated and remote. The physical involvement of personnel is small. The main activities are performed inside the shielded handling cell. This area can be compared to the industrial site from the operating point of view. In the risk matrix this area is from the operating point of view, considered as a low risk area. The risks during deposition work are mostly connected to the welding of fastening rings during installation of compartment plugs. Well functioning ventilation system and additional physical barriers including monitoring of oxygen concentrations in the breathing air are necessary.

As the design premises are not fully developed there are some identified uncertainties that need to be investigated further. Most uncertainties are related to the welding during installation of fastening rings in the deposition drift. To fulfil long-term safety criteria both from operational and personnel safety point of view it is recommended to investigate this area in more details.

Furthermore, the most critical physical barrier is the ventilation system. The dimensioning of the system for the final operation including the long-term consequences of welding in confined space should be further investigated.

The organisational safety is another issue, which should be worked out for the final deposition design in details according to the safety directives.

Table 9-3. Risks identified as unacceptable in the studies carried out, Table 9-4 shows the recommended solutions.

Event	Cause	Consequence	Technical barrier	Recommendation
Falling rocks, flying stones	Excavation of notches, drilling, reaming work	Serious injury person	Personnel protective equipment	6.1.5, 6.2.1
Shielding gas hose breaks	Welding in narrow space	Asphyxiation	Local ventilation outside	6.1.1, 6.1.3, 6.1.4
Gas cylinder leakage/rupture	Rounded bottom of the hole, narrow space	Displacement of oxygen, asphyxiation		6.1.1, 6.1.6, 6.1.3, 6.1.4
Welding fumes	Arc welding in confined space	Intoxication		6.1.1, 6.1.6, 6.1.3, 6.1.4

Table 9-4. Recommended safety measures.

No	Area	Recommendation
6.1.1	Ventilation Design	The ventilation system shall be sufficiently dimensioned for the final operation. The estimated amount of air contaminants in form of radon, dust, inert gases, etc shall be taken into consideration when dimensioning the ventilation system. Exhaust device and fresh air injection should be considered. The fan equipment used outside the drift shall be of an explosion-proof design. The concentration of contaminants in the supply air should be substantially below the occupational exposure limit values.
6.1.2	Alarm system	An alarm to warn for unforeseen fan/ventilation system stop and risk for fire shall be installed.
6.1.3	Emergency exists	Normally, underground work shall have at least two separate emergency exits. Installation of a rescue chamber designed for the actual number of workers is mandatory. Equipment giving access to respiratory air shall be provided. As an alternative a mobile rescue chambers can be used. All emergency exists shall be clearly marked.
6.1.4	Oxygen deficiency	It is recommended to measure the concentration of oxygen content in the air in order to assess the level of risk. The oxygen concentration in the breathing air shall not be lower than 18% vol. If there is a risk for oxygen deficiency, or heavy concentrations of air contaminations, compressed air equipment is necessary.
6.1.5	Falling stones/ flying rocks	The use of helmets and other necessary personnel protective clothing is mandatory.
6.1.6	Welding in confined space,	The main risks during arc welding in confined space are electricity, fire due to splash, contaminated air with welding gases and radiation. Splash can cause fires and burns. Protective clothing should be of suitable material. To avoid the electric chock use protective equipment, shoes with rubber soles and leather gloves. Protection from arc welding rays. UV radiation from the arc is dangerous. Use protective clothing, and suitable welding helmet. During TIG welding ozone gas is produced. It is irritating to the respiratory system. Use local exhaust which is moving in the welding direction during longer welding. Tungsten electrode emits small radioactivity. It should be placed in closed container before welding work starts. The air in the welding area should be monitored for amounts of welding fumes. Mechanical ventilation or exhaust hood is required. Place the source of electricity at least 1m away from the welder. Gas cylinders shall be chained in upright position. For work in a confined space a special work permit for classified welders is required.
6.2.1	Personnel protective equipment	It is mandatory to use safety helmets with chinstrap, safety shoes with protective toe caps and nail-proof soles during work with preparation of the drift. Other personnel equipment which shall be used includes hearing protectors, safety goggles, breathing protection, and protective clothing and leather gloves.

10 Future work

The preceding chapters of this report have covered KBS-3H background information and results from the latest project phase, *KBS-3HComplementary studies 2008–2010*. This chapter describes the upcoming project phase named *"KBS-3H System Design". The overarching goals and objectives are presented. In addition, the included full-scale sub-system tests are further detailed.* The KBS-3H System Design phase is closely connected to the recent phase and their joint goal is to produce KBS-3H basis for a decision on a possible future change of reference design from KBS-3V to KBS-3H.

10.1 Goals and objectives

The final goal of the upcoming KBS-3H project phase is to elevate the KBS-3H design and system understanding to such a level that a PSAR can be prepared and that a comparison between KBS-3V and KBS-3H is possible. For components and sub-systems this will be achieved by assessing the design basis and requirements, and based on this, reaching the system design level in accordance with SKB's model of delivery, Figure 10-1. The basis to achieve this shall be produced by the end of 2015.

10.1.1 Objectives

In order for the components and sub-systems to reach the desired system design level implies that:

a) the design of a sub-system or component, meets the set requirements in a verifiable manner, and

b) there exists suggestions for manufacturing, control and maintenance plans for the sub-system or component.

For the optimisation of the system it may be necessary to iterate the design steps. High priority will be given to requirements related to long-term safety. Design issues related to operational safety will also be in focus.

The first and fundamental step in the system design phase is that the design premises (SKB)/design basis (Posiva) should be updated and checked against the safety evaluations and the operational organisation and then decided upon. Thereafter the system design shall follow the steps below:

- The requirement specification for the design solution shall be revised to be in line with the updated design premises/design basis.
- The conceptual design that was selected in the conceptual phase (in most cases the previous project phase) shall be developed/updated based on the revised requirement specification, this generally means developing prototypes. The step also includes double-checking that the developed/updated design fulfils the requirement specification in the end.
- A plan shall be devised for industrialisation/implementation including control programmes that shows how the sub-system/component can be implemented and controlled so that the requirement specification is fulfilled.
- A programme for safe operation shall be devised and quality assured so that it ensures that the qualitative and quantitative demands that are set concerning the operational safety can be fulfilled.
- Verification:
  a) That the design solution meets the requirement specification.
  b) That the product can be manufactured so that the requirement specification is fulfilled (control programme).
- A risk assessment of both design and plan for industrialisation/implementation with control programmes shall be carried out.
- Basis for a decision to go ahead with the detailed design phase shall be delivered to the client.

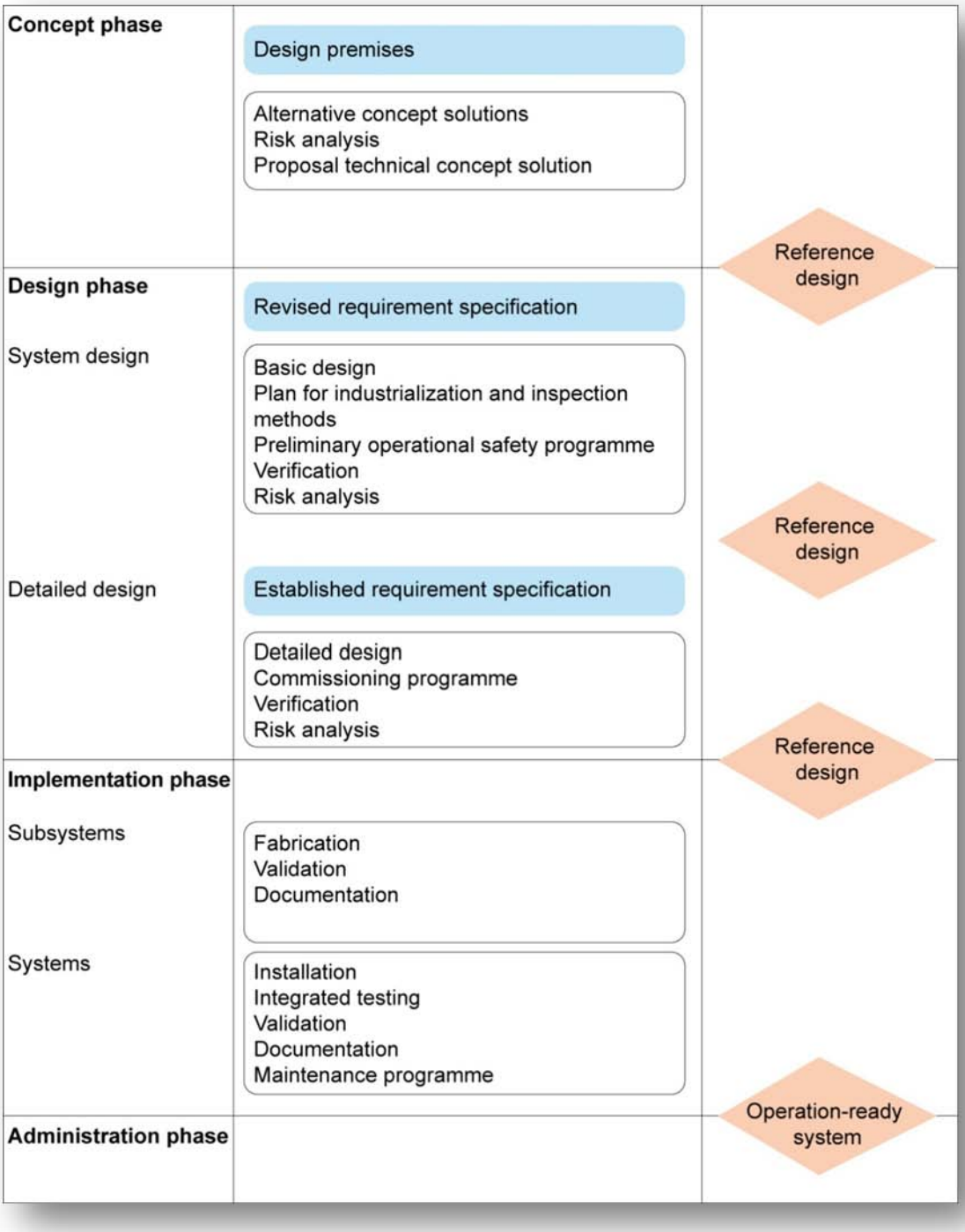

Figure 10-1. *SKB:s model of delivery, the KBS-3H project will proceed with the system design phase during 2011–2015.*

Vital in reaching the project's main objective is to produce the basis and carry out a safety evaluation for Forsmark and for Olkiluoto. This work will be based on earlier safety assessment work and make use of the SR Site (SKB 2011) for Forsmark and Posiva's safety case for KBS-3V for Olkiluoto.

Some issues noted as critical in the recent project phase shall be handled early in the new project phase. For example issues like compression shear due to earthquake and chemical erosion of the buffer due to penetration of glacial waters.

10.2 Full-scale sub-system tests

The reference design (DAWE) shall be verified in order to reach the system design level; this means verifying that the design solutions meet their requirement specifications. To achieve this two full-scale sub-system tests are planned:

- Excavation and preparation of a KBS-3H deposition drift.
- Multi Purpose Test.

The two tests are presented in the Sections below.

10.2.1 Excavation and preparation of a KBS-3H deposition drift

A KBS-3H repository is highly dependent on deposition drifts within the stipulated geometrical requirements; this is both due to long-term safety as well as practical aspects of emplacement. Excavation of the 95 metre drift at the –220 metre level at Äspö rendered a drift that fulfils the criteria. So far no full length drift has been excavated, which is required to fully verify the ability to excavate drifts that can be used for the KBS-3H design.

Full length pilot holes shall be drilled and the straightness measured in a quality assured way to verify that the technology both for drilling and verifying measurements of pilot hole and drift geometry is available. The pilot holes can be drilled using either steered or unsteered drilling, involving collection of drill core or not.

The pilot hole shall then be reamed to full drift size and measurements are to be carried out to evaluate if the drift requirements are met and to verify that quality assured measurement technologies are available. There is currently no need to ream the entire pilot hole (300 m long) to full drift size. Approximately 100 m should be enough to demonstrate the technology. The exact length can be adjusted to allow for plans for future tests in the drift.

Hydrogeological conditions are critical for a KBS-3H repository and a successful characterisation and integration in models of information from pilot boreholes and existing tunnels and drifts is essential to enable its construction. The hydrogeological conditions are decisive for potential erosion of and piping in the buffer. Once the hydrogeological situation is assessed, various grouting techniques can be used to control the inflow conditions; either as pre-grouting in pilot boreholes or as post-grouting made in the drift using the Mega-Packer. The ability to accurately predict the hydrogeological conditions in a completed drift from characterisation made in the corresponding pilot hole is important and will be tested in conjunction with the development of the planned KBS-3H experimental drift.

The planned tests shall be carried out at the Äspö HRL. The development of the KBS-3H drift is part of the planned Äspö expansion at the –420 m level at the Äspö HRL. The objectives of the excavation are related to:

- **Verification of pilot hole drilling performance (steered/without steering)**
  During the excavation of the 95 metre drift at the –220 m level the steering equipment for the full face pilot borehole failed. Despite this, the drift reamed using the pilot borehole fulfils the criteria specified by the KBS-3H design. Given the outcome of the drift development at the –220 m level, the drilling alternative without steering is still considered viable. It is, however, deemed more difficult to fulfil the geometrical criteria in the case of a 300 m drift, and its associated pilot borehole. For this reason the pilot hole drilling for the experimental drift should be verified by drilling full length pilot holes i.e. 300 m at the –420 m level at Äspö.
- **Assessment of pilot drilling involving full face boring or core drilling**
  Full face drilling will not produce any drill cores. The demand for a drill core to characterise and model the bedrock may entail that the use of full face boring is not sufficient. Hence, the planned work involves test and assessment of both full face and cored drilled pilot boreholes. It is noted that currently available site investigation methods in boreholes available with SKB and Posiva are developed for 76 mm core boreholes. Investigation of full face boreholes of larger diameter requires adaptation and development of available methods/tools to a variable degree.

- **Fulfilment of stipulated geometrical drift requirements**
  A pilot hole that fulfils the geometrical requirements is the base for further drift excavation. Reaming of the drift to full diameter is, however, also an important process. Apart from the straightness and inclination of the eventual drift there are other parameters that must be fulfilled, related to drift wall smoothness, drift steps, drift undulation etc. (Section 9.2).
- **Quality-assured measurement technology applicable to both pilot hole and full drift**
  The ability to develop drifts acceptable for deposition by way of a successive drilling and reaming process relies on verifying measurements of relevant parameters, thereby verifying the usability of the drift. Such methods and tools are important both for identifying drifts that may not be suitable for further use or for identifying problems associated with the excavation methods. Suitable measurement techniques will therefore be investigated, developed and tested.
- **Assessment of drift hydrogeological conditions from observations in pilot boreholes**
  The ability to early identify sections of a drift or the entire drift that might not be suitable for deposition is important for optimisation of the repository. Decisions related to performance of pre-grouting in the pilot boreholes and reaming of the pilot hole to full drift diameter are based on observations of inflows in the pilot borehole. These decisions therefore need to be founded on a proper assessment of the conductive fracture network, including effects of scale and near-drift conditions. Various tests will be carried out in conjunction with planned tunnel and drift developments.

Mega-Packer tests at repository depth

Successful test of the Mega-packer have earlier been completed at the –220 metre level of the Äspö Hard Rock Laboratory (Section 4.9 and Eriksson and Lindström 2008). The tests successfully demonstrated the ability to seal conductive fractures and fracture zones with both high and low inflows. The groundwater pressure at repository depth proposed by both Posiva and SKB is higher than at the –220 metre level. A recommendation arising from the performed tests at Äspö is to do additional tests at repository depth to verify the Mega-Packer function further at a more relevant depth and hydraulic pressure.

The tests will follow the same routine as at the –220 metre level of the Äspö laboratory where characterisation of the hydraulic conditions of the drift was done both prior to and after the Mega-Packer test.

The tests shall be carried out at the Äspö HRL at repository depth and will be a part of the drift excavation and preparation.

The objectives of the Mega-Packer test are:

- **Verification of Mega-Packer functionality at a repository depth**
  Fractures and zones associated with both high and low inflows will be tested.

Post-grouting using the Mega-Packer has to be verified at repository level if it is to be established as a KBS-3H post- grouting method. The tests should follow the procedures used at the –220 metre level.

10.2.2 Multi Purpose Test

The Multi Purpose Test is a full-scale sub-system test addressing several issues, hence the test name, and the test is included in the EC LucoeX-project. It will be carried out in the 95 m test drift at the KBS-3H test site at Äspö HRL. A preliminary test layout is presented in Figure 10-2. The location is chosen based on the KBS-3H projects time schedule and site accessibility. The deposition equipment is already located here and the site enables an earlier start than a site at repository level, which will take additional time to excavate and prepare. The limitations imposed by the lower groundwater pressure at the –220 metre level are not that large for this particular test, the buffer behaviour should not be affected in a critical way by the lower groundwater pressure and the emplacement technology is the same.

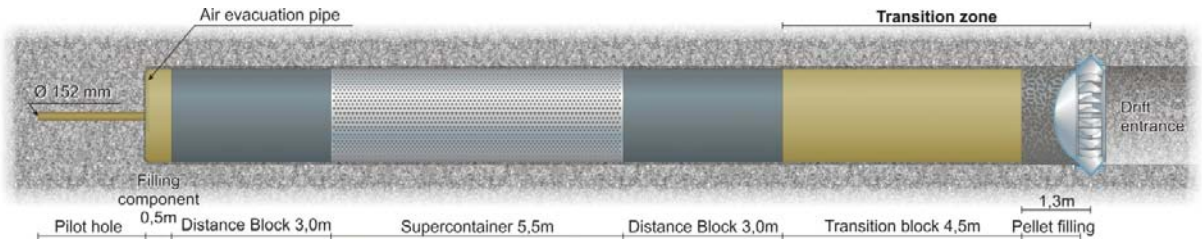

Figure 10-2. *Schematic illustration of the preliminary Multi Purpose Test layout.*

The test consists of one Supercontainer surrounded by distance blocks. At the drift bottom filling components are used to fill the pilot hole and drift bottom. The section is sealed off with a plug with a transition zone consisting of pellets and a transition block inside. The installation will follow the procedures of the reference design, DAWE. Multiple sensors will be installed in the drift to monitor swelling and pore pressure, moisture, temperature and water leakages. After test termination, excavation of the drift will give additional data on e.g. buffer homogenization. The test duration after installation is planned to be in excess of 400 days.

The test can be described as a simplified rehearsal before a system test is carried out. A full system test will only be carried out if it is decided to change the reference design from KBS-3V to KBS-3H.

Objectives and scope of the Multi Purpose Test:

Main objectives

- Test the system components in full scale and in combination with each other to obtain an initial verification of design implementation and component function.
- This includes the ability to manufacture full-scale components, carry out installation (according to DAWE)n and monitor the initial system state of the MPT and its subsequent evolution.

An objective of the test is to demonstrate the manufacturing of the KBS-3H components, their transportation and installation into a drift and the subsequent execution of drainage, artificial watering and air evacuation of DAWE, although for a shorter drift section than in the repository case. Thus one of the objectives is to gain experiences from working in the full-scale at ambient in situ conditions and recognising the implementation issues of the design. Another objective is to study the system behaviour during the early transition period without using heaters.

An additional objective is to study the buffer behaviour during the early part of the buffer evolution, including buffer swelling pressure at the rock interface. The constraints imposed by boundary conditions acting on the KBS-3H test site at Äspö HRL do not allow for rock spalling studies but the swelling pressure data generated can still be used when studying the buffer's ability to prevent thermally induced spalling of rock. The development of swelling pressure exerted on the plug during the operational phase (due to transition zone and distance blocks) will also be addressed.

As the experiment will be ongoing for about 400 days, the buffer will not reach full saturation within the test time. Depending on the test outcome a decision to prolong the test duration could be made. Buffer saturation/homogenization is also studied extensively within KBS-3V and the large/lab-scale test planning will address KBS-3H specific questions as well.

A further objective is to increase the understanding of the degree to which the desired initial state can be accomplished for each component.

The scope of work is summarised and detailed below:

- **Manufacturing of distance blocks, filling components and buffer blocks for the Supercontainer**
  KBS-3H bentonite buffer blocks have not previously been manufactured. Doing this will identify possible issues with the manufacturing process as well as the handing of the buffer blocks. This also includes manufacturing of a buffer mould.
- **Supercontainer assembly and transportation with bentonite buffer blocks**
  The buffer in the Supercontainers used so far has been simulated using concrete blocks. The use of real bentonite buffer blocks will verify the ability to assemble and handle a complete Supercontainer.
- **Emplacement of Supercontainer and distance blocks using the KBS-3H deposition machine**
  So far only Supercontainer and distance block dummies made of concrete have been emplaced. Installation of the Multi Purpose Test will verify the ability to correctly handle and emplace bentonite components.
- **Insight to buffer stability after emplacement but prior to wetting**
  Bentonite buffer blocks will be affected by the high humidity in the drift. This can lead to unwanted block damage or irregularities. Understanding of this process is important to optimise the design and routines for emplacement.
- **Studying buffer saturation and homogenization of Supercontainer buffer and distance blocks with artificial watering**
  Artificial watering is a key operation in the DAWE design. The ability to fill the voids in the test and then remove the water and air evacuation pipes is vital in order to reach the initial state. Complete buffer homogenization requires a very long test time, longer than what is currently planned for tests associated with DAWE. Despite this the initial buffer condition, moisture, temperature, swelling pressure and pore-pressure can be monitored with sensors and the conditions at the end of testing can be analysed with buffer samples during excavation of the test. It is also planned to pre-model the experiment and compare it with the outcome with an objective to add more understanding in buffer behaviour, see below.
- **Measuring swelling pressure achieved in situ from Supercontainer buffer and distance blocks with regards to rock spalling**
  The ability to quickly develop buffer counter pressure on the rock wall to mitigate/prevent rock spalling will be studied in the Multi Purpose Test. A number of sensors will monitor the buffer swelling pressure. Calculations show that the pressure needed will be reached regardless of whether heaters are used in the test or not.
- **Verification of plug functionality**
  The compartment plug test performed in 2009–2010 was successful in that the leakage criterion was met (Section 4.7). The test time in the Multi Purpose Test is longer than in the plug test which will provide useful data regarding the plug performance. This also includes the manufacturing of the plug.
- **Modelling**
  Modelling of the Multi Purpose Test will be carried out prior to installation; the models will later be evaluated relative the actual outcome. The magnitude of the swelling pressure and especially the time from installation to when the buffer generates a sufficient swelling pressure against rock are still uncertain. The development of swelling pressure by the distance blocks and the buffer blocks in the Supercontainer will be studied in the Multi Purpose Test. Modelling of MPT preceded by the BB test with e.g. a combination of distance block and Supercontainer types of bentonite blocks to provide more knowledge for MPT has been suggested. The BB test provides a well defined situation which will occur during the water filling. This would enhance the conditions to model the MPT. There are, however, problems regarding the mechanical model at unsaturated states, which will be the case if the buffer will be only partially saturated.

11 Conclusions

The main objectives of the KBS-3H project 2008–2010 was to develop the KBS-3H solution to such a state that a decision to go ahead with full-scale testing and demonstration could be made. This required evidence on:

- the behaviour of the buffer and other components (Supercontainer, plugs) after emplacement (initial state),
- the long-term performance of the buffer including interaction with other materials,
- and construction, manufacturing and installation of the system.

With respect to the restrictions imposed before the start of and during the execution of the project, mainly the fact that no safety evaluation was included in the Complementary studies phase, the main objectives have been met.

11.1 KBS-3H reference design

One of the highest priority targets of the recent project phase was the establishment of a robust drift design, a KBS-3H reference design. Two main design alternatives were identified in the preceding project phase, the DAWE and the STC design. Establishing one of these two designs as the KBS-3H reference design meant that several unique and some common uncertainties identified during earlier project phases had to be addressed. These were mainly related to buffer behaviour; piping and erosion, swelling and sealing in heterogeneous inflow conditions together with their ability to mitigate thermally induced spalling of rock.

DAWE was early recognized as the main alternative as STC faced problems primarily with erosion and cracking of buffer blocks. The artificial watering of DAWE gives a great advantage by producing an initial state with a water filled compartment of homogeneous water pressure. On the other hand artificial water filling also means potential problems with erosion during filling and a risk that the pipes used for filling and air evacuation are wedged in the drift by swelling buffer. These problems were, however, constrained; the long water filling pipes previously used can be exchanged for shorter pipes and by using fresh water to fill the compartments the erosion during filling should be kept well within the requirements. Using short water filling pipes means that only one long pipe, the air evacuation pipe, remains. Studies that have been carried out show that there is adequate time to remove this pipe before the buffer swell.

A potential advantage with the DAWE design is the mechanical pressure that develops as the buffer swells into contact with the rock wall due to the artificially introduced water. The counter pressure that will be required to prevent thermally induced spalling of rock at Forsmark and Olkiluoto is presently not established but studies have shown that the DAWE design will produce initial buffer swelling pressures are in the order of 50–500 kPa in a dry tunnel section. This may be sufficient to mitigate the thermally induced spalling of rock. Further research will be required in this area.

Establishing a KBS-3H reference design also meant that the KBS-3H components had to be brought to the conceptual design level. Development has been carried out on several components and has lead to an updated drift design which is a considerable simplification of the system and has an improved utilization degree. The filling components have been designed using the same material as the buffer and will hence behave in a similar manner. Tentative calculations and supporting studies indicate that filling blocks can be placed in sections with higher inflows, which possibly eliminates the previously used double compartment plug sections, it should be noted that this design is not ruled out and will be considered in future work as well. A new feature is the drift plug which replaces the combined

compartment and concrete drift end plug of the previous design. The drift plug shortens the installation time and increases the drift utilization degree. The buffer of the Supercontainers and the distance blocks has been re-evaluated and a conceptual design is now established. Drilling techniques, measurement techniques and the geometrical requirements of the drift have also been re-evaluated and recommendations have been made.

All issues concerning DAWE have not been solved, for instance buffer erosion remains, the remaining issues have, however, been further constrained and the understanding of the issues have been considerably improved, also see section 5.9 on remaining buffer issues and future buffer work. DAWE is presently expected to fulfil all requirements and a well founded selection of it as the KBS-3H reference design can be made.

Selection of the metal used for the reference for design, the Supercontainer shell, the drift end and compartment plugs and other supporting structure was another prioritised target of the recent project phase. Long-term safety aspects, mainly the possible negative impacts of the metals on the buffer, were the critical aspect in the selection process. Studies have shown that for the conditions existing at the buffer/rock interface titanium is expected to be the most inert, having lowest corrosion rate and lowest rate of production of hydrogen. In addition, this element is already present in natural bentonites which have been shown to display favourable properties as buffer material. Copper was the other possible material but its limited mechanical strength compared to titanium and steel was a disadvantage. Steel is not ruled out and can be considered again if additional evidence is provided that the iron-bentonite interactions do not compromise the buffer requirements. Titanium has been selected.

11.2 KBS-3H description

One essential part of the project phase was to update the compiled KBS-3H description.

Layout adaptations have been developed for both Forsmark and Olkiluoto. The KBS-3V layout was used as a basis and there are hence further optimizations with respect to utilization, rock strength, state of rock stress directions and fracture orientations will be made in a the upcoming project phase.

A structure for the KBS-3H specific production lines have been outlined. The Production line reports will provide information on how to produce, handle and inspect the engineered barriers and underground openings within the facilities of the KBS-3H system. The main work with the production lines will be carried out in the upcoming project phase.

The programme for hydraulic characterization has also been updated; characterization methodology and grouting techniques have been gone through. A model for predicting the conditions in the fully reamed drift from measurements taken in the pilot hole has also been proposed. This could serve as a starting point for a detailed investigations programme that will be developed in the upcoming project phase.

KBS-3H operational and personnel safety analysis have been carried out according to the “what if” methodology. The analysis focused on three main areas; preparation of drift, the reloading station and the deposition area. In addition to this analysis, a list of initiating events defined for the safety analysis of KBS-3V were checked to verify that no additional events had to be considered. Several risks have been identified and corresponding risk reducing measures proposed.

11.3 Full-scale demonstrations

The previous project phase 2004–2007 focused on demonstrating the KBS-3H technology. Some of the tests that were initiated then have continued throughout the recent project phase. The deposition machine has been run for 50 km both with a Supercontainer and distance blocks made of concrete as well as without any loads. The tests have proven that the technique works and continued development has been initiated to ensure a long-term functionality of the equipment. The Mega-Packer tests have also been completed with very good results, likely giving KBS-3H a solution if post-grouting would be required.

A full-scale demonstration of the compartment plug has also been carried out at the Äspö HRL. The test showed that the concept of compartment plugs is feasible and the compartment plug fulfilled the leakage criterion tentatively set to 0.1 l/min at 5 MPa. In the final step of the test the section behind the plug was filled with bentonite pellets. Leakage through the plug casting was already low but there was a leakage path by-passing the plug, likely through a fracture network, this leakage was sealed when the pellets were introduced and the pellets sealing ability was hence demonstrated.

11.4 KBS-3H, a potential repository solution

The most important conclusion from the recent project phase is that the KBS-3H design has potential as a repository solution and it would be of value to go ahead with the KBS-3H System Design phase. The horizontal design has potential as a more industrialised process during construction and disposal. It is expected to be robust and the prefabricated disposal container, the Supercontainer, will enable an easier quality assurance of the materials closest to the canister. The artificial water filling will also ensure a well defined initial state, which is beneficial for evaluating long-term safety aspects. Although the selection of titanium for the Supercontainer and plugs increase the costs there is still a reduction in total cost for the horizontal alternative when compared to the vertical reference design.

The knowledge gap between the KBS-3V reference design and the horizontal variant has been closed further during the recent project phase, both when it comes to the technical level as well as the design description. There is now a much higher degree of understanding when it comes to long-term performance of the buffer including interaction with other materials and a better understanding of the behaviour of the buffer and other critical components after emplacement. The decision to go ahead with DAWE as the reference design is an important milestone in the KBS-3H development; there is now a much clearer course towards a fully functioning horizontal repository. There is also better evidence on construction, manufacturing and installation of the system. If the planned drift performance and safety evaluations show that the KBS-3H design can provide the long-term safety required it could become a possible alternative to the vertical reference design.

References

SKB's (Svensk Kärnbränslehantering AB) publications can be found at www.skb.se/publications. References to SKB's unpublished documents are listed separately at the end of the reference list. Unpublished documents will be submitted upon request to document@skb.se.

Andersson C J, 2007. Äspö Hard Rock Laboratory. Äspö Pillar Stability Experiment, Final report. Rock mass response to coupled mechanical thermal loading. SKB TR-07-01, Svensk Kärnbränslehantering AB.

Andersson J, Ahokas H, Hudson J A, Koskinen L, Luukkonen A, Löfman J, Keto V, Pitkänen P, Mattila J, Ikonen A T K, Ylä-Mella M, 2007. Olkiluoto site description 2006. Posiva 2007-03, Posiva Oy, Finland.

Autio J, Hagros A, Johansson E, Börgesson L, Sandén T, Rönnqvist P-E, Eriksson M, Berghäll J, Kotola R, Parkkinen I, 2007. Design description 2006. Posiva Working Report 2007-105, Posiva Oy, Finland. (Also published as SKB R-08-32, Svensk Kärnbränslehantering AB.)

Autio J, Hagros A, Johansson E, Börgesson L, Sandén T, Anttila P, Rönnqvist P-E, Eriksson M, Halvarsson B, Berghäll J, Kotola R, Parkkinen I, 2008. KBS-3H design description 2007. Posiva 2008-01, Posiva Oy, Finland. (Also published as SKB R-08-44, Svensk Kärnbränslehantering AB.)

Back P-E, Wrafter J, Sundberg J, Rosén L, 2007. Thermal properties. Site descriptive modelling Forsmark – stage 2.2. SKB R-07-47 Svensk Kärnbränslehantering AB.

Birgersson M, Wersin P, 2013. KBS-3H. Reactive transport modelling of iron-bentonite interactions, an update for the Olkiluoto case. Posiva Working Report 2013-02, Posiva Oy, Finland.

Blanc P, Lassin A, Piantone P, 2007. THERMODDEM: A thermodynamic database devoted for modelling the alteration of waste minerals. Orléans: BRGM. Available at: http://thermoddem.brgm.fr

Buoro A, Dahlbo K, Wiren L, Holmén J, Hermanson J, Fox A (ed), 2009. Geological discrete-fracture network model (version 1) for the Olkiluoto site, Finland. Posiva Working Report 2009-77, Posiva Oy, Finland.

Bäckblom G, Lindgren E, 2005. KBS-3H – Excavation of two horizontal drifts at the Äspö Hard Rock Laboratory during year 2004–2005. Work description, summary of results, and experience. SKB R-05-44, Svensk Kärnbränslehantering AB.

Börgesson L, Hernelind J, 2010. Earthquake induced rock shear through a deposition hole. Modelling of three model tests scaled 1:10. Verification of the bentonite material model and the calculation technique. SKB TR-10-33, Svensk Kärnbränslehantering AB.

Börgesson L, Johannesson L-E, Sandén T, Hernelind J, 1995. Modelling of the physical behaviour of water saturated clay barriers. Laboratory tests, material models and finite element application. SKB TR 95-20, Svensk Kärnbränslehantering AB.

Börgesson L, Sandén T, Fälth B, Åkesson M, Lindgren E, 2005. Studies of buffers behaviour in KBS-3H concept. Work during 2002–2004. SKB R-05-50, Svensk Kärnbränslehantering AB.

Börgesson L, Dueck A, Johannesson L-E, 2010. Material model for shear of the buffer – evaluation of laboratory test results. SKB TR-10-31, Svensk Kärnbränslehantering AB.

Carslaw H S, Jaeger J C, 1959. Conduction of heat in solids. 2nd ed. Oxford: Clarendon. Eriksson M, Lindström L, 2008. KBS-3H post-grouting. Mega-Packer test at –220 m level at Äspö HRL. SKB R-08-42, Svensk Kärnbränslehantering AB.

Glamheden R, Fredriksson A, Röshoff K, Karlsson J, Hakami H, Christiansson R, 2007. Rock mechanics Forsmark. Site descriptive modelling Forsmark stage 2.2. SKB R-07-31, Svensk Kärnbränslehantering AB.

Glamheden R, Fälth B, Jacobsson L, Harrström J, Berglund J, Bergkvist L, 2010. Counterforce applied to prevent spalling. SKB TR-10-37, Svensk Kärnbränslehantering AB.

Grauer R, 1984. Behältermaterialien für die Endlagerung hochradioaktiver Abfälle: Korrosionschemische Aspekte. Nagra Technischer Bericht NTB 84-19, Nagra, Switzerland.

Gribi P, Johnson L, Suter D, Smith P, Pastina B, Snellman M, 2007. Safety assessment for a KBS-3H spent nuclear fuel repository at Olkiluoto. Process report. Posiva 2007-09, Posiva Oy, Finland. (Also published as SKB R-08-36, Svensk Kärnbränslehantering AB.)

Gustafson G, 2009. Hydrogeologi för bergbyggare. Stockholm: Formas.

Hartley L, Hoek J, Swan D, Roberts D, Joyce S, Follin S, 2009. Development of a hydrogeological discrete fracture network model for the Olkiluoto site descriptive model 2008. Posiva Working Report 2009-61, Posiva Oy, Finland.

Hartley L, Hoek J, Swan D, Roberts D, 2010. Hydrogeological discrete fracture network modelling of groundwater flow under open repository conditions. Posiva Working Report 2010-51, Posiva Oy, Finland.

Hellä P (ed), Ikonen A, Mattila J, Torvela T, Wikström L, 2009. RSC-programme – Interim report. Approach and basis for RSC development, layout determining features and preliminary criteria for tunnel and deposition holes scale. Posiva Working Report 2009-29, Posiva Oy, Finland.

Ikonen K, 2003. Thermal analyses of KBS-3H type repository. Posiva 2003-11, Posiva Oy, Finland.

Johansson E, Hagros A, Autio J, Kirkkomäki T, 2007. KBS-3H layout adaptation 2007 for the Olkiluoto site. Posiva Working Report 2007-77, Posiva Oy, Finland. (Also published as SKB R-08-31, Svensk Kärnbränslehantering AB.)

Karnland O, Birgersson M, 2009. Memorandum concerning the use of results from the LOT project at the Swedish National Council for Nuclear Waste seminar "Mechanisms of Copper Corrosion in Aqueous Environments". Swedish National Council for Nuclear Waste. Available at: http://www.karnavfallsradet.se/sites/default/files/dokument/Memo_SKB_on_coppercorrosion.pdf

Karnland O, Sandén T, Johannesson L-E, Eriksen T E, Jansson M, Wold S, Pedersen K, Motamedi M, Rosborg B, 2000. Long-term test of buffer material. Final report on the pilot parcels. SKB TR-00-22, Svensk Kärnbränslehantering AB.

Karnland O, Olsson S, Nilsson U, 2006. Mineralogy and sealing properties of various bentonites and smectite-rich clay materials. SKB TR-06-30, Svensk Kärnbränslehantering AB.

Kim S S, Chun K S, Kang K C, Baik M H, Kwon S H, Choi J W, 2007. Estimation of the corrosion thickness of a disposal container for high-level radioactive wastes in a wet bentonite. Journal of Industrial and Engineering Chemistry 13, 959–964.

King F, 2008. Corrosion of carbon steel under anaerobic conditions in a repository for SF and HLW in Opalinus Clay. Nagra Technical Report NTB 08-12, Nagra, Switzerland.

King F, Wersin P, 2013. Review of Supercontainer copper shell-bentonite interactions and possible effects on buffer performance for the KBS-3H design. Posiva Working Report 2013-03, Posiva Oy, Finland.

Kirkkomäki T, 2009. Loppusijoituslaitoksen asemointi ja vaiheittainen rakentaminen. Posiva Työraportti 2009-51, Posiva Oy, Finland. (In Finnish.)

Kirkkomäki T, Rönnqvist P-E, 2011. KBS-3H tekniikka, asemointi ja vaiheittainen rakentaminen. Posiva Työraportti 2010-77, Posiva Oy, Finland. (In Finnish with an English abstract.)

Kumpulainen S, Kiviranta L, Carlsson T, Muurinen A, Svensson D, Sasamoto H, Yui M, Wersin P, Rosch D, 2011. Long-term alteration of bentonite in the presence of metallic iron. Posiva Working Report 2010-71, Posiva Oy, Finland.

Lanyon G W, Marshall P, 2006. Discrete fracture network modelling of a KBS-3H repository at Olkiluoto. Posiva 2006-06, Posiva Oy, Finland. (Also published as SKB R-08-26, Svensk Kärnbränslehantering AB.)

Little B, Wagner P, Mansfeld F, 1991. Microbiologically influenced corrosion of metals and alloys. International Materials Reviews 36, 253–272.

Ludvigson J-E, Hansson K, Rouhianen P, 2002. Methodology study of Posiva difference flow meter in borehole KLX02 at Laxemar. SKB R-01-52, Svensk Kärnbränslehantering AB.

Löfman J, 1999. Site scale groundwater flow in Olkiluoto. Posiva 99-03, Posiva Oy, Finland.

Löfman J, Poteri A, 2008. Groundwater flow and transport simulations in support of RNT-2008 analysis. Posiva Working Report 2008-52, Posiva Oy, Finland.

Lönnqvist M, Hökmark H, 2007. Thermo-mechanical analyses of a KBS-3H deposition drift at Olkiluoto site. Posiva Working Report 2007-66, Posiva Oy, Finland. (Also published as SKB R-08-30, Svensk Kärnbränslehantering AB.)

Lönnqvist M, Hökmark H, Fälth B, 2010. THM-issues in repository rock. Thermal, mechanical, thermo-mechanical and hydro-mechanical evolution of the rock at the Forsmark and Laxemar sites. SKB TR-10-23, Svensk Kärnbränslehantering AB.

Martin C D, Christiansson R, 2009. Estimating the potential for spalling around a deep nuclear waste repository in crystalline rock. International Journal of Rock Mechanics and Mining Sciences 46, 219–228.

Marty N C M, Fritz B, Clément A, Michau N, 2010. Modelling the long-term alteration of the bentonite barrier in an underground radioactive waste repository. Applied Clay Science 47, 82–90.

Mattsson H, Olefjord I, 1984. General corrosion of Ti in hot water and water saturated bentonite clay. SKB TR 84-19, Svensk Kärnbränslehantering AB.

Neretnieks I, 2006. Flow and transport through a damaged buffer – exploration of the impact of a cemented and an eroded buffer. SKB TR-06-33, Svensk Kärnbränslehantering AB.

Neretnieks I, Liu L, Moreno L, 2010. Mass transfer between waste canister and water seeping in rock fractures. Revisiting the Q-equivalent model. SKB TR-10-42, Svensk Kärnbränslehantering AB.

Palandri J L, Kharaka Y K, 2004. A compilation of rate parameters of water-mineral interaction kinetics for application to geochemical modeling. Open File Report 2004-1068, U.S. Geological Survey, Denver, Colorado.

Pastina B, Hellä P, 2010. Models and data report 2010. Posiva 2010-01, Posiva Oy, Finland.

Pedersen K. 2008. Microbiology of Olkiluoto groundwater 2004–2006. Posiva 2008-02, Posiva Oy, Finland

Posiva, 2005. Olkiluoto site description 2004 (Vol 1–3). Posiva 2005-03, Posiva Oy, Finland.

Posiva 2009. Olkiluoto site description 2008. Posiva 2009-01, Posiva Oy, Finland.

Posiva, 2010. Nuclear waste management at Olkiluoto and Loviisa power plants. Review of current status and future plans for 2010–2012. Posiva TKS-2009, Posiva Oy, Finland.

Posiva, 2012. Safety case for the disposal of spent nuclear fuel at Olkiluoto – Design basis 2012, Eurajoki. Posiva 2012-03, Posiva Oy, Finland.

Puigdomenech I, Taxén C, 2000. Thermodynamic data for copper. Implications for the corrosion of copper under repository conditions. SKB TR-00-13, Svensk Kärnbränslehantering AB.

Sandén T, Börgesson L, Dueck A, Goudarzi R, Lönnqvist M, Nilsson U, Åkesson M, 2008a. KBS-3H. Description of buffer tests in 2005–2007. Results of laboratory tests. SKB R-08-40, Svensk Kärnbränslehantering AB.

Sandén T, Börgesson L, Dueck A, Goudarzi R, Lönnqvist M, 2008b. Deep repository – Engineered barrier system. Erosion and sealing processes in tunnel backfill materials investigated in laboratory. SKB R-08-135, Svensk Kärnbränslehantering AB.

Sandstedt H, Pers K, Birgersson L, Ageskog L, Munier R, 2001. Project JADE. Comparison of repository systems. Executive summary of results. SKB TR-01-17, Svensk Kärnbränslehantering AB.

Scholz C H, 2002. The mechanics of earthquakes and faulting. 2nd ed. Cambridge: Cambridge University Press.

Schultz R W, 2005. Corrosion of titanium and titanium alloys. In Cramer S D, Covino B S (eds). ASM handbook. Vol 13B, Corrosion: materials. Materials Park, OH: ASM International, 252–299.

Shoesmith D W, 2006. Assessing the corrosion performance of high-level nuclear waste containers. Corrosion 62, 703–722.

SKB, 1989. WP-Cave – assessment of feasibility, safety and development potential. SKB TR 89-20, Svensk Kärnbränslehantering AB.

SKB, 1993. Project on Alternative System Study (PASS). Final report. SKB TR 93-04, Svensk Kärnbränslehantering AB.

SKB, 2001a. Forsknings-, utvecklings- och demonstrationsprogram för ett KBS-3-förvar med horisontell deponering [Research, development and demonstration programme for a KBS-3H repository with horizontal deposition]. SKB R-01-55, Svensk Kärnbränslehantering AB. (In Swedish.)

SKB, 2001b. RD&D-Programme 2001. Programme for research, development and demonstration of methods for the management and disposal of nuclear waste. SKB TR-01-31, Svensk Kärnbränslehantering AB.

SKB, 2004. RD&D-Programme 2004. Programme for research, development and demonstration of methods for the management and disposal of nuclear waste. SKB TR-04-21, Svensk Kärnbränslehantering AB.

SKB, 2007. Final repository facility. Underground design premises/D2. SKB R-07-33, Svensk Kärnbränslehantering AB.

SKB, 2008. Horizontal deposition of canisters for spent nuclear fuel; Summary of the KBS-3H project 2004–2007. SKB TR-08-03, Svensk Kärnbränslehantering AB.

SKB, 2009a. Site engineering report Forsmark. Guidelines for underground design Step D2. SKB R-08-83, Svensk Kärnbränslehantering AB.

SKB, 2009b. Design premises for a KBS-3V repository based on results from the safety assessment SR-Can and some subsequent analyses. SKB TR-09-22, Svensk Kärnbränslehantering AB.

SKB, 2009c. Underground design Forsmark. Layout D2. SKB R-08-116, Svensk Kärnbränslehantering AB.

SKB, 2010a. Ramprogram för detaljundersökningar vid uppförande och drift av slutförvar för använt kärnbränsle. SKB R-10-08, Svensk Kärnbränslehantering AB.

SKB, 2010b. RD&D Programme 2010. Programme for research, development and demonstration of methods for the management and disposal of nuclear waste. SKB TR-10-63, Svensk Kärnbränslehantering AB.

SKB, 2010c. Design and production of the KBS-3 repository. SKB TR-10-12, Svensk Kärnbränslehantering AB.

SKB, 2010d. Design, production and initial state of the backfill and plug in deposition tunnels. SKB TR-10-16, Svensk Kärnbränslehantering AB.

SKB, 2010e. Design, production and initial state of the buffer. SKB TR-10-15, Svensk Kärnbränslehantering AB.

SKB, 2011. Long-term safety for the final repository for spent nuclear fuel at Forsmark. Main report of the SR-Site project. SKB TR-11-01, Svensk Kärnbränslehantering AB.

Smart N R, Rance A P, Werme L O, 2004. Anaerobic corrosion of steel in bentonite. In Oversby V M, Werme L O (eds). Scientific basis for nuclear waste management XXVII: symposium held in Kalmar, Sweden, 15–19 June 2003. Warrendale, PA: Materials Research Society. (Materials Research Society Symposium Proceedings 807), 441–446.

Smith P, Neall F, Snellman M, Pastina B, Hjerpe T, Nordman H, Johnson L, 2007a. Safety assessment for a KBS-3H spent nuclear fuel repository at Olkiluoto. Summary report. Posiva 2007-06, Posiva Oy, Finland. (Also published as SKB R-08-39, Svensk Kärnbränslehantering AB.)

Smith P, Nordman H, Pastina B, Snellman M, Hjerpe T, Johnson L, 2007b. Safety assessment for a KBS-3H spent nuclear fuel repository at Olkiluoto. Radionuclide transport report. Posiva 2007-07, Posiva Oy, Finland. (Also published as SKB R-08-38, Svensk Kärnbränslehantering AB.)

Smith P, Johnson L, Snellman M, Pastina B, Gribi P, 2007c. Safety assessment for a KBS-3H spent nuclear fuel repository at Olkiluoto. Evolution report. Posiva 2007-08, Posiva Oy, Finland. (Also published as SKB R-08-37, Svensk Kärnbränslehantering AB.)

SSM, 2008a. Strålsäkerhetsmyndighetens föreskrifter och allmänna råd om skydd av människors hälsa och miljön vid slutligt omhändertagande av använt kärnbränsle och kärnavfall (The Swedish Radiation Safety Authority's regulations on the protection of human health and the environment in connection with the final management of spent nuclear fuel and nuclear waste). Stockholm: Strålsäkerhetsmyndigheten (Swedish Radiation Safety Authority). (SSMFS 2008:37) (In Swedish.)

SSM, 2008b. Strålsäkerhetsmyndighetens föreskrifter och allmänna råd om säkerhet vid slutförvaring av kärnämne och kärnavfall (The Swedish Radiation Safety Authority's regulations and general recommendations concerning safety in connection with the disposal of nuclear material and nuclear waste). Stockholm: Strålsäkerhetsmyndigheten (Swedish Radiation Safety Authority). (SSMFS 2008:21) (In Swedish.)

SSM, 2009. Evaluation of SKB/Posiva's report on the horizontal alternative of the KBS-3 method. SSM 2009:35, Strålsäkerhetsmyndigheten (Swedish Radiation Safety Authority).

Steefel C I, 2006. CrunchFlow. Software for modeling multicomponent reactive flow and transport. User's manual. Lawrence Berkeley National Laboratory, Berkeley, USA.

Sundberg J, Wrafter J, Ländell M, Back P-E, Rosén L, 2008. Thermal properties Forsmark. Modelling stage 2.3. Complementary analysis and verification of the thermal bedrock model, stage 2.2. SKB R-08-65, Svensk Kärnbränslehantering AB.

Taylor G, 1966. The force exerted by an electric field on a long cylindrical conductor. Proceedings of the Royal Society of London, Series A, 291, 145–158.

Thorsager P, Lindgren E, 2004. KBS-3H. Summary report of work done during Basic Design. SKB R-04-42, Svensk Kärnbränslehantering AB.

Wersin P, Curti E, Appelo C A J, 2004. Modelling bentonite–water interactions at high solid/liquid ratios: swelling and diffuse double layer effects. Applied Clay Science 26, 249–257.

Wersin P, Birgersson M, Olsson S, Karnland O, Snellman M, 2007. Impact of corrosion-derived iron on the bentonite buffer within the KBS-3H disposal concept. The Olkiluoto site as case study. Posiva 2007-11, Posiva Oy, Finland.

Wersin P, Grolimund D, Kumpulainen S, Kiviranta L, Brendlé J, Snellman M, 2011. Titanium alloys as alternative material for the supercontainer shell in the KBS-3H concept: a preliminary Ti-clay interaction study. Posiva Working Report 2010-72, Posiva Oy, Finland. (Also published as SKB R-10-51, Svensk Kärnbränslehantering AB.)

Wersin P, Kiczka M, Rosch D, 2012. Safety case for the disposal of spent nuclear fuel at Olkiluoto: Radionuclide solubility limits and migration parameters for the canister and the buffer. Posiva 2012-39, Posiva Oy, Finland.

Åkesson M, Kristensson O, Börgesson L, Dueck A, Hernelind J, 2010. THM modelling of buffer, backfill and other system components. Critical processes and scenarios. SKB TR-10-11, Svensk Kärnbränslehantering AB.

Öhberg A, 2006. Investigation equipment and methods used by Posiva. Posiva Working Report 2006-81, Posiva Oy, Finland.

Unpublished documents

SKBdoc id, version	Titel	Utfärdare, år
1203875 ver 1.0	Ritningsförteckning för kapselkomponenter (In Swedish)	SKB, 2009

Appendix A

Filling blocks in position of inflows, length calculations

As presented in the main chapter, filling blocks will be placed in drift positions intersected by fractures giving initial inflows to the drift above 0.1 l/min (Figure A-1).

Below it is discussed how to formulate a criterion that defines the length of the filling as a function of the initial inflow from the fracture. The criterion is provisional, being based solely on considerations of radionuclide release and transport. However, it should also be noted that the scenario analysed may not reflect the most severe impact of having high flows close to a deposited canister. This means that the appropriate distance between a canister and a flowing fracture needs to be reassessed once a complete safety assessment of 3H is carried out.

The proposed approach can be stated as follows:

- suppose the drift section containing the filling block is intersected by a fracture giving an initial inflow QA > 0.1 litre per minute,
- suppose a canister in a Supercontainer adjoining this filling block fails and releases all radionuclides not incorporated in the fuel matrix relatively quickly (i.e. the IRF and the inventory in Zircaloy and other metal parts) to the surrounding buffer inside the Supercontainer,
- the maximum rate of release of these radionuclides to the fracture following its diffusion through the buffer should be such that Finnish geo-bio flux constraints are satisfied by a significant margin.

Finnish safety assessments have shown that I-129, Cl-36 and C-14 generally dominate the release or dose maximum following canister failure, with C-14 often dominating in cases of early canister lifetime and a degraded effectiveness of the repository barriers, and I-129 and Cl-36 dominating in many other cases (this being due to the shorter half life of C-14). Table A-1 gives their activity inventories and its partitioning (Smith et al. 2007a) and their geo-bio flux constraints.

In Table A-1, the normalised release is the inventory in the IRF in Zircaloy and in other metal parts, divided by the geo-bio flux constrain. This normalised release is dominated by C-14 and hence, in the following, attention is focussed on this radionuclide.

It is further assumed that, at some distance L_f from the drift, the fracture is intersected by a larger feature, such that the hydraulic pressure difference between this feature and the drift, together with the transmissivities of the fracture, controls initial inflow. This allows a value for the fracture

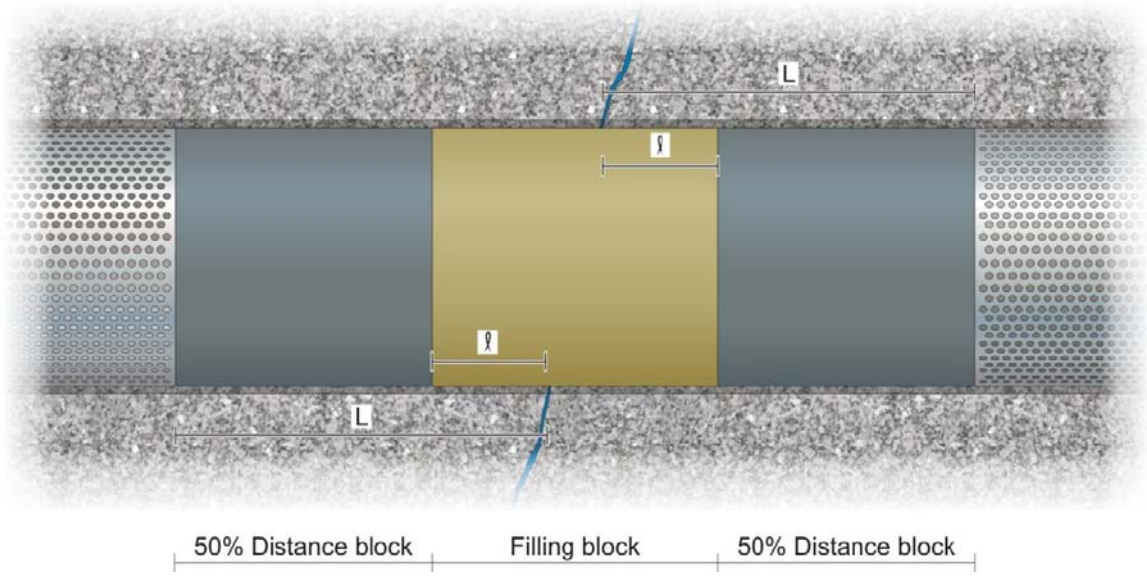

Figure A-1. *KBS-3H drift, showing the position of a filling block between split distance blocks and 2 Supercontainers. Note that the inclination of fracture has effect on the length of filling block.*

Table A-1. Data for key radionuclides.

RN	Activity inventory [GBq/tU]	Partitioning [%]				Geo-bio flux constrain [GBq a^{-1}]	Normalised release [a/tU]
		Fuel matrix	IRF	Zircaloy	Other metal parts		
C-14	$2.78 \cdot 10^{1}$	30	3	33	33	0.3	63.9
Cl-36	$1.04 \cdot 10^{0}$	45	5	50	0	0.3	1.90
I-129	$1.14 \cdot 10^{0}$	95	5	0	0	0.1	0.57

transmissivity to be inferred from the initial inflow. The long-term flow rate through the fracture can then be inferred from the transmissivity and the regional hydraulic gradient (*see Section below on Relationship between initial inflow and long-term flow)*. This simplistic approach is not well substantiated, but is deemed adequate for the present scoping calculations.

It is assumed that C-14, released as a pulse, is well mixed in the vertical direction, so that only 1-D diffusive transport along the drift is considered. Conservatively, only transport along the drift towards the fracture is considered (Figure A-1). Diffusion away from the fracture in the other direction along the drift is disregarded. Furthermore, also conservatively, all C-14 reaching the position in the drift where the fracture intersects is assumed to be transferred to the fracture, and not to diffuse further along the drift. The governing equation for diffusion along the drift is presented and solved in Appendix C.

Dimensioning

The results from the general approach described in Section 1 are shown in Figures A-2 and A-3. The figures plot the value of L required such that the flux to the fracture is either 0.03 GBq per year or 0.01 GBq i.e. 10% or 3% of the Finnish regulatory geo-bio flux constraint of 0.3GBq per year. f the ratio of transport aperture to hydraulic aperture of the fracture, is set to 10 in Figure A-2 and to 100 in Figure A-3.

The margin needed such that Finnish geo-bio flux constraints are satisfied is unclear. On the one hand, the model used here is quite conservative, especially in that spreading of the C-14 release during geo-sphere transport is not taken into account, but could be significant. Also, the entire inventory in the

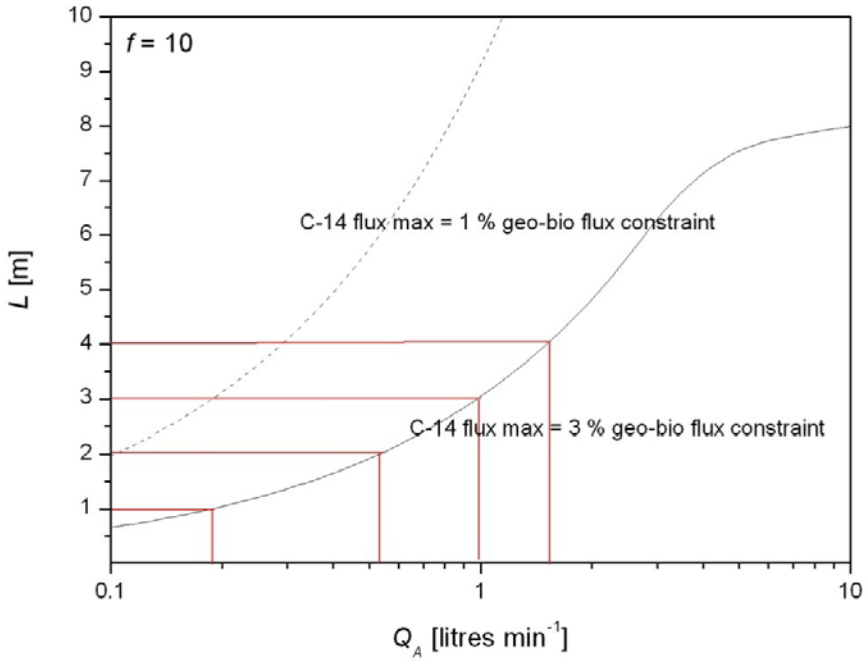

Figure A-2. *Proposed minimum respect distance (L) as a function of initial inflow to fracture and a ratio of transport aperture to hydraulic aperture of 10.*

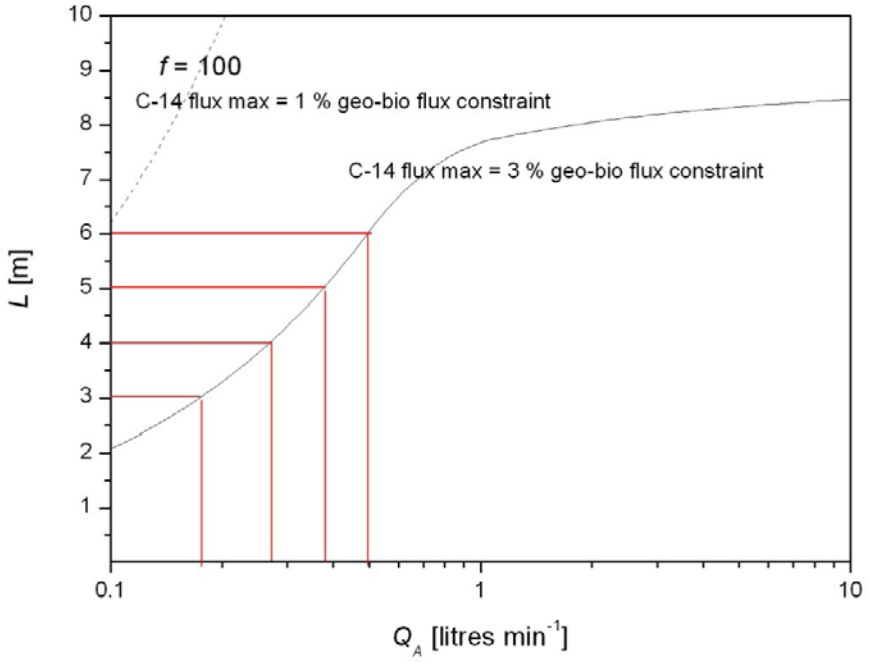

Figure A-3. *Proposed minimum respect distance (L) as a function of initial inflow to fracture and a ratio of transport aperture to hydraulic aperture of 100.*

Zircaloy and other metal parts are lumped together with the IRF. Note that the assumed fractional release rate from Zircaloy in safety assessments since TILA-99 has been 10^{-4} per year, and so a significant fraction of the C-14 in the Zircaloy will decay before it is ever released. On the other hand, the model considers only one failed canister, whereas the possibility of several failed canisters has to be accounted for.

Figure A-4 shows the results for $f = 100$, considering the C-14 IRF and inventory from other metal parts, but not the Zircaloy inventory.

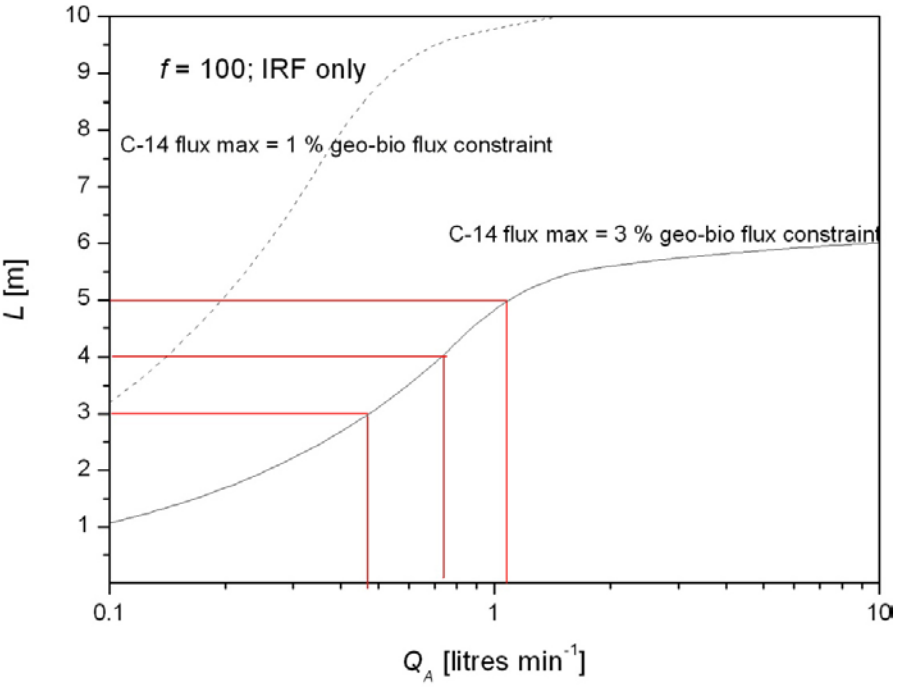

Figure A-4. *Proposed minimum respect distance (L) as a function of initial inflow to fracture and a ratio of transport aperture to hydraulic aperture of 100. Release from Zircaloy not included.*

On balance, however, it is tentatively proposed that a criterion that C-14 release to the fracture should not exceed 3% of the geo-bio flux maximum is appropriate, based on the results shown in Figure A-4. These results suggest the respect distances presented in Table A-2.

Relationship between initial inflow and long-term flow

A high initial inflow from a fracture intersecting an open drift clearly suggests that the long-term flow through this fracture around the drift once the EBS has been emplaced and early, transient processes associated with saturation and heat generation have ceased is also likely to be relatively high. Below, a simplified modelling approach is adopted to quantify this relationship. This approach is based on some assumptions that are not well substantiated. Nevertheless, the approach is deemed sufficient for the purposes of the present tentative calculations. Detailed groundwater flow modelling in which multiple realisations of the fracture network are considered would be needed to obtain a more accurate indication of the relationship between initial inflow and long-term flow.

Consider a fracture intersecting the drift that gives an initial inflow Q_A [$m^3\ s^{-1}$]. Assume that, at some distance L_f [m] from the drift, the fractures is intersected by a larger feature, such that the hydraulic pressure difference between this feature and the drift, together with the transmissivity of the fracture, controls initial inflow. From the solution of Darcy's Law in cylindrical polar coordinates, the transmissivity of the fracture, T[$m^2\ s^{-1}$] is given by:

$$T = \frac{\rho g Q_A}{2\pi P} \ln\left(\frac{L_f + r_t}{r_t}\right); \qquad \text{(A-1)}$$

with:

ρ density of water (1,000 kg m^{-3})

g gravitational acceleration (9.81 m s^{-2})

P hydrostatic pressure at repository depth ($4 \cdot 10^6$ Pa)

r_t drift radius (0.925 m).

In the long-term, flow around the drift is assumed be controlled by the fracture transmissivity and by the regional hydraulic gradient, such that the flow per unit width of fracture is given by:

$$Ti = \frac{\rho g Q_A i}{2\pi P} \ln\left(\frac{L_f + r_t}{r_t}\right) \qquad \text{(A-2)}$$

with:

i long-term hydraulic gradient (which may vary due to major climate change, see Appendix C).

Table A-2. Respect distances (L in Figure A-1) with respect to inflow rates based on the results shown in Figure A-4.

Initial inflow range [litre min^{-1}]	Respect distance [m]
0.1–0.5	3 m
0.5–1	5 m
> 1	6 m

Appendix B

Dimensioning of the transition zone

Below is the analytical calculations used to specify the length of the transition zone on the inside of the plugs.

Prerequisites

The initial conditions and geometries of the system are described in Figure B-1. The bentonite properties have been simplified so that it has been assumed to be completely saturated and homogenized from start. The highest average density allowed has been assumed since it yields the longest transition zone.

Geometry

- Radius = 0.925 m.
- Distance from the filling block to the plug filled with pellets: 1.3 m.

Initial properties

- Dry density of the pellets filling rdp = 1,000 kg/m^3.
- Dry density of the transition zone rdt = 1,635 kg/m^3.
- Swelling pressure of the distance block section ps = 10.8 MPa.

The relation between swelling pressure and dry density can for MX-80 be described by Equations B-1 and B-2 (Börgesson et al. 1995).

$$p = p_r \left(\frac{e}{e_r} \right)^{\frac{1}{\beta}} \tag{B-1}$$

where

e = void ratio

e_r = reference void ratio (= 1.1)

p = swelling pressure (at e)

p_r = reference swelling pressure (at e_0) (= 1,000 kPa)

β = –0.19

$$\rho_d = \frac{\rho_s}{1+e} \tag{B-2}$$

where

ρ_s = dry density

e = void ratio

ρ_s = density of solids = 2,780 kg/m^3

Dimensioning calculations

The calculations are made in the following way: The large difference in density and resulting swelling pressure of the bentonite in the transition zone and the bentonite in the pellets filling results in a swelling of the bentonite from the transition zone and compression of the bentonite in the pellets filling. There will not be a complete homogenization due to the shear resistance (friction angle) between the bentonite and the rock. Instead there will be a swelling pressure (and thus density) gradient between the plug and the end of the transition zone. The length of the transition zone will be dimensioned by the position where the density is unchanged.

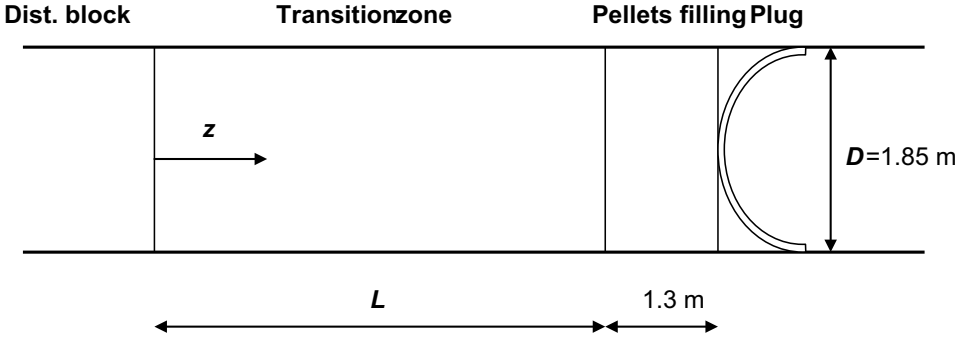

Figure B-1. *Basic geometry used for the calculation.*

The dry density distribution can be calculated from the swelling pressure distribution by combining Equations B-1 and B-2 with the following Equations B-3 and B-4 that describe the axial swelling pressure as a function of the axial distance from the unaffected bentonite at equilibrium after completed swelling in a cylindrical confinement.

$$p = p_0 \cdot e^{-\frac{2z\tan\phi}{r}} \tag{B-3}$$

$$z = -\frac{r}{2\tan\phi}\ln\frac{p}{p_0} \tag{B-4}$$

where

z = axial distance from the unaffected bentonite

r = radius

p = swelling pressure at z

p_0 = swelling pressure at $z = 0$

ϕ = friction angle (= 5°-30° depending on the swelling pressure and the roughness of the rock surface)

The swelling can be modelled according to Equations B-1 to B-3. Combining the expressions in Equations B-1 and B-3 for the swelling pressure yields Equation B-5.

$$p_r\left(\frac{e}{e_r}\right)^{\frac{1}{\beta}} = p_0 \cdot e^{-\frac{2z\tan\phi}{r}} \tag{B-5}$$

Applying Equation B-2 for the relation between void ratio and dry density and

e_r = 1.1 = reference void ratio

p_r =1,000 kPa = reference swelling pressure at e_r = 1.1

p_0 = 10,800 kPa = swelling pressure at $z = 0$

yield Equation B-6:

$$1{,}000 \cdot \left(\frac{\left(\frac{\rho_s}{\rho_d}\right)-1}{1.1}\right)^{\frac{1}{\beta}} = 10{,}800 \cdot e^{-\frac{2z\tan\phi}{r}} \tag{B-6}$$

$$\frac{\frac{\rho_s}{\rho_d}-1}{1.1} = \left(10.8 \cdot e^{-\frac{2z\tan\phi}{r}}\right)^{\beta} \tag{B-7}$$

$$\frac{\rho_s}{\rho_d} = 1.1 \cdot e^{-\frac{2z\tan\phi}{r}\beta} \cdot 10.8^{\beta} + 1 \tag{B-8}$$

Applying $\beta = -0.19$, $r = 0.925$ m and $\rho_s = 2.78$ t/m^3 yields

$$\frac{2.78}{\rho_d} = 0.70 \cdot e^{\frac{0.38 \cdot z \cdot \tan\phi}{0.925}} + 1 \tag{B-9}$$

$$\rho_d = \frac{2.78}{0.70 \cdot e^{0.41 \cdot z \cdot \tan\phi} + 1} \tag{B-10}$$

Equation B-10 thus yields the dry density distribution along the tunnel axis after force equilibrium. But in order to settle the required length of the transition zone L we need to use the fact that the mass of bentonite lost in the transition zone due to swelling is the same as the mass gained in the 1.3 m long pellets filling part due to the same swelling and subsequent compression of the pellets filling meaning that the total dry mass of bentonite between the plug and the unaffected distance block section is the same before and after swelling

The dry mass dm_s over an axial length of dz of the tunnel can be formulated with Equation B-11.

$$dm_S = \rho_d \cdot \pi r^2 dz = \frac{2.78}{0.70 \cdot e^{0.41 \cdot z \cdot \tan\phi} + 1} \cdot \pi r^2 dz \tag{B-11}$$

$$dm_S = \frac{2.78\pi 0.925^2 dz}{0.70 \cdot e^{0.41 \cdot z \cdot \tan\phi} + 1} = \frac{7.47}{0.70 \cdot e^{0.41 \cdot z \cdot \tan\phi} + 1} dz$$

$$dm_S = \frac{10.67}{e^{0.41 \cdot z \cdot \tan\phi} + 1.42} dz \tag{B-12}$$

In order to calculate the total mass M_{ST} we have to integrate the mass from $z = 0$ to $z = L+1.3$ m $= L_T$, but at first we change Equation B-12 to Equation B-13:

$$dm_S = \frac{a}{e^{b \cdot z} + c} dz \tag{B-13}$$

where

$a = 10.67$

$b = 0.41 \cdot \tan\phi$

$c = 1.43$

Integration according to Equation B-14 yields the total mass M_{ST} according to Equation B-15.

$$M_{ST} = \int_{z=0}^{z=L_T} dm_S = \int_{z=0}^{z=L_T} \frac{a}{e^{b \cdot z} + c} dz \tag{B-14}$$

$$M_{ST} = \frac{aL_T}{c} - \frac{a}{bc}\ln(c + e^{bL_T}) + \frac{a}{bc}\ln(c+1) \tag{B-15}$$

We thus have a general expression of the total dry mass over the length of the transition zone and the pellets filling after swelling.

The initial dry mass of bentonite in the transition zone (over the length L) is calculated according to Equation from B-16 to Equation B-17.

$$M_{S1} = \rho_d \pi r^2 L = 1.635 \cdot \pi \cdot 0.925^2 \cdot L = 4.395L \tag{B-16}$$

The initial mass of dry bentonite in the pellets filling is

$$M_{S2} = \rho_d \pi r^2 L_P = 1.0 \cdot \pi \cdot 0.925^2 \cdot 1.3 = 3.494 \quad \text{(B-17)}$$

The total dry mass is thus

$$M_{ST} = M_{S1} + M_{S2} = 4.395L + 3.494 = 4.395(L_T - 1.3) + 3.494 \quad \text{(B-18)}$$

By combining Equations B-15 and B-18 we can calculate L_T for different friction angles. By including the total length in Equation B-3 we can also calculate the swelling pressure on the plug. Table B-1 shows the results.

The required length of the transition zone and the resulting swelling pressure on the plug are thus very dependent on the friction angle. The friction angle for swelling pressures between 1 and 10 MPa is about $\phi = 10°$, which thus can be used as dimensioning value. However, the friction angle between bentonite and a smooth plane surface of rock can be lower (about 50% according to Börgesson et al. 1995), which would motivate using $\phi = 5°$.

Uncertainties

There are several simplifications and uncertainties related to these calculations. The following simplifications have been made:

1. The geometry of the plug is simplified.
2. No account has been taken to the initial slot between the bentonite blocks and the rock surface and the resulting radial density distribution.
3. No account has been taken to the water saturation phase, which in combination with the slot at the rock surface may affect the stress path during swelling.
4. The analytical calculation includes several simplified assumptions:
   a. No consideration of the hysteresis effects at loading and unloading has been taken.
   b. Potential radial stress gradients caused by the axi-symmetric swelling has not been taken into account.
   c. Potential differences between radial and axial stresses at uniaxial swelling and compression have not been taken into account.

It is difficult to estimate the importance of these simplifications. However, similar analytical calculation techniques have been used in different situations for KBS-3V and comparisons with FEM-calculations have shown reasonable agreement (Åkesson et al. 2010).

Another uncertainty is of course the friction angle between the bentonite and the rock and if future investigations or development of the drilling technique show that the rock surface is smooth this has to be taken into account.

Since there is a distance block section between the Supercontainer and the transition zone according to the present design, this is judged to yield sufficient safety margins for the uncertainties caused by the simplified calculation method. If, however, the distance block section is removed it is advisable to do more careful FEM-calculations of this case.

Table B-1. Results of the calculations.

Friction angle ϕ	Total length L_T	Length of transition zone L	Swelling pressure on the plug
5°	8.1 m	6.8 m	2.33 MPa
10°	5.8 m	4.5 m	1.40 MPa
20°	4.0 m	2.7 m	0.46 MPa
30°	3.2 m	1.9 m	0.20 MPa

Appendix C

Diffusion along the drift

The system to be modelled is shown in Figure C-1. Diffusion takes in the drift in both the r-direction (assumed relatively rapid, such that there are no concentration gradients in r) and in the x-direction. Conservatively, only the volume between $r = r_c$ (the canister radius) and $r = r_t$ (the drift radius) is assumed to be accessible by diffusion, i.e. diffusion takes place through a cross-sectional area:

$$A = \pi\left(r_t^2 - r_c^2\right) \tag{C-1}$$

The equation governing diffusion along the drift is:

$$\frac{\partial C}{\partial t} = D\frac{\partial^2 C}{\partial x^2}, \tag{C-2}$$

where C [Bq m^{-3}] is C-14 dissolved concentration and D is the pore diffusion coefficient of C-14 in bentonite, which is here taken to be $1.2 \cdot 10^{-10}$ m^2 s^{-1} (value for neutral and cationic species in Section 5.2 of Smith et al. 2007b).

No exact analytical solution is known to the author that would account both for transfer of C-14 from the drift to the fracture, and continuing diffusion along the drift beyond the fracture. Instead, two limiting cases are considered:

Case a: in which C-14 that exits the failed canister diffuses only in the positive x-direction towards the fracture, and is captured by the fracture, such that there is no diffusion along the fracture for $x < 0$ or for $x > L$.

Case b, in which C-14 that exits the failed canister diffuses in the positive and negative x-directions, and only a small fraction is captured by the fracture, such that the evolution of C-14 concentration in the drift can be assumed to be unaffected by the fracture.

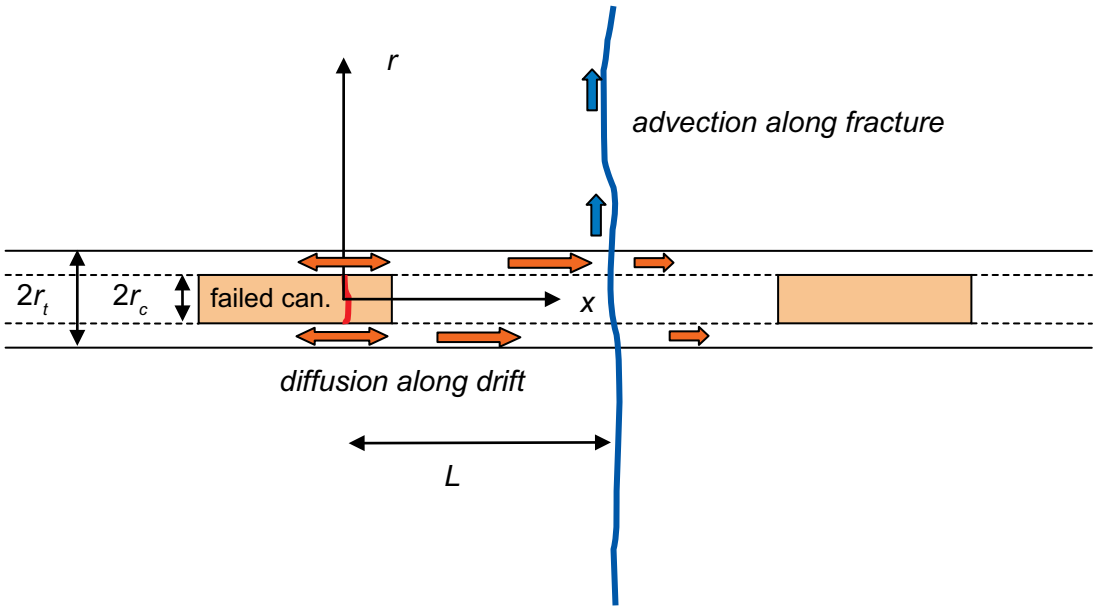

Figure C-1. *The system to be modelled*

Case a becomes an increasingly good approximation as the flow rate in the fracture increases. Case b is a good approximation for low flow rates in the fracture. Both are expected to be conservative, in the sense that they will tend to over-estimate C-14 release to the fracture. Thus, the release to the fracture, R [mol a^{-1}] is taken to be:

$$R = Q \begin{cases} C_a\big|_{x=L} = \varepsilon D A \dfrac{\partial C_a}{\partial x}\Big|_{x=L} \\ \\ C_b\big|_{x=L} \end{cases} \quad \text{the smaller} \tag{C-3}$$

where C_a and C_b are C-14 concentrations, evaluated for cases a and b, respectively, ε is the effective porosity for C-14, taken to be 0.43 (value for neutral and cationic species in Section 5.2 of Smith et al. 2007b) and Q is an effective flowrate through fracture that takes into account the transport resistance of the filling blow/rock interface. It is given by:

$$Q_{eff} = 4\sqrt{2 D_w T i r_t b} \tag{C-4}$$

where D_w is the diffusion coefficient of C-14 in water ($2 \cdot 10^{-9}$ m^2 s^{-1}). $2b$, the transport aperture of the fracture, is obtained using Eq. B.1. The product Ti is obtained using Eq. A-2.

Case a

In case a, where diffusion takes place only in the positive x-direction, the boundary condition at the failure location on the canister ($x = 0$) is:

$$\varepsilon D A \int_0^t \frac{\partial C_a}{\partial x}\bigg|_{x=0} dt = \begin{cases} 0 & t = 0 \\ M & t > 0 \end{cases} \tag{C-5}$$

where M is the mass of C-14 released from the canister to the drift upon canister failure and $t = 0$ is canister failure time.

In order to solve Eq. C-2, consider the parameter V, where:

$$V(x,t) = \int_0^t C_a(x,\tau) d\tau \,. \tag{C-6}$$

V is also governed by the diffusion equation:

$$\frac{\partial V}{\partial t} = D \frac{\partial^2 V}{\partial x^2}. \tag{C-7}$$

From Eq. C-5, boundary condition at the canister ($x = 0$) is:

$$\varepsilon D A \frac{\partial V}{\partial x}\bigg|_{x-0} = \begin{cases} 0 & t = 0 \\ M & t > 0 \end{cases}. \tag{C-8}$$

From Eq. C-3, the boundary condition where the drift intersects the fracture ($x = L$) is:

$$\varepsilon D A \frac{\partial V}{\partial x}\bigg|_{x=L} = VQ \tag{C-9}$$

The solution to this equation can be found in Carslaw and Jaeger (1959, problem iv, p 125):

$$V = \frac{M}{Q}\left\{1 + H\left(1 - \frac{x}{L}\right) - \sum_{n=1}^{\infty} \frac{2H\left(\alpha_n^2 + H^2\right)\cos\left(\alpha_n x / L\right)}{\alpha_n^2\left(H + H^2 + \alpha_n^2\right)} \exp\left(-\alpha_n^2 T\right)\right\}, \tag{C-10}$$

where:

$$T = \frac{Dt}{L^2}, \tag{C-11}$$

$$H = \frac{LQ}{\varepsilon DA}, \tag{C-12}$$

and α_n are the positive roots of:

$$\alpha \tan \alpha = H. \tag{C-13}$$

The flux to the fracture for this case is given by:

$$QC_a\big|_{x=L} = Q\frac{\partial V}{\partial t}\bigg|_{x=L} = \frac{2HMD}{L^2} \sum_{n=1}^{\infty} \frac{\left(\alpha_n^2 + H^2\right)\cos\left(\alpha_n\right)}{\left(H + H^2 + \alpha_n^2\right)} \exp\left(-\alpha_n^2 T\right). \tag{C-14}$$

Case b

In case b, where diffusion takes place only in the positive and negative x-directions, the boundary condition at the failure location on the canister ($x = 0$) is

$$\varepsilon DA \int_0^t \frac{\partial C_b}{\partial x}\bigg|_{x=0} dt = \begin{cases} 0 & t = 0 \\ M/2 & t > 0 \end{cases}, \tag{C-15}$$

where, in this case, only $M/2$ diffuses towards the fracture.

The fracture is assumed to have negligible influence on the diffusive transport of most C-14 along the drift. The boundary condition at large distances from the failed canister is:

$$C_b \to 0 \text{ as } x \to \infty. \tag{C-16}$$

In order to solve Eq. C-2 for these boundary conditions, we again consider the parameter V, as defined by Eq. C-6. From Eq. C-15, boundary condition at the canister ($x = 0$) is:

$$\varepsilon DA \frac{\partial V}{\partial x}\bigg|_{x=0} = \begin{cases} 0 & t = 0 \\ M/2 & t > 0 \end{cases}. \tag{C-17}$$

and, from Eq. C-16:

$$V \to 0 \text{ as } x \to \infty. \tag{C-18}$$

The solution to this equation can be found in Carslaw and Jaeger (1959, problem i, p75):

$$V = \frac{M}{\varepsilon D \pi r_t^2}\left\{\sqrt{\frac{Dt}{\pi}} \exp\left(-\frac{x^2}{4Dt}\right) - \frac{x}{2}\operatorname{erfc}\frac{\mathrm{x}}{2\sqrt{\mathrm{Dt}}}\right\}, \tag{C-19}$$

The flux to the fracture at $x = L$:

$$QC_b\big|_{x=L} = Q\frac{\partial V}{\partial t}\bigg|_{x=L} = \frac{MDH}{2L^2}\left\{\frac{1}{\sqrt{\pi T}}\exp\left(-\frac{1}{4T}\right)\right\} \tag{C-20}$$

The flux along the drift at $x = L$ is:

$$\varepsilon DA\frac{\partial C_b}{\partial x}\bigg|_{x=L} = \frac{MD}{4TL^2}\left\{\frac{1}{\sqrt{\pi T}}\exp\left(-\frac{1}{4T}\right)\right\} \tag{C-21}$$

Note that, in this case, the flux to the fracture has a maximum when:

$$Q\frac{\partial C_b}{\partial t}\bigg|_{x=L} = 0 \tag{C-22}$$

From Eq. C-20, this occurs when:

$$T = \frac{1}{2}. \tag{C-23}$$

At this time, the flux to the fracture at $x = L$ is:

$$QC_b\big|_{x=L} = \frac{MDH}{2L^2}\sqrt{\frac{2}{\pi e}} \tag{C-24}$$

and the flux along the drift is:

$$\varepsilon DA\frac{\partial C}{\partial x}\bigg|_{x=L} = \frac{MD}{2L^2}\sqrt{\frac{2}{\pi e}}. \tag{C-25}$$

Case b is a good approximation if the flux along the drift should be much greater than the flux to the fracture, i.e. if:

$$H >> 1. \tag{C-26}$$

Appendix D

KBS-3H specific nomenclature

Term	Description
Air evacuation	Removing of air from a drift compartment through pipes during artificial watering.
Artificial watering	Adding water through pipes to a Supercontainer section to facilitate buffer saturation.
Backfilling	Filling the deposition niche, transport tunnels and other parts of the repository.
Basic Design	KBS-3H design alternative.
BD	Basic Design.
BRITE	Barrier Review, Integration, Tracking and Evaluation group.
Buffer	Bentonite originally inside the Supercontainer and the bentonite distance blocks.
Candidate design	Design alternative to be used for selecting a suitable design.
Catching tube	Equipment for catching the copper canister during retrieval.
Compartment	Drift section used for emplacement of Supercontainers. Typically, the 300 m-long drift is divided into 2 compartments by a compartment plug.
Compartment plug	Titanium plug used to seal off drift sections where inflows are higher than 1 litre per minute after grouting, thus dividing the drift into compartments.
Cutting tool	Device for removal/cutting of Supercontainer end plate during retrieval.
DAWE	Drainage, Artificial Watering and air Evacuation. The SKB-3H reference design alternative.
DD-2005, DD-2006, DD-2007	KBS-3H Design Description 2005, 2006 and 2007 reports, respectively.
Deposition drift	A 100–300 m long horizontal drift with a diameter of 1.85 m.
Deposition equipment	Includes all equipment needed for the emplacement of Supercontainer and installation of distance blocks.
Deposition machine	The machine used in the deposition drift for emplacement of Supercontainers and distance blocks.
Deposition niche	A tunnel section in front of the deposition drift hosting the deposition equipment.
Design component	A component in design which fulfils a specific functional requirement, e.g. compartment plug, distance blocks.
Distance blocks	Bentonite blocks between the Supercontainers. The roles of the distance blocks are to provide hydraulic separation and thermal spacing.
Drift Plug	Drift plug. A titanium plug used to close the deposition drifts, designed to seal the deposition drift during the operational period. Built to withstand both groundwater and buffer swelling pressure. Basically a scaled up compartment plug.
Drift end plug	This was the original design for closing the drifts and has now been replaced by the drift plug. A steel-reinforced low-pH concrete bulkhead positioned in a notch situated at the end of deposition drift close to the intersection with the deposition niche.
Drip (and spray) shield	Thin metal sheets, steel or copper, sheets over inflow points preventing erosion of bentonite due to the spraying, dripping and squirting of water from the drift walls onto the distance blocks and Supercontainers.
EDZ	Excavation Damaged Zone; section of the rock damaged by the boring of deposition drifts.
End plate	Unperforated end plate for the Supercontainer shell.
Engineered and residual materials	Materials introduced during construction and operation of the repository that will remain underground after closure.
Erosion	Loss or redistribution of bentonite mass in the deposition drift due to physical or chemical processes, such as piping or chemical erosion by dilute water.
Fastening ring	Metallic ring used to fasten the steel compartment plug to the rock.
Filling block	Filling blocks are placed at positions where Supercontainer units cannot be positioned because inflow is higher than positioning criteria.
Filling material	Material between and in the vicinity of the compartment plugs to fill empty space which cannot be filled by using filling blocks.
FKA	Forsmarks Kraftaktiebolag (The Forsmark nuclear power station).
Fixing ring (BD design only)	Metallic rings installed, where necessary, to avoid displacement of the distance blocks prior to the installation of compartment and drift end plugs.
F.O.S	Factor of Safety.
FSAR	Final Safety Analysis Report. (The expression not used in Sweden where we use SAR instead).
Gamma gate	Sliding radiation protection gates located on the transport tube or at the entrance of the deposition drift.
Gripping tool	Device for removal of canister from the drift during retrieval.
Handling cell	A radiation shielded cell for handling of the spent fuel canister.

Term	Description
Handling equipment	Equipment for handling of the transport container for the spent fuel canister within the reloading station or the spent fuel canister inside the handling cell.
Horizontal push-reaming	Excavation method to ream the pilot hole to full drift size, known also as horizontal blindboring, reverse raiseboring or horizontal box-hole boring.
HRL	The Hard Rock Laboratory at Äspö.
KBS	(Kärnbränslesäkerhet). The method for implementing the spent fuel disposal concept based on multiple barriers (as required in Sweden and in Finland). KBS-1, KBS-2 and KBS-3 are variations of this method.
KBS-3H	(Kärnbränslesäkerhet 3-Horisontell). Design alternative of the KBS-3 method in which several spent fuel canisters are emplaced horizontally in each deposition drift.
KBS-3V	(Kärnbränslesäkerhet 3-Vertikal). The reference design alternative of the KBS-3 method in which the spent fuel canisters are emplaced in individual vertical deposition holes.
Low pH-cement, sometimes also called LHHP cement	Low-pH cement, used for spent fuel repository applications, characterized by a low pH value, below 11, low heat of hydration, and a lower release of free hydroxide ions.
Mega-Packer	Large-scale post-grouting device for grouting of rock.
Onkalo	Underground rock characterisation facility in Olkiluoto, Finland.
Parking feet	Feet on the Supercontainer.
Pilot hole	Drilled hole for guiding horizontal push-reaming excavation.
Piping	Formation of hydraulically conductive channels in the bentonite due to high water flow and hydraulic pressure difference along the drift.
Post-grouting	Grouting method used in deposition drift after excavation.
Pre-grouting	Grouting made through investigation or pilot holes before reaming the drift to full size.
Pre-pilot hole	Core-drilled investigation hole made before drilling the pilot hole. This may be used for guiding the boring of pilot holes.
PSAR	Preliminary Safety Analysis Report.
RSC	Criteria The Rock Suitability, a Finnish classification system.
Reloading station	Station at repository level where the spent fuel canister is transferred from the transport cask to the Supercontainer.
Retrievability	Possibility of removal of canisters after the buffer has absorbed water and started to swell within the deposition drift.
Retrieval	Removal of the canister after the buffer has absorbed water and started to swell within the deposition drift.
Reverse operation	Operation to remove the Supercontainer from the deposition drift before the buffer has absorbed water and started to swell within the deposition drift.
SFIC	Safety function indicator criterion.
Safety studies	Long-term safety studies performed for the 2004–2007 KBS-3H project consisting of five main reports: Process, Evolution, Radionuclide transport, Complementary Evaluations of Safety and Summary.
Sealing ring	Design component in the STC design (still at a conceptual stage) presented in DD-2007.
Silica Sol	Type of colloidal silica used for groundwater control purposes.
Spalling of rock	Breaking of the rock surface of deposition drift induced by high rock stresses into splinters, chips or fragments.
Start tube	Support structure for the deposition machine.
STC	Semi Tight Compartments design alternative.
Supercontainer	Assembly consisting of a canister surrounded by bentonite clay and a perforated shell.
Supercontainer section	Section of the drift (about 10 m long for the reference type BWR fuel from Olkiluoto 1–2) in which a Supercontainer and a distance block are located.
Supercontainer shell	Perforated shell that holds together the canister and the bentonite surrounding it.
TDS	Total Dissolved Solids.
Transition block	A component in the filling system adjacent to compartment plug.
Transport tube	Tube for the handling of the Supercontainer.
Transport vehicle	Vehicle for transportation of deposition equipment.
URL	Underground Research Laboratory.
UCS	Unconfined compressive strength.
VAHA	Posiva's requirements management system VAHA is an information system designed in Posiva to manage the requirements related to the geological disposal of spent nuclear fuel. VAHA aims to include all relevant requirements, origin and their rationale with existing solutions to fulfil them and enables an effective review of compliance and dependencies between separate specifications and requirements.
Water cushion system	System for the transportation of Supercontainers and distance blocks.